AD-A266 984

WL-TR-93-2047

ADVANCED COOLING FOR HIGH POWER ELECTRIC ACTUATORS

Michael G. Schneider

Timothy J. Bland

Sundstrand Corporation
P.O. Box 7002
Rockford, IL 61125-7002

DTIC
ELECTE
JUL 13 1993
S A D

January 1993

Interim Report for January 1992 to September 1992

APPROVED FOR PUBLIC RELEASE; DISTRIBUTION UNLIMITED

AERO PROPULSION AND POWER DIRECTORATE
WRIGHT LABORATORY
AIR FORCE MATERIEL COMMAND
WRIGHT-PATTERSON AFB OH 45433-7650

93-15784

93 7 12 062

NOTICE

When Government drawings, specifications, or other data are used for any purpose other than in connection with a definitely Government-related procurement, the United States Government incurs no responsibility or any obligation whatsoever. The fact that the government may have formulated or in any way supplied the said drawings, specifications, or other data, is not to be regarded by implication, or otherwise in any manner construed, as licensing the holder, or any other person or corporation; or as conveying any rights or permission to manufacture, use, or sell any patented invention that may in any way be related thereto.

This report is releasable to the National Technical Information Service (NTIS). At NTIS, it will be available to the general public, including foreign nations.

This technical report has been reviewed and is approved for publication.

Micheal J. Morgan
Project Engineer
Thermal Technology Section

Jerry E. Beam
Section Chief
Thermal Technology Section
Power Technology Branch

MICHAEL D. BRAYDICH, Lt Col, USAF
Deputy Chief
Aerospace Power Division
Aero Propulsion & Power Directorate

If your address has changed, if you wish to be removed from our mailing list, or if the addressee is no longer employed by your organization please notify WL/POOS-3 WPAFB, OH 45433-7251 to help us maintain a current mailing list.

Copies of this report should not be returned unless return is required by security considerations, contractual obligations, or notice on a specific document.

REPORT DOCUMENTATION PAGE

Form Approved
OMB No. 0704-0188

Public reporting burden for this collection of information is estimated to average 1 hour per response, including the time for reviewing instructions, searching existing data sources, gathering and maintaining the data needed, and completing and reviewing the collection of information. Send comments regarding this burden estimate or any other aspect of this collection of information, including suggestions for reducing this burden to Washington Headquarters Services, Directorate for Information Operations and Reports, 1215 Jefferson Davis Highway, Suite 1204, Arlington, VA 22202-4302, and to the Office of Management and Budget, Paperwork Reduction Project (0704-0188), Washington, DC 20503.

1. AGENCY USE ONLY (Leave blank)	2. REPORT DATE	3. REPORT TYPE AND DATES COVERED
	January 1993	Interim Jan 92 to Sep 92

4. TITLE AND SUBTITLE

Advanced Cooling for High Power Electric Actuators

5. FUNDING NUMBERS

C-F33615-91-C-2139
PE-62203F
PR-3145
TA-29
WU-14

6. AUTHOR(S)

Michael G. Schneider
Timothy J. Bland

7. PERFORMING ORGANIZATION NAME(S) AND ADDRESS(ES)

Sundstrand Corp.
PO Box 7002
Rockford IL 61125-7002

8. PERFORMING ORGANIZATION REPORT NUMBER

9. SPONSORING/MONITORING AGENCY NAME(S) AND ADDRESS(ES)

Aero Propulsion and Power Directorate
Wright Laboratory
Air Force Materiel Command
Wright-Patterson AFB OH 45433-7650

10. SPONSORING/MONITORING AGENCY REPORT NUMBER

WL-TR-93-2047

11. SUPPLEMENTARY NOTES

12a. DISTRIBUTION/AVAILABILITY STATEMENT

Approved for Public Release; Distribution Unlimited

12b. DISTRIBUTION CODE

13. ABSTRACT *(Maximum 200 words)*

The development of more electric technologies for future military aircraft promises to provide significant redundancy, reliability, maintainability, and performance benefits. Advanced Cooling For High Power Electric Actuators particularly address the use electro-mechanical actuators (EMAs), and an approach for cooling EMAs using the combined concepts of passive reflux cooling and phase change materials (PCMs) for energy storage. The planned program involves four Phases:

Phase I - Requirements and Trade Studies.
Phase II - Detailed Design.
Phase III - Fabrication and Test Plans.
Phase IV - Test/Data Correlation.

During Phase I Sundstrand identified actuator cooling requirements and evaluated the effects of several critical parameters on the use of passive reflux cooling in combination with PCM.

14. SUBJECT TERMS

Electric Actuators
Heat Exchanger
Thermal Management
Phase Change Material

15. NUMBER OF PAGES

146

16. PRICE CODE

17. SECURITY CLASSIFICATION OF REPORT	18. SECURITY CLASSIFICATION OF THIS PAGE	19. SECURITY CLASSIFICATION OF ABSTRACT	20. LIMITATION OF ABSTRACT
Unclassified	Unclassified	Unclassified	UL

TABLE OF CONTENTS

		PAGE NUMBER
1.0	INTRODUCTION	1
	1.1 Background	1
	1.2 EMA Passive Cooling Approach	1
2.0	SPECIFICATIONS	8
3.0	DEMONSTRATION REFLUX COOLER DESIGN SUMMARY	13
4.0	ANALYTICAL METHODS	14
	4.1 SINDA Model Description	14
	4.2 Model Inputs/Defaults	14
	4.3 Correlations	20
5.0	TRADE STUDIES	23
	5.1 Actuator Comparison	23
	5.2 Steady State Analysis	23
	5.2.1 Geometry/Design Considerations	
	5.2.2 Mission Considerations	
	5.2.3 Type of Motor	
	5.3 Motor Comparison	53
	5.4 Transient Analysis	57
	5.4.1 Frequency Response	
	5.4.2 Combat Phase	
	5.4.3 Typical Combat Mission	
	5.5 Working Fluid Comparison	77
	5.6 Phase Change Material Comparison	87
	5.7 Demonstration Motor Selection	90
	5.8 Manufacturing Approach	92
6.0	CONCLUSIONS	94
7.0	RECOMMENDATIONS	95
8.0	REFERENCES	96
	APPENDIX A - FIGURES IN BRITISH UNITS	98

DTIC QUALITY INSPECTED 3

Accesion For
NTIS CRA&I ☑
DTIC TAB ☐
Unannounced ☐
Justification
By
Distribution /
Availability Codes
Dist | Avail and / or Special
A-1

LIST OF FIGURES

Figure No.	Title	Page No.
1.1	Thermosyphon Concept	2
1.2	Reflux Cooler in Normal Operation	4
1.3	Reflux Cooler in Inverted Operation	5
1.4	Effect of PCM on Reflux Temperature	6
2.1	Typical EMA Mission Duty Cycle	9
2.2	PC Cycles, Frequency, System Pressure vs. Phase	10
2.3	Analysis of F-18 Aileron Actuator Flight Data	11
2.4	Worse Case EMA Mission Duty Cycle	12
4.1	Passive Cooling Concept	15
4.2	SINDA Model Schematic	16
4.3	SINDA Models Inputs/Defaults	17 18
4.4	Motor Loss Distributions (Percentage of Total Losses)	19
5.1	Actuator Comparison	24
5.2	Advanced Actuator Cooling - Steady State Temperature vs Condenser Width Parameter	25
5.3	Advanced Actuator Cooling - Steady State Temp. Differences vs Condenser Width Parameter	26
5.4	Advanced Actuator Cooling - Steady State Temperature vs Evaporator Width Parameter	27
5.5	Advanced Actuator Cooling - Steady State Temp. Differences vs Evaporator Width Parameter	28
5.6	Advanced Actuator Cooling - Steady State Temperature vs Cooler Height Parameter	29
5.7	Advanced Actuator Cooling - Steady State Temp. Differences vs Cooler Height Parameter	30
5.8	Advanced Actuator Cooling - Steady State Temperature vs Fin Count	31
5.9	Advanced Actuator Cooling - Steady State Temp. Differences vs Fin Count	32
5.10	Advanced Actuator Cooling - Steady State Temp vs Ambient Heat Transfer Coefficient	34
5.11	Advanced Actuator Cooling - Steady State Temp Diff vs Ambient Heat Trans Coef	35
5.12	Advanced Actuator Cooling - Steady State Temperature vs Structure Conductance	36
5.13	Advanced Actuator Cooling - Steady State Temp Differences vs Structure Conductance	37
5.14	Advanced Actuator Cooling - Steady State Temperature vs Structure Plate Thickness	38
5.15	Advanced Actuator Cooling - Steady State Temp Differences vs Structure Plate Thickness	39
5.16	Advanced Actuator Cooling - Steady State Temperature vs Altitude	40
5.17	Advanced Actuator Cooling - Steady State Temp Differences vs Altitude	41
5.18	Advanced Actuator Cooling - Steady State Temperature vs Altitude	42
5.19	Advanced Actuator Cooling - Steady State Temp Differences vs Altitude	43

Figure No.	Title	Page No.
5.20	Advanced Actuator Cooling - Steady State Temperature vs Altitude	44
5.21	Advanced Actuator Cooling - Steady State Temp Differences vs Altitude	45
5.22	Advanced Actuator Cooling - Steady State Temperature vs Altitude	46
5.23	Advanced Actuator Cooling - Steady State Temp Differences vs Altitude	47
5.24	Advanced Actuator Cooling - Steady State Temperature vs Altitude	48
5.25	Advanced Actuator Cooling - Steady State Temp Differences vs Altitude	49
5.26	Advanced Actuator Cooling - Steady State Temperature vs Altitude	50
5.27	Advanced Actuator Cooling - Steady State Temp Differences vs Altitude	51
5.28	Advanced Actuator Cooling - Steady State Rotor Temperature vs Altitude	52
5.29	Electric Motor Comparison	54
5.30	Advanced Actuator Cooling - Frequency Response-Motor Power vs Time	58
5.31	Advanced Actuator Cooling - Frequency Response-Motor Power vs Time	59
5.32	Advanced Actuator Cooling - Frequency Response-Temperature vs Time	60
5.33	Advanced Actuator Cooling - Frequency Response-Temperature vs Time	61
5.34	Advanced Actuator Cooling - Frequency Response-Temperature vs Time	62
5.35	Advanced Actuator Cooling - Frequency Response-Temperature vs Time	63
5.36	Advanced Actuator Cooling - Frequency Response	65
5.37	Advanced Actuator Cooling - Frequency Response	66
5.38	Advanced Actuator Cooling - Actuator Motor Power vs Time	67
5.39	Advanced Actuator Cooling - Temperature vs Time	68
5.40	Advanced Actuator Cooling - Temperature vs Time	69
5.41	Advanced Actuator Cooling - PCM Liquid Mass Fraction vs Time	70
5.42	Advanced Actuator Cooling - Temperature vs Time	71
5.43	Advanced Actuator Cooling - Temperature vs Time	72
5.44	Advanced Actuator Cooling - PCM Liquid Mass Fraction vs Time	73
5.45	Advanced Actuator Cooling - Temperature vs Time	74
5.46	Advanced Actuator Cooling - Temperature vs Time	75
5.47	Advanced Actuator Cooling - PCM Liquid Mass Fraction vs Time	76
5.48	Advanced Actuator Cooling - Temperature vs Time	78
5.49	Advanced Actuator Cooling - Temperature vs Time	79
5.50	Advanced Actuator Cooling - Temperature vs Time	80
5.51	Advanced Actuator Cooling - Temperature vs Time	81
5.52	Advanced Actuator Cooling - Temperature vs Time	82

Figure No.	Title	Page No.
5.53	Advanced Actuator Cooling - Temperature vs Time	83
5.54	Reflux Working Fluids Comparison	85
5.55	Advanced Actuator Cooling - Fluids Comparison	86
5.56	Candidate PCMs	88 89
5.57	Electric Motor Comparison	91
5.58	Advanced Actuator Cooling - Passive Cooling Concept	93
A.1	Advanced Actuator Cooling - Steady State Temperature vs Condenser Width Parameter	99
A.2	Advanced Actuator Cooling - Steady State Temp. Differences vs Condenser Width Parameter	100
A.3	Advanced Actuator Cooling - Steady State Temperature vs Evaporator Width Parameter	101
A.4	Advanced Actuator Cooling - Steady State Temp. Differences vs Evaporator Width Parameter	102
A.5	Advanced Actuator Cooling - Steady State Temperature vs Cooler Height Parameter	103
A.6	Advanced Actuator Cooling - Steady State Temp. Differences vs Cooler Height Parameter	104
A.7	Advanced Actuator Cooling - Steady State Temperature vs Fin Count	105
A.8	Advanced Actuator Cooling - Steady State Temp. Differences vs Fin Count	106
A.9	Advanced Actuator Cooling - Steady State Temp vs Ambient Heat Transfer Coefficient	107
A.10	Advanced Actuator Cooling - Steady State Temp Diff vs Ambient Heat Trans Coef	108
A.11	Advanced Actuator Cooling - Steady State Temperature vs Structure Conductance	109
A.12	Advanced Actuator Cooling - Steady State Temp Differences vs Structure Conductance	110
A.13	Advanced Actuator Cooling - Steady State Temperature vs Structure Plate Thickness	111
A.14	Advanced Actuator Cooling - Steady State Temp Differences vs Structure Plate Thickness	112
A.15	Advanced Actuator Cooling - Steady State Temperature vs Altitude	113
A.16	Advanced Actuator Cooling - Steady State Temp Differences vs Altitude	114
A.17	Advanced Actuator Cooling - Steady State Temperature vs Altitude	115
A.18	Advanced Actuator Cooling - Steady State Temp Differences vs Altitude	116
A.19	Advanced Actuator Cooling - Steady State Temperature vs Altitude	117
A.20	Advanced Actuator Cooling - Steady State Temp Differences vs Altitude	118
A.21	Advanced Actuator Cooling - Steady State Temperature vs Altitude	119
A.22	Advanced Actuator Cooling - Steady State Temp Differences vs Altitude	120
A.23	Advanced Actuator Cooling - Steady State Temperature vs Altitude	121
A.24	Advanced Actuator Cooling - Steady State Temp Differences vs Altitude	122
A.25	Advanced Actuator Cooling - Steady State Temperature vs Altitude	123
A.26	Advanced Actuator Cooling - Steady State Temp Differences vs Altitude	124
A.27	Advanced Actuator Cooling - Steady State Rotor Temperature vs Altitude	125

Figure No.	Title	Page No.
A.28	Advanced Actuator Cooling - Frequency Response-Temperature vs Time	126
A.29	Advanced Actuator Cooling - Frequency Response-Temperature vs Time	127
A.30	Advanced Actuator Cooling - Frequency Response-Temperature vs Time	128
A.31	Advanced Actuator Cooling - Frequency Response-Temperature vs Time	129
A.32	Advanced Actuator Cooling - Frequency Response	130
A.33	Advanced Actuator Cooling - Frequency Response	131
A.34	Advanced Actuator Cooling - Temperature vs Time	132
A.35	Advanced Actuator Cooling - Temperature vs Time	133
A.36	Advanced Actuator Cooling - PCM Liquid Mass Fraction vs Time	134
A.37	Advanced Actuator Cooling - Temperature vs Time	135
A.38	Advanced Actuator Cooling - Temperature vs Time	136
A.39	Advanced Actuator Cooling - PCM Liquid Mass Fraction vs Time	137
A.40	Advanced Actuator Cooling - Temperature vs Time	138
A.41	Advanced Actuator Cooling - Temperature vs Time	139
A.42	Advanced Actuator Cooling - PCM Liquid Mass Fraction vs Time	140
A.43	Advanced Actuator Cooling - Temperature vs Time	141
A.44	Advanced Actuator Cooling - Temperature vs Time	142
A.45	Advanced Actuator Cooling - Temperature vs Time	143
A.46	Advanced Actuator Cooling - Temperature vs Time	144
A.47	Advanced Actuator Cooling - Temperature vs Time	145
A.48	Advanced Actuator Cooling - Temperature vs Time	146

1.0 INTRODUCTION

1.1 Background

The development of more electric technologies for future military aircraft promises to provide significant redundancy, reliability, maintainability and performance benefits. In particular, the use of electrically driven actuators for flight control surfaces, as well as engine thrust control, allows elimination of actuator hydraulic circuits throughout the aircraft that often leak, require high maintenance, and damage easily during battle.

Many of these actuators, such as flaperons and stabilators, operate at high powers during certain flight segments such as takeoff, combat, and landing. The development of inherently unstable aircraft, for improved maneuverability, particularly results in large actuator powers. The hydraulic oil circuit carries the associated waste heat away from conventional hydraulic actuators, whereas, electro-mechanical actuators (EMAs) possess no inherent means of removing waste heat. Moreover, the use of an active cooling loop for EMAs would re-introduce reliability/ maintainability/safety issues eliminated with the removal of conventional hydraulic circuits. Therefore, cooling becomes an issue for EMAs because of limited accessibility or availability of appropriate heat sinks.

The aircraft structure and skin, and ultimately the ambient air, provide the most feasible heat sink for EMAs. Peak power levels for flaperons and other high power control surface actuators may reach 50 hp which, with a motor efficiency of 95 percent, places a heat load of 2.5 hp on the heat sink during peak conditions. However, these actuators typically operate at peak power for brief durations, and operate at significantly reduced power levels during most of a flight duty cycle. This characteristic of aircraft actuator duty cycles suggests the use of energy storage techniques that would store energy during peak power periods and dissipate that stored energy during low power periods. Energy storage techniques would allow the design of a heat rejection system for average heat loads rather than peak heat loads.

Thus, the replacement of hydraulic actuators with EMAs introduces a motor cooling issue, and the challenge for the design of an EMA cooling system involves designing a simple, lightweight, passive heat transfer means between the actuator and ambient air that uses energy storage to reduce heat exchanger heat duty during transient peak power periods. The Sundstrand approach for EMA cooling uses the two-phase fluid thermosyphon concept, to provide passive energy transport, and a phase change material (PCM), to provide energy storage.

1.2 EMA Passive Cooling Approach

Sundstrand's approach for passive cooling of EMAs uses a passive reflux or thermosyphon concept to transfer heat from the motor housing to the aircraft skin. This technology depends upon submerging the heat source in a liquid that boils when heated. The generated vapor rises due to the density difference between the vapor and liquid phases and condenses on a cooler surface favorably located above the heat source. The condensate returns to the pool of liquid surrounding the heat source to complete the cycle. Figure 1.1 illustrates the thermosyphon concept.

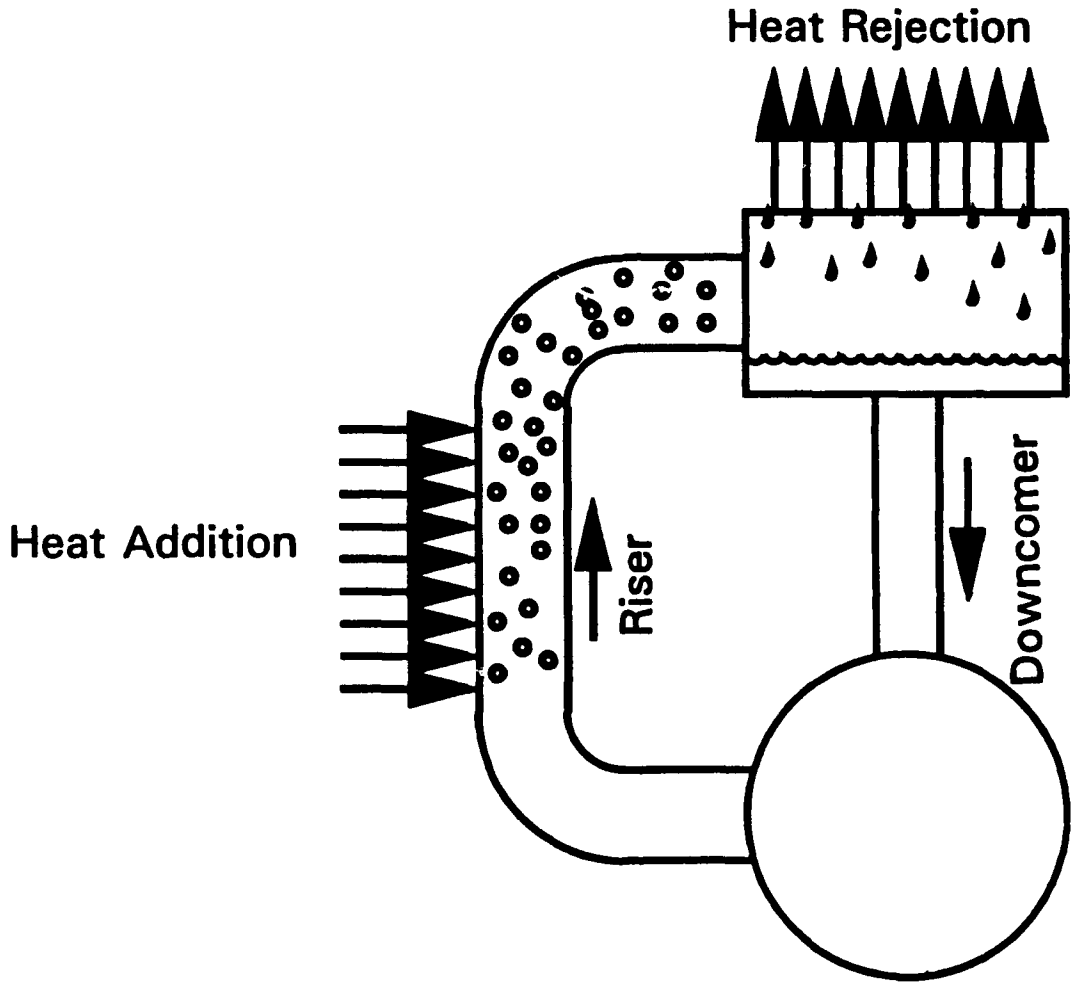

Figure 1.1 Thermosyphon Concept

A two-phase fluid provides significantly enhanced heat transfer compared to conduction or single phase convection, and heat transport can occur across large distances by virtue of vapor flow from the hot source to the cold sink. The reflux heat exchanger operates under the same principle as large scale thermosyphon boilers used in Rankine cycle power plants, relying upon the density difference between the liquid phase and vapor phase, and gravity to provide the motive force for the natural circulation of fluid. Heat pipes, somewhat similar devices, rely upon surface tension and a wicking structure rather than gravity to provide the motive force for liquid circulation. In general, the allowable heat flux at the heat source for a reflux heat exchanger exceeds the allowable heat flux for a heat pipe using the same working fluid.

Figure 1.2 illustrates the implementation of this concept for motor cooling. The design completely wets the motor housing with the liquid phase of the two-phase fluid selected for the application, and waste heat from the motor boils the liquid, generating vapor. This vapor flows upward due to density difference through centrally located vapor channels called "risers" and then condenses on the colder surface associated with the aircraft skin. Liquid condensate then flows downwards though "downcomers" to reenter the liquid pool surrounding the motor housing.

This cooling approach must also provide heat rejection in attitudes other than with the gravity vector in the downward direction. This requires careful consideration for providing a pool of liquid surrounding the heat source for any attitude, especially inverted flight. Figure 1.3 shows the location of the liquid level during inverted operation, keeping the motor submerged. Provided the heat exchanger uses only one heat rejection surface, heat transfer will occur at a lower rate since single phase convection replaces the two-phase condensation process at the submerged heat sink during inverted operation. Condensation in the vapor space continues, but energy reaches the ultimate heat rejection area by conduction through the heat exchanger metal and the subcooled liquid phase. Therefore, generated vapor tends to raise the system saturation temperature and pressure since this condition increases the heat transfer resistance between the heat source and heat sink. The rate of temperature rise depends upon the total thermal capacitance. The use of upper and lower heat rejection surfaces would allow condensation heat rejection under either orientation.

Heat load changes with this passive cooling approach result in changes in operating temperature and pressure for a given sink temperature. In its simplest form, the peak load defines the design condition for the cooling system, and the series thermal conductances between the motor and ambient air determines the motor temperatures.

Enhancement of the system thermal capacitance through energy storage allows the heat rejection surfaces to be designed for the average load, reducing motor temperatures to those associated with the average heat load. Energy storage occurs through the use of either sensible storage, i.e., addition of mass and specific heat, or the use of a PCM that stores energy in latent heat. This latter approach typically results in minimum mass and volume impacts on the system. The Sundstrand EMA cooling concept uses the PCM approach to minimize weight.

Figure 1.4 depicts the concept of using a PCM for energy storage. The figure illustrates the two-phase working fluid through the duty cycle represented by the square wave in the upper half of the figure. Starting at point A, the actuator goes to peak load after a

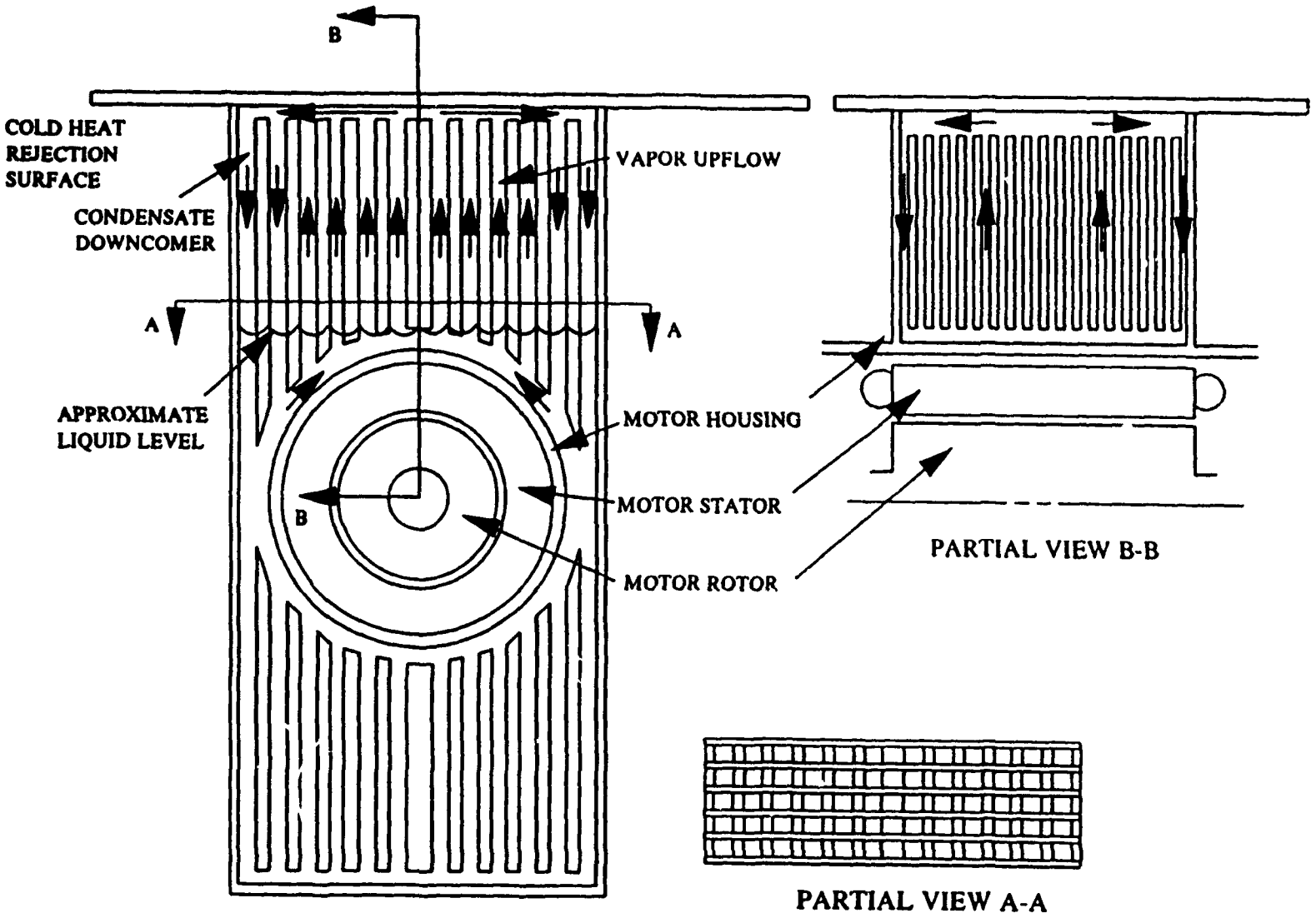

FIGURE 1.2 REFLUX COOLER IN NORMAL OPERATION

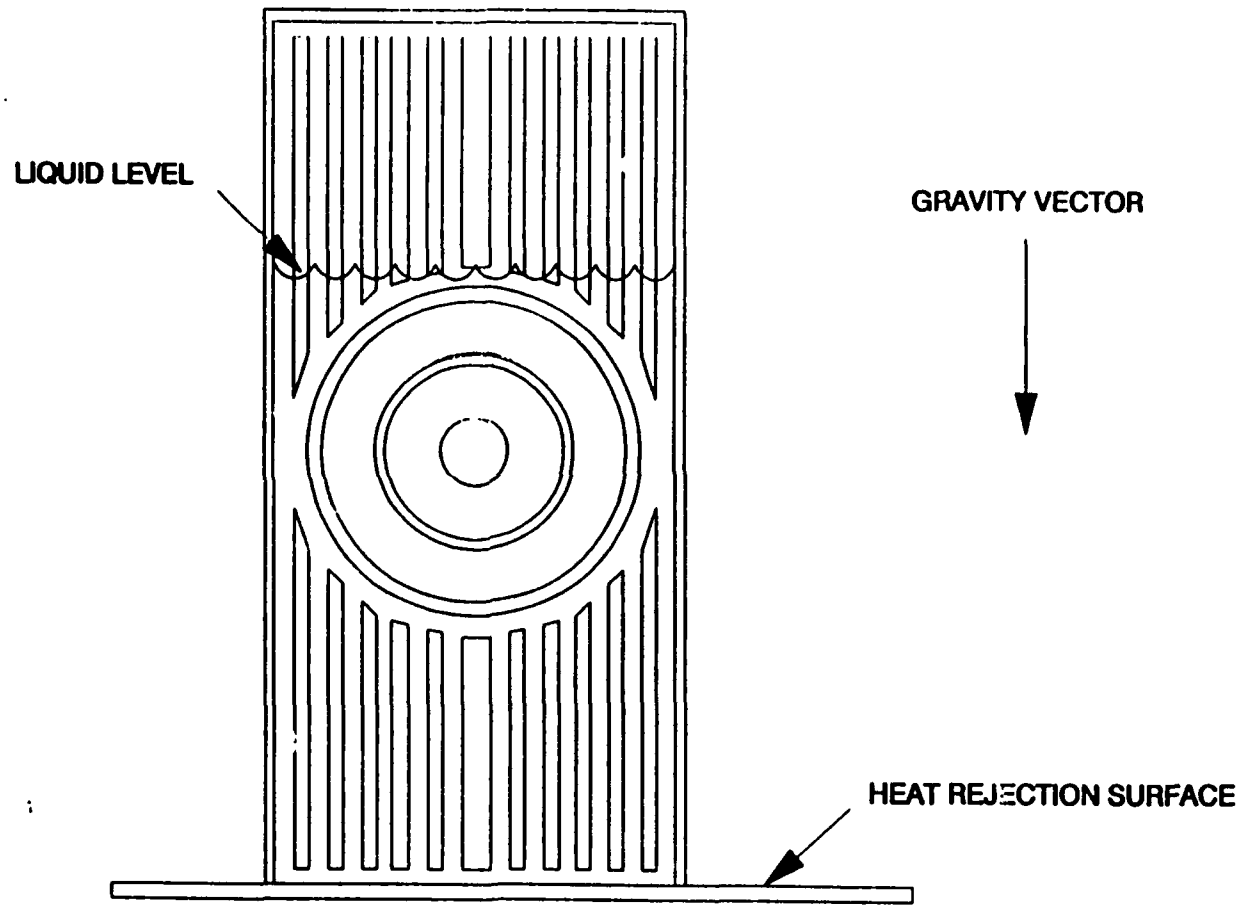

FIGURE 1.3 REFLUX COOLER IN INVERTED OPERATION

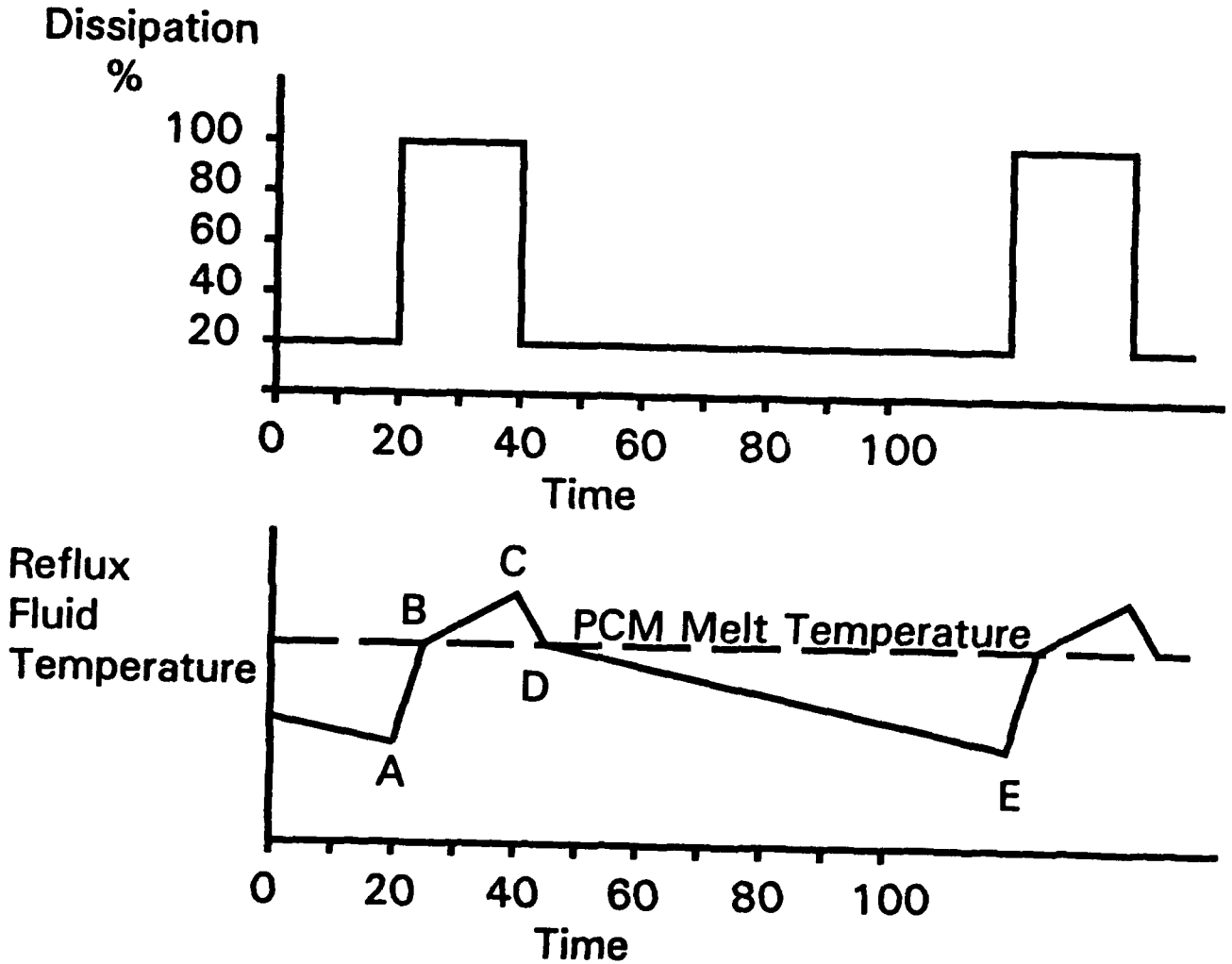

Figure 1.4 Effect of PCM on Reflux Temperature

period of low load operation. The phase change material, stored within a containment structure is completely solid. As the dissipation rises to full load, the fluid temperature (and saturation pressure) rises at a rate dependent on structure specific heat and heat transfer rates. At point B, the fluid temperature reaches the melting temperature of the PCM and it starts to melt, storing energy in the form of latent heat. As the solid material melts, the coolant temperature continues to rise, but at a much lower rate, as the heat conducts through the molten material to access the remaining solid material in its container.

At point C, the motor heat load drops from its peak value to a value of 20 percent of the peak and much lower than the design average heat rejection value of 36 percent of peak. The PCM now acts as a heat source, additive to the motor load, and the temperature starts to fall as the molten PCM cools off to its freezing point D. At this temperature, freezing occurs at the surface of the container and a freeze front starts to move inward within the PCM. The temperature continues to drop during this process until the actuator again experiences peak load at point E.

2.0 SPECIFICATIONS

One of the difficulties encountered in designing a heat rejection system for EMAs involves defining the design specifications. Limited relevant design data exists from the previous use of hydraulic actuators and the advent of inherently unstable aircraft designs. Because hydraulic actuators relied upon the hydraulic circuit to carry away waste heat, the design of these actuators did not require detailed heat rejection requirements, and therefore limited actuator heat rejection experimental data. On the other hand the minimum weight design of a heat rejection system for EMAs requires detailed heat rejection data in order to make effective use of limited available heat sinks. Designing for the use of a PCM particularly requires actuator duty cycle data. In addition to the limited available data, actuator design data for previous aircraft designs may not apply to next generation aircraft which depend upon inherently unstable aircraft designs for improved maneuverability. These aircraft use aircraft control surfaces more actively to maintain control of the aircraft, even during level flight.

Given the shortage of design data, Sundstrand formulated design specifications based upon actuator design experience and limited experimental data for the F-15 aileron actuator. The following requirements served as the design specifications for the EMA heat rejection system for Phase I of the program:

- Design Power 34 hp
- Maximum Ambient Temperature 115 °F
- Minimum Ambient Temperature -65 °F
- Limit motor designs to those using conventional windings insulation systems (windings temperatures limited to approximately 250 °F).
- Typical mission duty cycle defined based upon design requirements data received by Sundstrand for F-15 actuators and F-15 aileron actuator flight data (see Figure 2.1).

Of these specifications the mission duty cycle particularly affects the design of the heat rejection system. Figure 2.1 breaks a mission into different phases and provides phase duration, actuator power, range of altitude and range of aircraft velocity for each of the phases. Sundstrand defined the mission duty cycle using the actuator design data provided for the F-15 and illustrated in Figure 2.2. Figure 2.2 provides data as a function of the type of actuator; whereas, Figure 2.1 defines a duty cycle for a generic actuator. Sundstrand used the worst case conditions from Figure 2.2 to arrive at composite conditions presented in Figure 2.1.

Design of a heat rejection system using a PCM relies upon the low power phases (cruise phases) of a mission in order to reduce the overall mission average power. In order to confirm the validity of 5 percent power during the cruise phase, Sundstrand evaluated experimental data provided by the Air Force for an F-15 aileron actuator. Figure 2.3 presents average power levels for each of the evaluated data files, and shows power levels well below 1 percent for all of the cases. Therefore, Sundstrand used a cruise power level of 5 percent for all Phase I design activities.

Because Figure 2.1 defines ranges of altitude and aircraft speed, Sundstrand used the worst case heat rejection conditions over the ranges to arrive at a representative duty cycle used for mission analysis presented in Figure 2.4. Worst case heat rejection conditions and obtained for maximum altitudes and minimum aircraft speed due to degraded ambient convection heat transfer coefficients.

MISSION PHASE	TOTAL TIME OF MISSION PHASE (MINUTES)	ACTUATOR POWER (%)	ALTITUDE (FEET)	MACH NUMBER
TAXI	PREFLIGHT CHECKS	100	0	0.0
STOL	0.5	85	0-5,000	0.0-0.25
CLIMB	7.0	50	5,000-45,000	0.25-0.80
CRUISE	20.0	5	10,000-45,000	0.50-1.50
COMBAT - PHASE I	14.0	65	10,000-30,000	0.50-0.80
- PHASE II	1.0	100	10,000-30,000	0.50-0.80
CRUISE	20.0	5	10,000-45,000	0.5-1.5
DESCENT	18.0	50	45,000-5,000	0.25-0.80
STOL	3.0	80	5,000-0	0.25-0.0

FIGURE 2.1 TYPICAL EMA MISSION DUTY CYCLE

Mission Phase / Actuator	Warm Up	Taxi	STOL	Climb	Cruise	Combat	Cruise	Descent	STOL	Reverse	Taxi	Cool Down
Stabilator	0	2-100%	2-80% 2-70%	30-50% 30-30% 400-2%	500-10% 2000-2%	6-100% 6-90% 30-80% 68-70% 80-50%	1000-10% 3500-2%	90-50% 70-30% 1000-2%	2-90% 8-80% 30-70% 100-2%	0	0	0
Freq. (Hz)		.448	.235	1.153	1.871	.31	1.76	1.082	.777			
Canard	0	2-90% 200-0%	2-80% 2-70%	30-50% 30-30% 600-2%	700-10% 1600-2%	14-90% 30-80% 68-70% 80-50%	1300-10% 2800-2%	90-50% 70-30% 1200-2%	8-80% 30-70%	0	0	0
Freq. (Hz)		.448	.235	1.654	1.572	.313	1.603	1.269	.211			
Flaperon	0	2-100%	2-100% 10-80%	2-90% 100-70% 50-50% 100-30%	500-10% 1750-2%	2-100% 50-80% 150-70% 150-30% 1000-10%	1000-10% 3250-2%	4-90% 250-70% 200-50% 250-30%	2-100% 2-90% 140-80%	0	0	0
Freq. (Hz)		.56	.705	.631	1.684	2.209	1.662	.656	.8			
Rudder	0	2-100%	2-80% 2-70%	30-50% 30-30% 400-2%	500-10% 2000-2%	6-100% 6-90% 30-80% 68-70% 80-50%	1000-10% 3500-2%	90-50% 70-30% 1000-2%	2-90% 8-80% 30-70% 100-2%	0	0	0
Freq. (Hz)		.704	.235	1.153	1.871	.31	1.76	1.082	.777			
Total Time (Sec)	60	450	17	399	1336	612	2557	1072	180	7	450	60
Cum. Time (sec.)	60	510	527	926	2262	2874	5431	6503	6683	6690	7140	7200
Ave Pump Pressure (psi)	3000	3150	8000	6800	4200	8000	4000	6900	8000	3000	3000	3000

FIGURE 2.2 PC CYCLES, FREQUENCY, SYSTEM PRESSURE VS. PHASE

CASE DESCRIPTION	MEAN POWER (hp)	MEAN POWER (%)[1]
FILE 1. OUT - POWER APPROACH, MODERATE TURBULENCE	0.023	0.24
FILE 2. OUT - POWER APPROACH, HEAVY TURBULENCE	0.055	0.58
FILE 3. OUT - MACH # = 0.6, 15000 FEET, MODERATE TURBULENCE	0.0014	0.01
FILE 4. OUT - MACH # = 0.6, 15000 FEET, HEAVY TURBULENCE	0.0028	0.03
FILE 5. OUT - MACH # = 0.7, 30000 FEET, MODERATE TURBULENCE	0.0025	0.03
FILE 6. OUT - MACH # = 0.7, 30000 FEET, HEAVY TURBULENCE	0.0047	0.05
FILE 7. OUT - MACH # = 1.5, 30000 FEET, MODERATE TURBULENCE	0.0024	0.03
FILE 8. OUT - MACH # = 1.5, 30000 FEET, HEAVY TURBULENCE	0.0048	0.05

1. BASED ON TWO 5.7HP MOTORS ACTUATING THE FLIGHT SURFACE WITH AN OVERALL ACTUATOR EFFICIENCY OF 83%.

FIGURE 2.3 ANALYSIS OF F-18 AILERON ACTUATOR FLIGHT DATA

MISSION PHASE	TOTAL TIME OF MISSION PHASE (MINUTES)	ACTUATOR POWER (%)	ALTITUDE (FEET)	MACH NUMBER
TAXI	--	--	--	--
STOL	0.5	85	5,000	0.25
CLIMB	7.0	50	25,000	0.50
CRUISE	20.0	5	45,00	0.50
COMBAT - PHASE I	14.0	65	30,000	0.50
- PHASE II	1.0	100	30,000	0.50
CRUISE	20.0	5	45,000	0.50
DESCENT	18.0	50	25,000	0.50
STOL	3.0	80	5,000	0.25

FIGURE 2.4 WORSE CASE EMA MISSION DUTY CYCLE

3.0 DEMONSTRATION REFLUX COOLER DESIGN SUMMARY

As a result of the trade studies completed during Phase I (see Chapter 5 discussion) Sundstrand makes the following recommendations for the demonstration reflux cooler design:

- Demonstration Motor - Modified National Launch System (NLS) induction motor. Modifications include removal of the resolver, replacement of the housing with a reflux cooler, and simplifications of the end plate and shaft.
- Working Fluid - 3M Company's fluorinated organic compound, FC-75.
- PCM - Acetamide.
- Heat Exchanger - Brazed, plate fin construction with alternating working fluid and PCM layers.

4.0 ANALYTICAL METHODS

4.1 SINDA Model Description

Sundstrand developed a nodal thermal model of an EMA incorporating a reflux cooler, using SINDA (Systems Improved Numerical Differencing Analyzer). The model includes all significant conductances between the motor (heat source) and ambient air (heat sink). Figure 5.1 illustrates the use of a reflux cooler for motor cooling and the heat transfer conductances separating the motor and ambient air. Conductances include boiling, condensation, convection across the motor air gap, conduction through the reflux cooler, interface contact conductances, conduction through the aircraft structure, heat spreading across the aircraft wing and convection to the ambient air. Figure 5.2 schematically illustrates the node and conductor network that models the heat rejection system.

The model calculates heat transfer areas within the cooler assuming a brazed plate fin heat exchanger construction, and requires the user to specify fin geometry and the generalized cooler geometry parameters illustrated in Figure 5.1. The model calculates all geometric parameters on a per unit length basis axially along the shaft, and requires user input data on a per unit length basis. In effect, the model assumes an infinitely long motor. This approach results in a more generalized modelling approach.

Using the input data and internally calculated data, the model estimates heat transfer coefficients on the working fluid side of the heat exchanger and calculates required conductance and capacitance values. This model does not perform a detailed thermal-hydraulic analysis of the reflux process, but estimates the boiling heat transfer coefficient using a pool boiling correlation and condensing heat transfer coefficient using a derivation for film condensation on a vertical flat plate. In result, the model estimates motor and cooler temperatures as a function of operating conditions, and performs both steady state and transient analysis. Sundstrand used the model to parametrically identify controlling heat transfer conductances, characterize the effects of cooler geometry, study the effects of using PCM, and select the working fluid and PCM.

4.2 Model Inputs/Defaults

Figure 5.3 presents the SINDA model input parameters and default values where applicable. Several of the parameters depend upon the analysis condition or the PCM selection, and do not have default values. As previously mentioned, the units on several of the parameters illustrate the modelling of the motor and cooler on a per unit length basis. In addition to the parameters illustrated in Figure 5.3, the model also uses working fluid property arrays, that depend upon the fluid selection, in order to estimate heat transfer coefficients on the fluid side of the heat exchanger.

Several of the motor input parameters presented in Figure 5.3 reflect the National Launch System (NLS) induction motor design that Sundstrand originally proposed as the demonstration motor for the program. During the trade studies Sundstrand evaluated the effects of motor types including induction motors, switched reluctance motors and brushless DC motors. For these motor trades the study relied upon the NLS induction motor finite difference model, but varied the loss distributions within the rotor and stator as a function of the type of motor. Varying the motor finite difference motor model would have required detailed design activities for each of the three types, which was beyond the scope of the program. Figure 5.4 presents the distribution of losses used for the trade studies. These distributions result from Sundstrand's motor design experience.

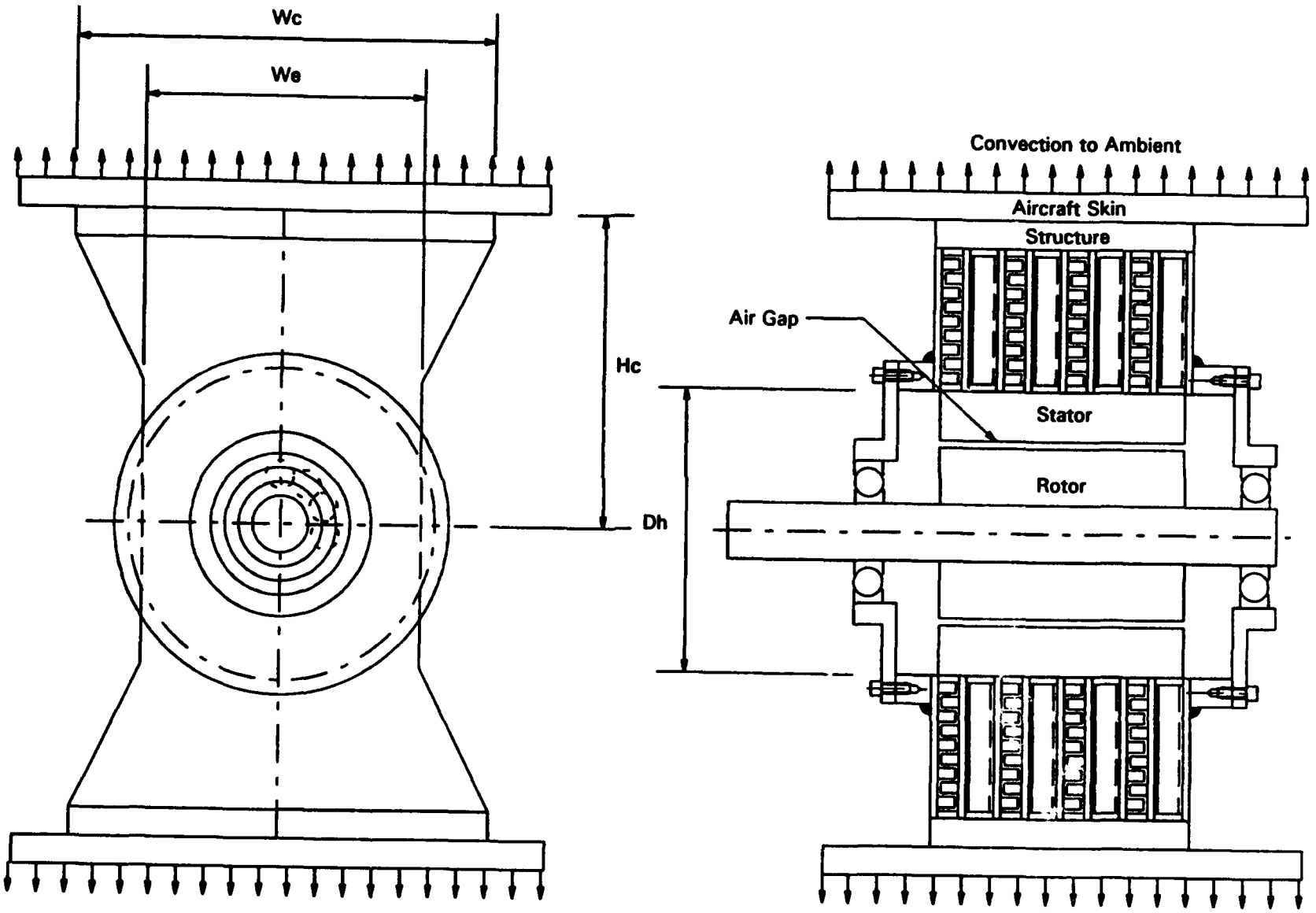

Figure 4.1 Passive Cooling Concept

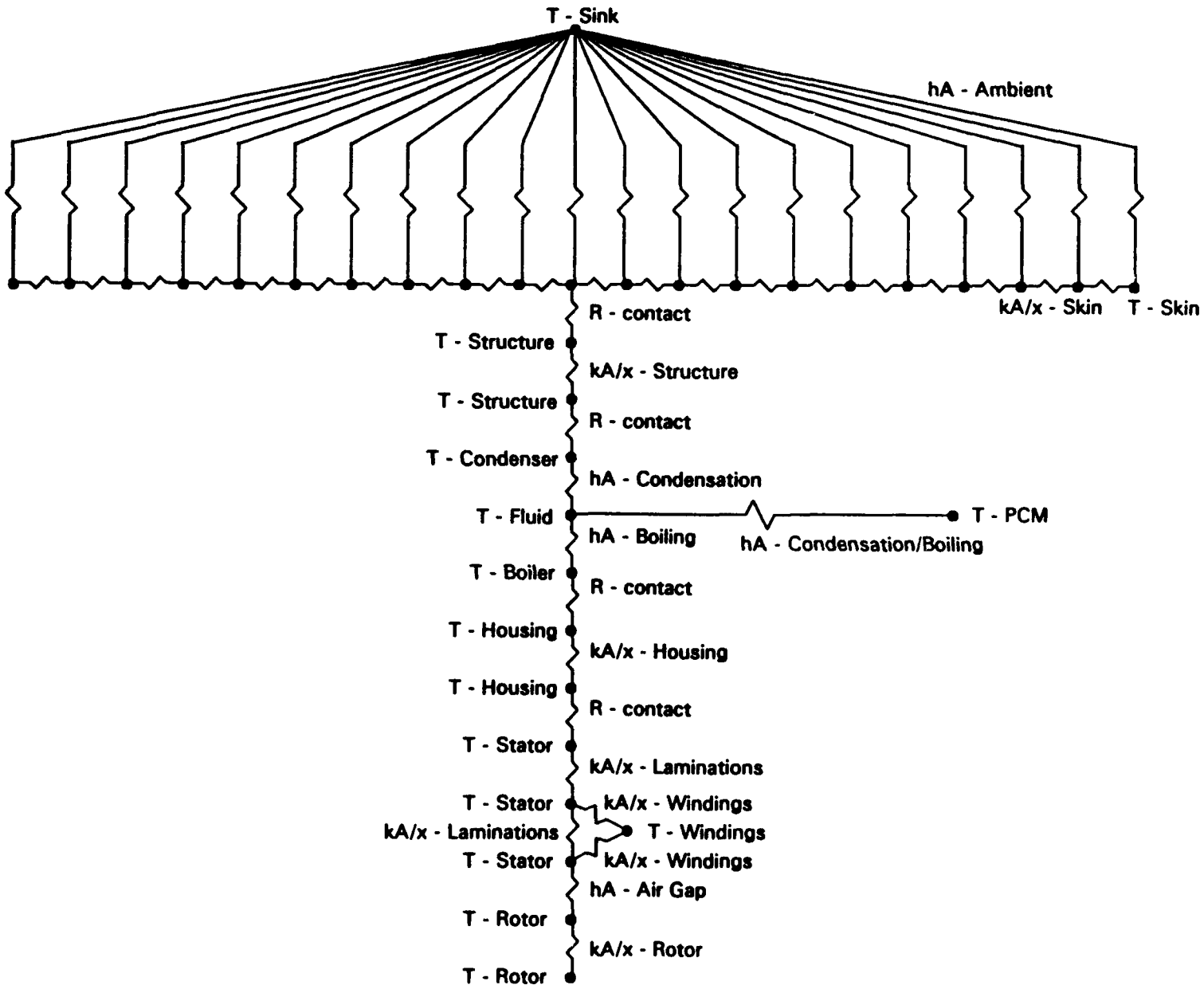

Figure 4.2 SINDA Model Schematic

	Defaults
Ambient Boundary Conditions	
Sink temperature	(parameter)
Ambient heat transfer coefficient	(variable)
Motor air gap heat transfer coefficient	(variable)
Geometry Data	
Motor Geometry:	
Housing OD	4.25 in.
Stator OD	3.75 in.
Rotor OD	2.25 in.
Cooler Generalized Geometry Ratios:	
Structure width to motor OD (Ws/Dh)	3.0
Condenser width to motor OD (Wc/Dh)	3.0
Evaporator width to motor OD (We/Dh)	2.0
Cooler height to motor OD (Hc/Dh)	1.0
Aircraft Skin:	
Aircraft skin thickness	0.050 in.
Plate Fin Geometry:	
Fin thickness	0.010 in.
Fin count	10.0 fins/in.
Fin length	0.25 in.
Fraction of cooler occupied by working fluid (remainder occupied by PCM)	0.50
Conductance/Capacitance Data	
Aircraft Structure:	
Thickness	0.75 in.
Density (aluminum)	0.098 lbm/in^3
Specific heat	0.23 Btu/lbm-°F
Thermal conductivity	100.0 Btu/hr-ft-°F
Motor Housing:	
Capacitance	0.0732 Btu/°F/in.
Conductance	418.3 Btu/hr-°F/in.

FIGURE 4.3 SINDA MODEL INPUTS/DEFAULTS

	Defaults
Motor Stator:	
Lamination capacitance	0.142 Btu/°F/in.
Windings capacitance	0.0906 Btu/°F/in.
Lamination conductance (OD to core)	89.43 Btu/hr-°F/in.
Lamination conductance (core to ID)	10.89 Btu/hr-°F/in.
Winding conductance (OD to core)	20.2 Btu/hr-°F/in.
Winding conductance (core to ID)	20.2 Btu/hr-°F/in.
Motor Rotor:	
Capacitance	0.0936 Btu/°F/in.
Conductance	160.4 Btu/hr-°F/in.
Material Properties	
Aircraft Skin:	
Density (aluminum)	0.098 lbm/in^3
Specific heat	0.23 Btu/lbm-°F
Thermal conductivity	100.0 Btu/hr-ft-°F
Cooler:	
Density (aluminum)	0.098 lbm/in^3
Specific heat	0.23 Btu/lbm-°F
Thermal conductivity	100.0 Btu/hr-ft-°F
Phase Change Material Data	
Transition temperature	
Heat of transition	
Density	
Specific heat	
Contact Conductances	
Aircraft skin to structure	2000.0 Btu/hr-ft^2-°F
Aircraft structure to cooler	2000.0 Btu/hr-ft^2-°F
Cooler to motor housing	2000.0 Btu/hr-ft^2-°F
Motor housing to stator	2000.0 Btu/hr-ft^2-°F
Motor Performance Data	
Maximum shaft power	6.19 hp/in.
Fractional power	
Motor efficiency	0.90
Fraction of losses in rotor laminations	(variable)
Fraction of losses in rotor windings	(variable)
Fraction of losses in stator	(variable)

FIGURE 4.3 (CONT'D) SINDA MODEL INPUTS/DEFAULTS

TYPE OF MOTOR	STATOR LAMINATIONS %	STATOR WINDINGS %	ROTOR %
SWITCHED RELUCTANCE	37.28	51.12	11.60
INDUCTION	25.13	49.74	25.13
BRUSHLESS DC	33.41	66.34	0.25

FIGURE 4.4 MOTOR LOSS DISTRIBUTIONS (PERCENTAGE OF TOTAL LOSSES)

4.3 Correlations

Analysis of the EMA cooling approach required the use of a number of correlations either calculated directly within the model or used to estimate model input data. The EMA cooler analysis required correlations for the following parameters:

- Ambient heat transfer coefficient.
- Viscous boundary layer heating.
- Air gap heat transfer coefficient.
- Boiling heat transfer coefficient.
- Condensation heat transfer coefficient.
- Fin efficiency.

The paragraphs which follow present the correlations selected for calculations.

<u>Ambient Heat Transfer Coefficient</u>

Correlation for turbulent flow over a flat plate (reference [17]):

$$Nu_L = Pr^{1/3} (0.037Re^{0.8} - 850)$$

where:

Nu_L	= Nusselt number.
Pr	= Prandtl number.
Re	= Free stream Reynolds number.
L	= Characteristic length.
	= 3.0 ft.

<u>Viscous Boundary Layer Heating</u>

Correlation for viscous heating within the boundary layer (reference [18]):

$$T_{BL} = T_\infty + CU_\infty^2/2C_p$$

where:

T_{BL}	= Fluid temperature within the boundary layer (used as the sink temperature).
T_∞	= Freestream temperature.
U_∞	= Freestream velocity.
C_p	= Fluid specific heat.
C	= $Pr^{1/2}$ - laminar boundary layer.
	= $Pr^{1/3}$ - turbulent boundary layer.

Air Gap Heat Transfer Coefficient.

Rotating, enclosed cylinder with zero axial flow (reference [19]):

$Nu = 1.00$ $\quad Ta<41$

$Nu = 0.106Ta^{0.63}Pr^{0.27}$ $\quad 41<Ta<100$

$Nu = 0.193Ta^{0.5}Pr^{0.27}$ $\quad 100<Ta$

where:

Nu	=	Nusselt number.
	=	Ub/k
Ta	=	Taylor number.
	=	$(\rho\omega r_i b/\mu)(b/r_i)$
b	=	Radial clearance.
r_i	=	Rotor radius.
ρ	=	Fluid density.
ω	=	Rotational speed.
μ	=	Fluid viscosity.
k	=	Fluid thermal conductivity.

Boiling Heat Transfer Coefficient.

Nucleate pool boiling (reference [17]):

$$T_w - T_{sat} = C_{sf}(h_{fg}Pr^s/C_{pl})\{(q''/\mu_l h_{fg})[g_c\sigma/g(\rho_l - \rho_v)]^{0.5}\}^{0.33}$$

where:

T_w	=	Wall temperature.
T_{sat}	=	Saturation temperature.
C_{sf}	=	Fluid/surface factor.
	=	0.013 - applies to a number of fluid/surface combinations.
s	=	1.0 - water.
	=	1.7 - other fluids.
h_{fg}	=	Fluid heat of vaporization.
C_{pl}	=	Liquid specific heat.
q''	=	Heat flux.
μ_l	=	Liquid viscosity.
σ	=	Surface tension.
ρ_l	=	Liquid density.
ρ_v	=	Vapor density.

Condensation Heat Transfer Coefficient

Laminar film condensation on a vertical flat plate (reference [17]):

$$h = 0.943\{[\rho_l(\rho_l-\rho_v)gh_{fg}k_l^3]/[l\mu_l(T_{sat} - T_w)]\}^{1/4}$$

where:

- h = Heat transfer coefficient.
- k_l = Liquid thermal conductivity.
- l = Condensation length.
  = Equated to one quarter of the heat exchanger height.

Fin Efficiency.

Fin efficiency for a fin of constant cross section with an insulated tip (reference [17]). Model uses the fin efficiency correlation to approximate heat transfer within the plate fin structure of the heat exchanger:

$$\eta_f = \tanh(ml)/ml$$

where:

- m = $(hP/kA)^{1/2}$
- h = Convective heat transfer coefficient.
- P = Perimeter of fin.
- A = Cross sectional area of fin.
- l = Fin length.

5.0 TRADE STUDIES

5.1 Actuator Comparison

Figure 5.1 presents a comparison of actuator types and their requirements. This figure illustrates widely varying power levels and duty cycles dependent upon the type of actuator. Some actuators on aircraft experience very active duty cycles, while many operate for very brief periods with lengthy periods of inactivity. Characterization of actuator duty cycles presents one of the more difficult challenges to actuator designers, due to limited actuator flight data, and yet, duty cycle effects selection of the actuator cooling approach. Inactive actuators may not require any external means of cooling, due to significant thermal mass; actuators with very active and consistent duty cycles may require an external means of cooling; and active actuators with high, intermittent loads may require an external means of cooling coupled with PCM.

In addition, Figure 5.1 illustrates differences in the availability of heat sinks between types of actuators. The location of thrust vector control actuators provides easy access to aircraft fuel as a viable heat sink; whereas, the aircraft skin and ambient air serves as the most feasible heat sink for the majority of actuators.

Application of reflux cooling coupled with PCM depends upon:

- actuator power levels.
- actuator duty cycles.
- heat sink availability.

Given the varying requirements between actuator types and changing aircraft configurations (inherently unstable aircraft), application of the reflux cooling method requires evaluation on an individual actuator basis.

5.2 Steady State Analysis

5.2.1 Geometry/Design Considerations

The geometry/design analyses involved parametric studies of some of the parameters that affect overall cooler performance. These studies helped to identify those parameters that most dominate the overall heat transfer process and provided guidelines for defining the cooler geometry. The parameters studied included:

- Generalized cooler geometry (condenser width, evaporator width, cooler height)
- Fin stock fin count (fins/inch).
- Ambient heat transfer coefficient.
- Structure conductance.

Figures 5.2 through Figure 5.7 present results of the generalized cooler geometry (illustrated in Figure 4.1) parametric studies. These figures present the data in two forms; as actual temperatures, and as temperature differences for the primary conductances in the finite difference node/conductor network. The plots illustrating actual temperatures illustrate the effects of the parameters upon overall cooler

PARAMETER	SYSTEM					
	LEADING EDGE FLAPS	TRAILING EDGE FLAPS	RUDDER	STABILIZER	AILERONS	THRUST VECTOR CONTROL
HP (OPER)	1-7 HP					1-10
HP (PEAK)	17 HP		4 HP	10-12 HP	10-12 HP	15-20 HP
OPER LOAD	350 K IN-LB					80 K IN-LB
OPER RATE	25°/SEC		105°/SEC			40°/SEC
MOTOR SPEED	11,000 RPM					5,000 RPM
STALL TORQUE	500 K IN-LB		21,700 LB	43,100 LB	43,700 LB	140 K IN-LB
FREQ RESP	18 HZ @ 10%		20 HZ @ 5%	13.5 HZ @ 2%		8 HZ $\pm$5%
ACCEL/AXIS						20 G's
DUTY CYCLE	90% N.L.		$\frac{356}{8956}$ >50%	$\frac{356}{8956}$ >50%		ACTIVE DITHER
ORIENTATION	H	H	V	V	H	H
MOVE (Y/N)	NO	NO	NO	YES	YES	YES
HEAT SINK	WING SKIN				WING SKIN	FUEL
AMB TEMP	-65 TO -275°					500-700°F

FIGURE 5.1 ACTUATOR COMPARISON

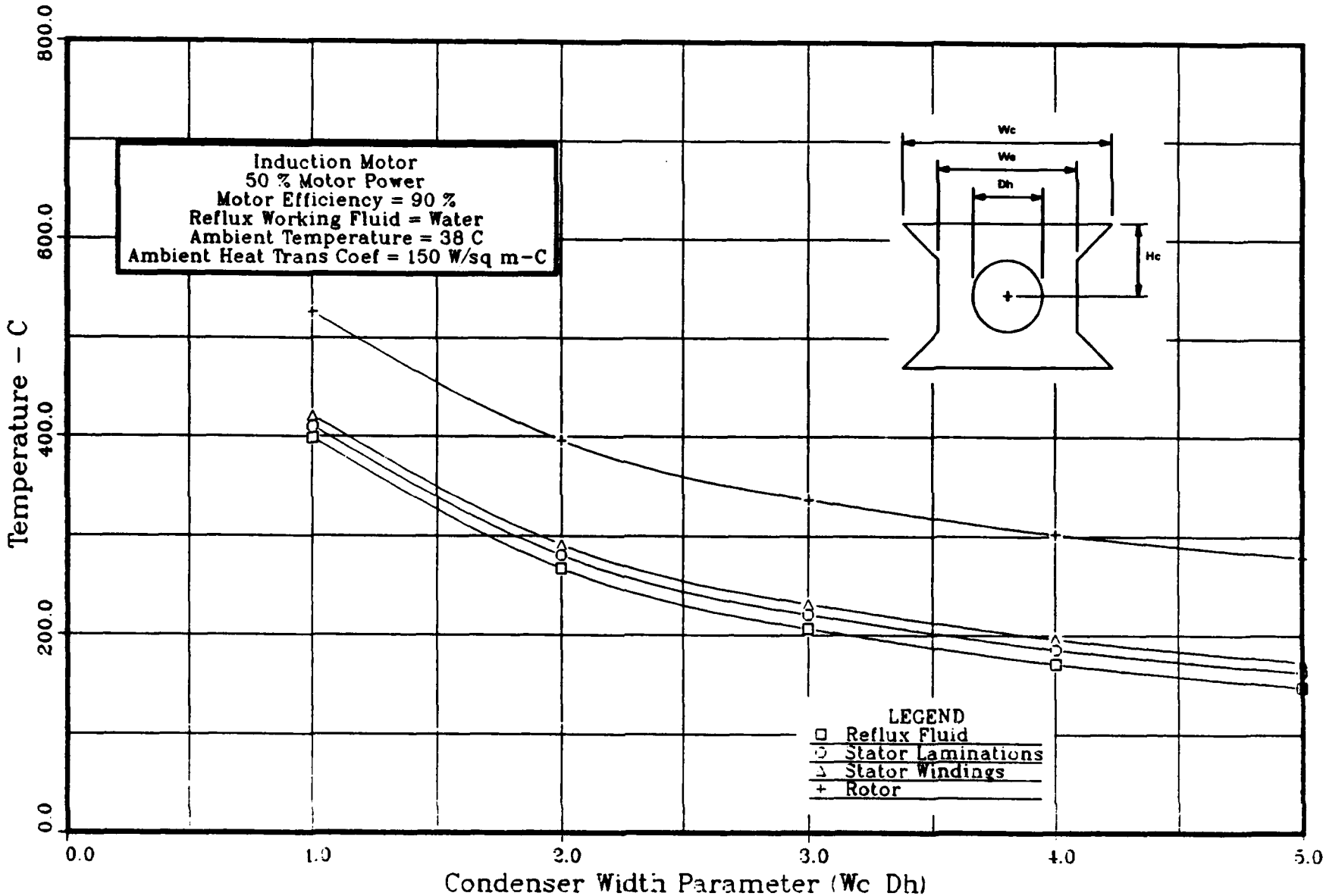

FIGURE 5.2 ADVANCED ACTUATOR COOLING
Steady State Temperature vs Condenser Width Parameter

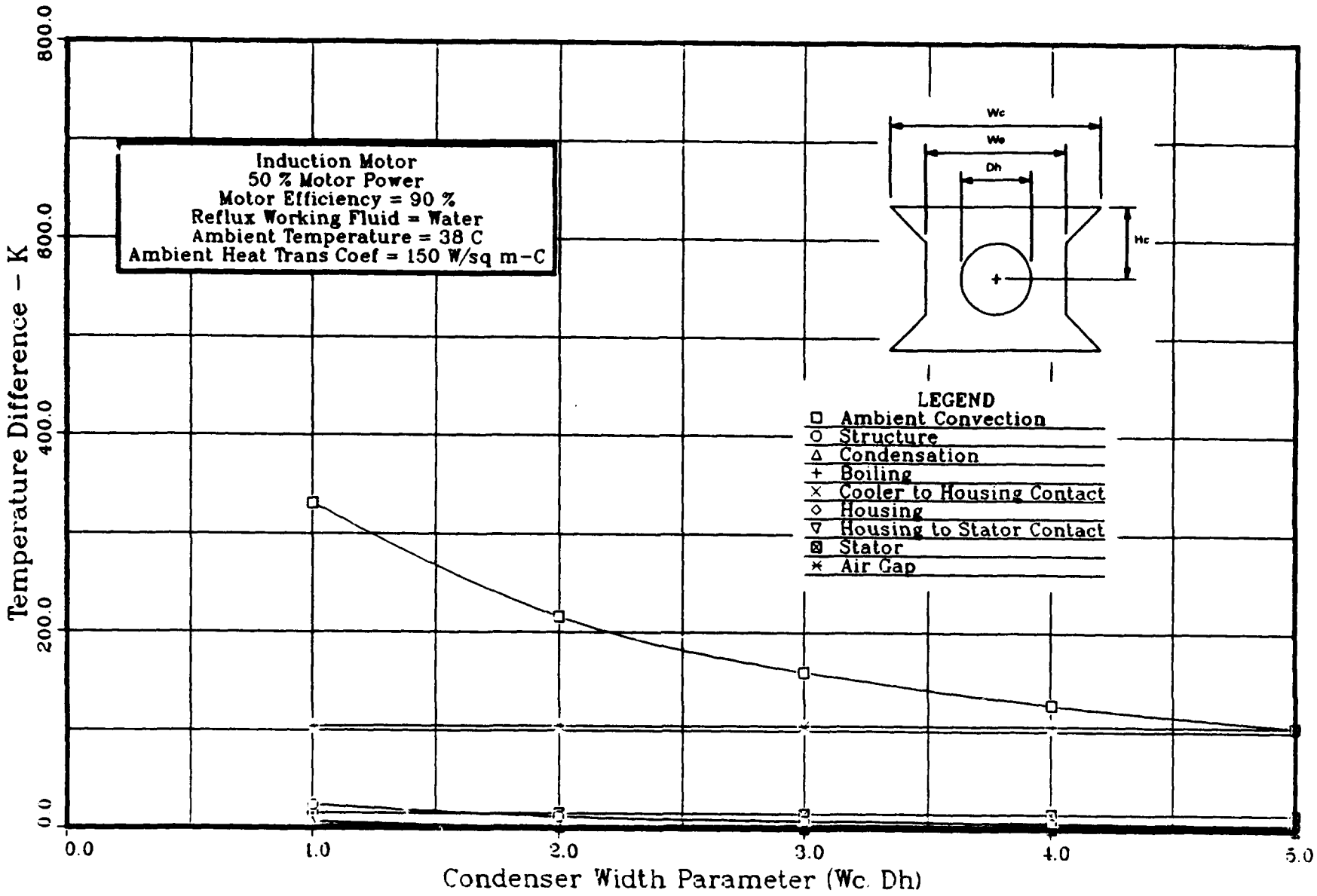

FIGURE 5.3 ADVANCED ACTUATOR COOLING
Steady State Temp. Differences vs Condenser Width Parameter

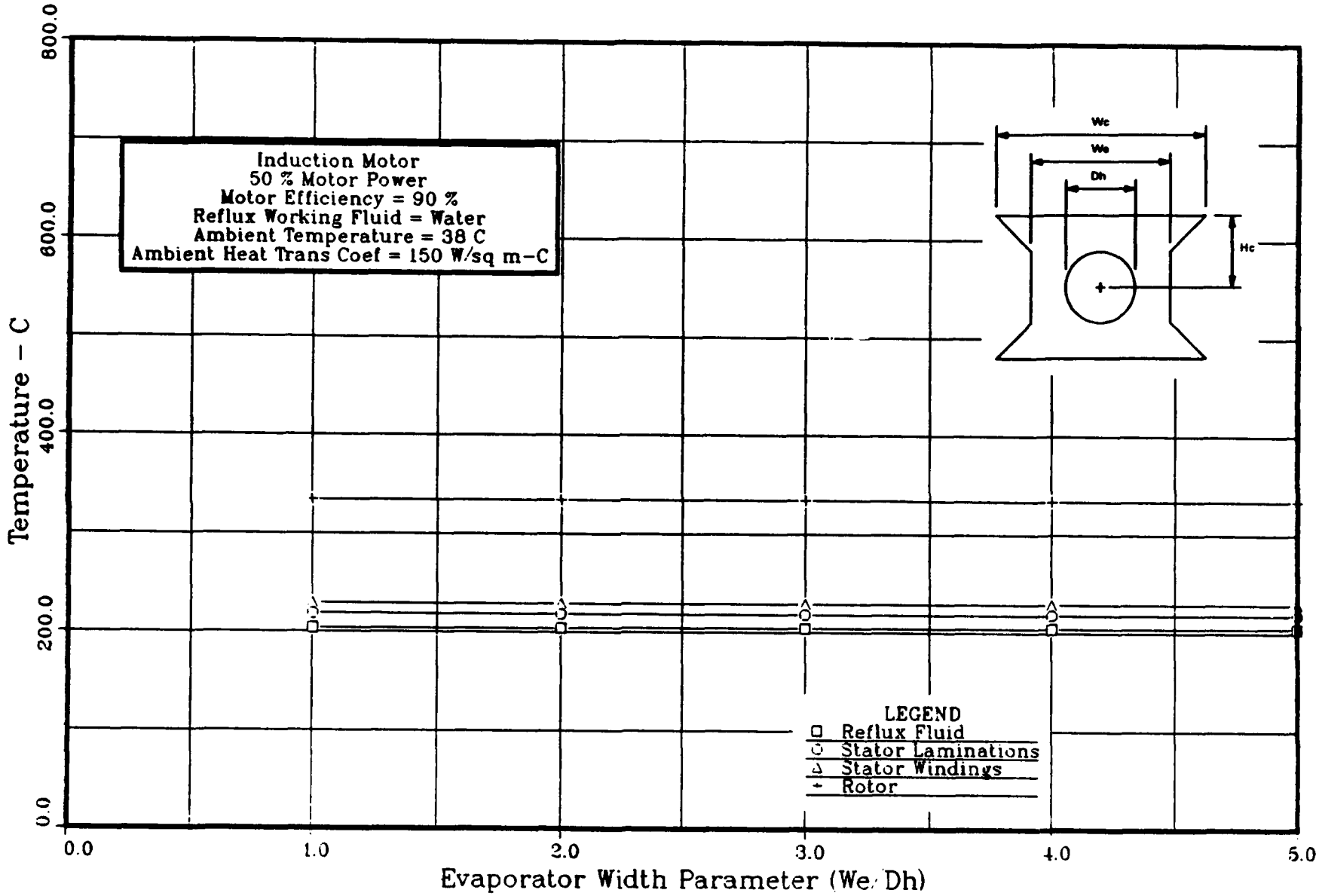

FIGURE 5.4 ADVANCED ACTUATOR COOLING
Steady State Temperature vs Evaporator Width Parameter

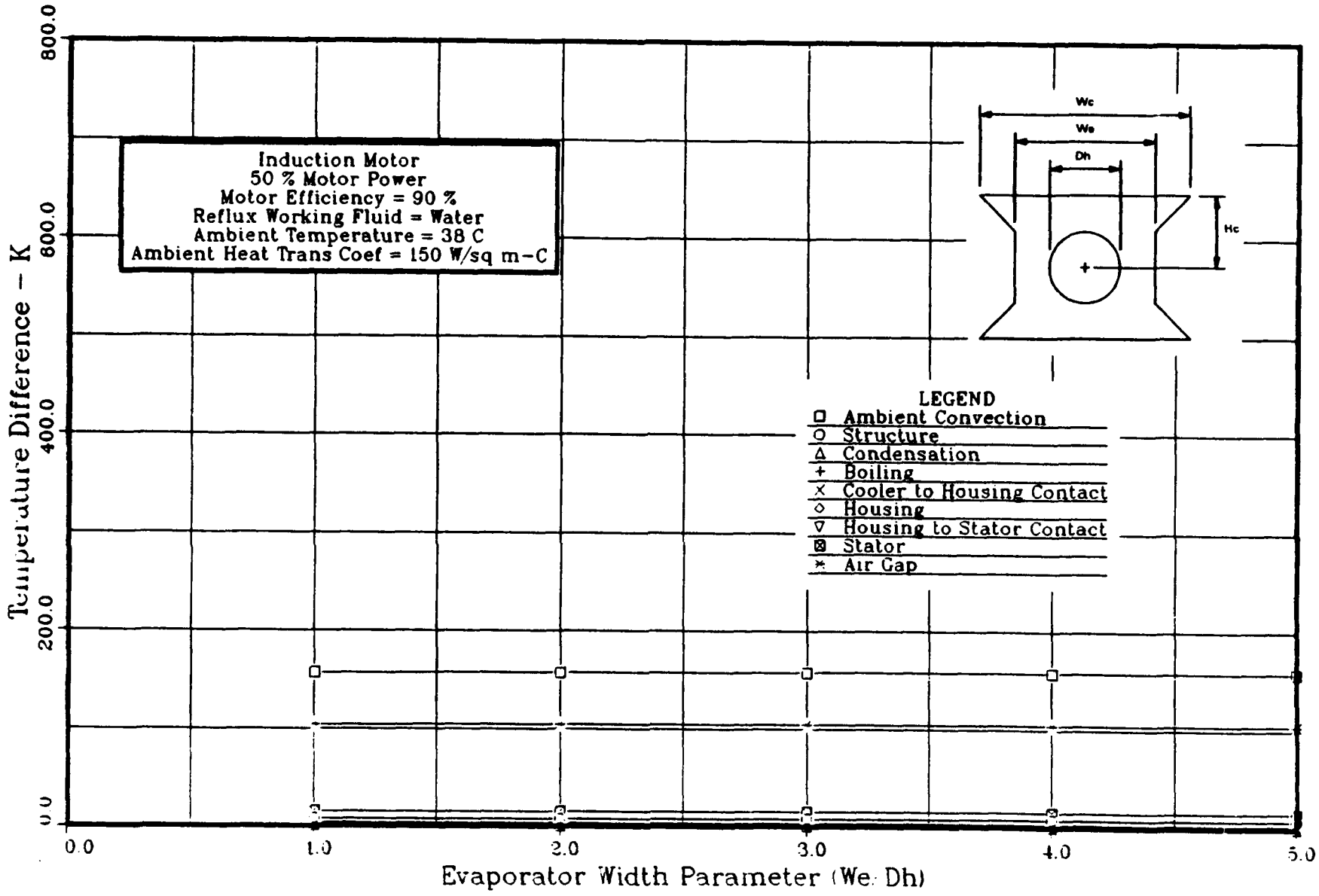

FIGURE 5.5 ADVANCED ACTUATOR COOLING
Steady State Temp. Differences vs Evaporator Width Parameter

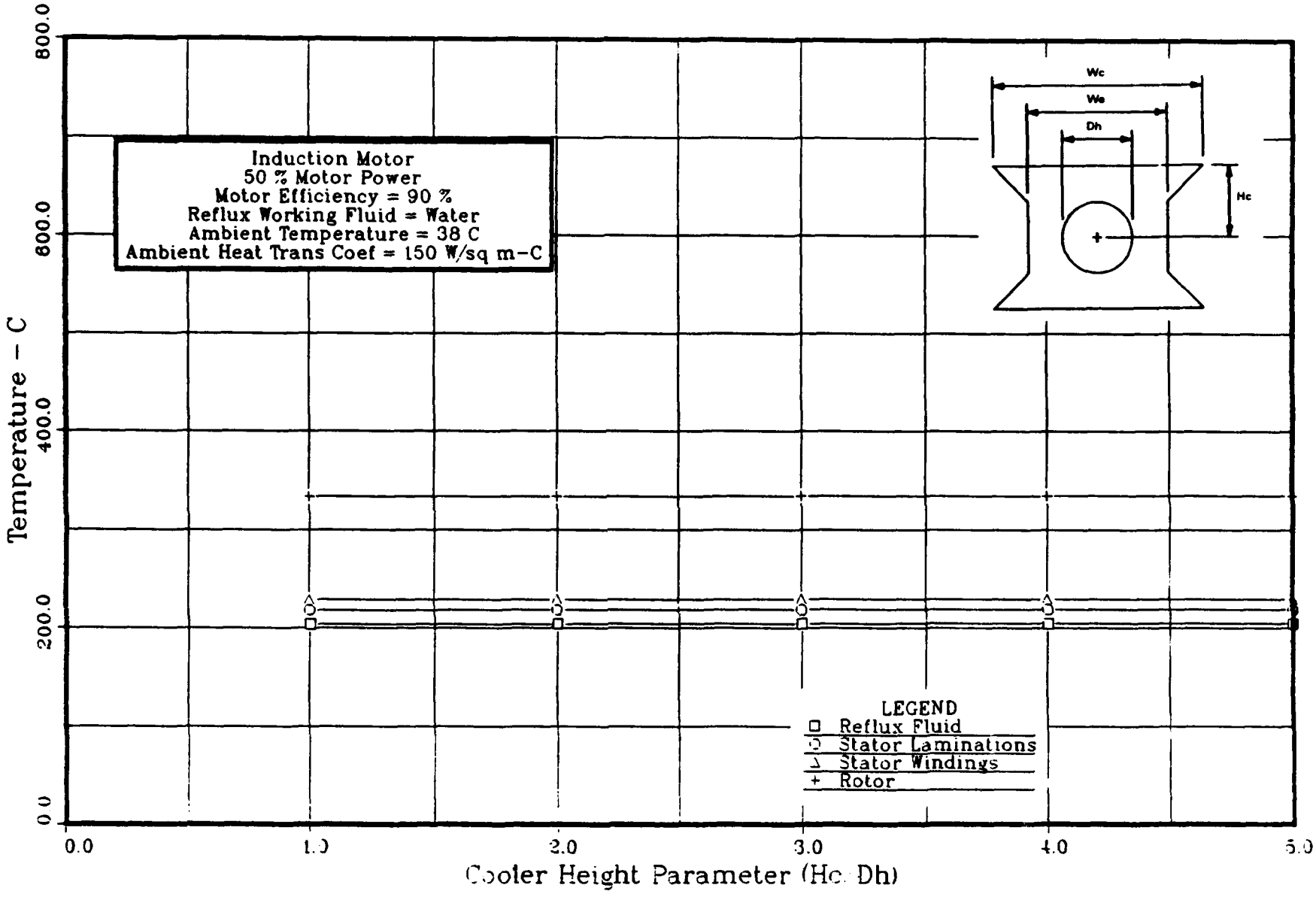

FIGURE 5.6 ADVANCED ACTUATOR COOLING
Steady State Temperature vs Cooler Height Parameter

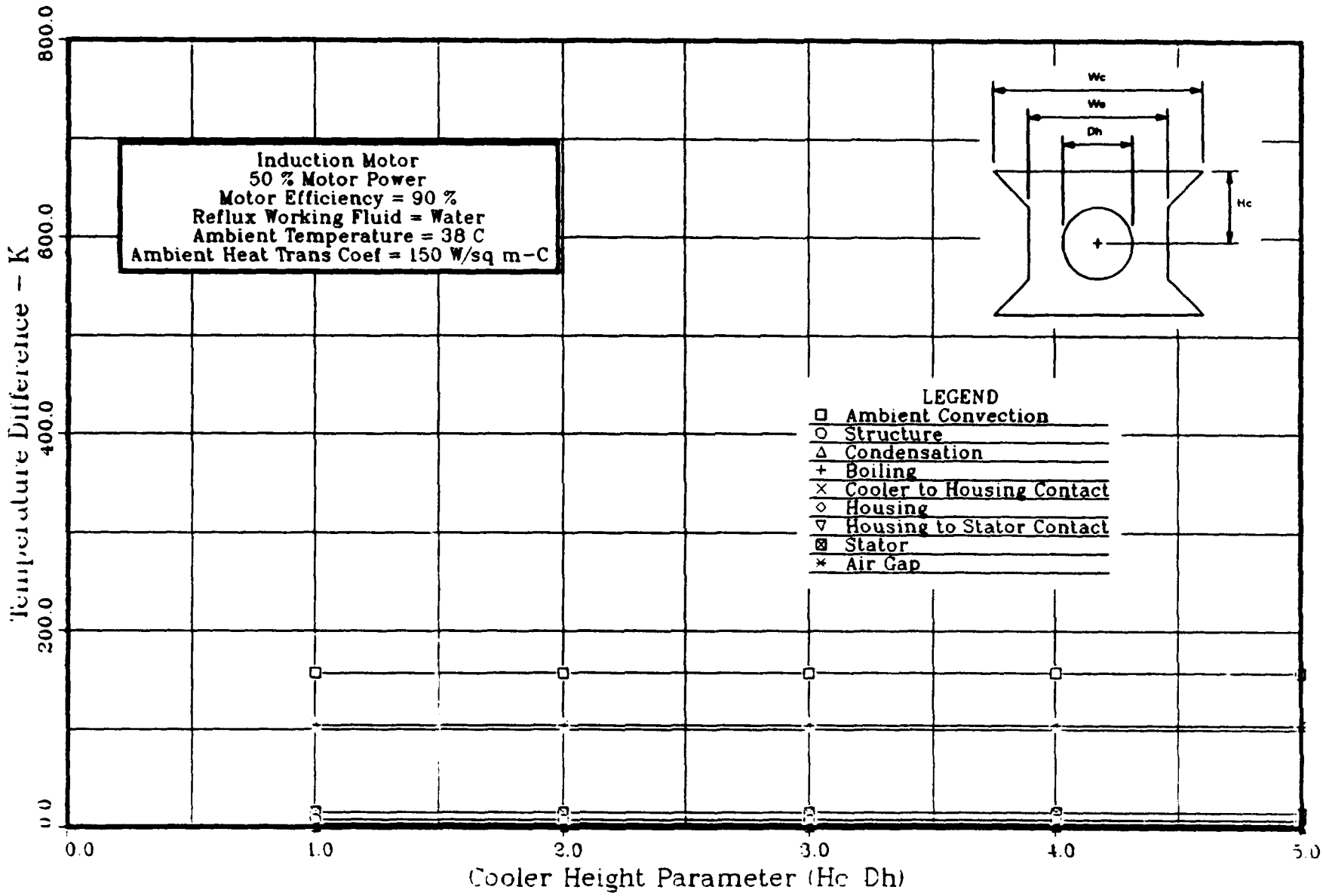

FIGURE 5.7 ADVANCED ACTUATOR COOLING
Steady State Temp. Differences vs Cooler Height Parameter

performance, while the temperature difference plots help identify the controlling conductances in the overall heat transfer process. Similarly, Figures 5.8 and 5.9 present the effects of fin stock fin counts upon cooler performance and Figures 5.10 and 5.11 present the effects of ambient heat transfer coefficient.

Additionally, Figures 5.12 through 5.15 present the effects of structure conductance studied in two forms. Figures 5.12 and 5.13 present temperatures and temperature differences as a function of conductance value, and Figures 5.14 and 5.15 present temperatures and temperature differences as a function of the thickness of an aluminum plate separating the cooler and aircraft skin. As a point of reference, reference [24] measured a structural conductance of 21 W/^{0}C/m for a heat pipe attached to a wing strut on an F/A-18 wing section.

Based upon Figures 5.2 through 5.15 one can make the following observations:

- The controlling heat transfer conductances in the overall heat transfer process include ambient convection and convection across the air gap.
- Structure conductance becomes significant below values of 30 Btu/hr-^{0}F/in.
- The condenser width parameter dominates the other geometry parameters as a controlling conductance due to the dominance of ambient convection.

All of these observations suggest that successful implementation of a reflux cooler requires the minimization of the heat transfer resistances separating the cooler and aircraft skin, and a maximization of the effective aircraft skin area used for actuator cooling.

5.2.2 Mission Considerations

Mission considerations involved the parametric study of aircraft operating conditions that affect cooler performance, including altitude and aircraft speed (Mach number). These studies included the effects of altitude and Mach number upon ambient temperature and pressure, aerodynamic heating within the boundary layer, ambient convection coefficient, and the motor air gap heat transfer coefficient. Figures 5.16 through 5.27 present temperatures and temperature differences for the three types of motors studied at Mach numbers of 0.6 and 1.5 over altitudes ranging from sea level to 60,000 feet.

Based on Figures 5.16 through 5.27 one can make the following observation:

- Motor temperatures increase with increasing altitude, despite decreasing ambient temperature, due to the dominance of ambient convection.

5.2.3 Type of Motor

Figure 5.28 selectively presents rotor temperature for the three motor types from the data presented in the previous section. This plot illustrates the differences in rotor temperature for the three motors due to differences in rotor losses. Larger temperature differences resulted in the rotors for the three motors than in the stators since a passive reflux cooling approach directly cools the stators but indirectly cools the rotors.

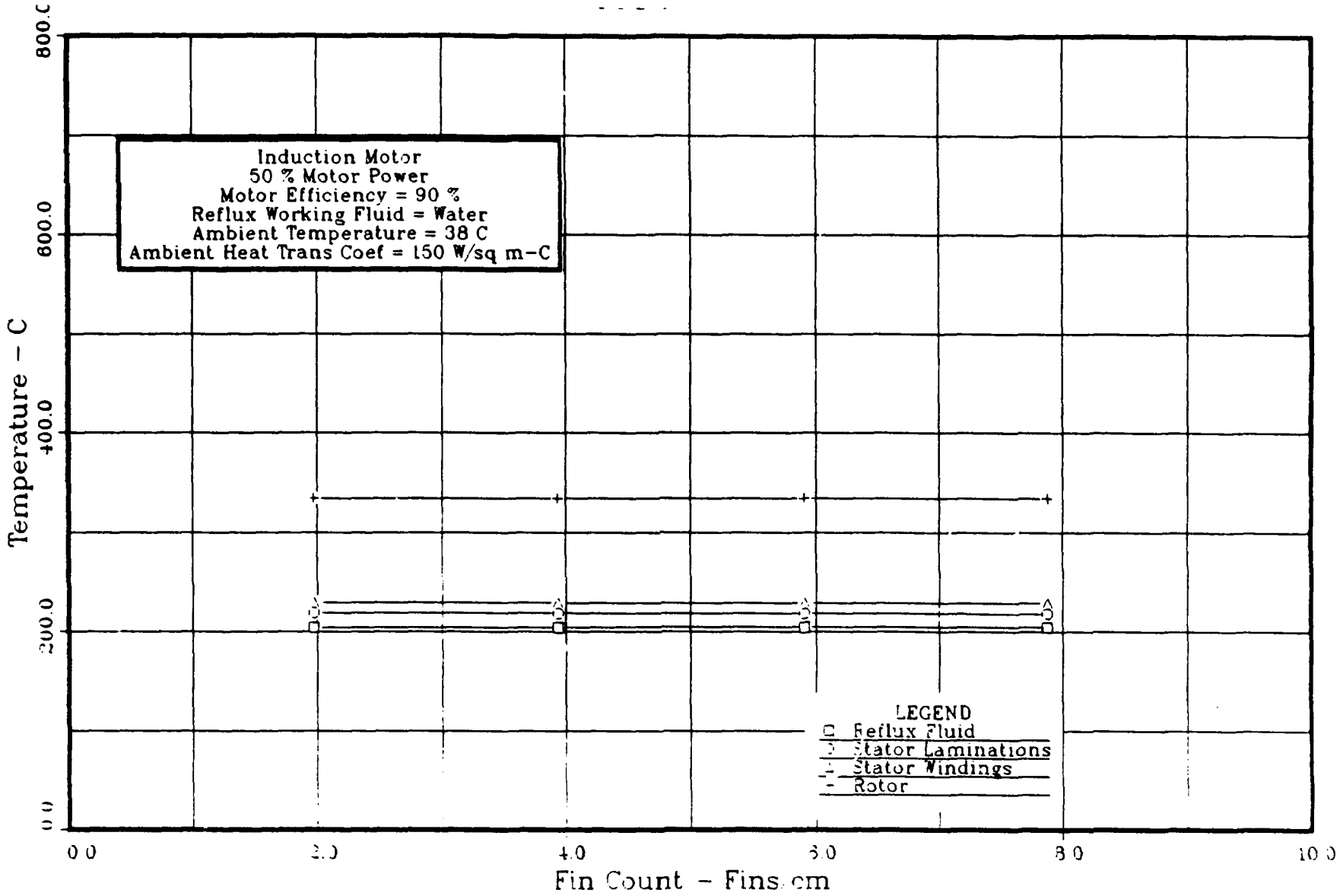

FIGURE 5.8 ADVANCED ACTUATOR COOLING
Steady State Temperature vs Fin Count

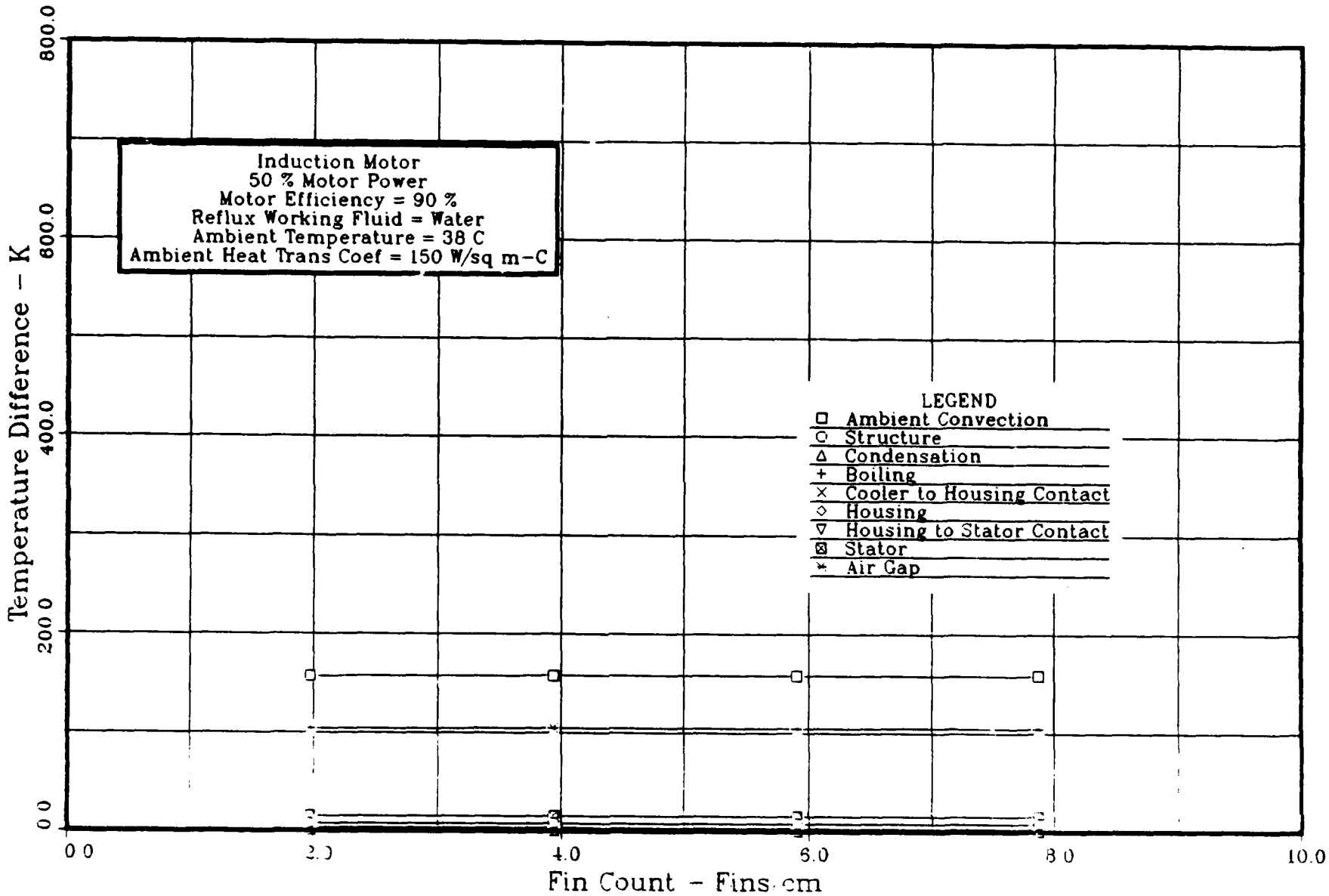

FIGURE 5.9 ADVANCED ACTUATOR COOLING
Steady State Temp. Differences vs Fin Count

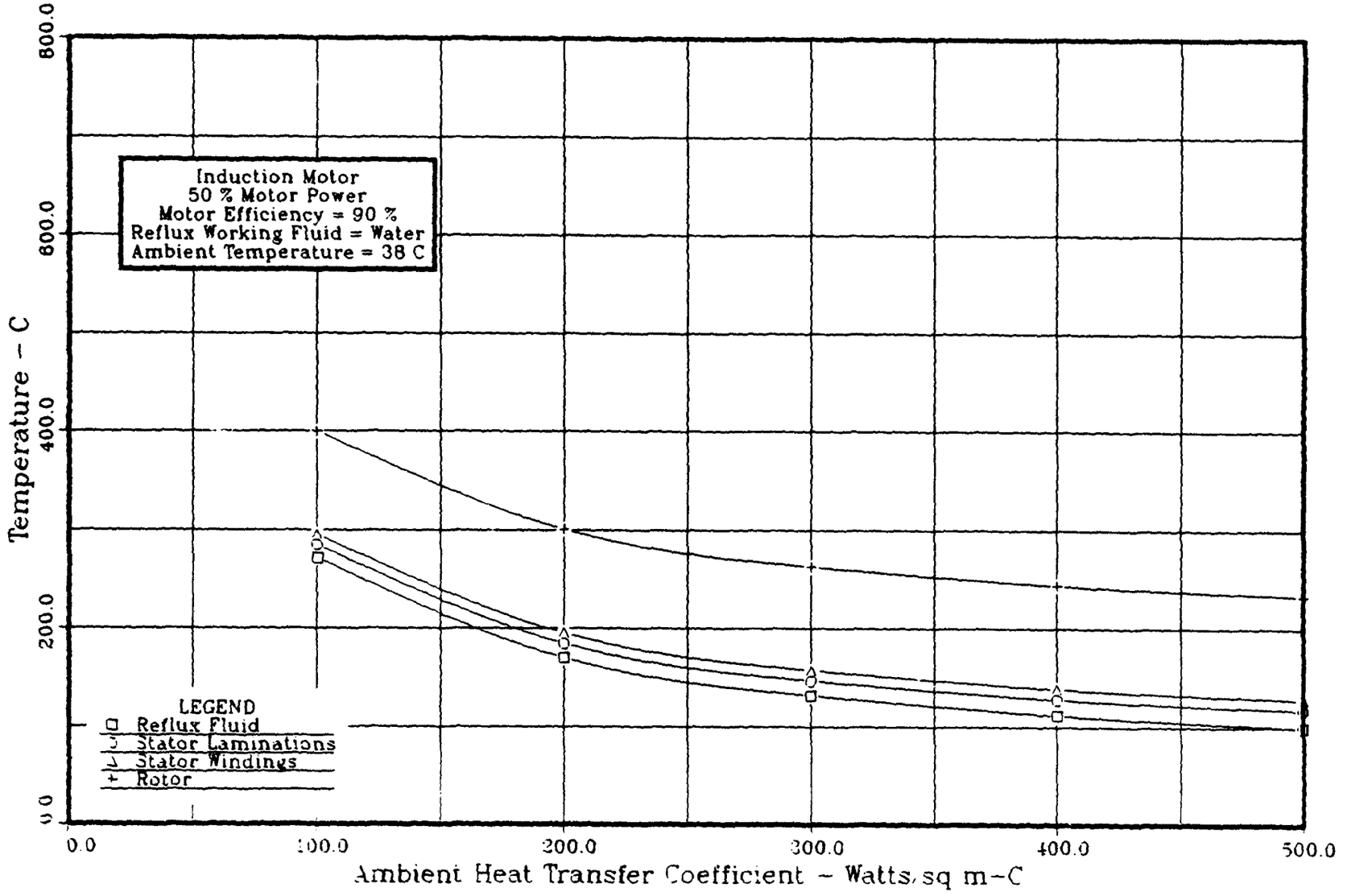

FIGURE 5.10 ADVANCED ACTUATOR COOLING
Steady State Temp vs Ambient Heat Transfer Coefficient

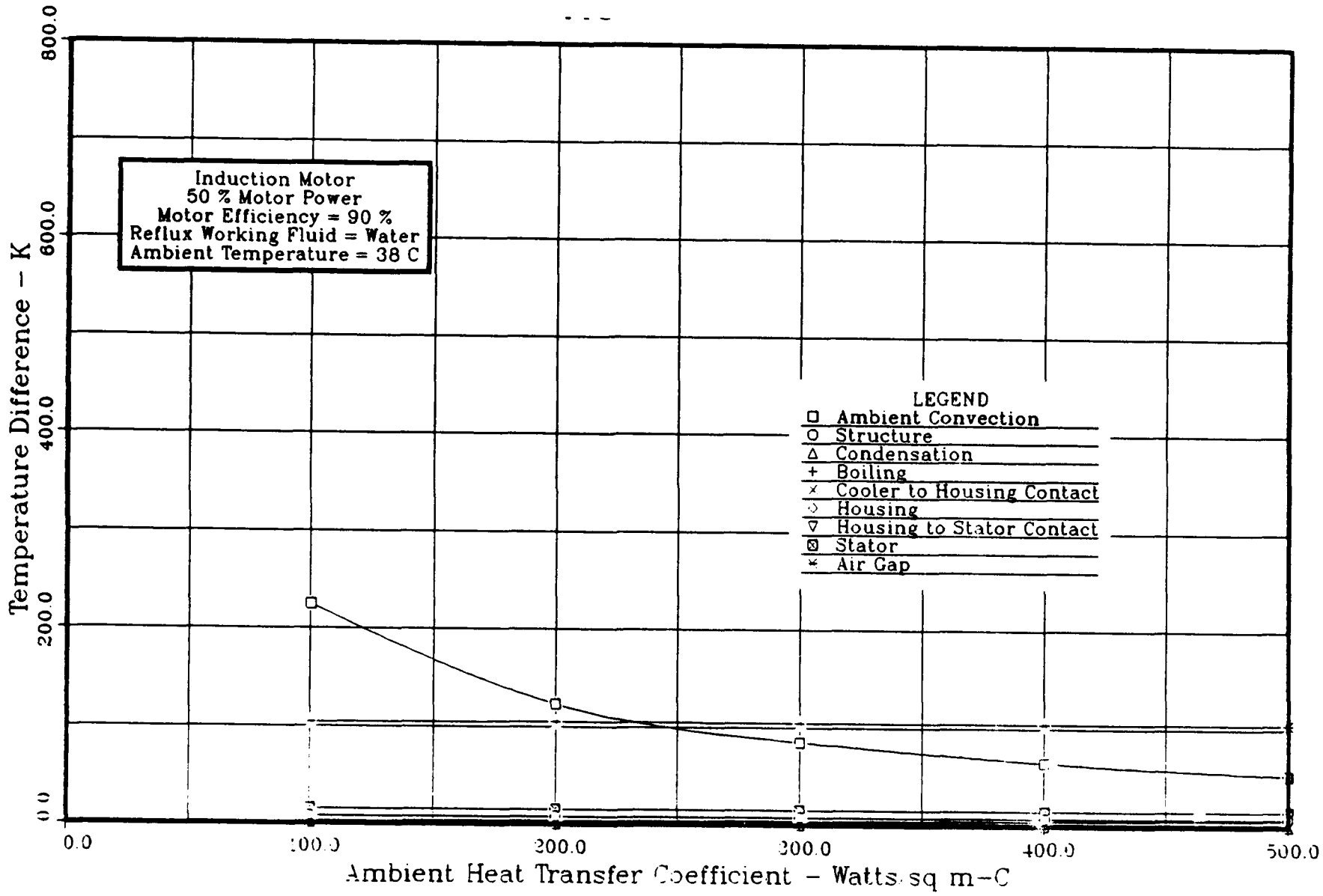

FIGURE 5.11 ADVANCED ACTUATOR COOLING
Steady State Temp Diff vs Ambient Heat Trans Coef

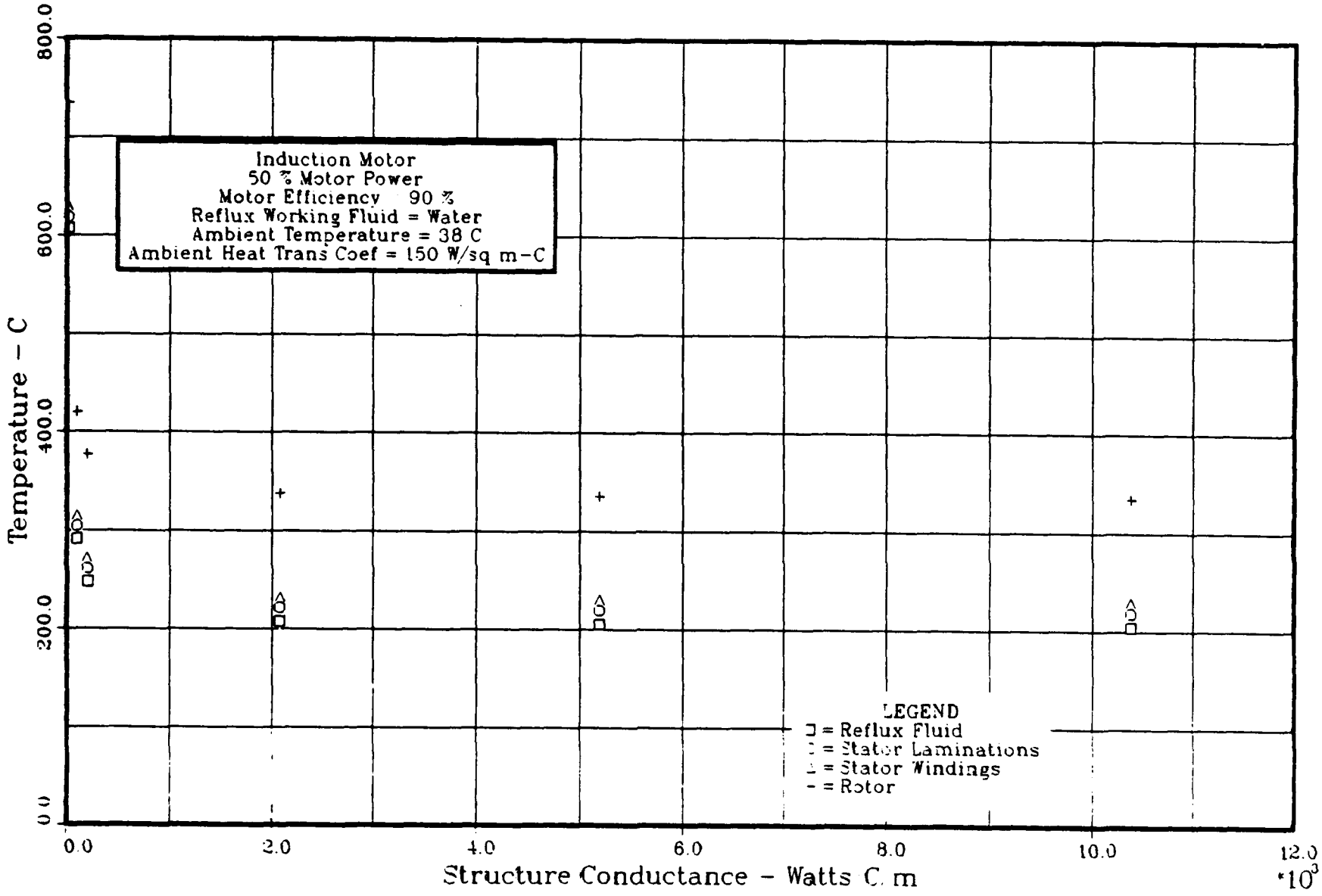

FIGURE 5.12 ADVANCED ACTUATOR COOLING
Steady State Temperature vs Structure Conductance

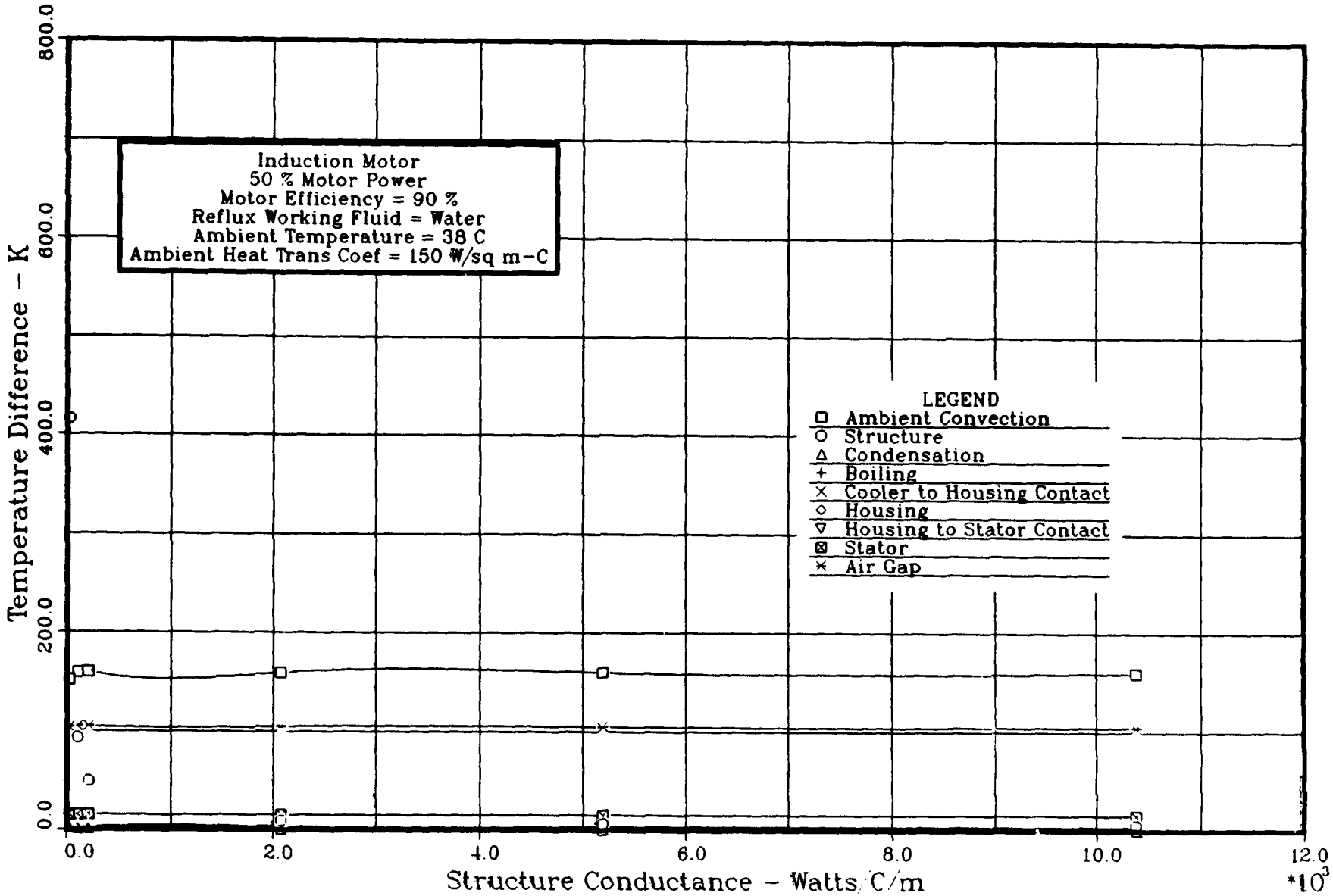

FIGURE 5.13 ADVANCED ACTUATOR COOLING
Steady State Temp Differences vs Structure Conductance

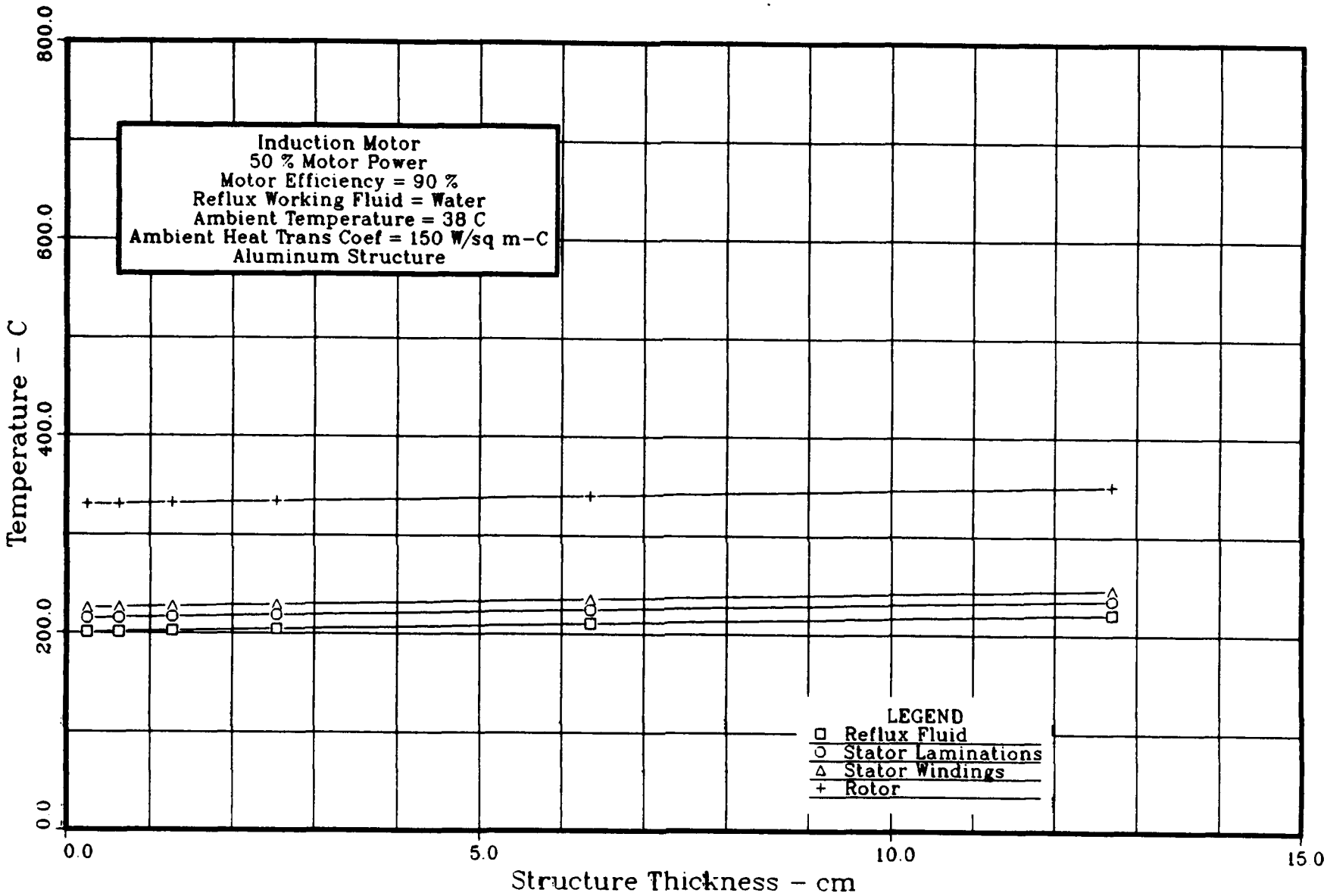

FIGURE 5.14 ADVANCED ACTUATOR COOLING
Steady State Temperature vs Structure Plate Thickness

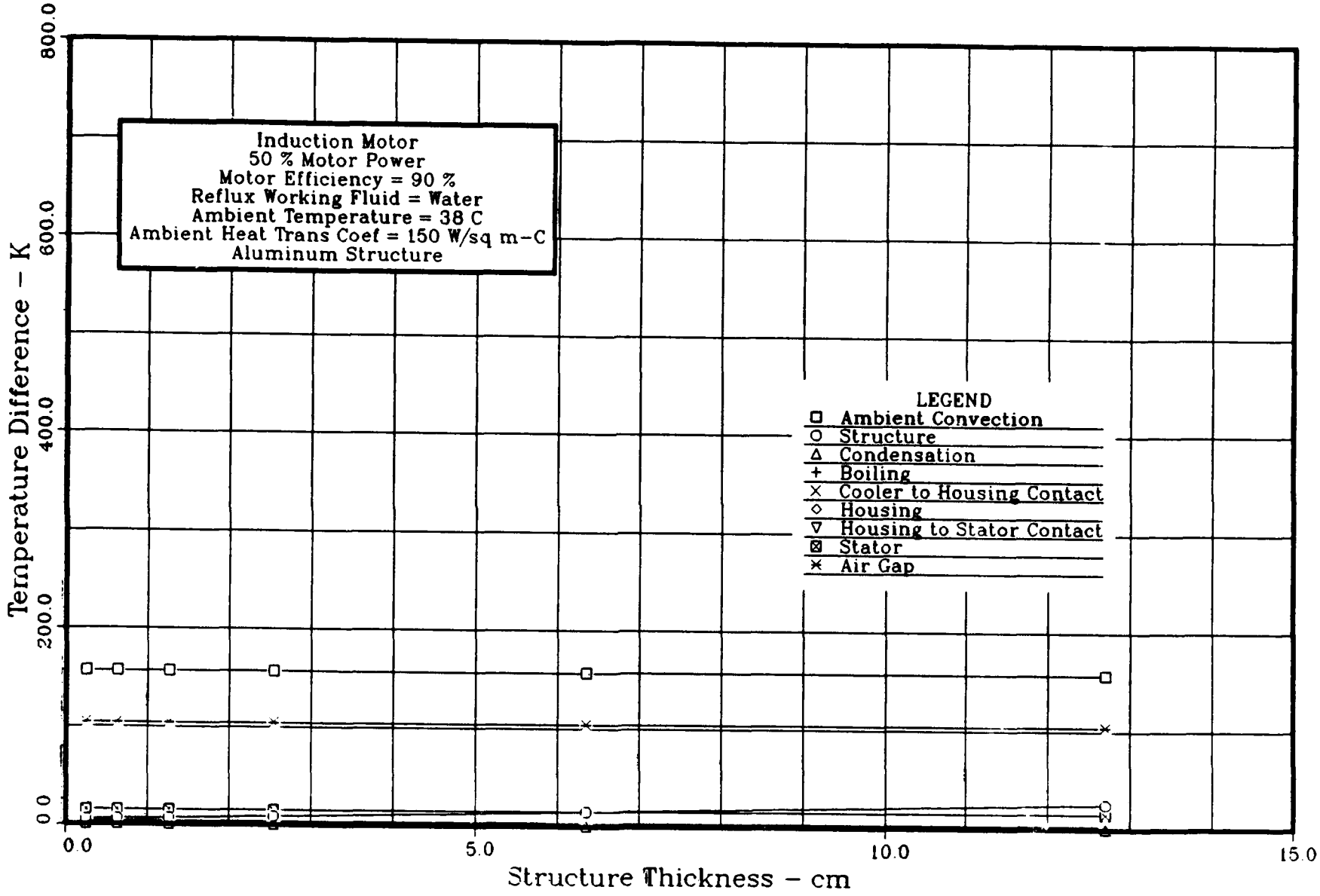

FIGURE 5.15 ADVANCED ACTUATOR COOLING
Steady State Temp Differences vs Structure Plate Thickness

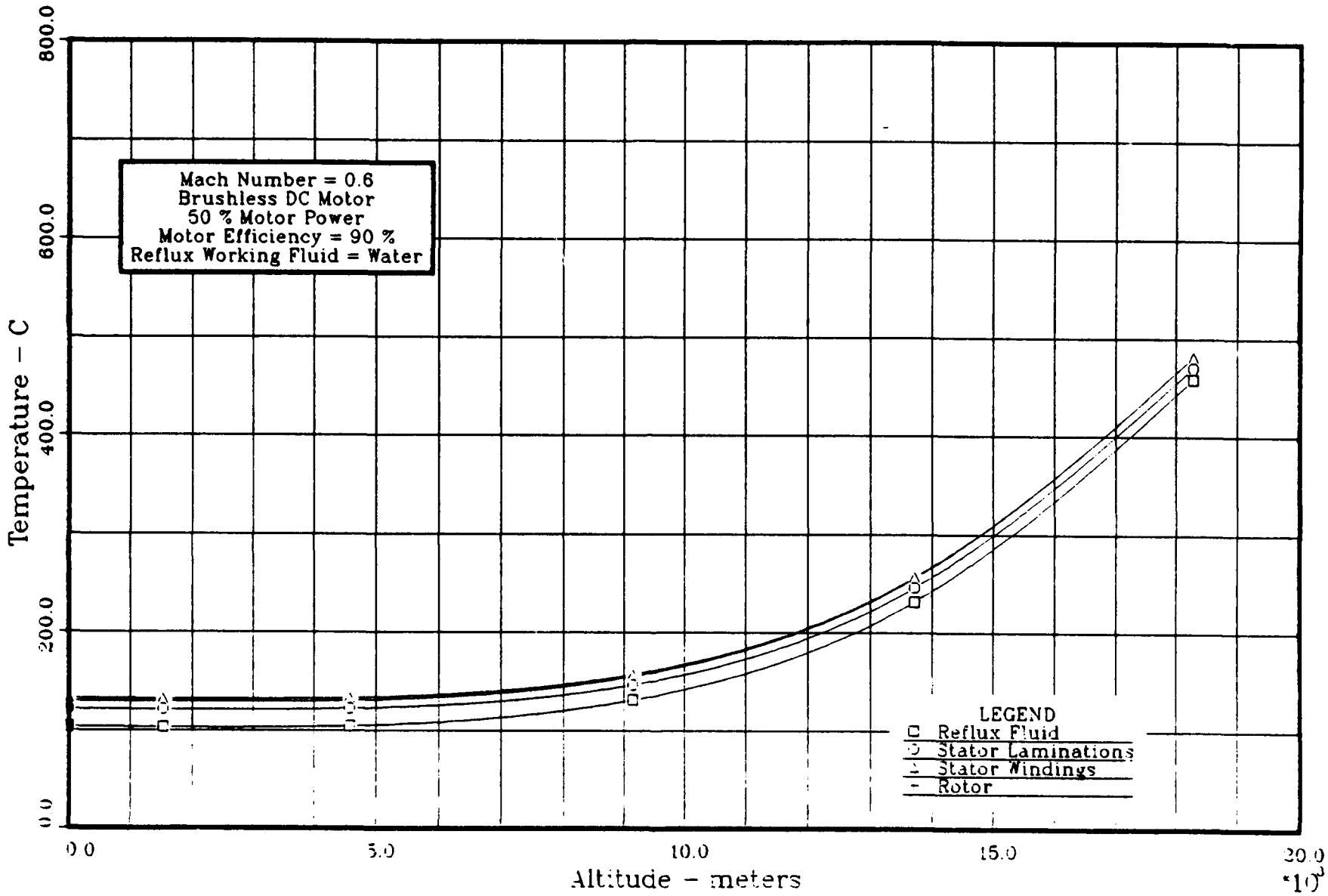

FIGURE 5.16 ADVANCED ACTUATOR COOLING
Steady State Temperature vs Altitude

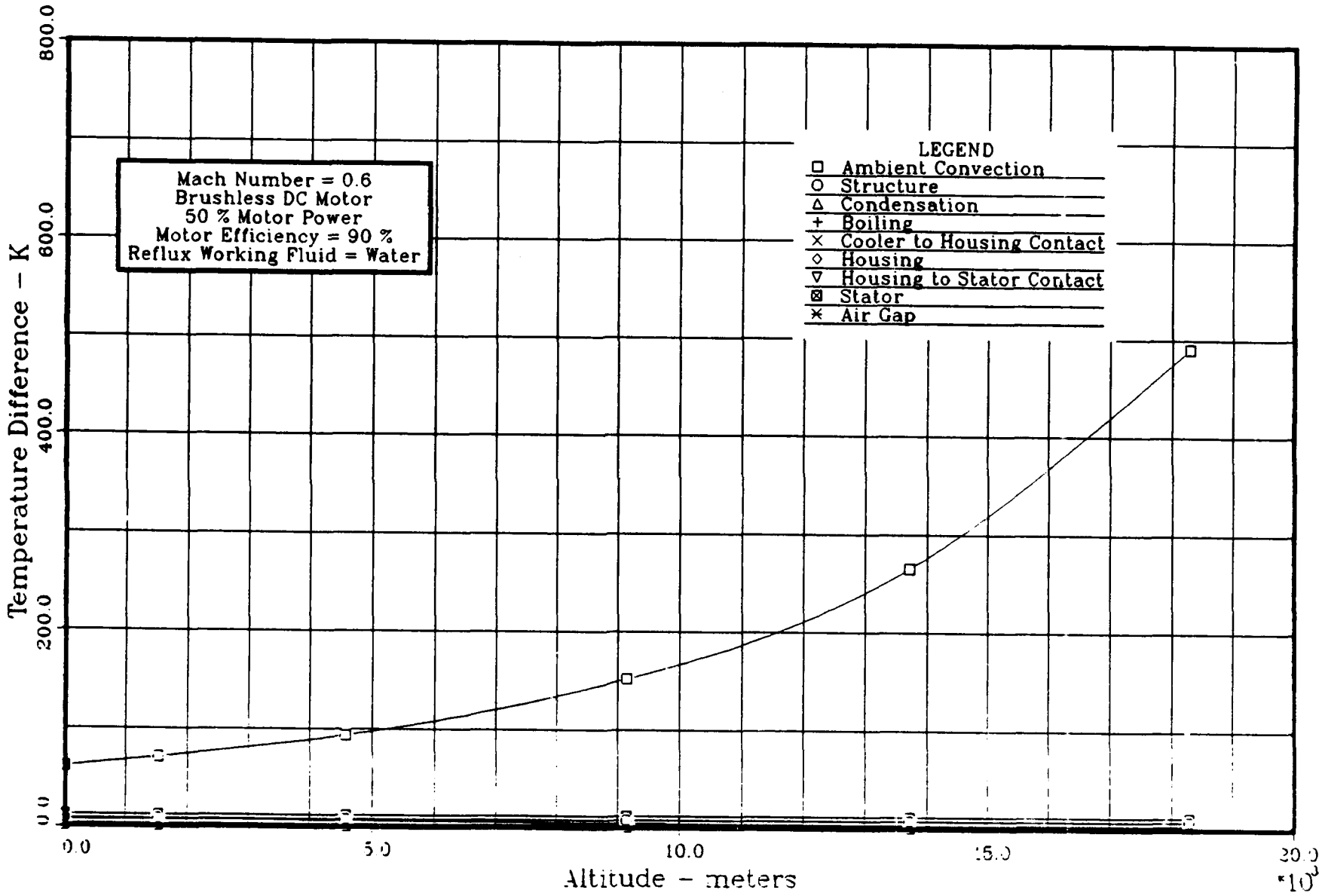

FIGURE 5.17 ADVANCED ACTUATOR COOLING
Steady State Temp Differences vs Altitude

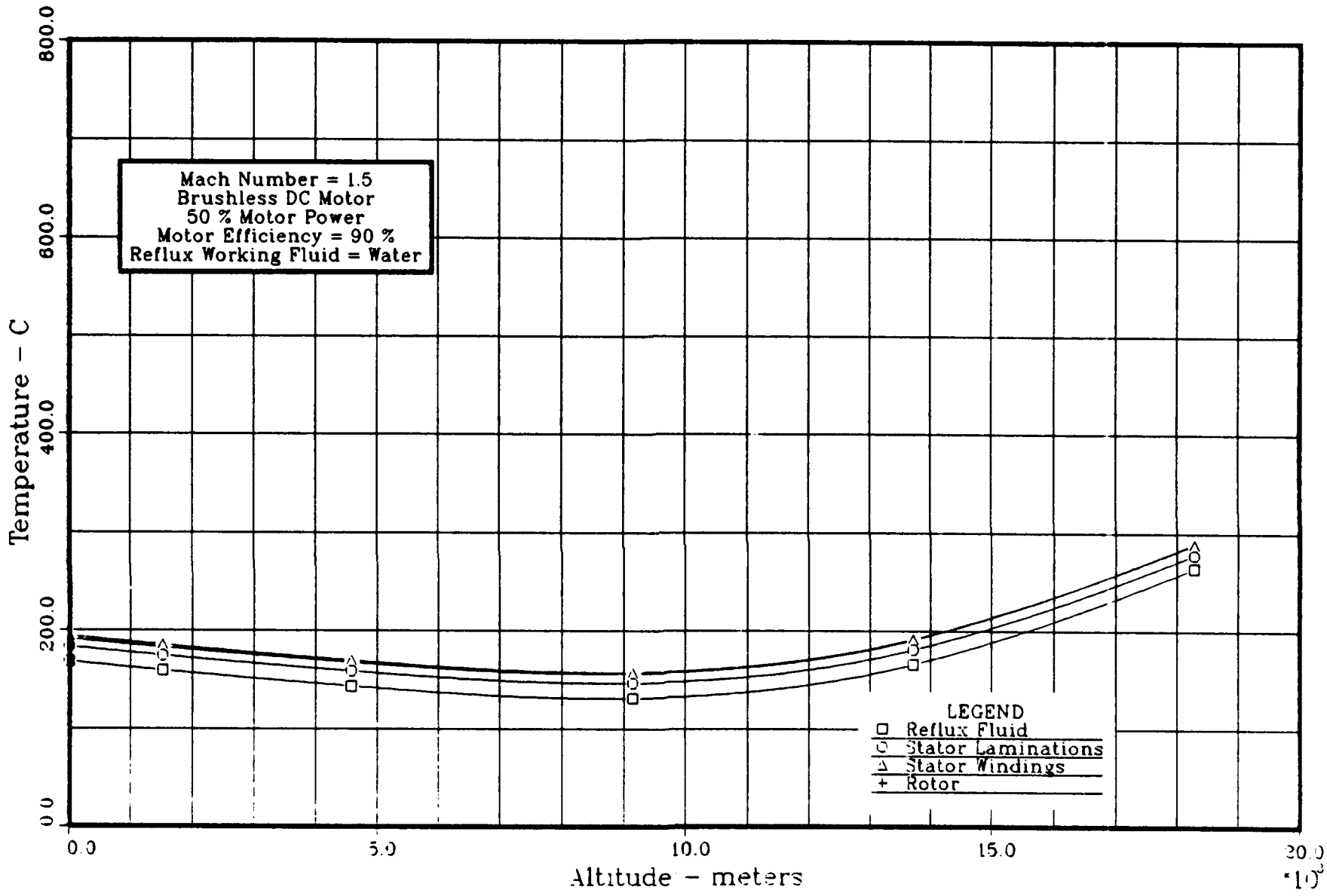

FIGURE 5.18 ADVANCED ACTUATOR COOLING
Steady State Temperature vs Altitude

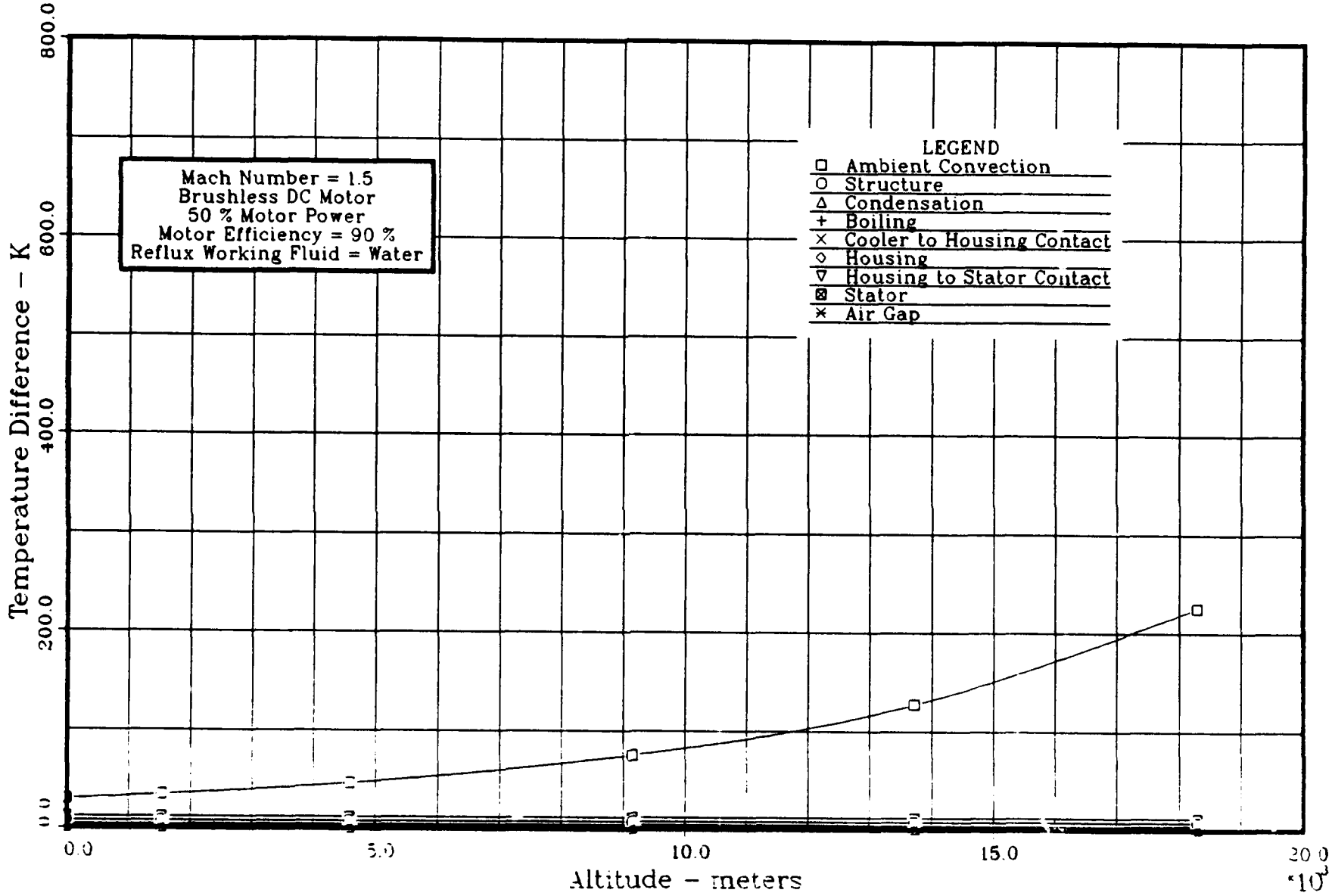

FIGURE 5.19 ADVANCED ACTUATOR COOLING
Steady State Temp Differences vs Altitude

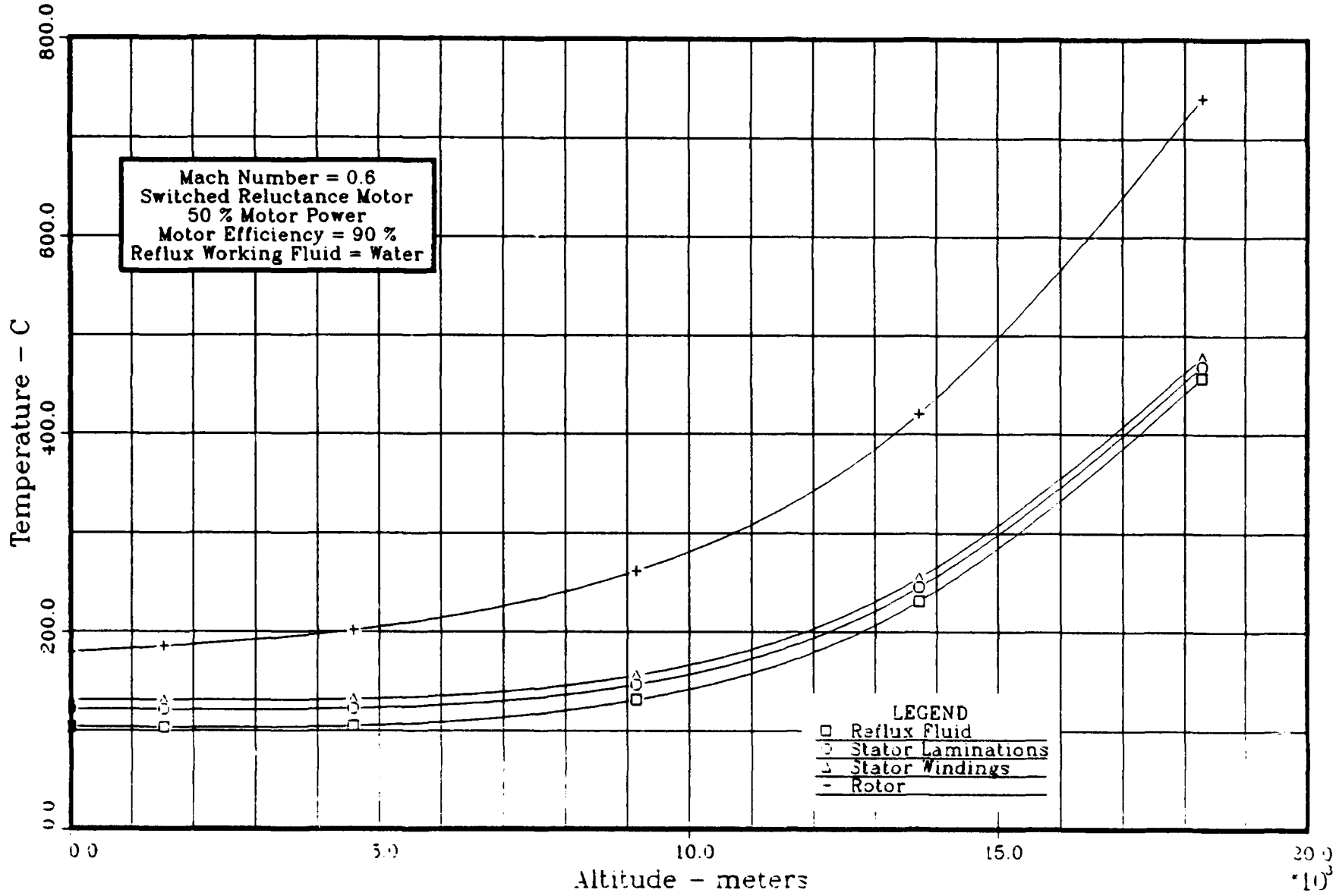

FIGURE 5.20 ADVANCED ACTUATOR COOLING
Steady State Temperature vs Altitude

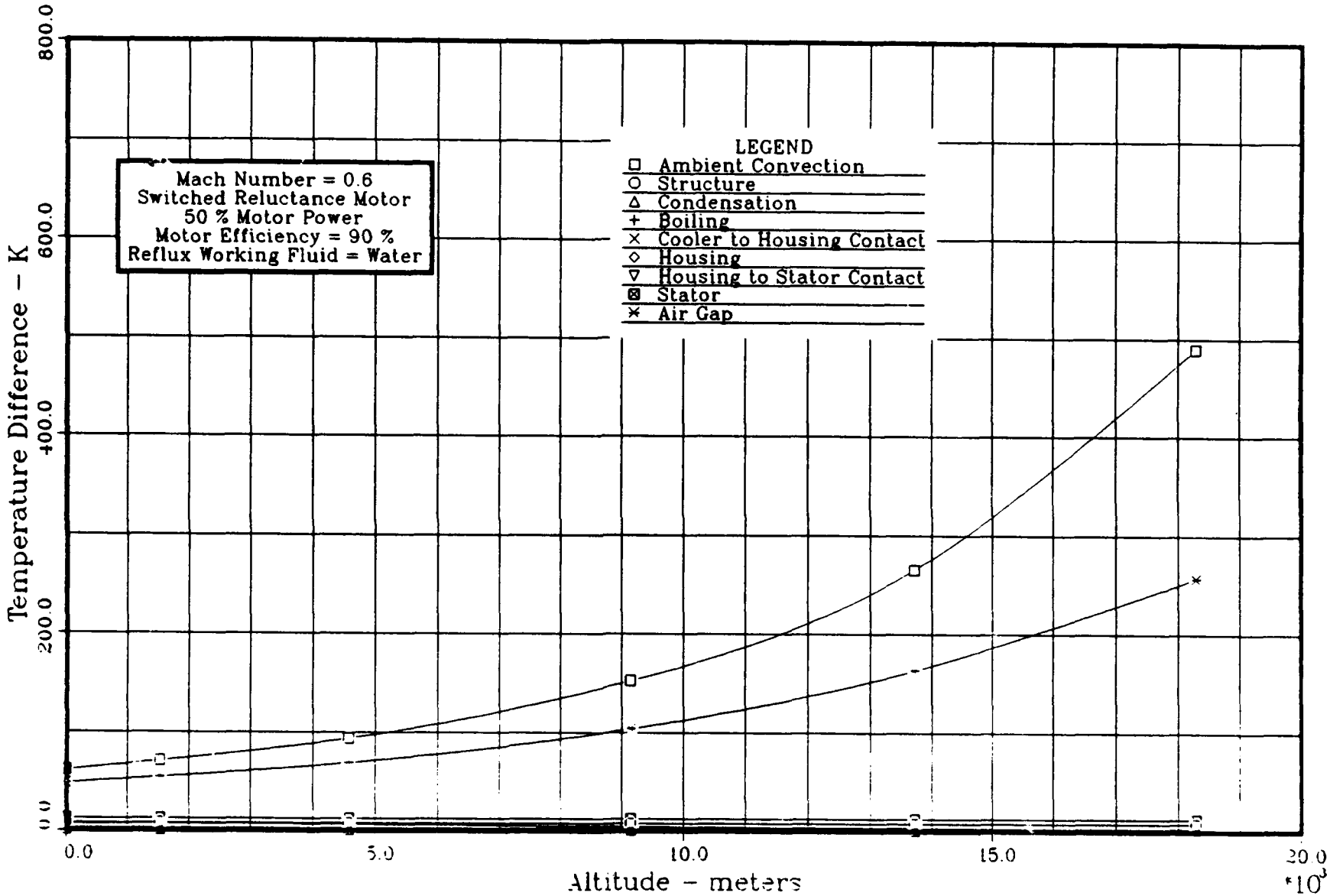

FIGURE 5.21 ADVANCED ACTUATOR COOLING
Steady State Temp Differences vs Altitude

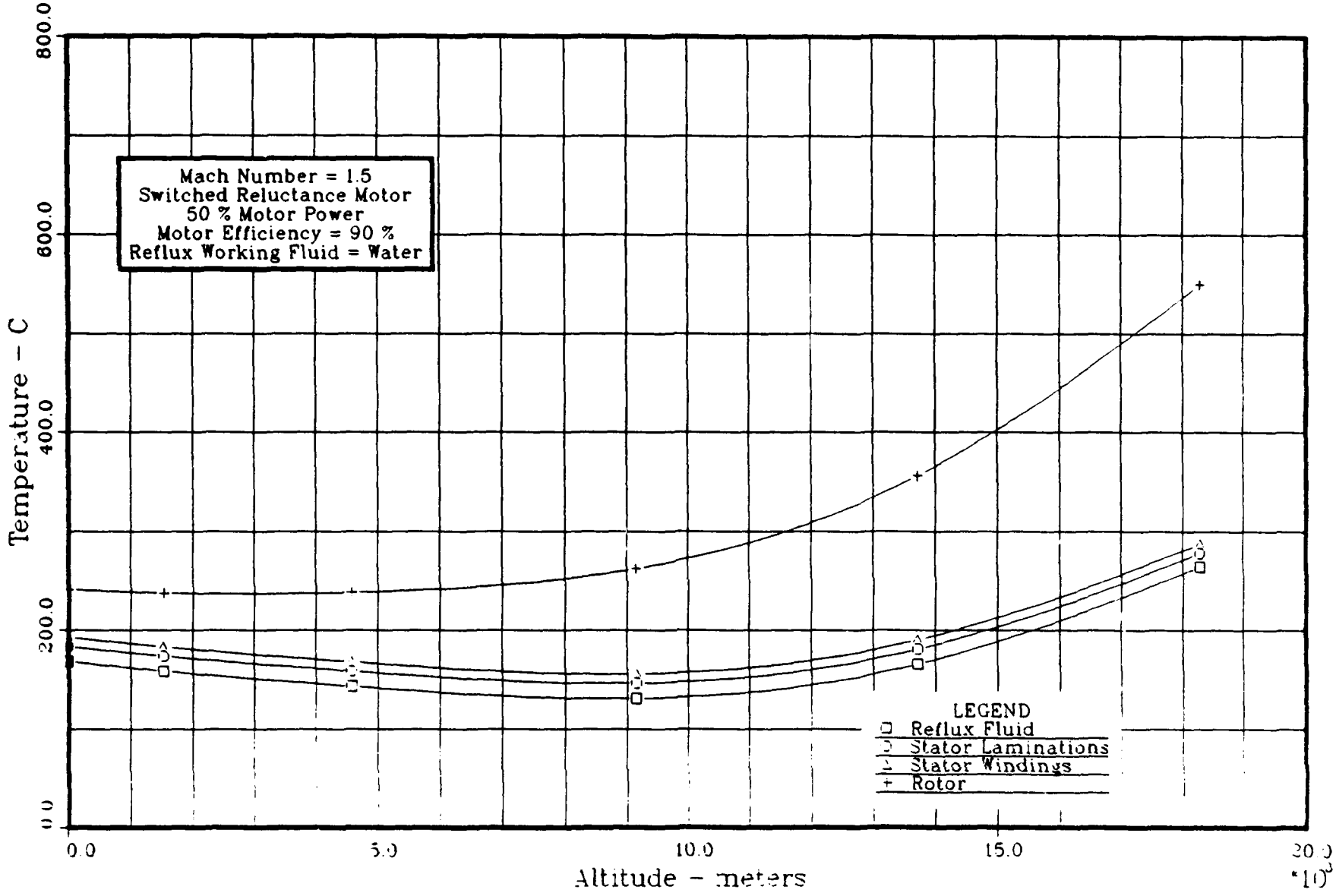

FIGURE 5.22 ADVANCED ACTUATOR COOLING
Steady State Temperature vs Altitude

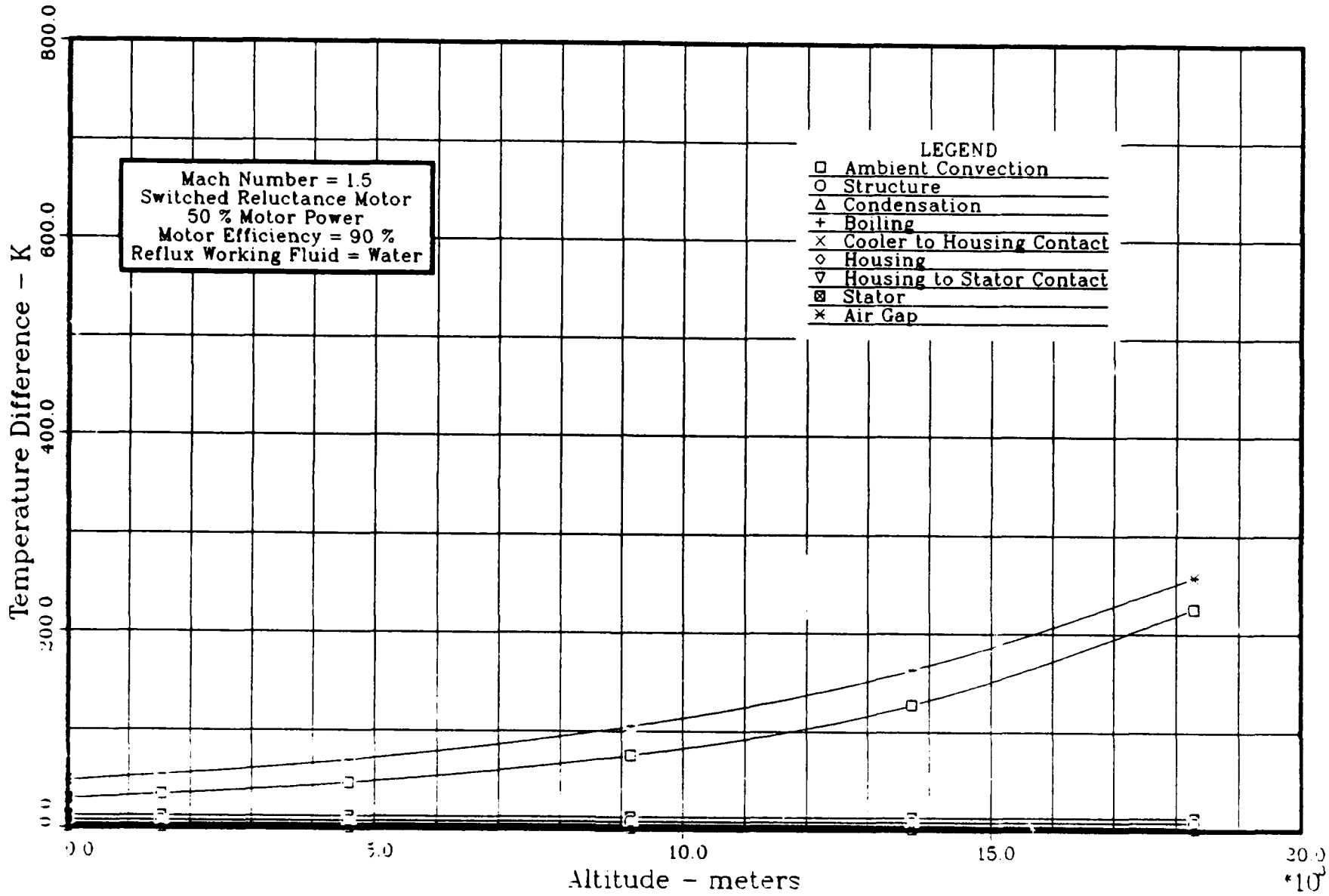

FIGURE 5.23 ADVANCED ACTUATOR COOLING
Steady State Temp Differences vs Altitude

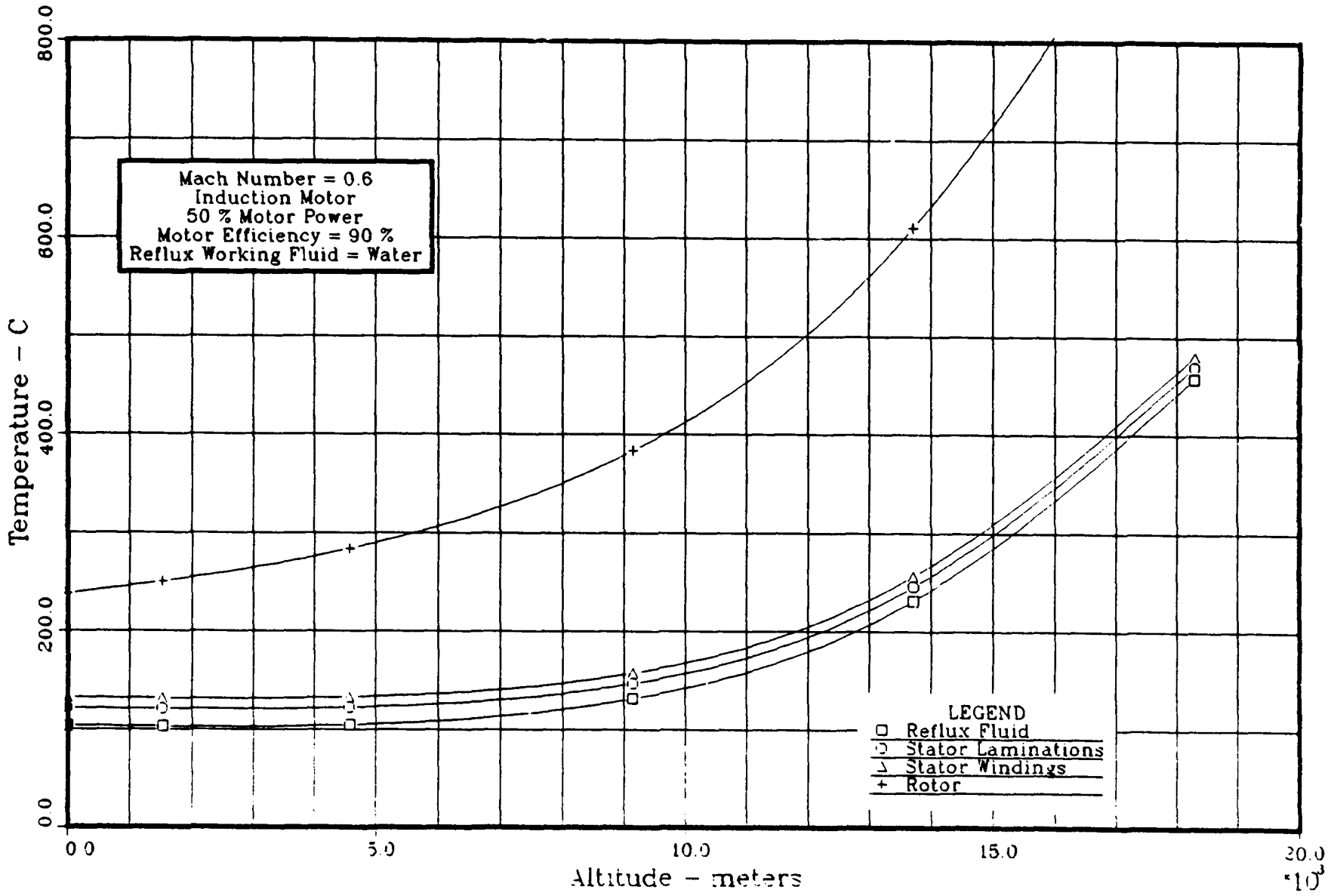

FIGURE 5.24 ADVANCED ACTUATOR COOLING
Steady State Temperature vs Altitude

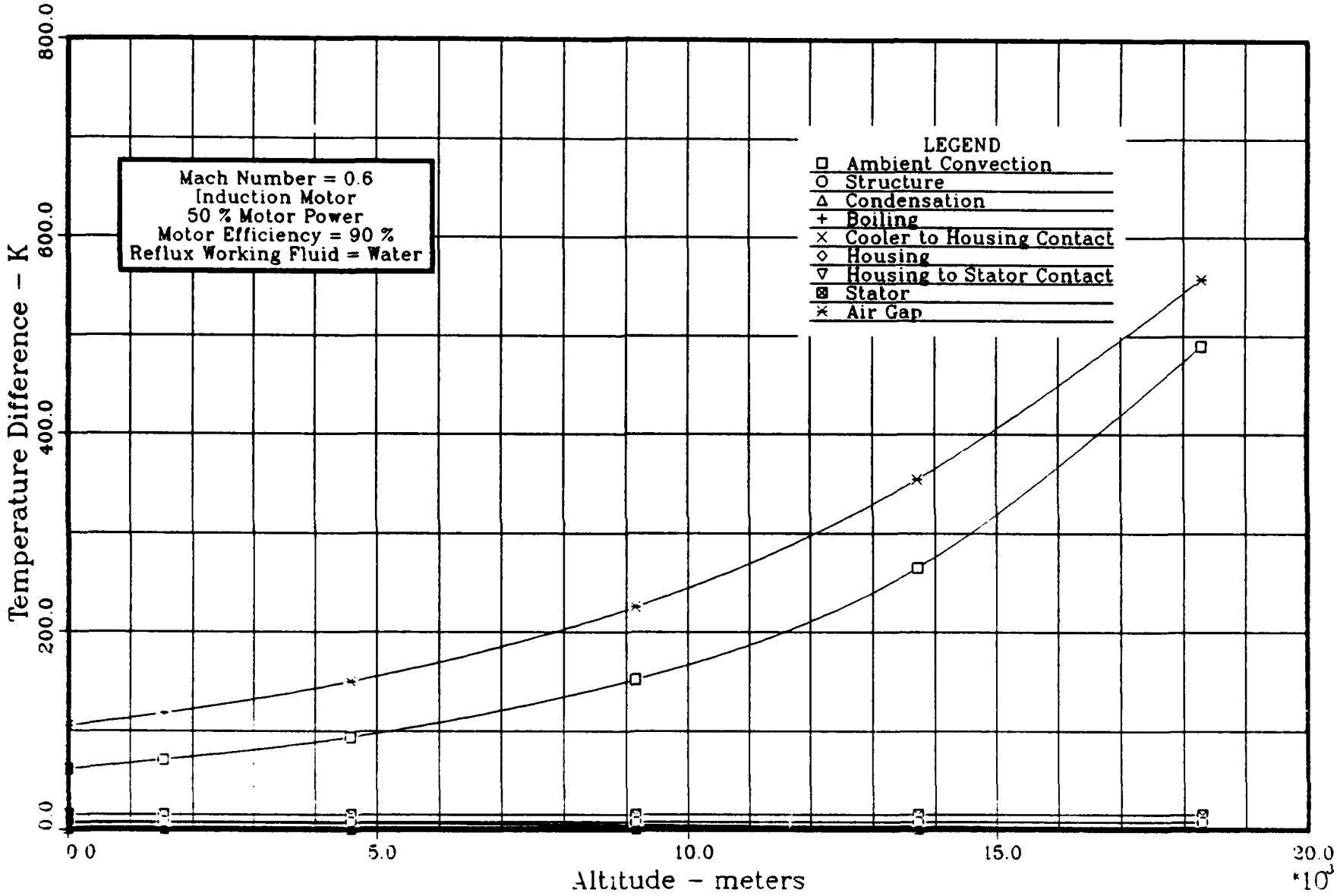

FIGURE 5.25 ADVANCED ACTUATOR COOLING
Steady State Temp Differences vs Altitude

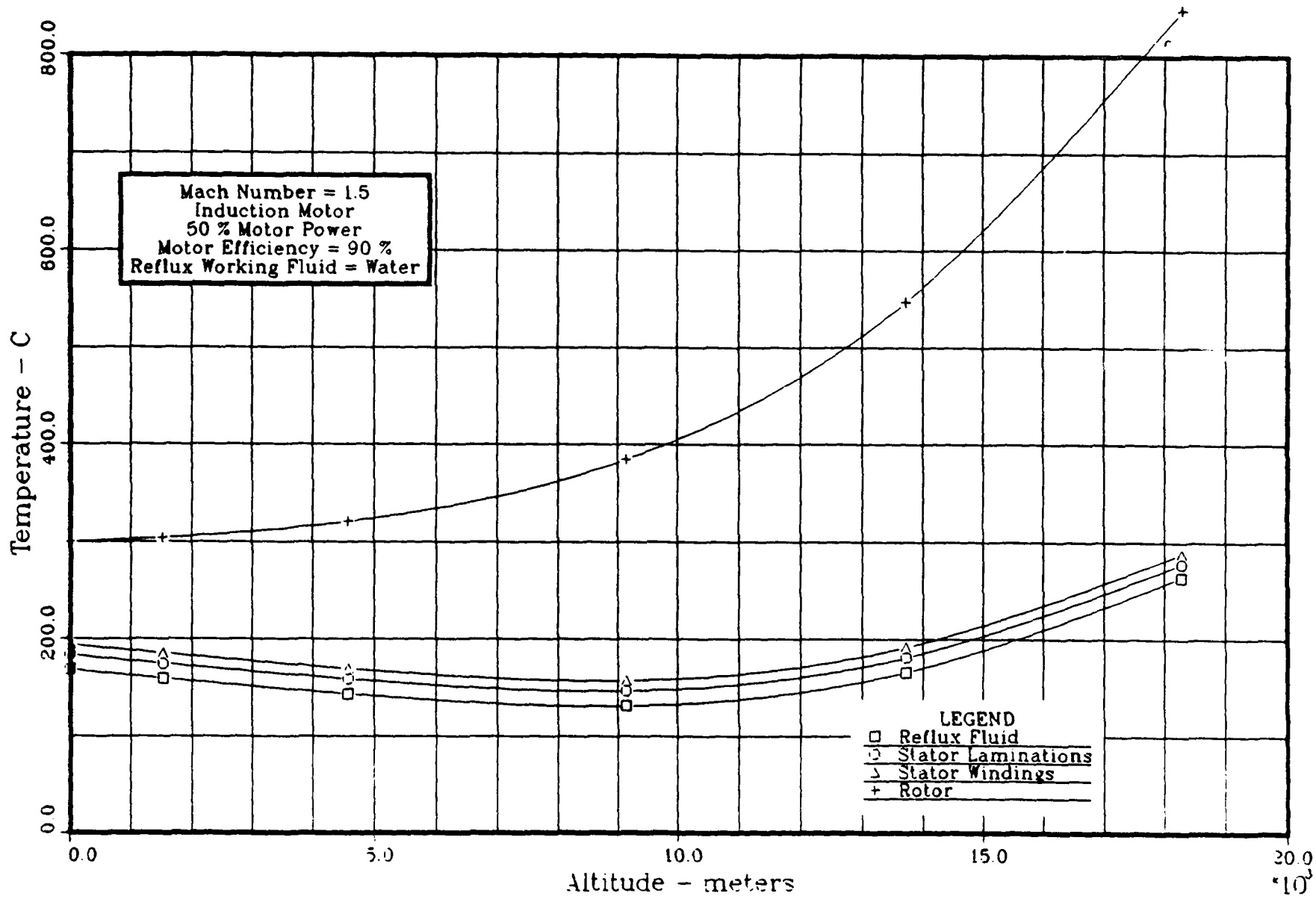

FIGURE 5.26 ADVANCED ACTUATOR COOLING
Steady State Temperature vs Altitude

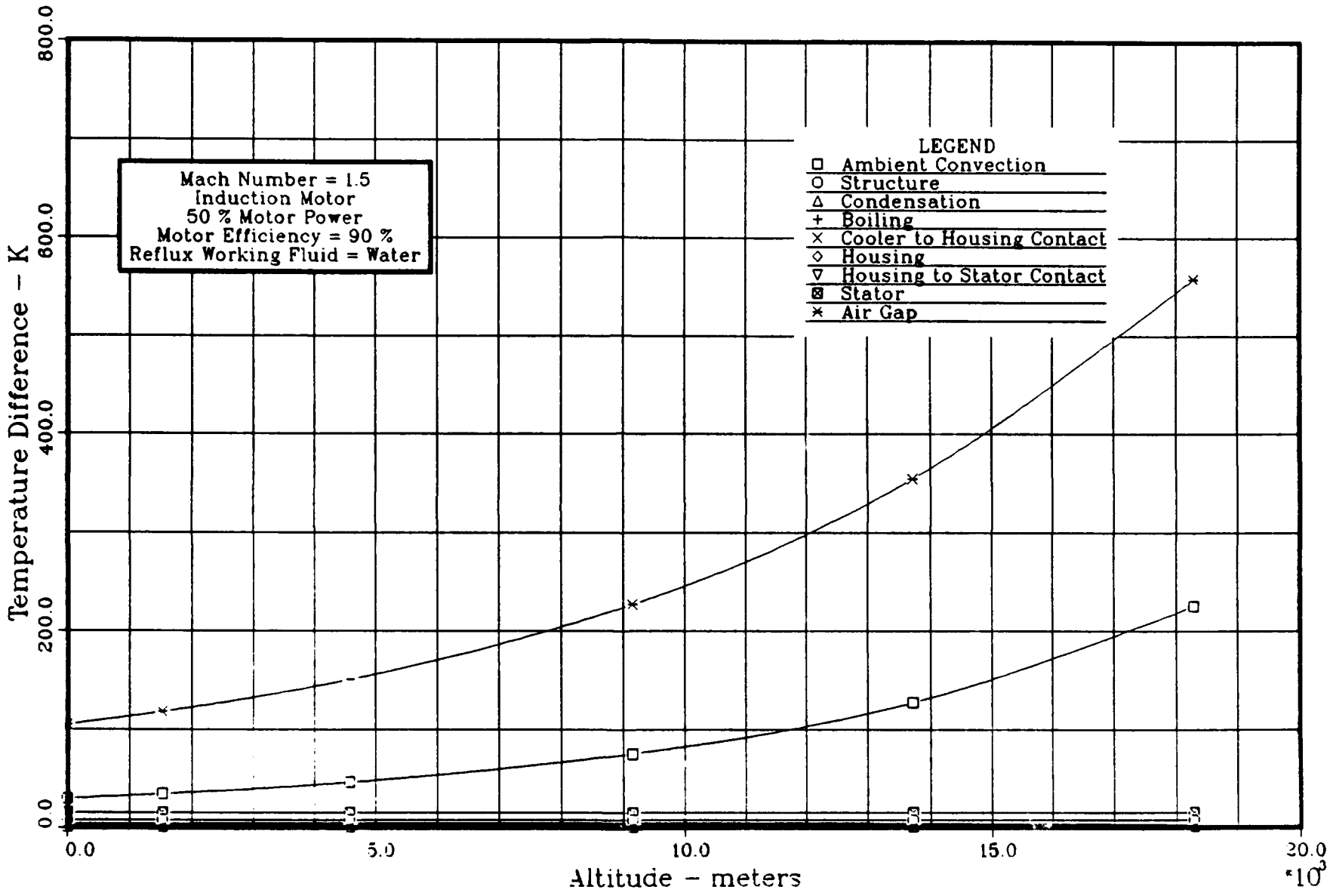

FIGURE 5.27 ADVANCED ACTUATOR COOLING
Steady State Temp Differences vs Altitude

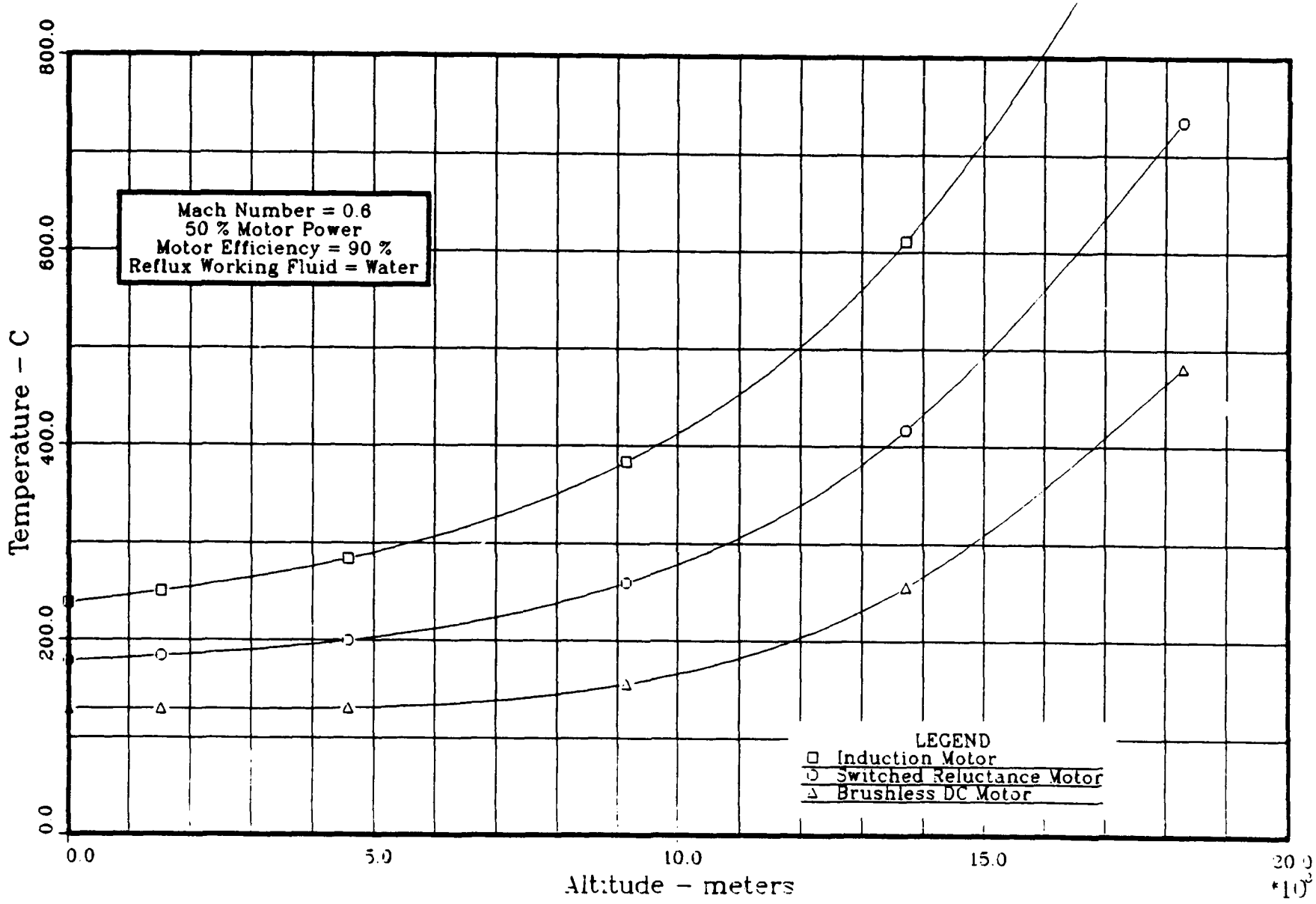

FIGURE 5.28 ADVANCED ACTUATOR COOLING
Steady State Rotor Temperature vs Altitude

Figure 5.28 illustrates the following observation:

- Passive reflux cooling indirectly cools motor rotors requiring careful control of rotor losses and consideration of rotor temperature limitations.

As discussed in section 5.3, rotor cooling may particularly become a problem for brushless DC motors and induction motors. Permanent magnet magnetic properties limit brushless DC rotor temperatures, while the mechanical strength of copper rotor bars limit induction rotor temperatures.

Additionally, direct cooling of the stator provides significant improvements in motor reliability, since motor reliability depends more upon stator temperatures than rotor temperatures, as long as allowable rotor magnet temperatures are not included for the PM rotor.

5.3 Motor Comparison

Sundstrand evaluated three types of motors for application in EMAs: induction motors, permanent magnet brushless DC motors, and switched reluctance motors. Figure 5.29 compares some of the features of the three motor types, and the paragraphs which follow provide a more detailed discussion of the motors.

Based on the discussion which follows and the previously discussed steady state analyses, switched reluctance proved to be the most compatible motor design for the reflux cooling approach. Moderate rotor losses combined with a more robust rotor design result in less restrictive temperature limitations for switched reluctance motors than induction and brushless DC motors. In addition, the inherent fail degraded performance characteristics of switched reluctance motors result in an EMA consistent with the more electric airplane technologies approach.

<u>Induction Motor</u>

Limitations:

- Insulation properties limit the stator operating temperatures. The following describes temperature limitations for insulation systems:

  Conventional Insulation: 220 - 250 °C
  (HML magnet wire with ML or epoxy varnish)

  High Temperature Insulation: 400 °C
  (ceramic insulation)

- Typically, the mechanical strength of the rotor bars and the design rotor stress levels (rotor speed, rotor diameter, etc.) limit the rotor operating temperatures. Therefore, a motor designer possesses limited control of the rotor temperature limitation through selection of the rotor bar material, motor design speed, and rotor diameter. As an additional design consideration, rotor losses typically increase with increasing temperature.

	INDUCTION	PERMANENT MAGNET BRUSHLESS DC	SWITCHED RELUCTANCE
RATING	FRACTIONAL TO 1000'S OF KW	FRACTIONAL TO 100'S OF KW	FRACTIONAL TO 1000'S OF KW
SPEED	< 200 M/SEC PERIPHERAL SPEED	< 250 M/SEC PERIPHERAL SPEED	< 300 M/SEC PERIPHERAL SPEED
EFFICIENCY	85 - 92%	HIGH: 90 - 95%	LOW: APPROX 85%
LOSSES	IRON AND COPPER ROTOR AND STATOR	IRON AND COPPER STATOR ONLY	IRON/COPPER STATOR IRON ROTOR
WEIGHT	INTERMEDIATE	MINIMUM	HIGHEST
TEMPERATURE	INSULATION LIMITED	MAGNET LIMITED (150 DEGREES C)	INSULATION LIMITED
STALL TORQUE	GOOD	GOOD	VERY GOOD - MINIMAL LOSSES
FAULT TOLERANCE	NO	NO	YES
COST	INTERMEDIATE	HIGH	LOW

FIGURE 5.29 ELECTRIC MOTOR COMPARISON

Advantages:

- Most commonly used motor with many applications within the aerospace industry.

- Motor designs allow canning of stator with minimal affect upon motor performance. Stator canning allows hermetically sealing the stator from the rotor and air gap, and permits the use of direct fluid cooling of the stator. In the case of reflux cooling, the use of stator canning would allow the working fluid to directly contact the stator windings and laminations, thus eliminating some of the series thermal conductances separating the stator and working fluid.

- Control of induction motors does not require position feedback, therefore simplifying motor design.

- Interference fits between the motor stator and motor housing does not adversely affect induction motor performance. Interference fits improve the contact conductance between the stator and housing, reducing the temperature drop across the interface.

Disadvantages:

- Rotor losses for induction motors exceed the rotor losses for brushless DC or switched reluctance motors. Therefore, rotor temperature limitations often limit motor operating temperatures with a cooling method, like reflux cooling, which indirectly provides rotor cooling.

- A single failure to an induction motor often results in complete motor failure. Splitting the stator and rotor into effectively two motors on the same shaft, provides a degree of fail degraded performance.

<u>Permanent Magnet Brushless DC Motor</u>

Limitations:

- Insulation properties limit the stator operating temperatures; therefore, the same temperature limitations as induction motor stators apply to brushless DC motor stators.

- The magnetic properties of the rotor permanent magnets, as a function of temperature, limit the rotor operating temperatures. Above 150 ^{0}C rotor losses rapidly increase due to degraded magnet properties.

Advantages:

- Motor designs allow canning of stator with minimal affect upon motor performance. Stator canning offers similar advantages for reflux cooling as it offers induction motors.

- Interference fits between the motor stator and motor housing does not adversely affect induction motor performance. Interference fits improve the contact conductance between the stator and housing, reducing the temperature drop across the interface.

- Motor efficiencies for brushless DC motors exceed the efficiencies for induction and switched reluctance motors, reducing heating loads on motor cooling systems.

- Brushless DC motors weigh less than induction and switched reluctance motors of the same power.

- Brushless DC motor designs result in minimal rotor losses. However, the temperature limitations of the rotor magnets often outweighs the advantages of low rotor losses.

Disadvantages:

- Rotor permanent magnet temperature limitations severely limit motor operating temperatures. This particularly applies to cooling methods like reflux cooling which indirectly cools the rotor through cooling of the stator outer diameter.

- A single failure to a brushless DC motor often results in complete motor failure. Splitting the stator and rotor into effectively two motors on the same shaft, provides a degree of fail degraded performance.

- Control of brushless DC motors requires shaft position feedback and high power switching.

- Brushless DC motors cost more than induction and switched reluctance motors.

<u>Switched Reluctance Motor</u>

Limitations:

- Insulation properties limit the stator operating temperatures; therefore, the same temperature limitations as induction motor stators apply to switched reluctance motor stators.

- Typically, the mechanical strength of the rotor laminations and the design rotor stress levels (rotor speed, rotor diameter, etc.) limit the rotor operating temperatures. Therefore, a motor designer possesses limited control of the rotor temperature limitation through selection of the rotor lamination material, motor design speed, and rotor diameter. Though similar rotor constraints apply for both switched reluctance and brushless DC motors, the mechanical strength of laminations exceeds copper rotor bars, resulting in less restrictive temperature limitations upon switched reluctance rotors.

- Interference fits between the motor stator and motor housing adversely affect switched reluctance motor performance. A loose fit between the stator and housing reduces the contact conductance between the stator and housing. Since the reflux cooling concept provides cooling across this interface, reflux cooling may require some method of contact conductance enhancement in order to reduce the temperature drop across this interface.

- Switched reluctance motor performance has proven sensitive to the size of the air gap. This sensitivity to the size of the air gap prevents the use of stator canning, which prevents a direct cooling approach with the reflux working fluid in direct contact with the stator laminations and windings.

Advantages:

- Switched reluctance motors inherently provide fail degraded performance due to the number of individual stator poles. This feature may prove particularly valuable on military applications due to combat environments.
- The temperature limitations on switched reluctance rotors typically exceed the limitations on induction and brushless DC motors.
- Switched reluctance motor designs result in lower rotor losses than induction motors.
- Switched reluctance motors cost less than induction and brushless DC motors.

Disadvantages:

- Switched reluctance motors have relatively low efficiency (approximately 85% versus 90% and 95% efficiencies for induction and permanent magnet motor, respectively).
- As mentioned earlier, motor performance is adversely affected by hoop pressure applied to the stator.

5.4 Transient Analysis

5.4.1 Frequency Response

Sundstrand performed a frequency response study in order to characterize the advantages of using PCM as a function of the frequency of actuator power variations. Sundstrand performed the study by applying square wave actuator power variations to the reflux cooler model for coolers with and without PCM. For this study Sundstrand used a mixture of 78.3 molar percent pentaerythritol with pentaglycerine, solid-solid PCMs.

Figure 5.30 presents the actuator power for a square wave period of two minutes, while Figure 5.31 presents the actuator power for a square wave period of 30 minutes. These figures illustrate the variation of actuator power between five percent and 65 percent of maximum power (note change of scale).

Figures 5.32 and 5.33 present transient cooler and motor temperatures as a function of time for a power cycle period of two minutes for coolers without and with PCM, respectively. Similarly, Figures 5.34 and 5.35 present data for a power cycle period of 30 minutes.

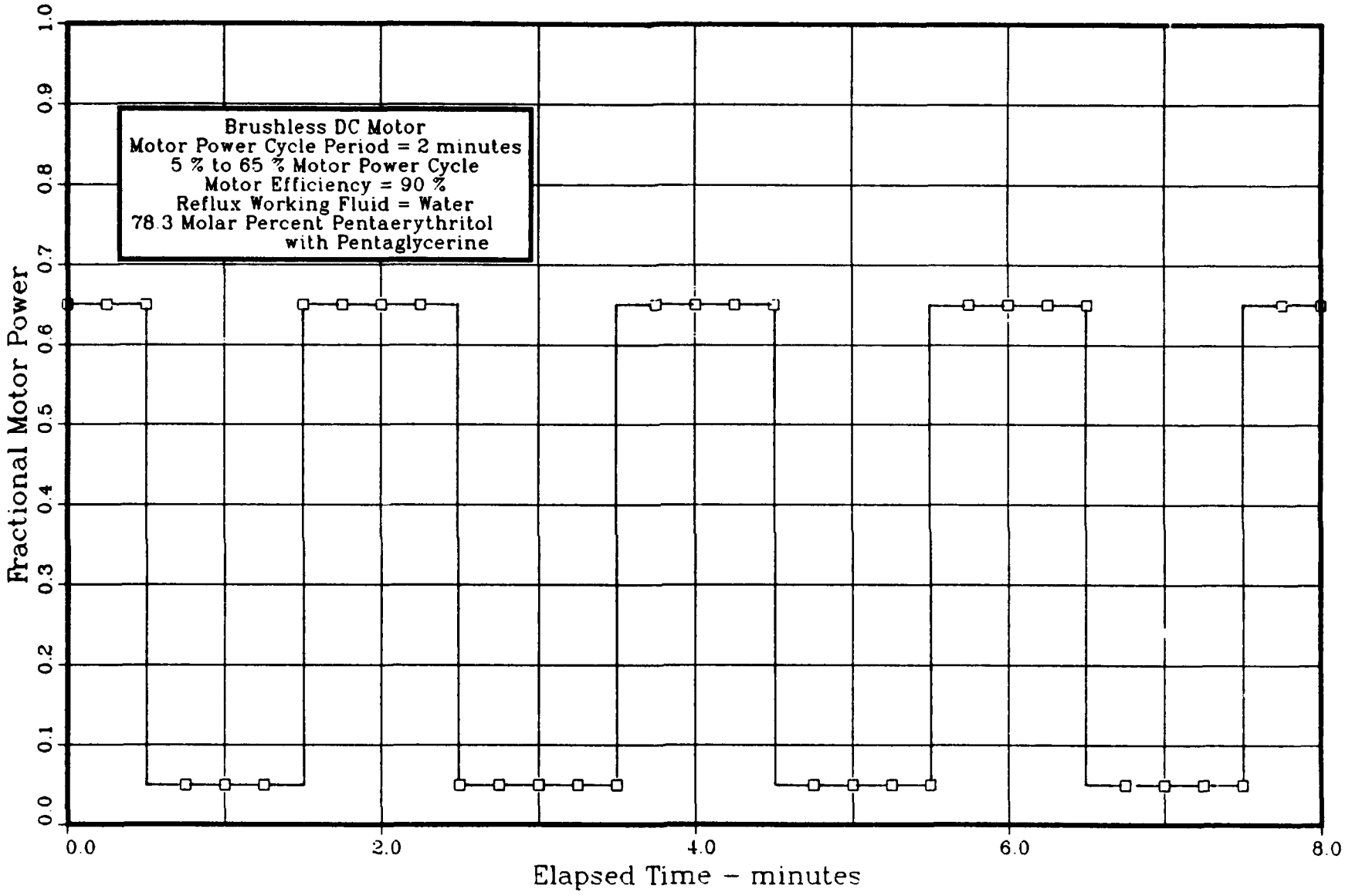

FIGURE 5.30 ADVANCED ACTUATOR COOLING
Frequency Response - Motor Power vs Time

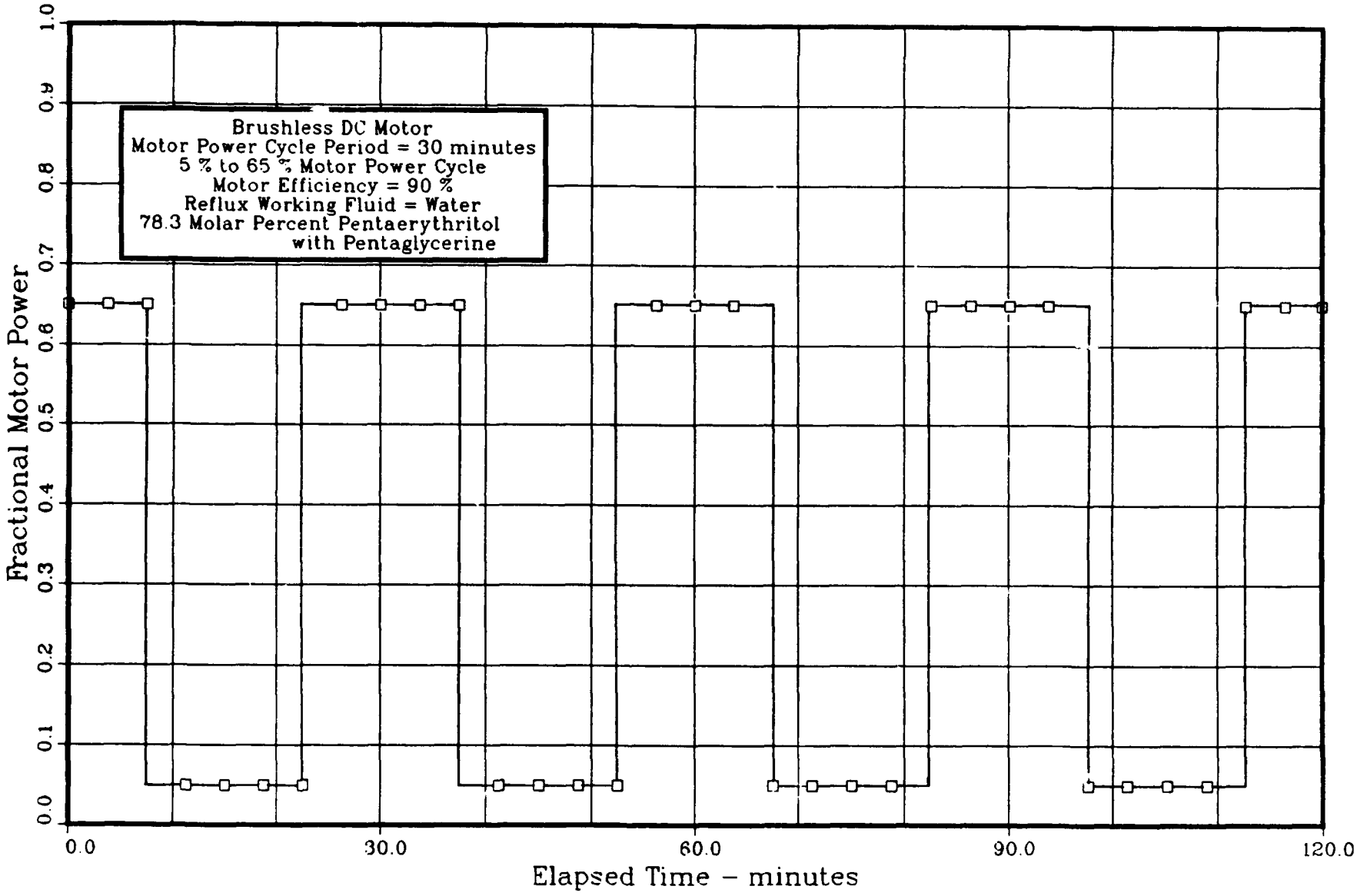

FIGURE 5.31 ADVANCED ACTUATOR COOLING
Frequency Response - Motor Power vs Time

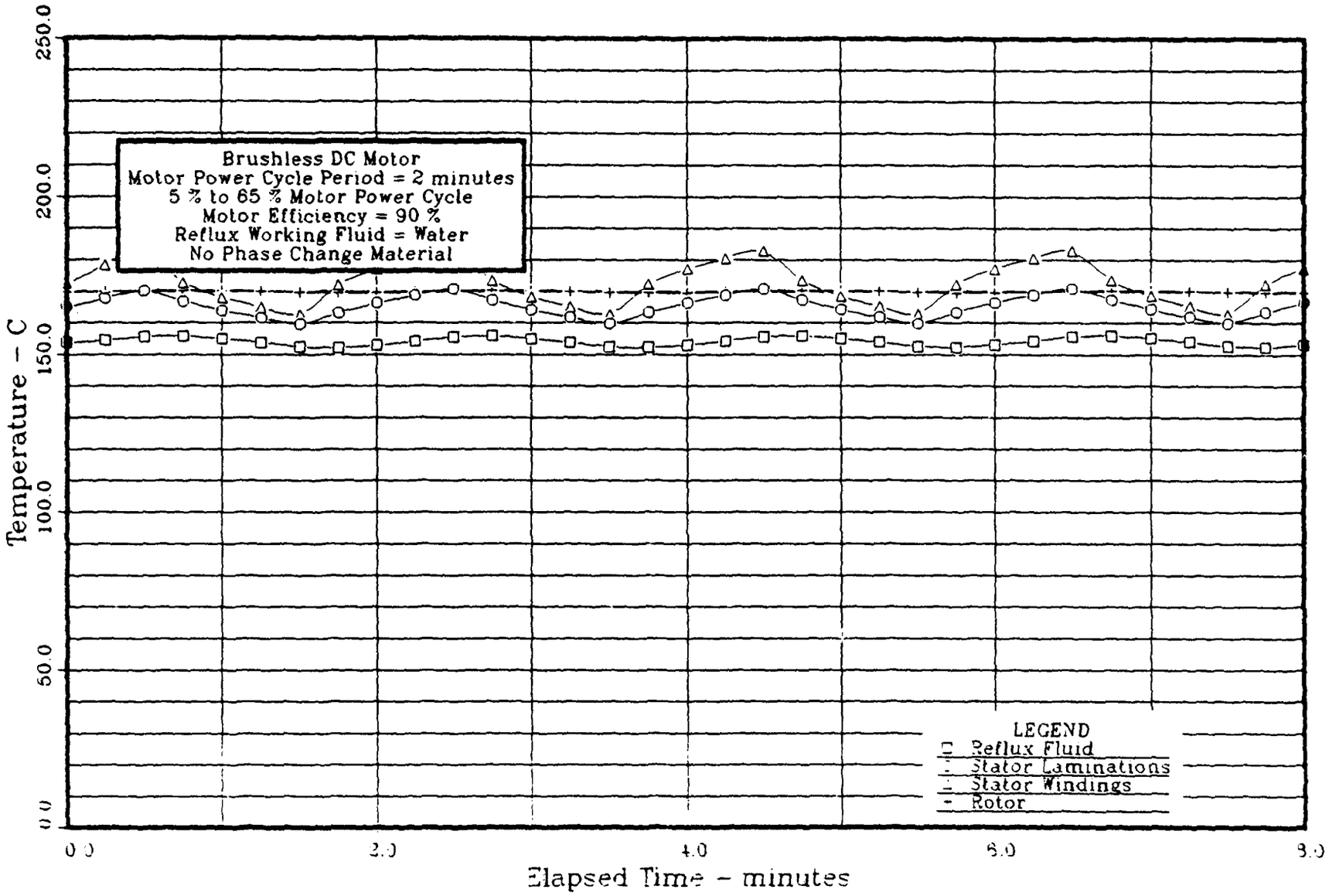

FIGURE 5.32 ADVANCED ACTUATOR COOLING
Frequency Response - Temperature vs Time

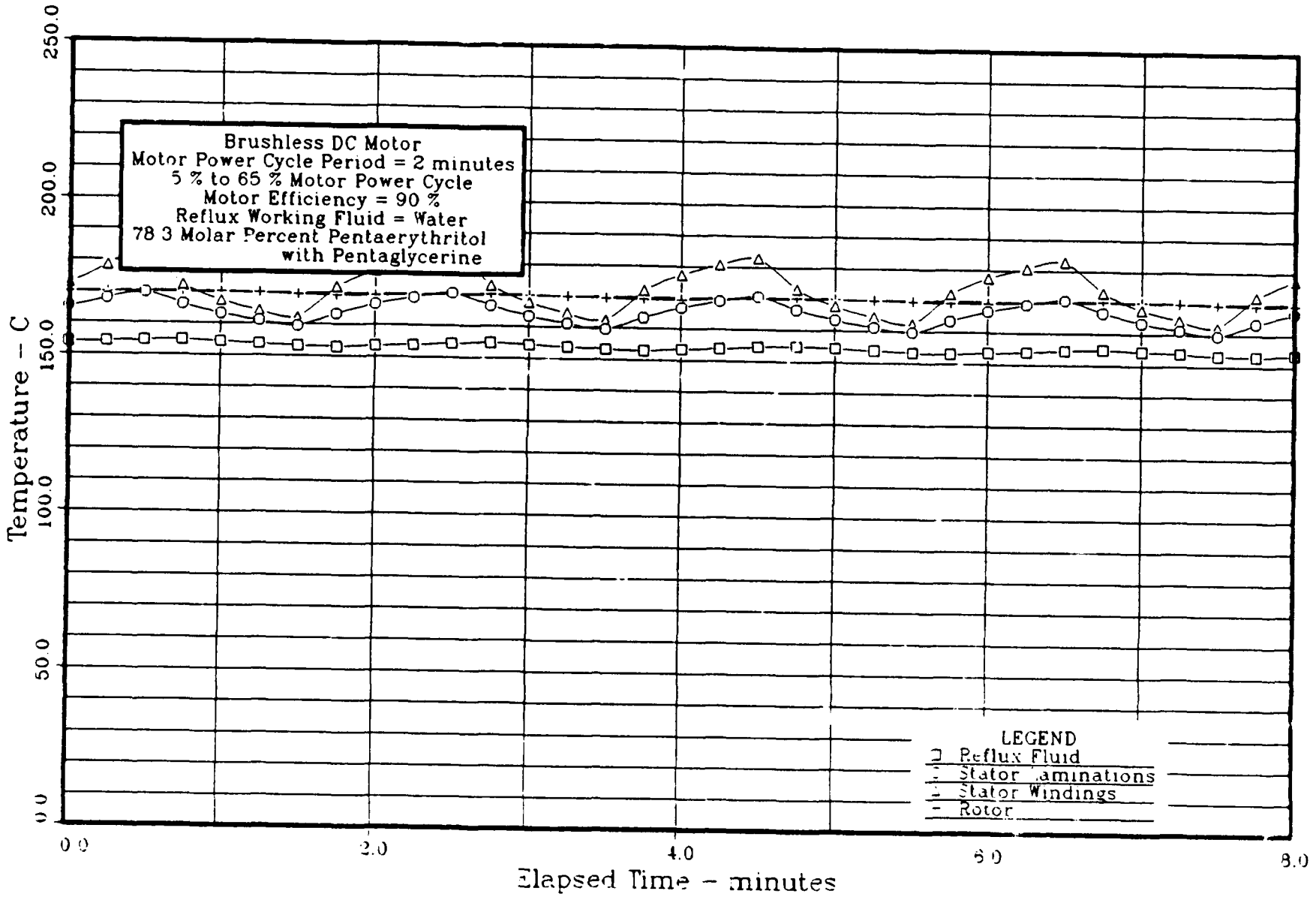

FIGURE 5.33 ADVANCED ACTUATOR COOLING
Frequency Response - Temperature vs Time

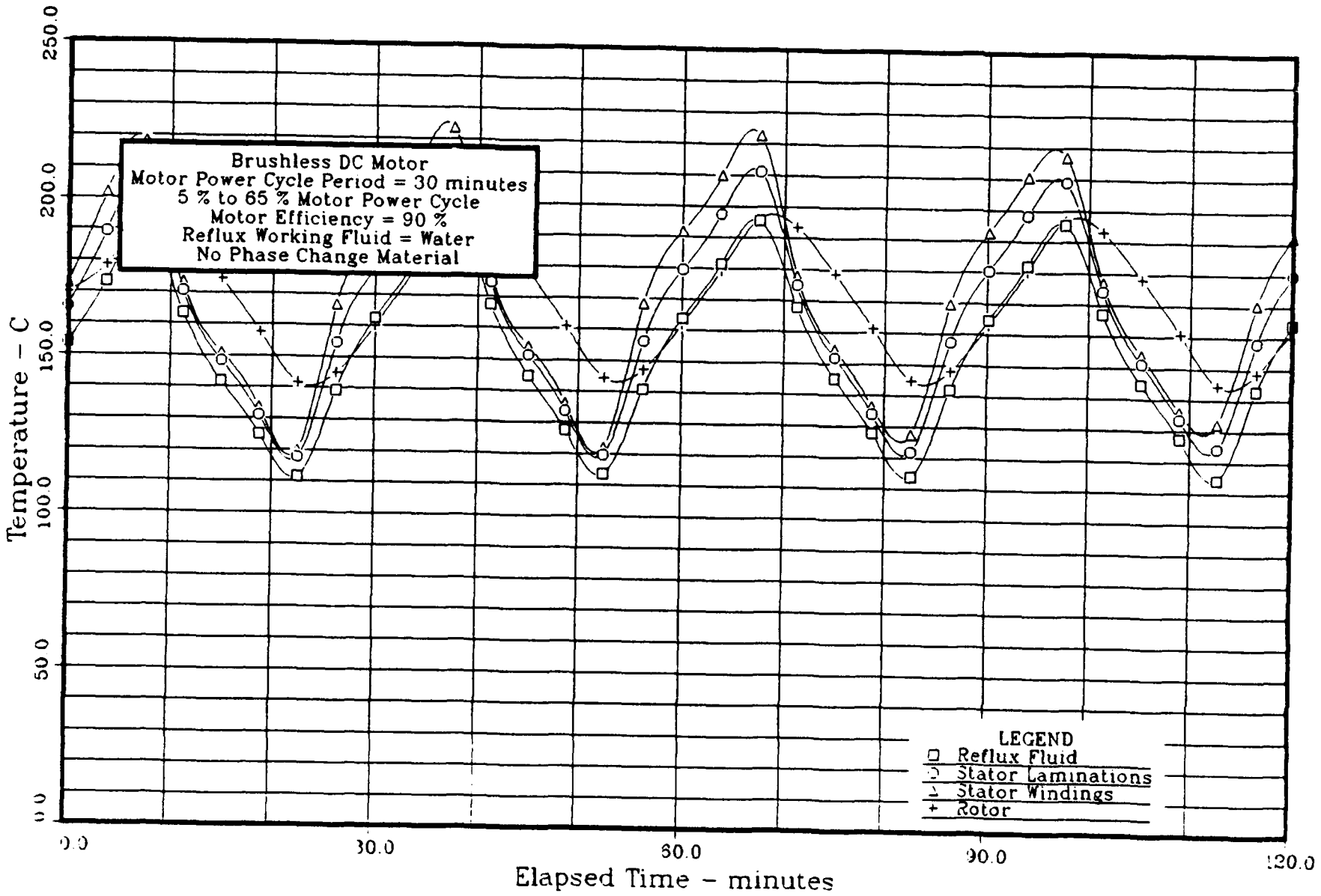

FIGURE 5.34 ADVANCED ACTUATOR COOLING
Frequency Response - Temperature vs Time

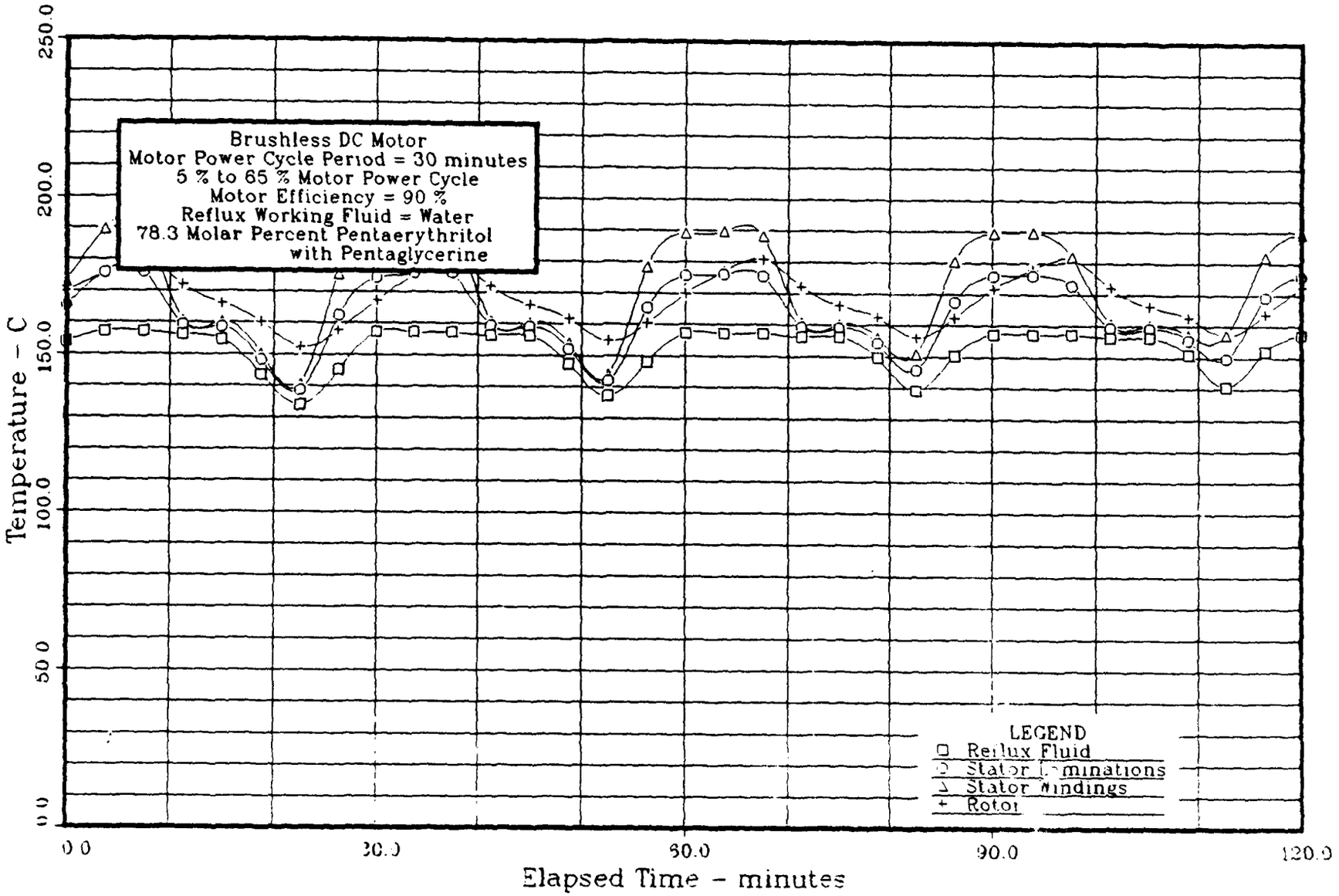

FIGURE 5.35 ADVANCED ACTUATOR COOLING
Frequency Response - Temperature vs Time

Figures 5.36 and 5.57 compile data for all of the cases studied between periods of two minutes and 30 minutes and plot the periodic amplitude of the temperatures as a function of power cycle period for coolers without and with PCM, respectively.

The data in Figures 5.32 through 5.37 illustrates increasing benefits of using PCM as the power cycle period increases (frequency decreases) and little benefit of PCM for characteristically low power cycle periods (higher frequencies). This data suggests that PCM provides little benefit for phenomenon characterized by high frequencies such as turbulence or active actuator dither, but PCM provides benefit for phenomenon characterized by low frequencies such as high load periods during a mission duty cycle (takeoff, combat, and descent). Therefore, the data support the following observation:

- Inherent motor thermal inertia attenuates frequency response for cycle periods less than five minutes; therefore, PCM provides little benefit for high frequency actuator duty cycles.

5.4.2 Combat Phase

The combat phase analysis involved estimating cooler performance with and without PCM during a combat maneuver. This analysis simply considered the combat phase of a mission, and served as a preliminary analysis before performing a more detailed mission analysis (presented in section 5.4.3).

Figure 5.38 illustrates the actuator power cycle applied to the model in order to simulate the transient combat phase of a mission. The analysis used a five percent power level before entering a fifteen minute combat phase and then a five percent power level followed as a recovery period. A five percent power level represents cruise powers (see section 2.0).

Figures 5.39 and 5.40 present temperatures as a function of time for an induction motor for coolers without and with PCM, respectively, and Figure 5.41 presents the PCM liquid mass fraction as a function of time. Figures 5.42 through 5.44 and Figures 5.45 through 5.47 present similar data for a brushless DC motor and a switched reluctance motor, respectively. The major difference between data for the three motors lies in the rotor temperatures, as demonstrated in steady state analyses.

These figures further illustrate the advantages of PCM for characteristically low frequency actuator power variations such as combat maneuvers.

5.4.3 Typical Combat Mission

The combat mission analyses involved an analysis of the worst case combat mission duty cycle presented in Figure 2.1, and included variations in actuator power, Mach number, and altitude. The analysis included the effects of altitude and Mach number on ambient temperature and pressure, aerodynamic heating with the boundary layer, ambient convection coefficient, and motor air gap convection coefficient.

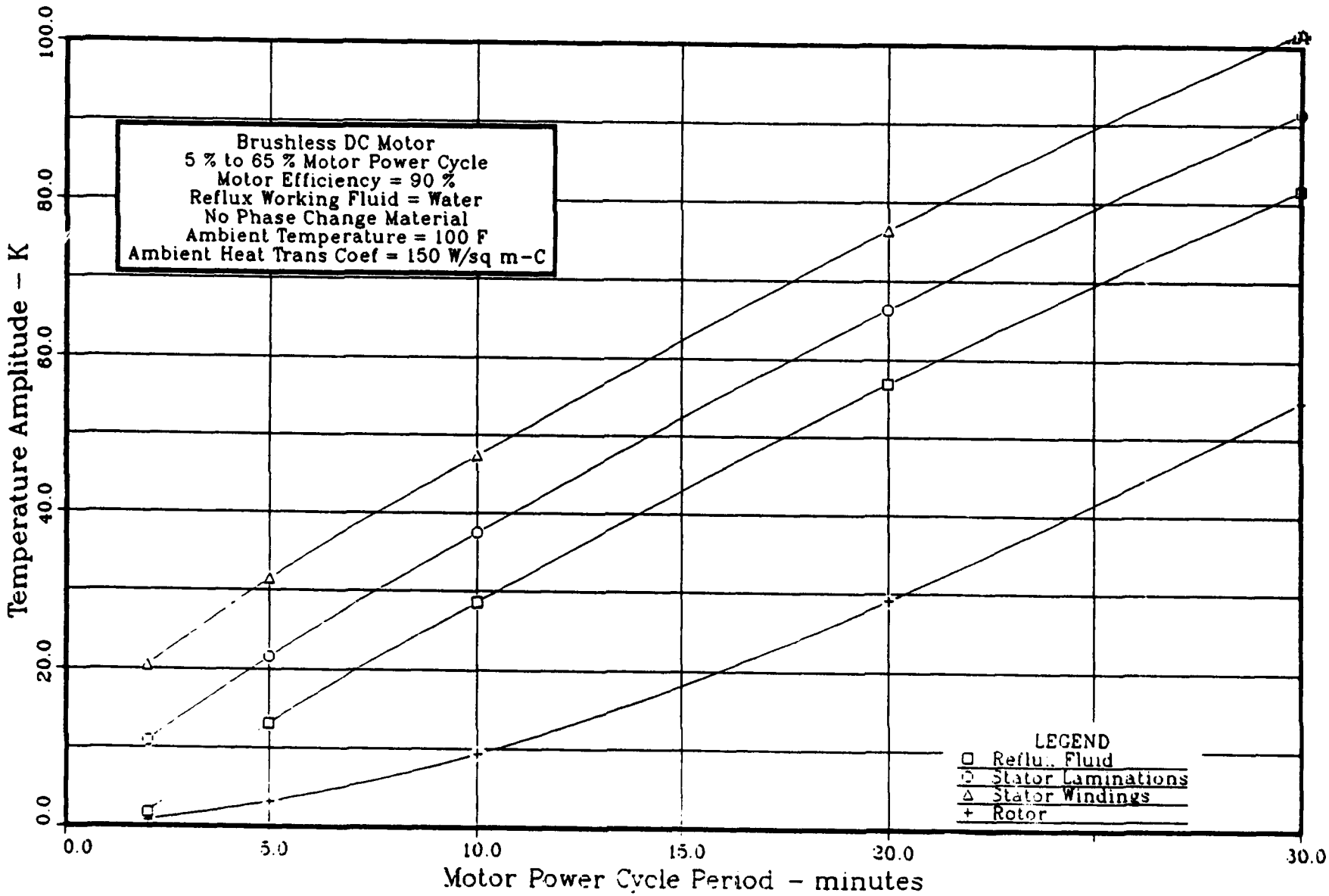

FIGURE 5.36 ADVANCED ACTUATOR COOLING
Frequency Response

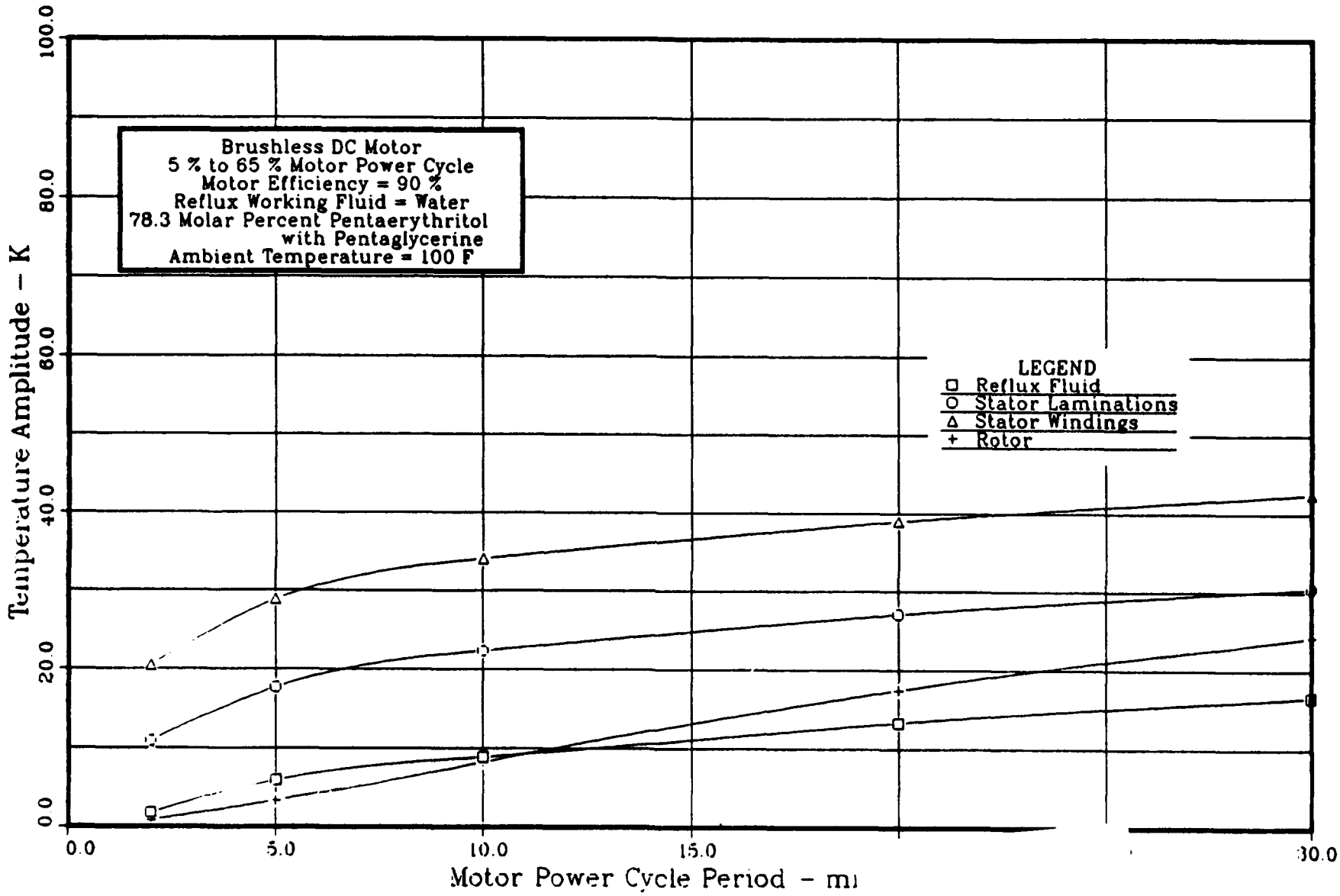

FIGURE 5.37 ADVANCED ACTUATOR COOLING
Frequency Response

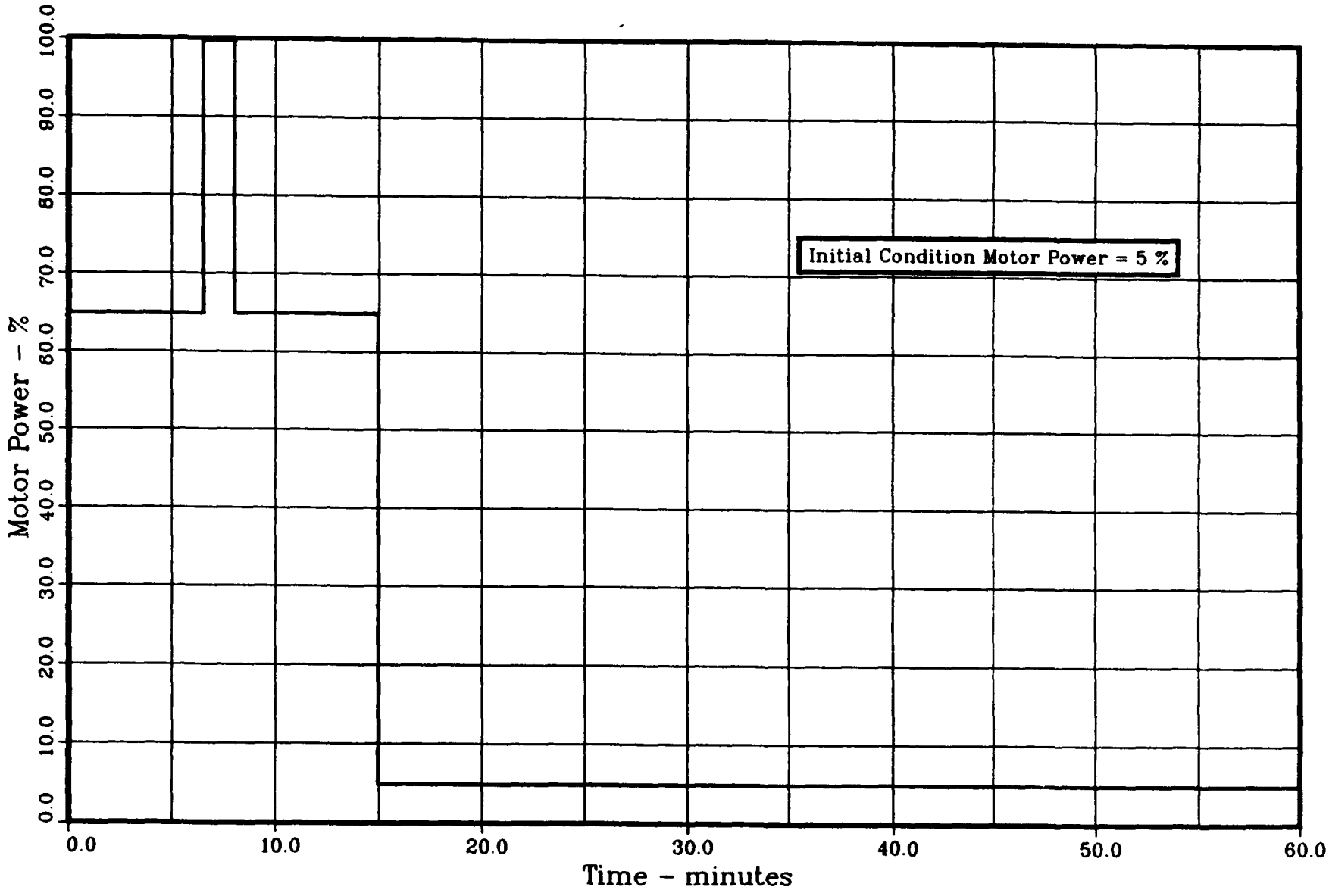

FIGURE 5.38 ADVANCED ACTUATOR COOLING
Actuator Motor Power vs Time

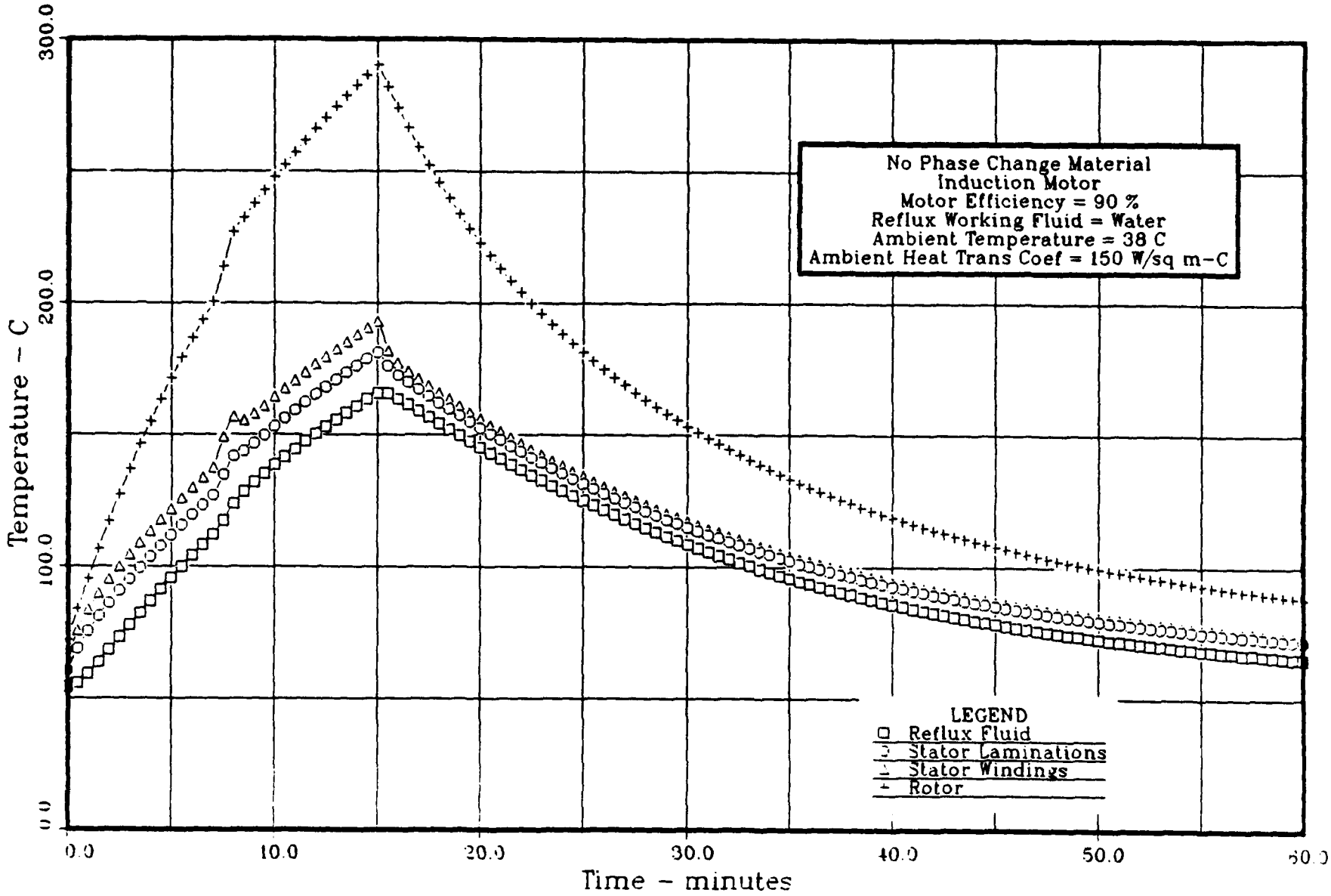

FIGURE 5.39 ADVANCED ACTUATOR COOLING
Temperature vs Time

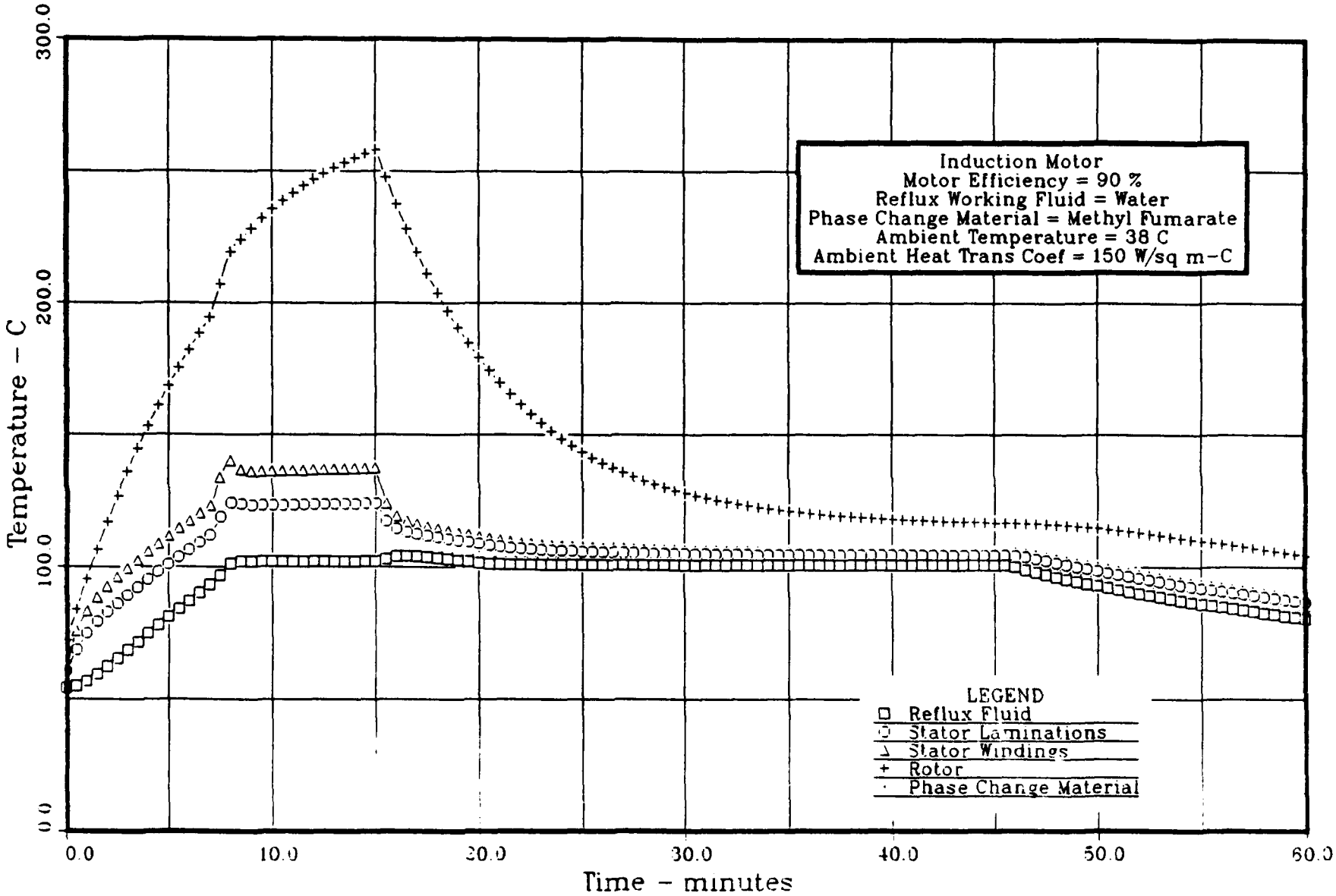

FIGURE 5.40 ADVANCED ACTUATOR COOLING
Temperature vs Time

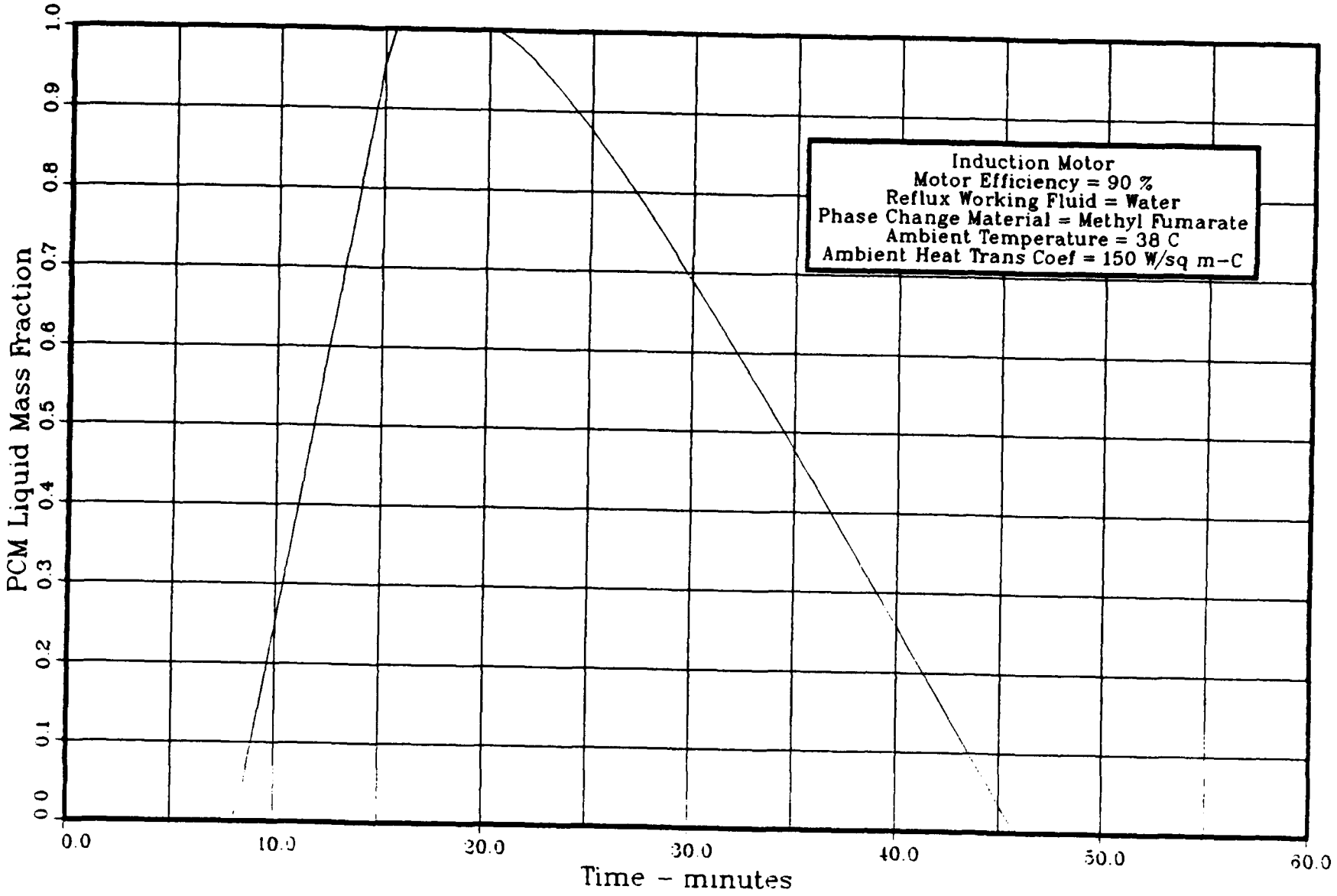

FIGURE 5.41 ADVANCED ACTUATOR COOLING
PCM Liquid Mass Fraction vs Time

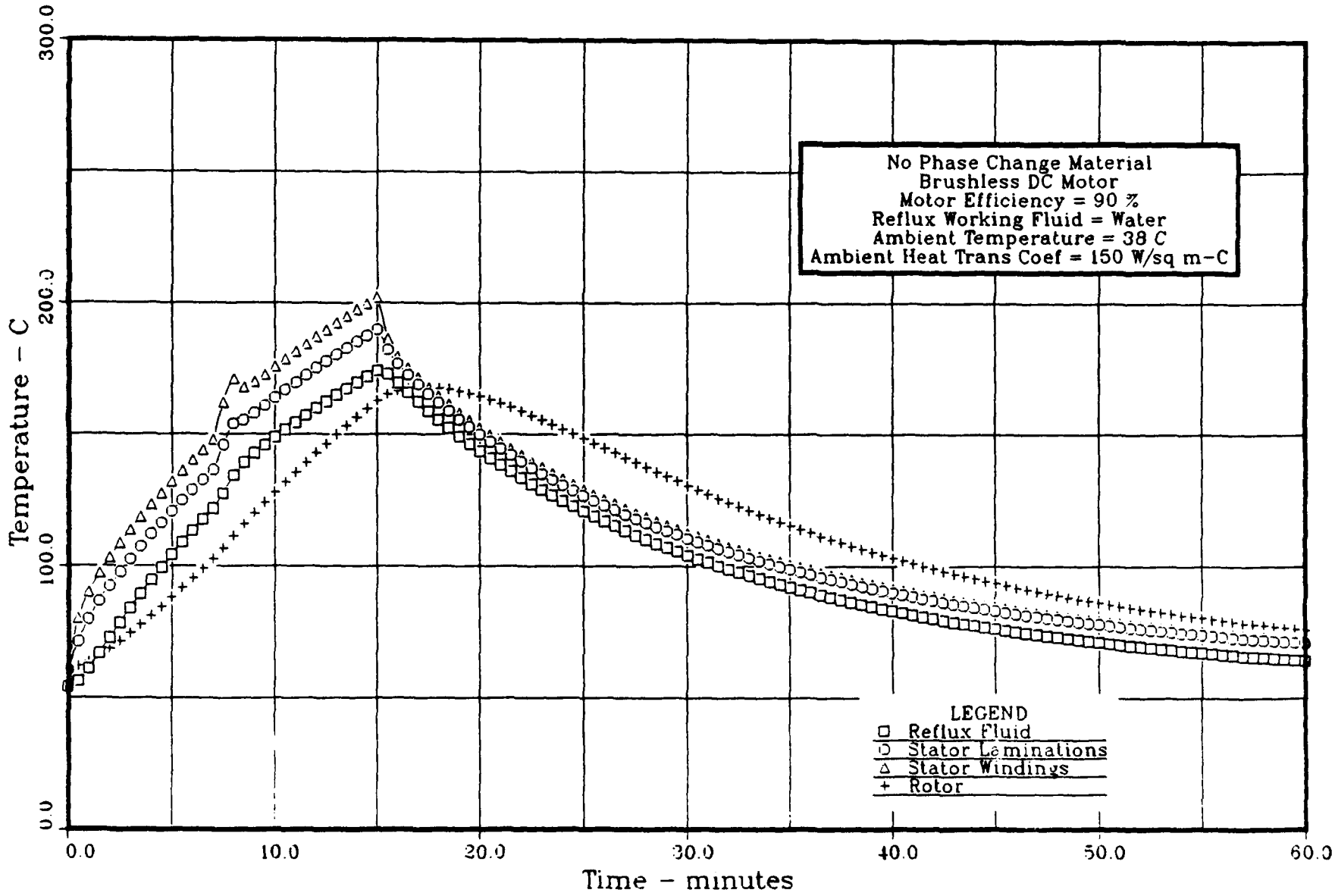

FIGURE 5.42 ADVANCED ACTUATOR COOLING
Temperature vs Time

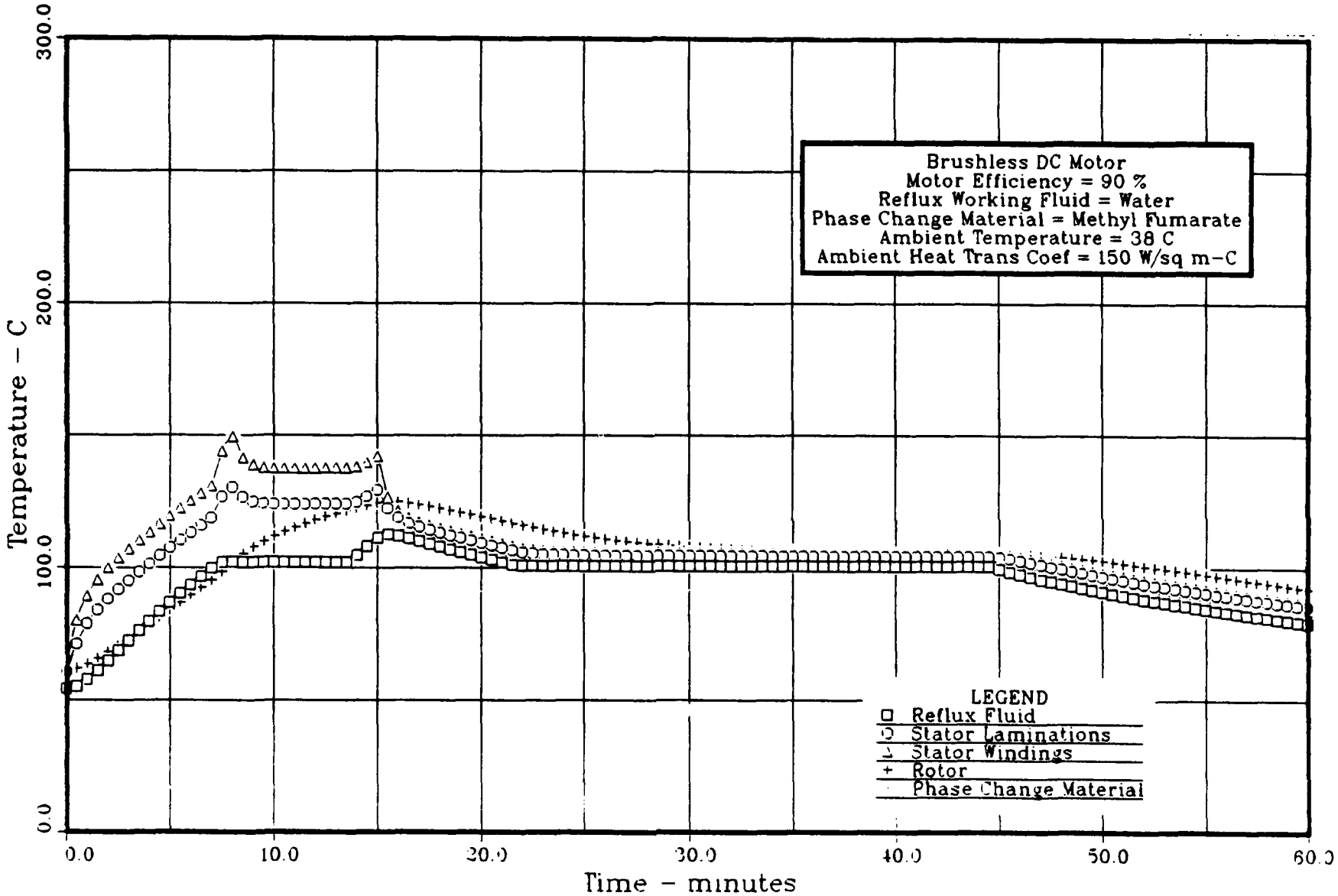

FIGURE 5.43 ADVANCED ACTUATOR COOLING
Temperature vs Time

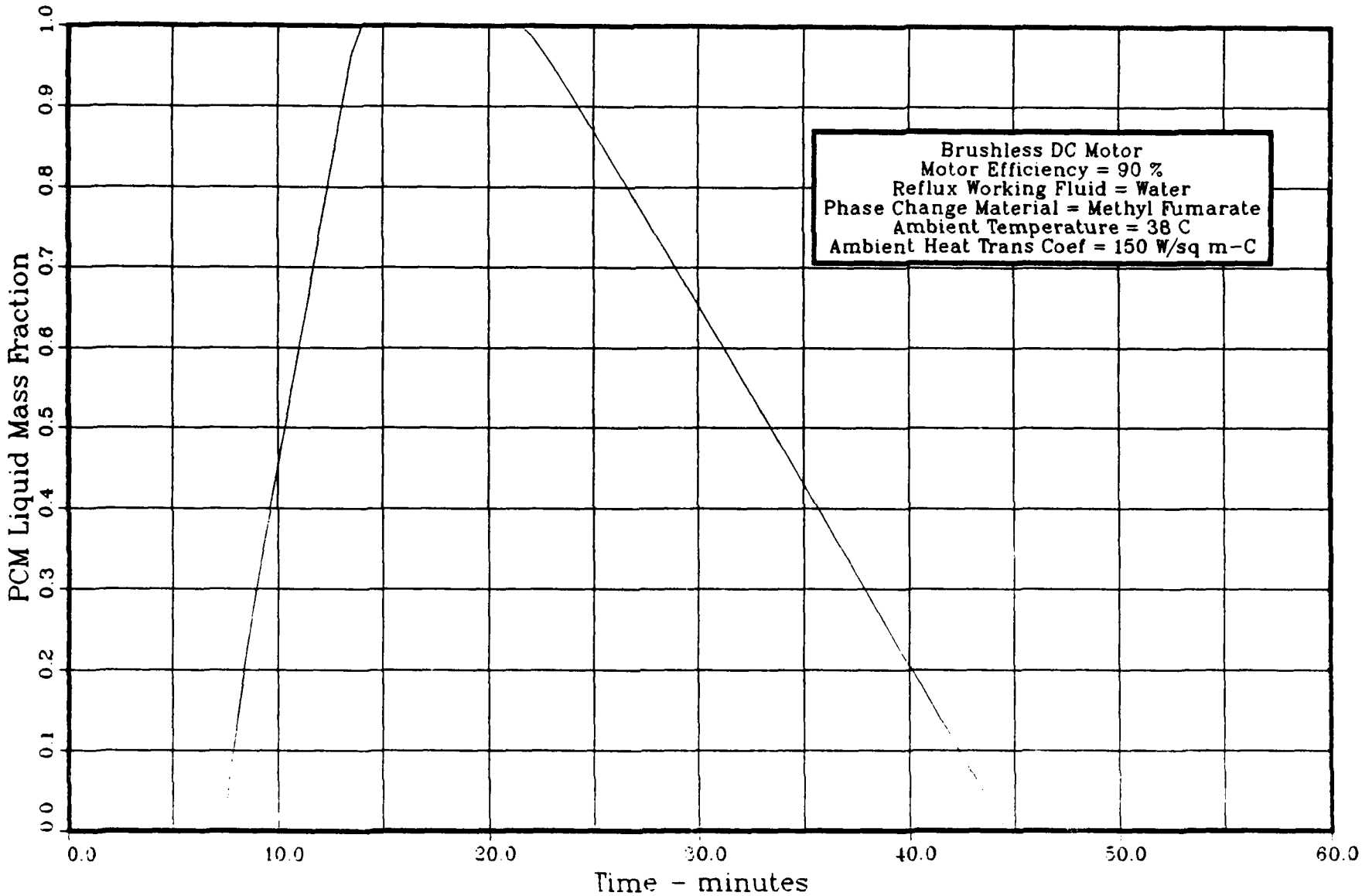

FIGURE 5.44 ADVANCED ACTUATOR COOLING
PCM Liquid Mass Fraction vs Time

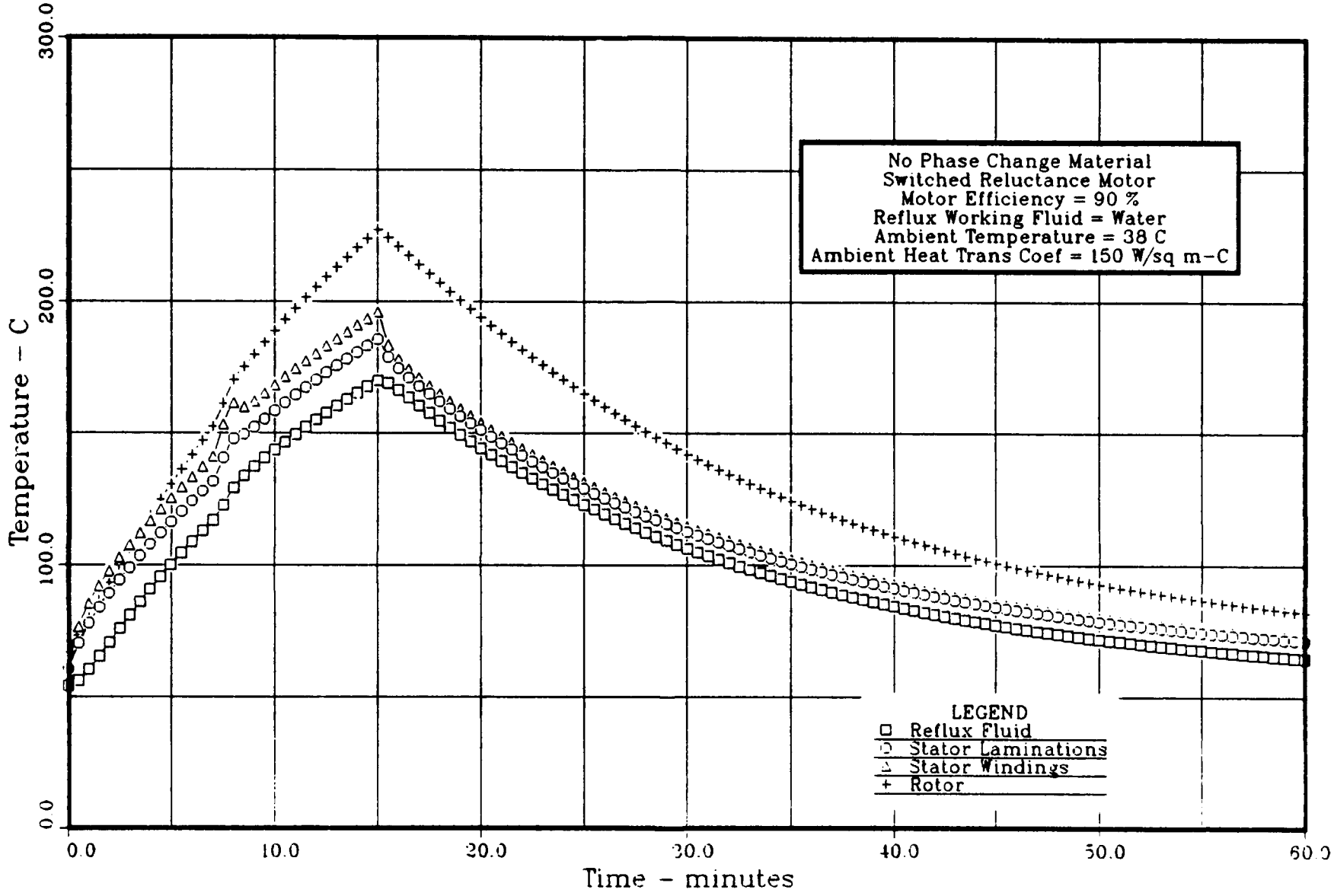

FIGURE 5.45 ADVANCED ACTUATOR COOLING
Temperature vs Time

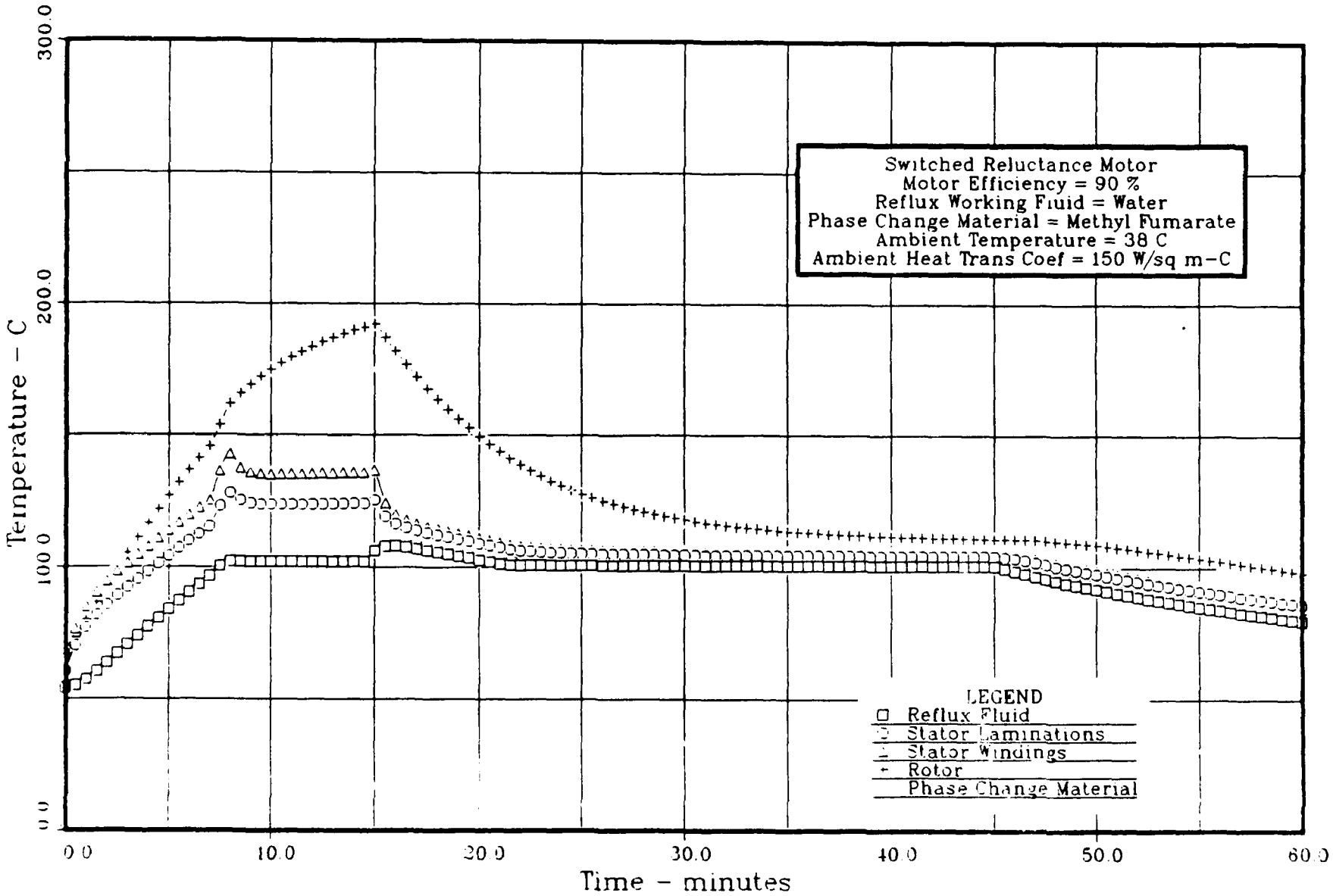

FIGURE 5.46 ADVANCED ACTUATOR COOLING
Temperature vs Time

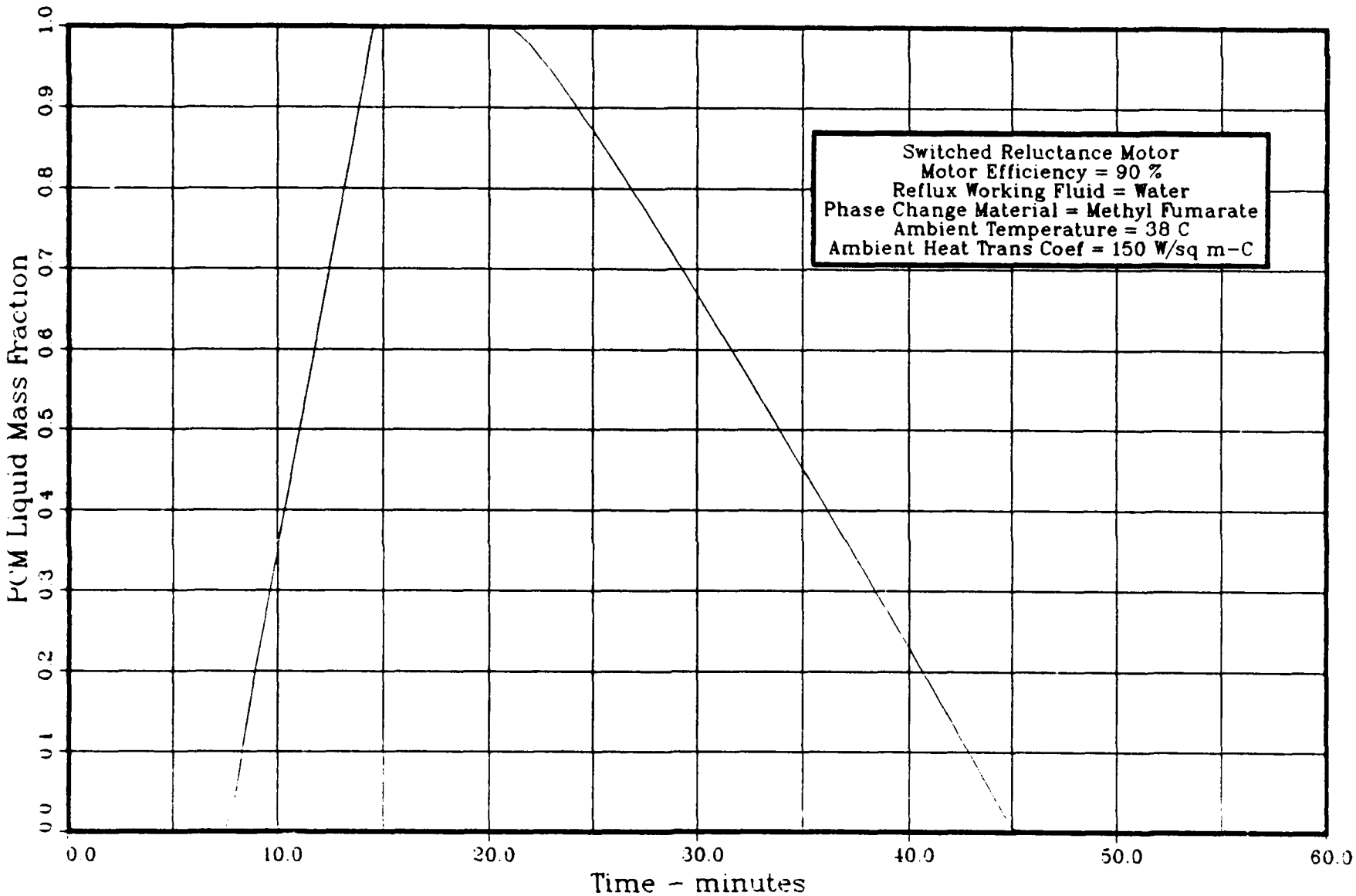

FIGURE 5.47 ADVANCED ACTUATOR COOLING
PCM Liquid Mass Fraction vs Time

Figures 5.48, 5.49 and 5.50 present temperatures as a function of time using toluene as a working fluid for coolers using no PCM, barium hydroxide octahydrate as a PCM, and acetamide as a PCM, respectively. Barium hydroxide octahydrate undergoes a phase change at 78 °C (172 °F) and acetamide transitions at 81 °C (178 °F). Figures 5.51 through 5.53 present similar data for a reflux cooler using FC-75 as a working fluid.

The following observations result from these figures:

- PCM reduces rotor temperatures by approximately 56 °C (100 °F) for typical hot day mission conditions.
- Working fluid temperatures for hot day mission conditions range from 46 °C to 177 °C (115 °F to 350 °F).
- Suitable PCM transition temperature for hot day mission conditions ranges from 77 °C to 107 °C (170 °F to 225 °F).
- Barium hydroxide octahydrate and acetamide thermally perform similarly since they undergo a phase transition at nearly the same temperature.
- Toluene and FC-75 perform similarly as working fluids since the working fluid boiling and condensation conductances do not dominate the overall cooler heat transfer process.
- Rotor temperatures lag behind stator temperatures during transients due to the low thermal conductance across the air gap which reduces the effective time constant of the rotor.
- PCM will increase motor reliability due to the reduction in peak stator temperatures.

The results of the transient mission analysis provide the guidelines for selection of the reflux working fluid and the PCM (see sections 5.5 and 5.6).

5.5 Working Fluid Comparison

Properties which affect the selection of a working fluid include the following:

- Freezing temperature.
- Critical temperature.
- Saturation temperature and pressure.
- Heat of vaporization.
- Liquid/vapor density difference.
- Boiling wall superheat.
- Critical heat flux.
- Boiling incipience.

Freezing temperature as a selection criteria particularly applies to water as working fluid, since water freezes at a temperature within the temperature limitations of expected actuator ambients and water expands upon freezing. Therefore, water introduces heat exchanger mechanical design considerations due to freezing, though often desirable as a heat transfer fluid.

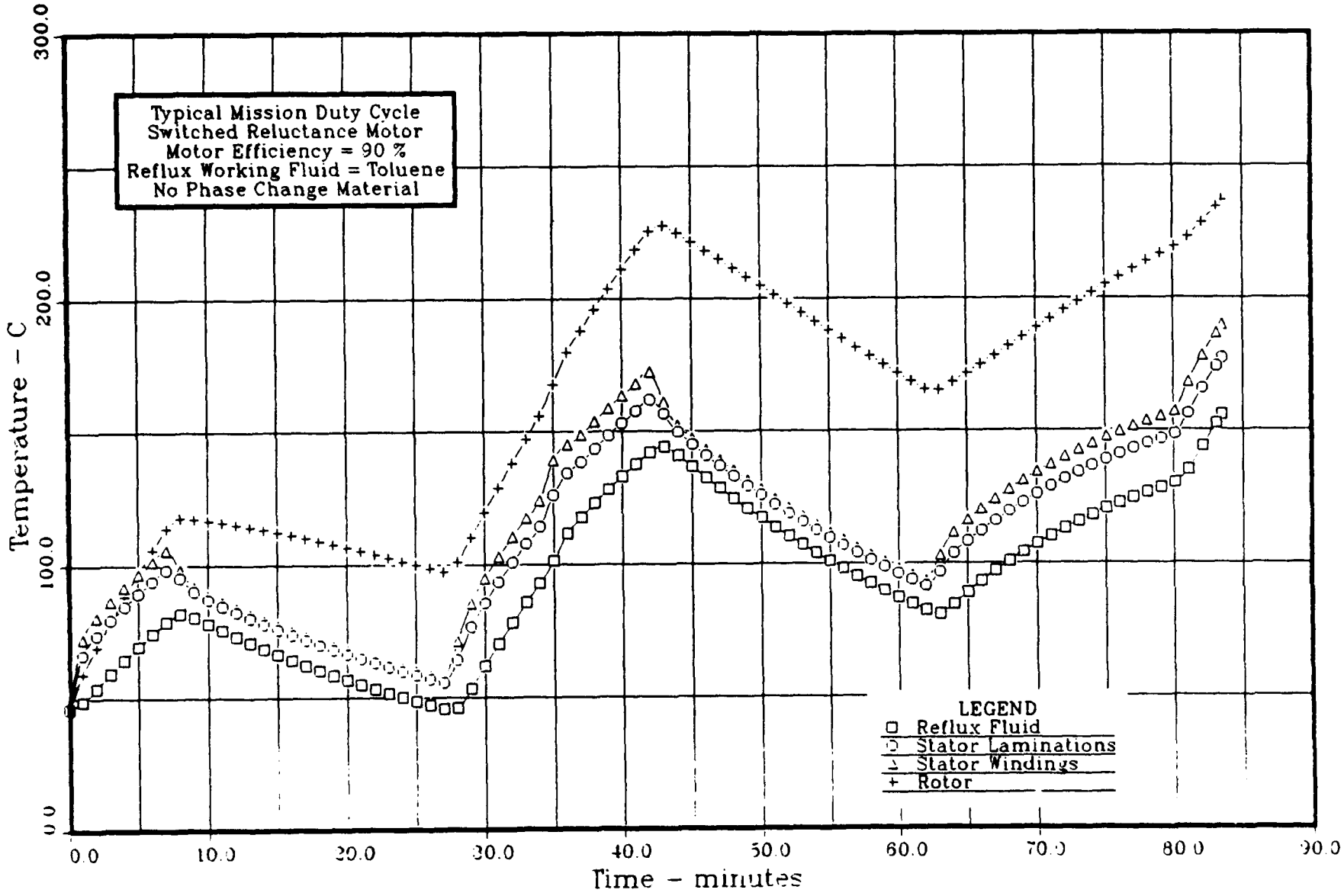

FIGURE 5.48 ADVANCED ACTUATOR COOLING
Temperature vs Time

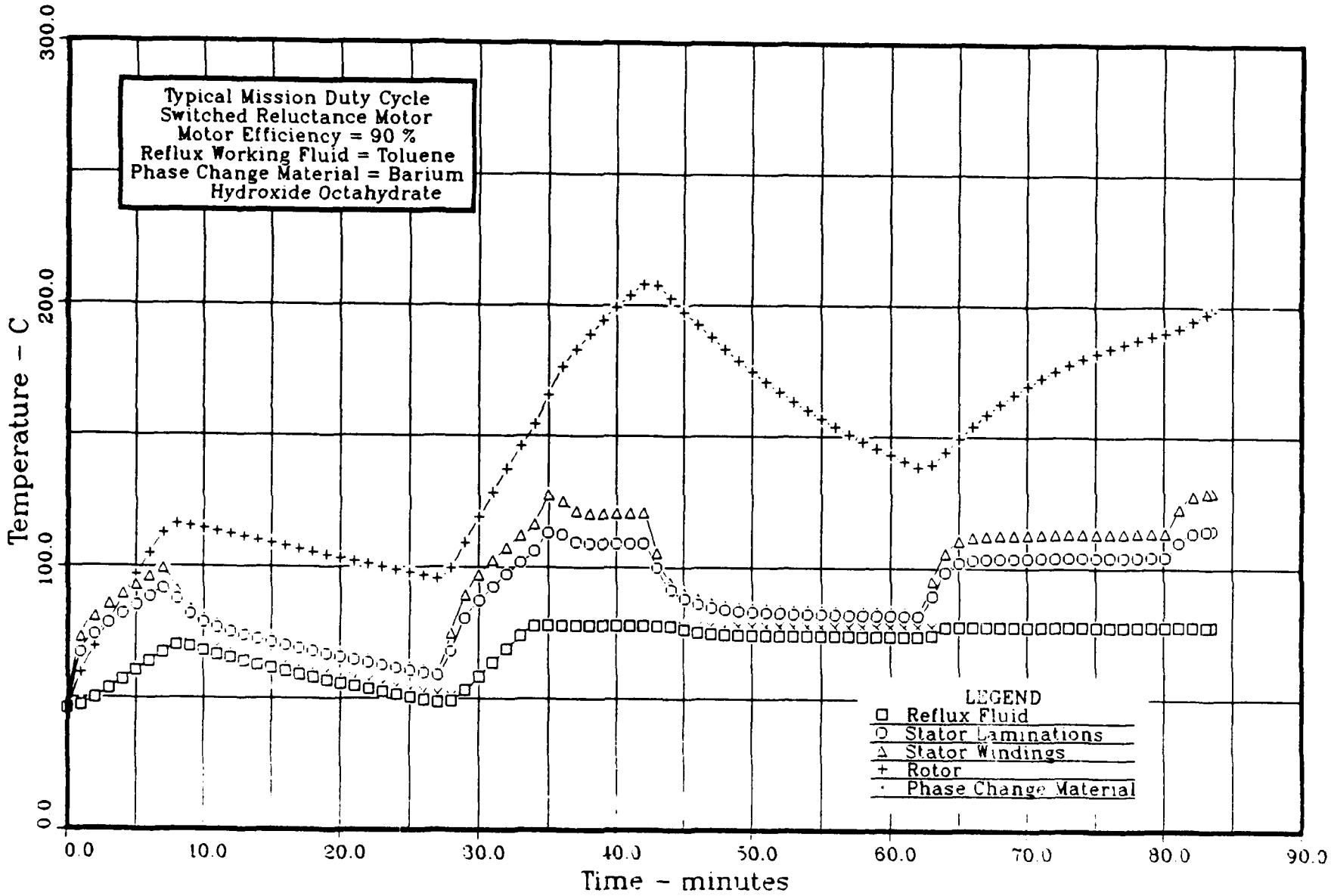

FIGURE 5.49 ADVANCED ACTUATOR COOLING
Temperature vs Time

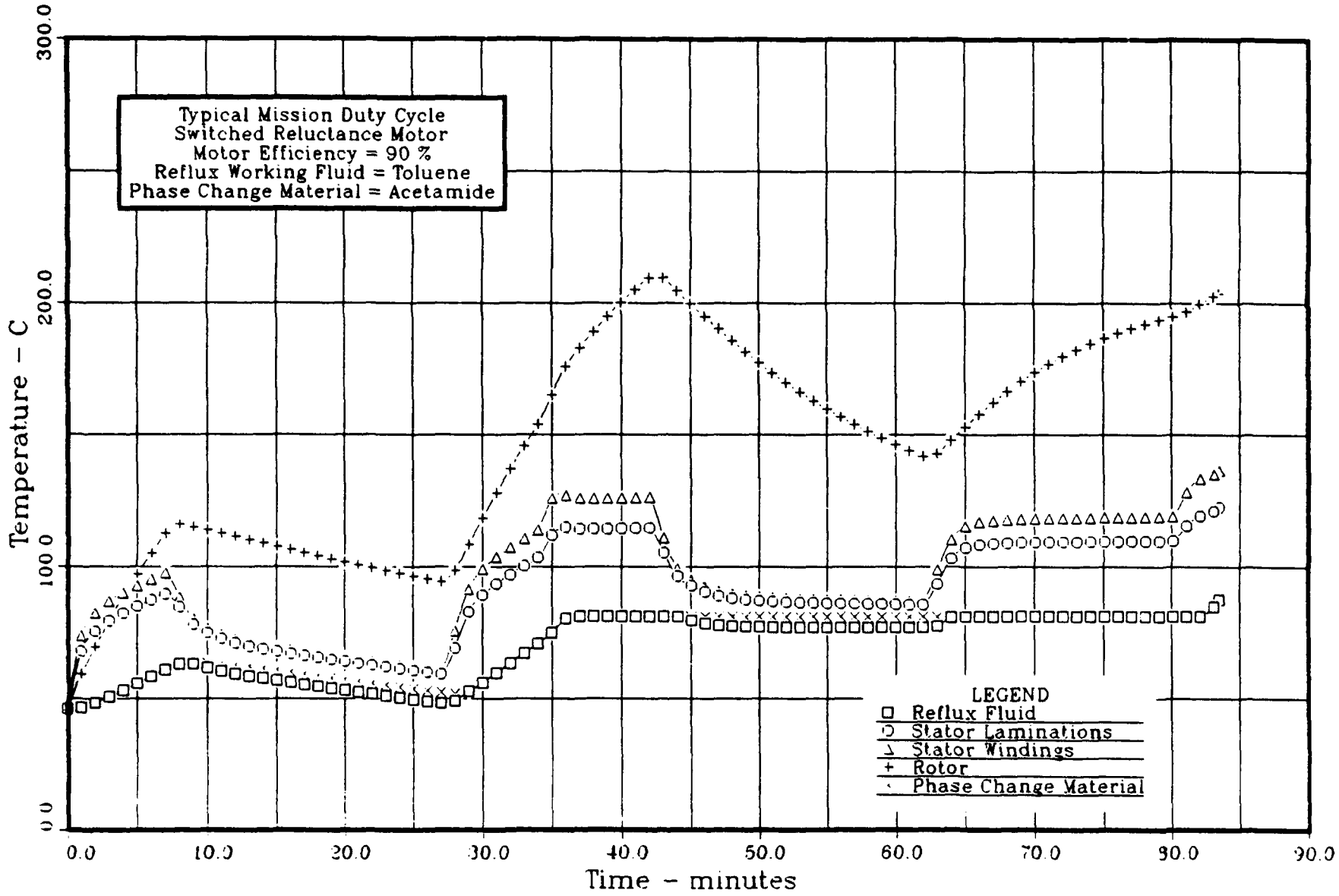

FIGURE 5.50 ADVANCED ACTUATOR COOLING
Temperature vs Time

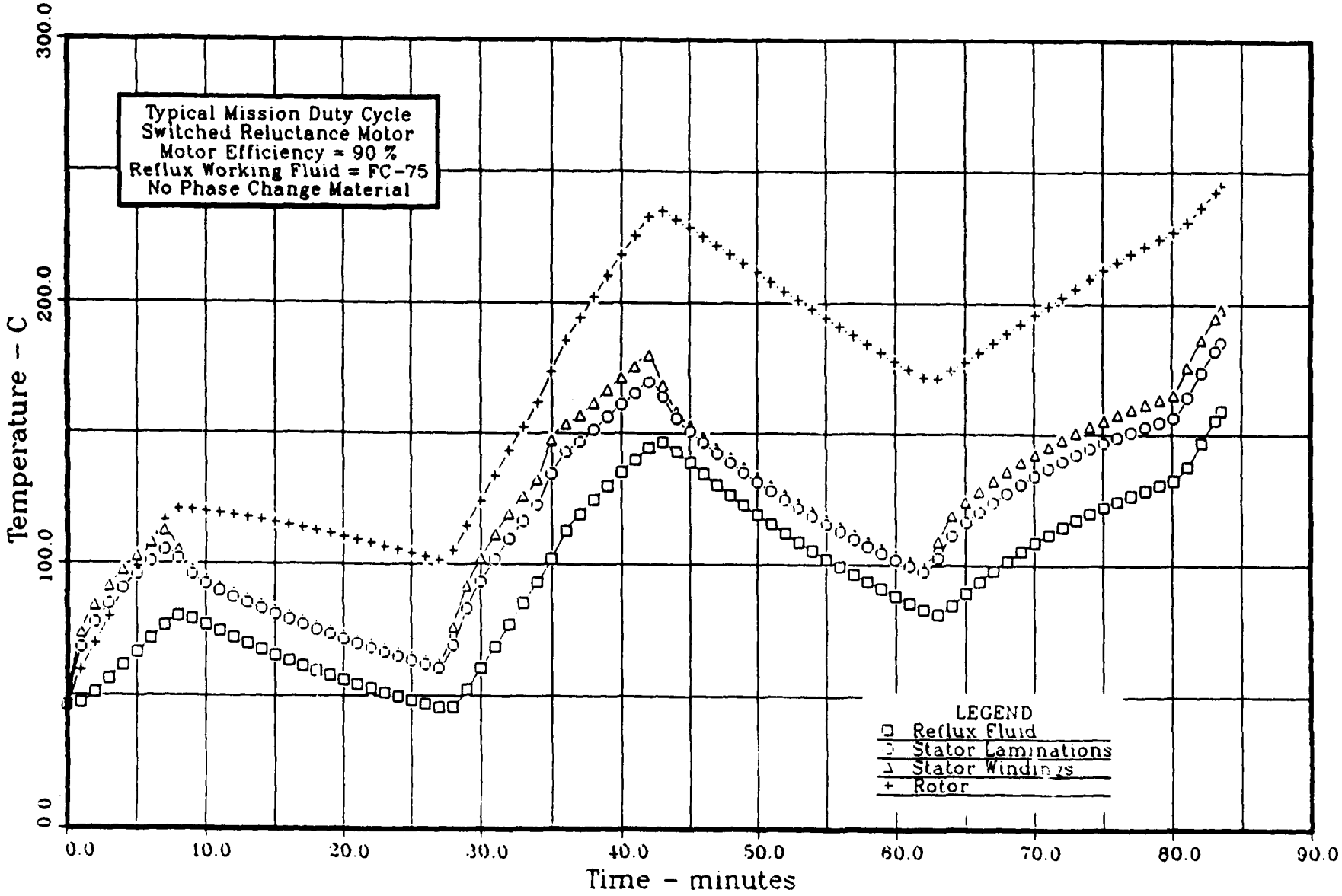

FIGURE 5.51 ADVANCED ACTUATOR COOLING
Temperature vs Time

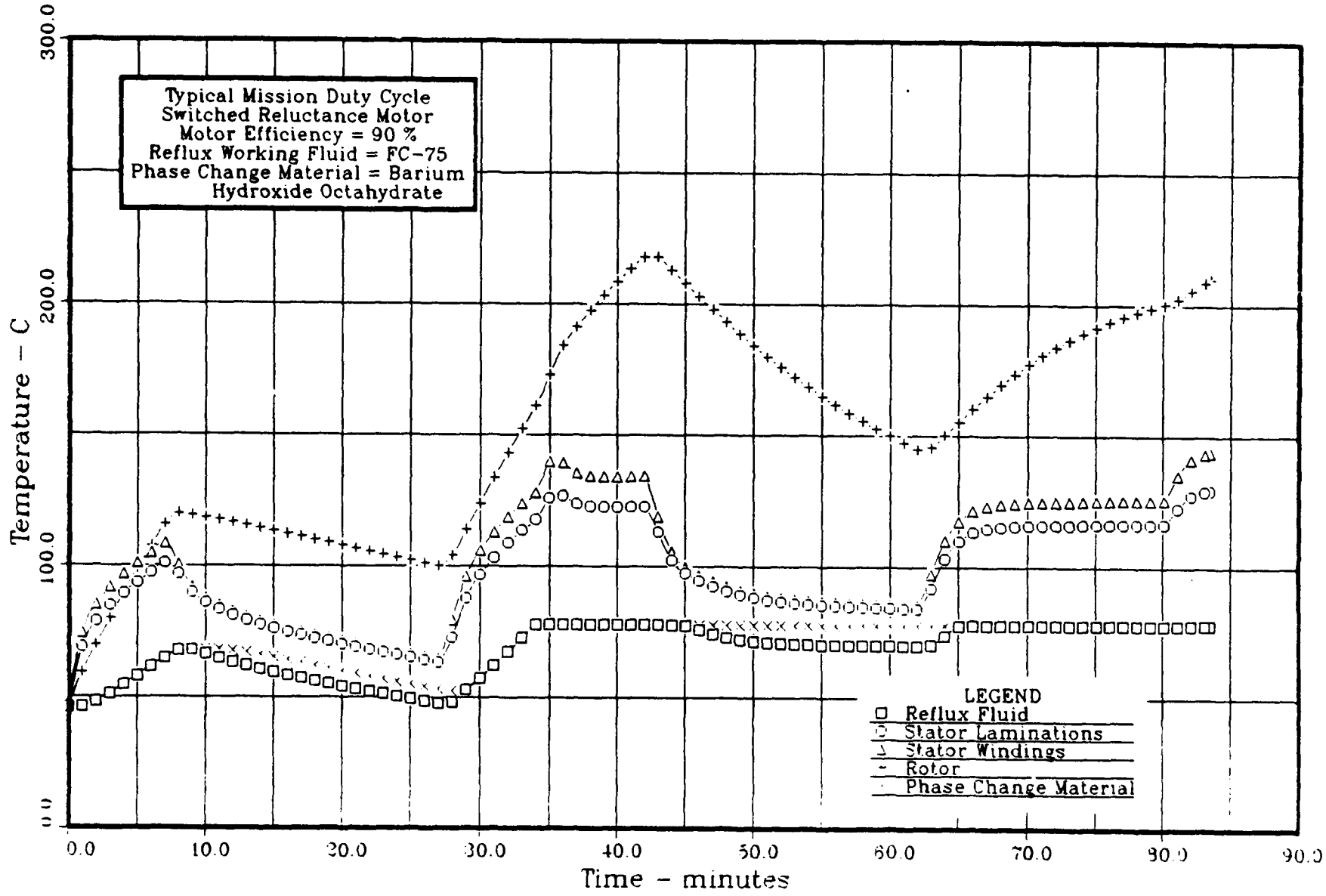

FIGURE 5.52 ADVANCED ACTUATOR COOLING
Temperature vs Time

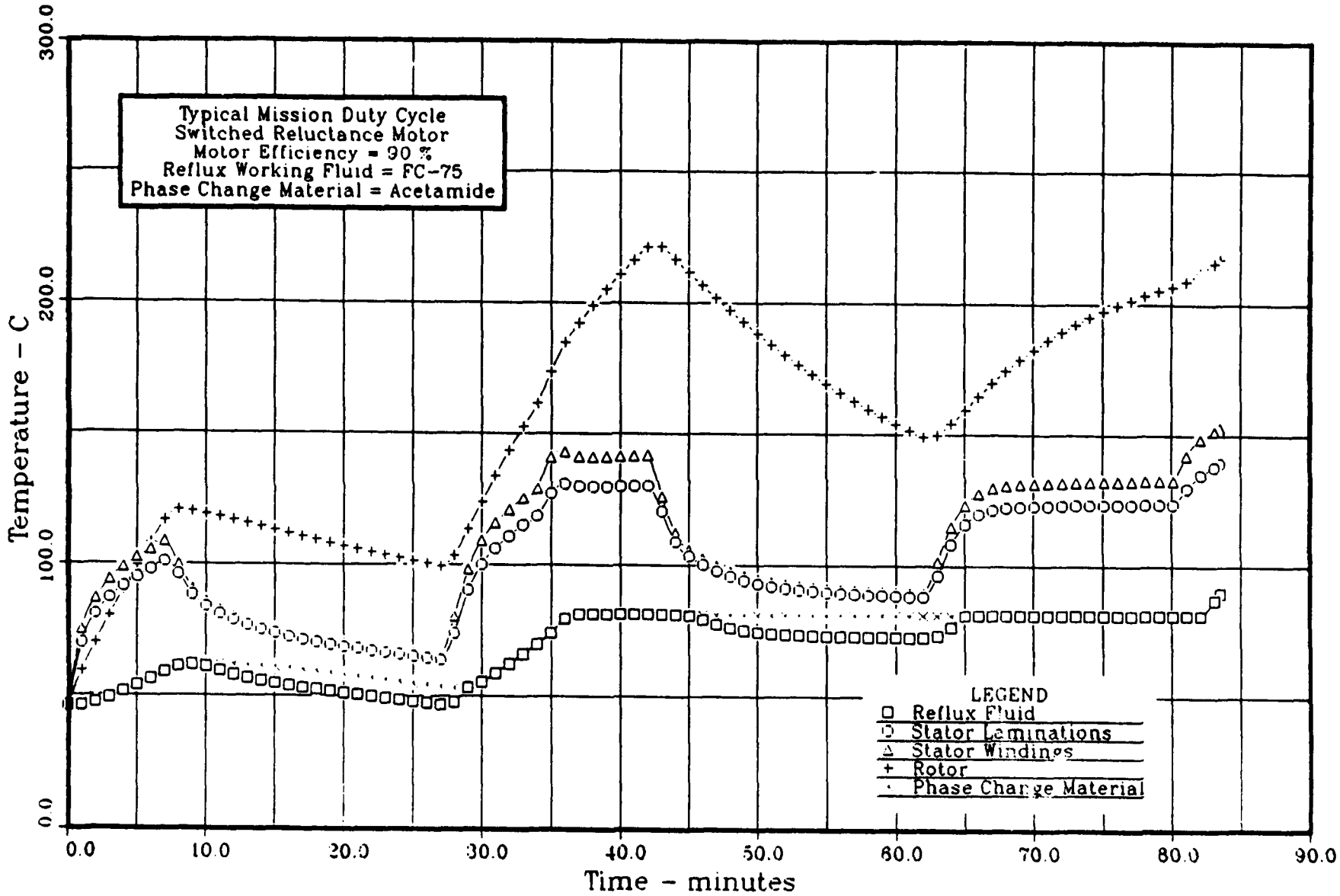

FIGURE 5.53 ADVANCED ACTUATOR COOLING
Temperature vs Time

Critical temperature becomes an issue when operating temperatures exceed critical fluid temperature, since the density difference between the liquid phase and the vapor phase provides the motive force for fluid circulation. Supercritical fluids would not exhibit the distinct density difference between phases.

The relationship between fluid saturation temperature and pressure effect the mechanical design of the heat exchanger since the heat exchanger must contain the fluid pressure. Large saturation pressures within the operating temperature range would result in a heavier heat exchanger in order to carry the loads of containing the fluid pressure.

Heat of vaporization affects the recirculating fluid flow rate required to carry the heat duty.

The density difference between the liquid and vapor phases provides the motive force for fluid recirculation. Fluids operating above the critical point would have little density difference between the phases and poor recirculation rates.

The boiling wall superheat provides a measure of fluid boiling characteristics. The results of the steady state parametric trade studies suggest that the boiling and condensation heat transfer processes do not control the overall heat transfer process, therefore lessening the importance of boiling wall superheat as a selection criteria.

Critical heat flux provides a measure of the limiting value of heat flux that results in nucleate boiling. Heat fluxes that exceed the critical heat flux result in transition or film boiling, and subsequently higher wall superheats.

Boiling incipience represents the heat flux required to initiate the change from single phase convection to two phase boiling. Sundstrand experience with reflux coolers has shown that boiling incipience critically affects reflux cooler performance. Heat fluxes which do not result in boiling result in nonisothermal heat exchangers and very poor heat transfer rates.

Figure 5.54 presents a comparison of the candidate fluids and the properties of interest, with the exception of boiling incipience. Of the properties illustrated, the saturation pressure provides a more critical selection criterion than other properties, since the boiling and condensation heat transfer conductances did not control the overall heat transfer process of the reflux cooler.

Figure 5.55 compares boiling incipience for the candidate fluids estimated by three methods:

- Homogenous nucleation [22].
- Heterogeneous nucleation based on nucleation site size [20].
- Heterogeneous nucleation neglecting available nucleation site size [21].

Figure 5.55 illustrates large variations between the three methods. Homogeneous nucleation involves bulk boiling within the fluid itself; whereas, heterogeneous boiling involves boiling at a surface. Homogeneous boiling requires larger superheats, therefore providing a worst case analysis of boiling incipience. Sundstrand estimated heterogeneous boiling using two methods. The one method does not account for the available sites for nucleation, while the other method uses an estimate of the nucleation site availability as its basis. Neglecting the availability of nucleation sites may lead to overly optimistic boiling incipience estimates; whereas, some estimate of nucleation site availability leads to more realistic boiling incipience estimates.

Fluid	Freezing Temperature (°C)	Critical Temperature (°C)	Sat. Temperature (°C)	Sat. Pressure (kPa)	Heat of Vapor (kJ/kg)	Density Difference (ρ_l-ρ_v) (kg/m³)	Wall[1] Superheat (°K)	Critical Heat Flux (W/cm²)
Water	0	374	121 316	205.6 10625	2195 1276	942.9 619.2	9.32 3.68	146.7 372.3
Toluene	-	320.8	121 316	135.3 3837	357.5 114.0	760.1 259.0	33.82 4.04	31.4 14.3
Dowtherm A*	12.0	497	121 316	1.39 312.6	355.0 264.9	979.0 779.5	162.12 29.90	5.1 36.1
Dowtherm E*	<-17.8	-	121 316	18.2 1211	301.3 200.6	1193 862.3	79.62 24.23	15.3 55.0
FC-72*	<-53.9	178	121 316	593.1 -	63.7	1310	12.92	17.7
FC-75*	<-53.9	227	121 316	171.5 -	76.49	1468	52.72	12.7
EGW 60% by volume	-52.2	-	121 316	147.6	2195	1010	35.36	149.3

[1] Evaluated for a heat flux of 20 W/cm².

* Dowtherm is a registered trademark of Dow Chemical Company.

* FC-72 and FC-75 are registered trademarks of 3M Company.

* Selected based upon saturation pressure, freezing temperature, wall superheat, boiling incipience, non-flammability, and dielectric strength.

FIGURE 5.54 REFLUX WORKING FLUIDS COMPARISON

FLUID	HOMOGENEOUS NUCLEATION [7,4]		HETEROGENEOUS NUCLEATION [5,4] -based on bubble radius-		HETEROGENEOUS NUCLEATION [6,4] -based on heat flux-					
	Boiling Incipience ΔT (°R)	Boiling Incipience Heat Flux (Watts/cm²) [1]	Boiling Incipience ΔT (°R)	Boiling Incipience Heat Flux (Watts/cm²) [1]	Boiling Incipience ΔT (°R)	Boiling Incipience Heat Flux (Watts/cm²) [1]	Critical Heat Flux (Watts/cm²) [4]	Wall Superheat (°R) [2,4]	Saturation Pressure @ 250°F (psia)	Saturation Pressure @ 350°F (psia)
Water	347	34	12.1	0.5	0.03	0.0003	147	10.6	30	135
Tolerance	262	6	69.7	1.2	0.02	0.0001	31	38.4	19.6	70
Dowtherm A	546	12	8154	346	8.7	0.07	5.3	190	0.2	1.7
Dowtherm E	458	10	848	21.2	0.6	0.002	16	95	2.6	13.5
FC-72	51	0.6	2.8	0.02	0.0008	0.0000	18	3.3-14.6 [3]	86	259
FC-75	118	1.6	10.1	0.07	0.003	0.000	13	13.8-59.9 [3]	25	94
EGW (60% by/lb)	347	17	12.1	0.25	0.03	0.001	149	40.4	21	–

1. Based on a natural convection on a vertical flat plate.
2. Based on pool boiling with a heat flux of 5 Watts/cm².
3. C_{sf} in Rohsenhow's pool boiling correlation ranging from 0.003 to 0.013.
4. Data for saturation temperature of 250°F.
5. Rohsenow, W.M., 1982, "Pool Boiling," Handbook of Multiphase Systems, ed. Hestroni, G., McGraw Hill-Hemisphere, New York, 1982.
6. Bergles, A.E. and Rohsenow, W.M., 1964, "The Determination of Forced Convection Surface Boiling Heat Transfer," J. Heat Transfer, Vol. 86, pp. 365-372.
7. Lienhard, J.H., 1976, "Correlation of Limiting Liquid Superheat," Chem. Engng. Sci., Vol. 31, pp. 847-849.

FIGURE 5.55 ADVANCED ACTUATOR COOLING - FLUIDS COMPARISON

Based on the comparison of candidate fluids and observations noted as a result of steady state parametric studies, Sundstrand recommends 3M company's fluorinated organic compound, FC-75, as the demonstration working fluid. Sundstrand based this recommendation upon saturation pressure, freezing temperature, wall superheat, boiling incipience, non-flammability, and dielectric strength.

5.6 Phase Change Material Comparison

Figure 5.56 presents a comparison of PCMs and their properties for PCMs with transition temperatures ranging from 65 to 190 °C (150 to 375 °F). The figure presents transition temperature and heat of transition on both a per unit mass and per unit volume basis. Selection of the transition depends upon the nominal operating temperatures of the reflux system. During low power conditions the PCM transition temperature should exceed the reflux fluid saturation temperature; whereas, during transient high power conditions the steady state saturation temperature should exceed the PCM transition temperature in order to take advantage of the PCM latent heat. The heat of transition on a per unit mass and a per unit volume basis effects the required PCM mass and volume required to meet known transient heat duty requirements.

Figure 5.56 breaks the PCMs into four categories:

- Nonparaffin organics.
- Hydrated salts.
- Solid-Solid.
- Metallic.

According to reference [4] the following statements apply to the four categories of PCMs:

Nonparaffin Organics:

- Most numerous of PCMs.
- Flammable.
- Some are toxic.
- Relatively low thermal conductivities.
- Attractively high heats of fusion on both a per unit mass and per unit volume basis.

Salt Hydrates:

- Attractively high heats of fusion on both a per unit mass and per unit volume basis.
- Small volume change upon melting.
- Relatively high thermal conductivities.
- Corrosive.

Solid-Solid:

- Do not require containment structure.
- Small volume change upon melting.
- Mixtures of pentaerythritol and pentaglycerine allow tailoring of transition temperature.

Material	Trans. Temp. (°F)	Heat of Trans. (Btu/lbm)	Heat of Trans. (Btu/ft^3)	Ref.
Nonparaffin Organics:				
P-Chloroanaline	156	66.8	5060	4
Stearic Acid	157	85.5	4520	4
Bromcamphor	171	74.7	6760	4
Durene	174.7	67.2	3510	4
Acetamide	178	104	7510	4
Methyl Brombenzoate	178	54.2		4
Dimethytartrate	189	63.0	5110	4
Ethyl Lithium	203	167		4
α Napthol	205	69.9	4780	4
Glutaric Acid	207.5	37.4	5990	4
P-Xylene Dichloride	212	59.1		4
Methyl Fumarate	216	104	11660	4
Catechol	219.7	88.7	7590	4
Resorcinol	230			4
Quinone	239	73.5	6040	4
Acetanilide	239	65.2	4920	4
Succinic Anhydride	246	87.5	6030	4
Benzoic Acid	251.1	60.9	4813	4
Stilbene	255	71.7	5200	4
Benzamide	261.0	72.7	6080	4
Phenacetin	279	58.7		4
α Glucose	286	74.9	7220	4
Acetal-p-toluidine	295	77.2		4
Phenylhydrazone	311	57.9		4
Salicylic Acid	318	85.5	7700	4

FIGURE 5.56 CANDIDATE PCMs

Benzanilide	322	69.7		4
o-Mannitol	331	126.1	11740	4
Hydroquinone	342.3	111	9390	4
p-Aminobenzoic Acid	369	65.6		4
Hydrated Salts:				
$Al(NO_3)_3 \bullet 9H_2O$	158	67		5
Barium Hydroxide Octahydrate	172	129	17600	4
$Mg(NO_4)_2 \bullet 6H_2O$	192	70	7140	2
Aluminum Potassium Sulfate Dodecahydrate	195.8	79		4
$Mg(NO_3)_3 \bullet 6H_2O$	203	68.8	6271	5
Magnesium Chloride Hexahydrate	243	72.5	7105	2,4
Sodium Acetate Trihydrate	279	74	6610	4
Solid-Solid:				
Neopentyl Glycol	118	51.2	3379	15
Pentaglycerine	192	59.8	4545	15
Polyethylene	270	86	5160	3
Pentaerythritol	363	115.7	9625	1,15
Metallic:				
Corrobend Eutectic	158	14.0	8180	4

FIGURE 5.56 (CONT'D) CANDIDATE PCMs

Metallics:

- Low heat of transition per unit mass.
- High heat of transition per unit volume.
- High thermal conductivities.

Based upon the transient mission analysis presented in section 5.4.2, the transition temperature of the PCM for the demonstration cooler should fall in the range of 77 to 107 °C (170 to 225 °F). Sundstrand narrowed the selection to acetamide and barium hydroxide octahydrate based upon the transition temperatures and heats of transition. However, consideration of compatibility with aluminum eliminates barium hydroxide octahydrate due to corrosiveness with aluminum. Therefore, Sundstrand recommends acetamide as the PCM for the demonstration reflux cooler.

5.7 Demonstration Motor Selection

Based on a trade study of three Sundstrand motor designs, Sundstrand recommends modifying a National Launch System (NLS) actuator motor design for the demonstration motor. Sundstrand recommended an approach using the NLS motor in the original motor, but performed the trade study to confirm the motor selection. The recommended motor uses an induction design with sealed bearings, and provides 35 hp at 15,000 rpm. Sundstrand selected the design based upon its proven mechanical design, prototypic bearing approach, power supply availability, parts availability, and less complex motor design. The availability of laminations and rotor bars and the less complex motor design promise to provide cost advantages.

The three motors studied included:

- Selected NLS motor design.
- Modified NLS motor design using a split rotor/stator.
- LV-100 switched reluctance motor.

Figure 5.57 provides a comparison of the three motors. All of the motors require modification in order to include the passive reflux cooled heat exchanger as an integral part of the motor housing.

Though switched reluctance motors are more consistent with the 270 VDC More Electric Airplane (MEA) technology than induction or brushless DC motors, Sundstrand did not select the LV-100 motor for a number of reasons. The LV-100 motor uses an oil flow loop to provide bearing lubrication and rotor cooling which would result in compromised testing of the passive cooling approach proposed for EMA cooling. Elimination of active rotor cooling would require major modifications to the bearing lubrication flow loop or replacement of the oil lubricated bearing with a sealed bearing design. In addition, testing of the switched reluctance motor would require use of an Army power supply (requiring approval) or the purchase of a power supply at a considerable cost penalty (approximately $130,000). Since the primary objective of the program involves demonstrating the passive cooling approach for EMAs, selection of an induction motor rather than a switched reluctance motor will not invalidate results of the development program.

	INDUCTION	PERMANENT MAGNET BRUSHLESS DC	SWITCH RELUCTANCE
RATING	FRACTIONAL TO 1000'S OF KW	FRACTIONAL TO 100'S OF KW	FRACTIONAL TO 1000'S OF KW
SPEED	< 200 M/SEC PERIPHERAL SPEED	< 250 M/SEC PERIPHERAL SPEED	< 300 M/SEC PERIPHERAL SPEED
EFFICIENCY	85 - 92%	HIGH: 90 - 95%	LOW: APROX 85%
LOSSES	IRON AND COPPER ROTOR AND STATOR	IRON AND COPPER STATOR ONLY	IRON/COPPER STATOR IRON ROTOR
WEIGHT	INTERMEDIATE	MINIMUM	HIGHEST
TEMPERATURE	INSULATION LIMITED	MAGNET LIMITED (150 DEGREES C)	INSULATION LIMITED
STALL TORQUE	GOOD	GOOD	VERY GOOD - MINIMAL LOSSES
FAULT TOLERANCE	NO	NO	YES
COST	INTERMEDIATE	HIGH	LOW

FIGURE 5.57 ELECTRIC MOTOR COMPARISON

Sundstrand also evaluated a variation of the NLS motor design currently in development that uses a split rotor/stator design that provides fail degraded performance. Sundstrand did not select the NLS split motor design since the motor uses a nonprototypic rotor/stator design, and the motor mechanical design has not been proved by test.

5.8 Manufacturing Approach

Sundstrand selected the brazed plate fin heat exchanger manufacturing approach illustrated in Figure 5.58. The selected manufacturing approach offers the following advantages:

- Proven manufacturing approach.
- Integral motor housing/cooler.
- Provides extended surface.
- Alternating layers of working fluid and PCM reduces conduction lengths.
- Vertically oriented fins in the working fluid layers provides direction of recirculating flows.
- Horizontally oriented fins enhance conductivity within PCM layers and promote lateral heat spreading.

Though Figure 5.58 illustrates horizontally oriented fins within the PCM layers consideration of the freeze and thaw process may suggest vertically oriented fins. Vertically oriented fins would allow free movement of the liquid within the heat exchanger during the thaw process.

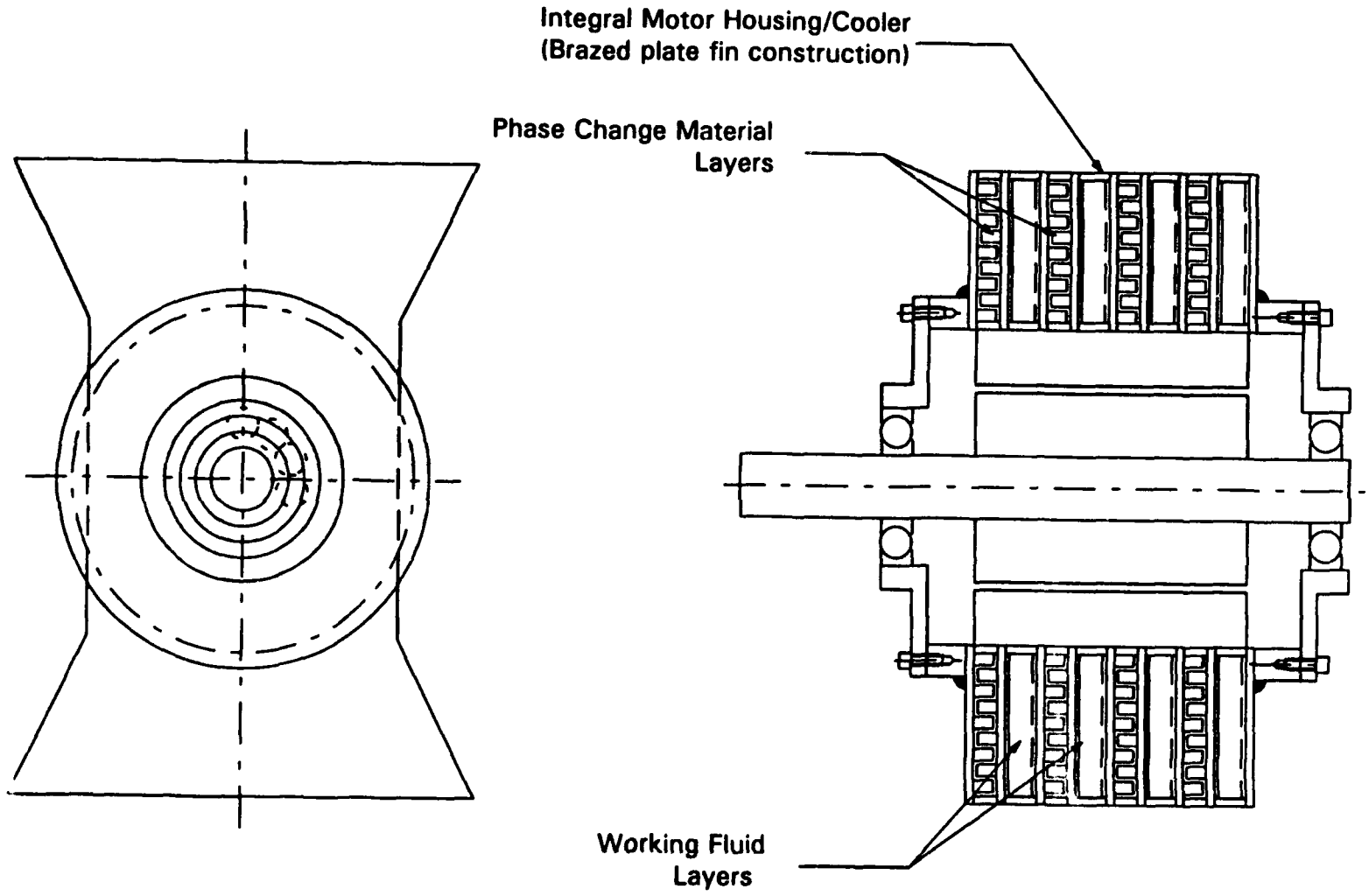

Figure 5.58 Advanced Actuator Cooling - Passive Cooling Concept.

6.0 CONCLUSIONS

Based on the tasks completed during Phase I Sundstrand has reached the following conclusions:

- EMA cooling offers several challenges due to actuator power levels approaching a level of 50 hp, limited heat sink availability for passive cooling approaches, and weakly defined actuator duty cycles, dependent upon type of actuator.

- Capitalizing upon the advantages of EMAs over conventional hydraulic actuators (i.e., elimination of hydraulic lines) requires a passive actuator cooling approach like reflux cooling.

- The controlling heat transfer conductances for a passive reflux EMA cooler include ambient convection and convection across the motor air gap. These conclusions suggest the use of a large condenser foot print area to make use of a large aircraft skin area for convection, and result in difficult cooling of motor rotors.

- The passive reflux cooling approach provides direct cooling of motor stators but indirectly cools motor rotors; however, motor reliability depends more upon stator temperatures than rotor temperatures.

- Magnet temperature limitations result in difficult passive cooling of brushless DC motors despite the fact that rotor losses for the other motors considered exceed those of brushless DC motor.

- High rotor losses result in difficult cooling of induction motors despite the fact that the upper temperature limitation for induction motors exceeds brushless DC motors.

- Rotor materials and moderate rotor losses suggest switched reluctance motors as the most likely candidate for passive reflux cooled EMAs.

- PCM reduces motor temperatures for lower frequency power transients such as high power phases of combat missions with the inherent thermal inertia of the motor dominating at lower frequencies.

7.0 RECOMMENDATIONS

Based upon the tasks completed during Phase I Sundstrand makes the following recommendations:

- The robust nature of switched reluctance rotors and inherent fail degraded performance justify switched reluctance motors as the motor selection for future passive reflux cooled EMAs.

- Low frequency actuator power transients, such as the combat phase of a mission, justify the use of PCMs, while PCMs provide no advantage for high frequency transients, such as turbulence.

- Sundstrand recommends a modified NLS induction motor for the demonstration motor based upon proven mechanical design, prototypic bearing approach, power supply availability, and less complex motor design.

- Sundstrand recommends acetamide as the demonstration PCM based upon transition temperature, heat of transition, and compatibility with aluminum. This selection could vary depending on mission requirements.

- Sundstrand recommends FC-75 as the demonstration working fluid based upon saturation pressure, wall superheat, boiling incipience, nonflammability, and dielectric strength.

- Sundstrand recommends a brazed plate fin heat exchanger construction since this approach provides a proven manufacturing technique, extended surface, reduced conduction lengths, and enhanced conduction within the PCM layers.

8.0 REFERENCES

[1] Glen E. Thorncraft and Fred S. Gunnerson, Performance Evaluation of a Solid State Phase Change Material for Thermal Storage Applications, Proceedings of the 26th Intersociety Energy Conversion Engineering Conference, Boston, Massachusetts, August 4-9, 1991.

[2] W.M. Rohsenow, J.P. Hartnett and E.N. Ganić, Handbook of Heat Transfer Applications, 2nd Edition, McGraw-Hill Book Company, 1985.

[3] Eric C. Guyer, Handbook of Applied Thermal Design, McGraw-Hill Inc., 1989.

[4] D.V. Hale, M.J. Hoover and M.J. O'Neill, Phase Change Materials Handbook, Lockheed Missiles and Space Company, NASA Contractor Report CR-61363, September 1971.

[5] William R. Humphries and Edwin O. Griggs, A Design Handbook for Phase Change Thermal Control and Energy Storage Devices, NASA Technical Paper 1074, November 1977.

[6] "Dowtherm Heat Transfer Fluids," The Dow Chemical Company, 1969.

[7] "Fluorinert Electronic Liquids - Product Manual," 3M Company, 1990.

[8] "Prestone II - Physical Properties Data," Union Carbide Corporation, Eighth Edition, 1980.

[9] Sundstrand Toluene Properties Handbook, 1974.

[10] G.J. Ganz, C.B. Allen, J.R. Downey, Jr., and R.P.T. Tomkins, "Physical Properties Data Compilations Relative to Energy Storage, I. Molten Salts: Eutectic Data," Report NSRDS-NBS 61, Part I, 1978.

[11] G.J. Ganz, C.B. Allen, N.P. Bansal, R.M. Murphy, and R.P.T. Tomkins, "Physical Properties Data Compilations Relative to Energy Storage, I. Molten Salts: Data on Single and Multi-Component Salt Systems," Report NSRDS-NBS61, Part II, 1979.

[12] G.J. Ganz and R.P.T. Tomkins, "Physical Properties Data Compilations Relative to Energy Storage. IV. Molten Salts: Data on Additional Single and Multi-Component Salt Systems," Report NSRDS-NBS 61, Part IV, 1981.

[13] 1989 ASHRAE Handbook - Fundamentals, American Society of Heating, Refrigerating and Air-Conditioning Engineers, Inc., 1989.

[14] "Therminol 66 Heat Transfer Fluid," Technical Bulletin (T-66), Monsanto Company, 1973.

[15] Benson, D.K., Webb, J.D., Burrows, R.W., McFadden, J.D.O., Christensen, C., "Materials Research for Passive Solar Systems: Solid-State Phase-Change Materials," Solar Energy Research Institute Report, Task Nos. 1275.00 and 1464.00 WPA304, March 1985 (Available through NTIS, SERI/TR 255-1828 Category 62A).

[16] Benson, D.K., Burrows, R.W., and Webb, J.D., "Solid State Phase Transitions in Pentaerythritol and Related Polyhedric Alcohols," Solar Energy Materials, Vol. 13, North-Holland, 1986, 133-152.

[17] Holman J.P., Heat Transfer, Fifth Edition, McGraw-Hill Book Company, 1981.

[18] Telecon between Kirk Yerkes, Wright-Patterson Air Force Base, and Kevin Funke, Sundstrand, May 26, 1992.

[19] Heat Transfer and Fluid Flow Data Book, General Electric Company, 1970.

[20] Rohsenow, W.M., "Pool Boiling," Handbook of Multiphase Systems, Editor, Hestroni, G., McGraw-Hill-Hemisphere, New York, 1982.

[21] Bergles, A.E. and Rohsenow, W.M., "The Determination of Forced Convection Surface Boiling Heat Transfer," Journal of Heat Transfer, Vol. 86, pp. 365-372, 1964.

[22] Lienhard, J.H., "Correlation of Limiting Liquid Superheat," Chemical Engineering Science, Vol. 31, pp. 847-849, 1976.

[23] Bland, T.J. and Funke, K.D., "Advanced Cooling for High Power Electric Actuators," SAE Paper 921022, April 7-10, 1992.

[24] Gersurt, Nelson J. and Sarraf, David B., "A Thermal Analysis of an F/A-18 Wing Section for Actuator Thermal Management," SAE Paper 921023, April 7-10, 1992.

APPENDIX

FIGURES IN BRITISH UNITS

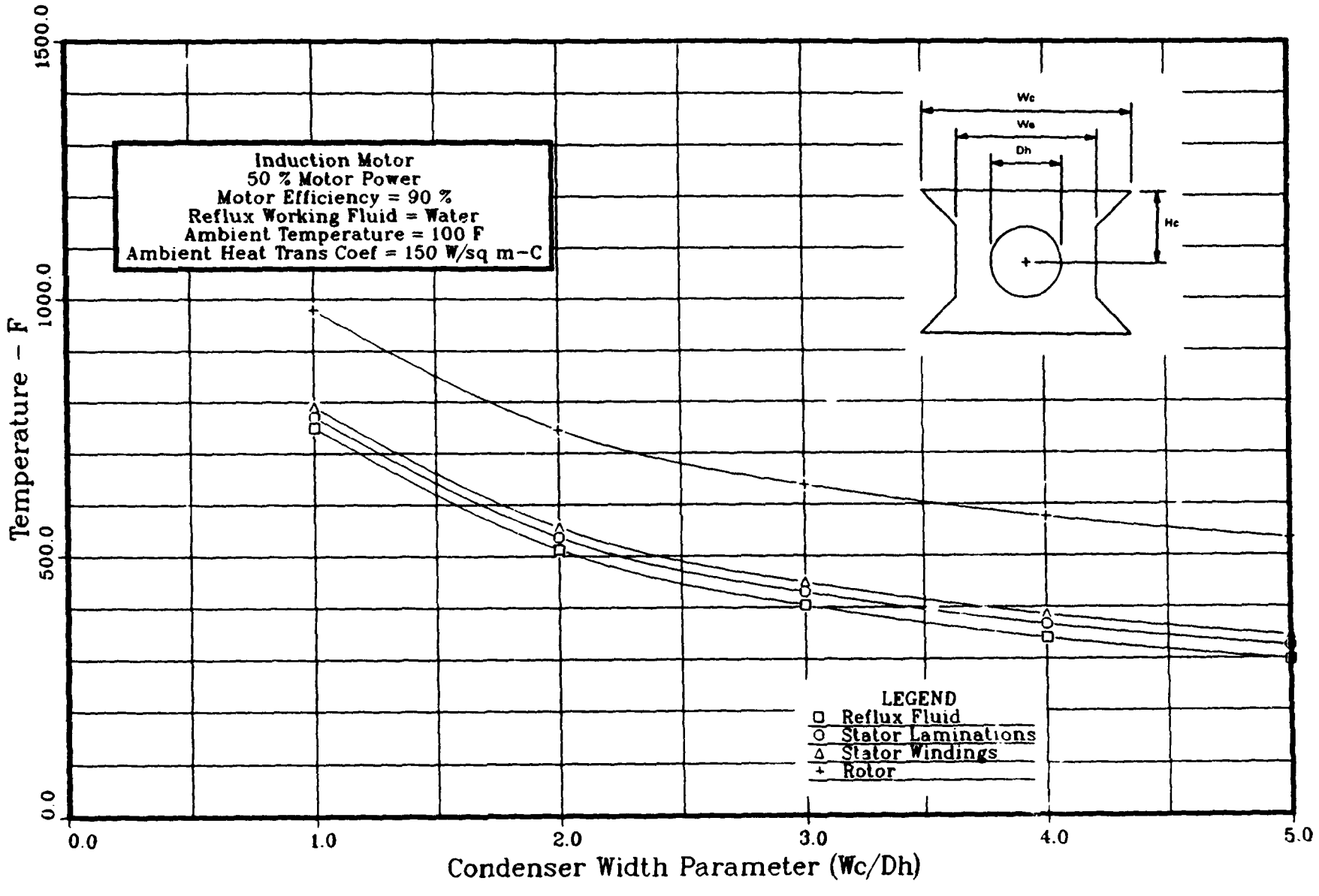

FIGURE A.1 ADVANCED ACTUATOR COOLING
Steady State Temperature vs. Condenser Width Parameter

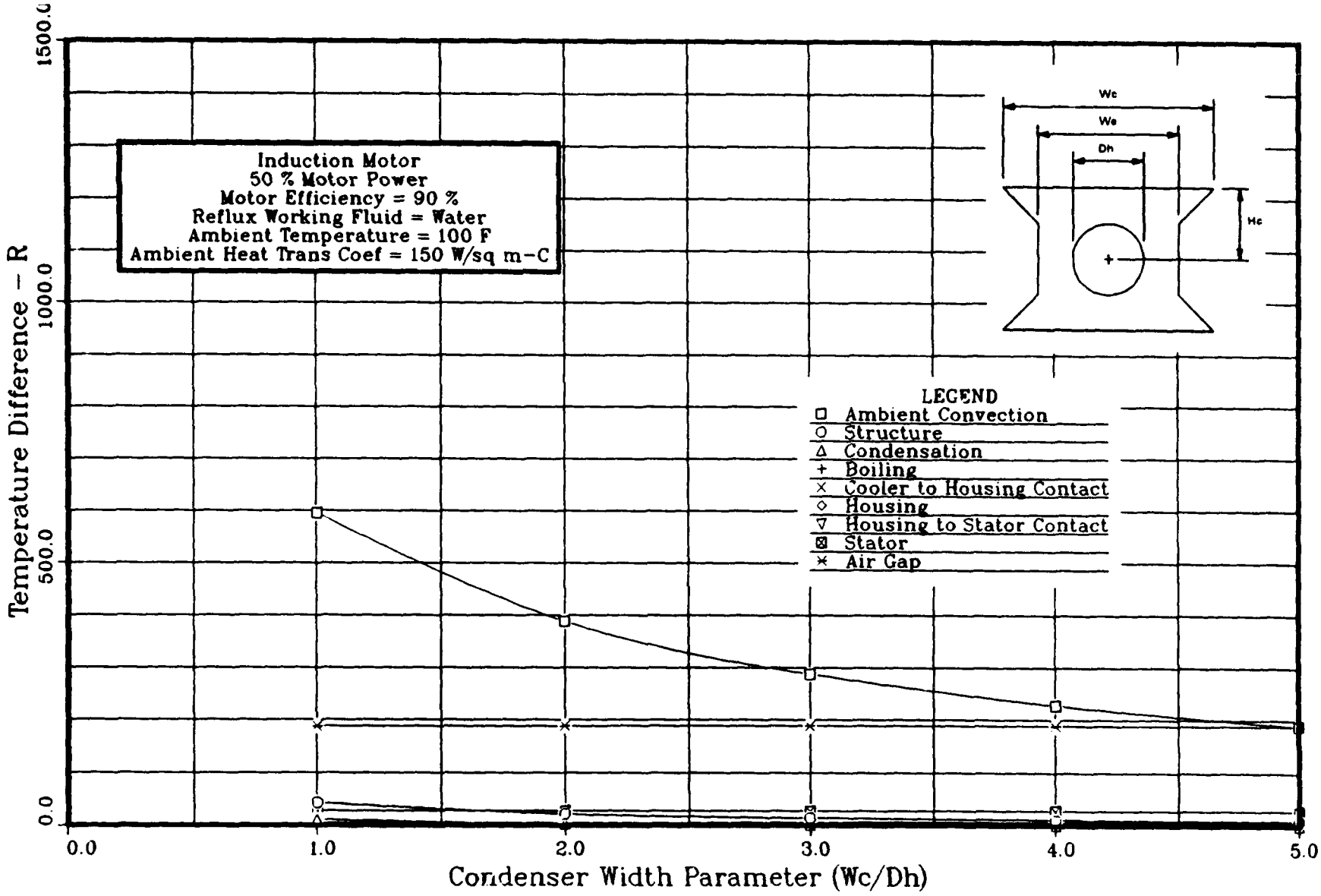

FIGURE A.2 ADVANCED ACTUATOR COOLING
Steady State Temp. Differences vs Condenser Width Parameter

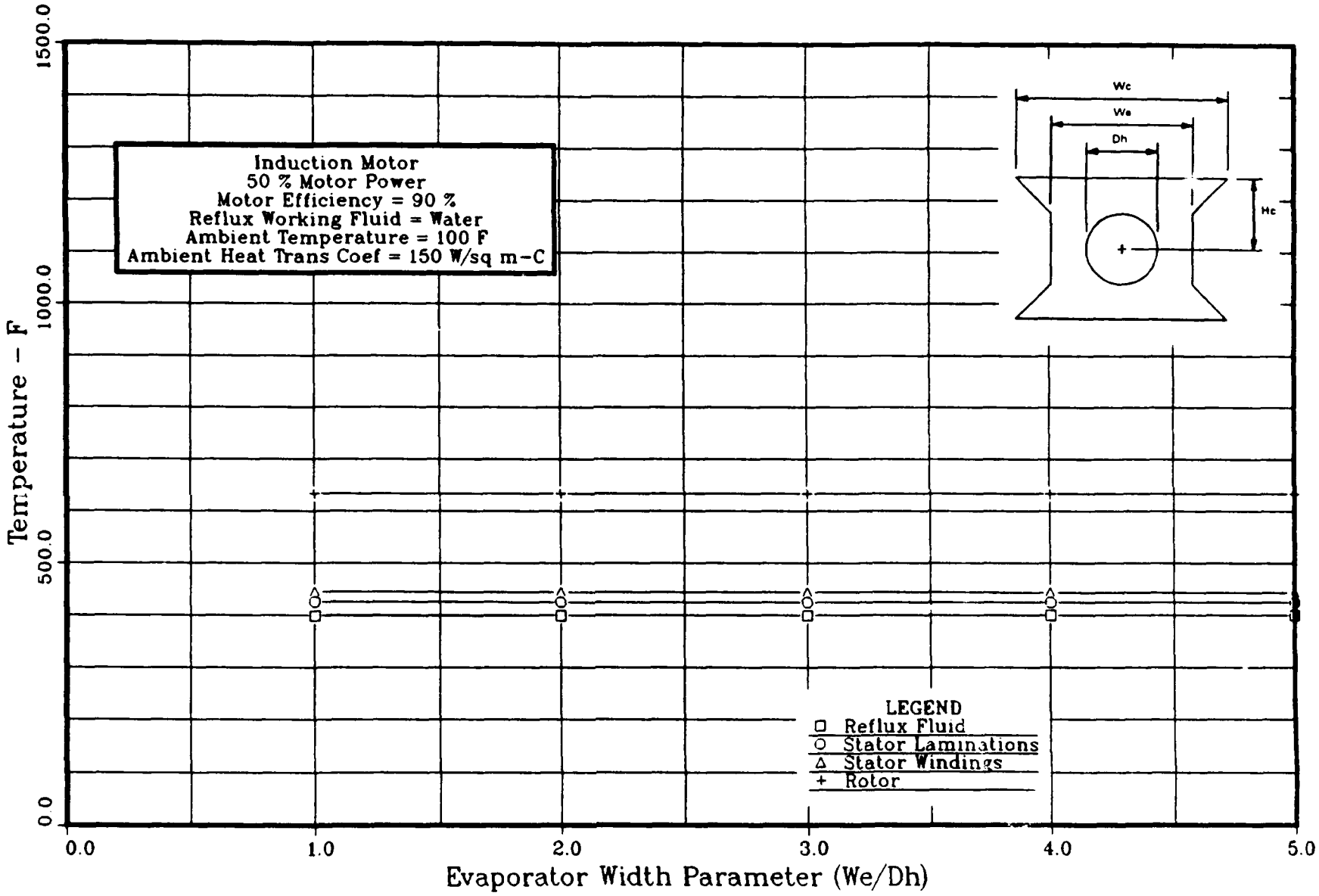

FIGURE A.3 ADVANCED ACTUATOR COOLING
Steady State Temperature vs Evaporator Width Parameter

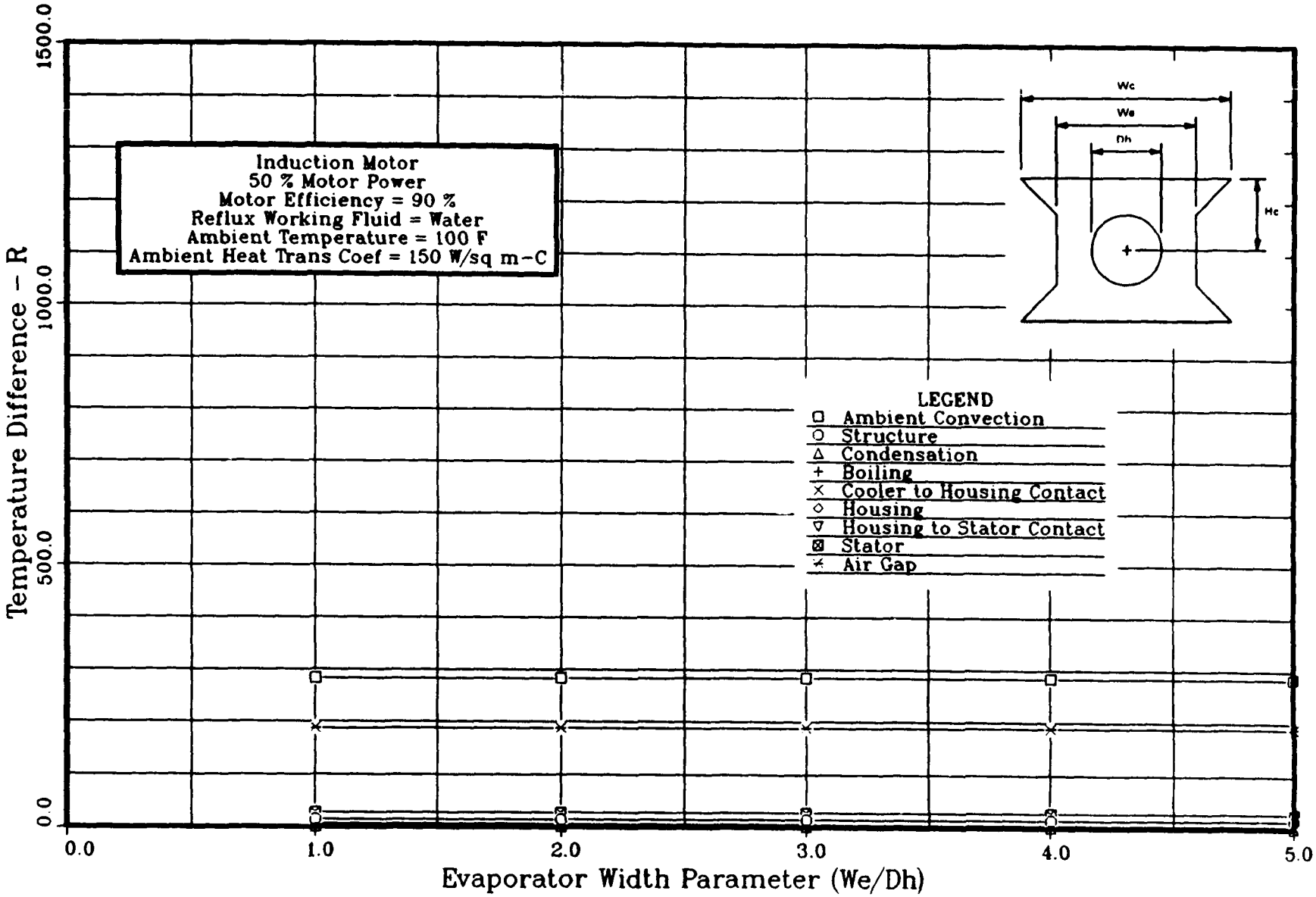

FIGURE A.4 ADVANCED ACTUATOR COOLING
Steady State Temp. Differences vs Evaporator Width Parameter

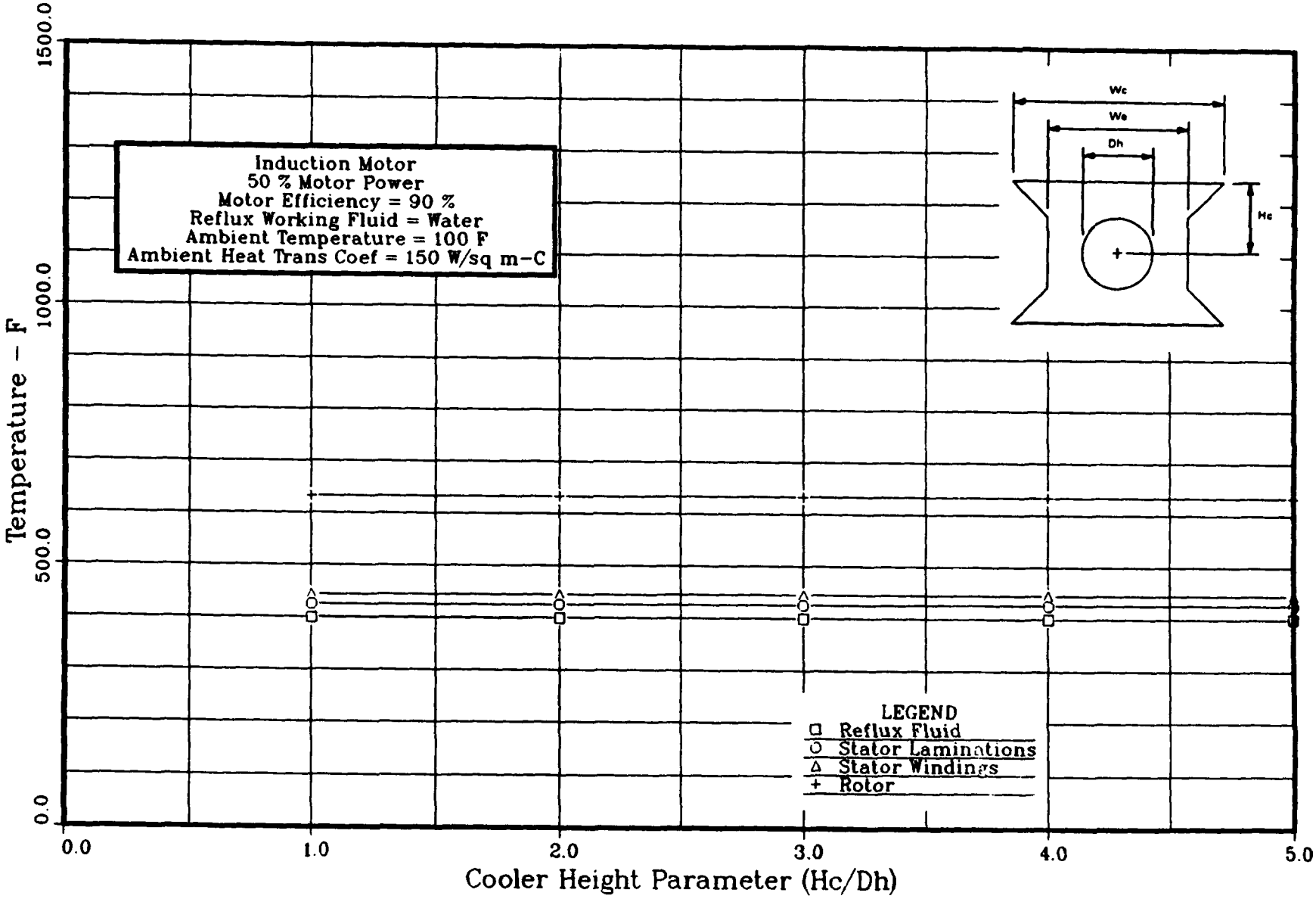

FIGURE A.5 ADVANCED ACTUATOR COOLING
Steady State Temperature vs Cooler Height Parameter

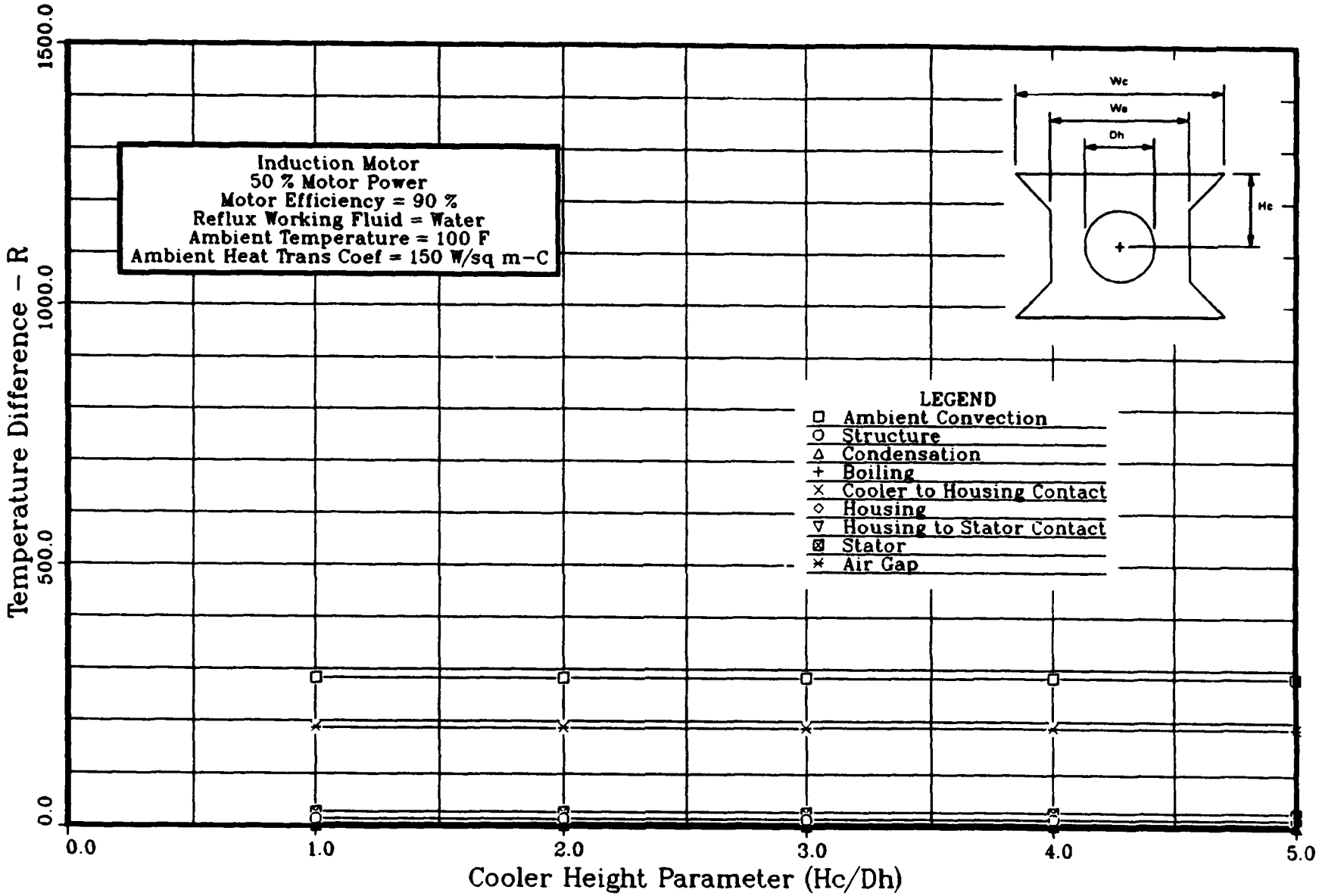

FIGURE A.6 ADVANCED ACTUATOR COOLING
Steady State Temp. Differences vs Cooler Height Parameter

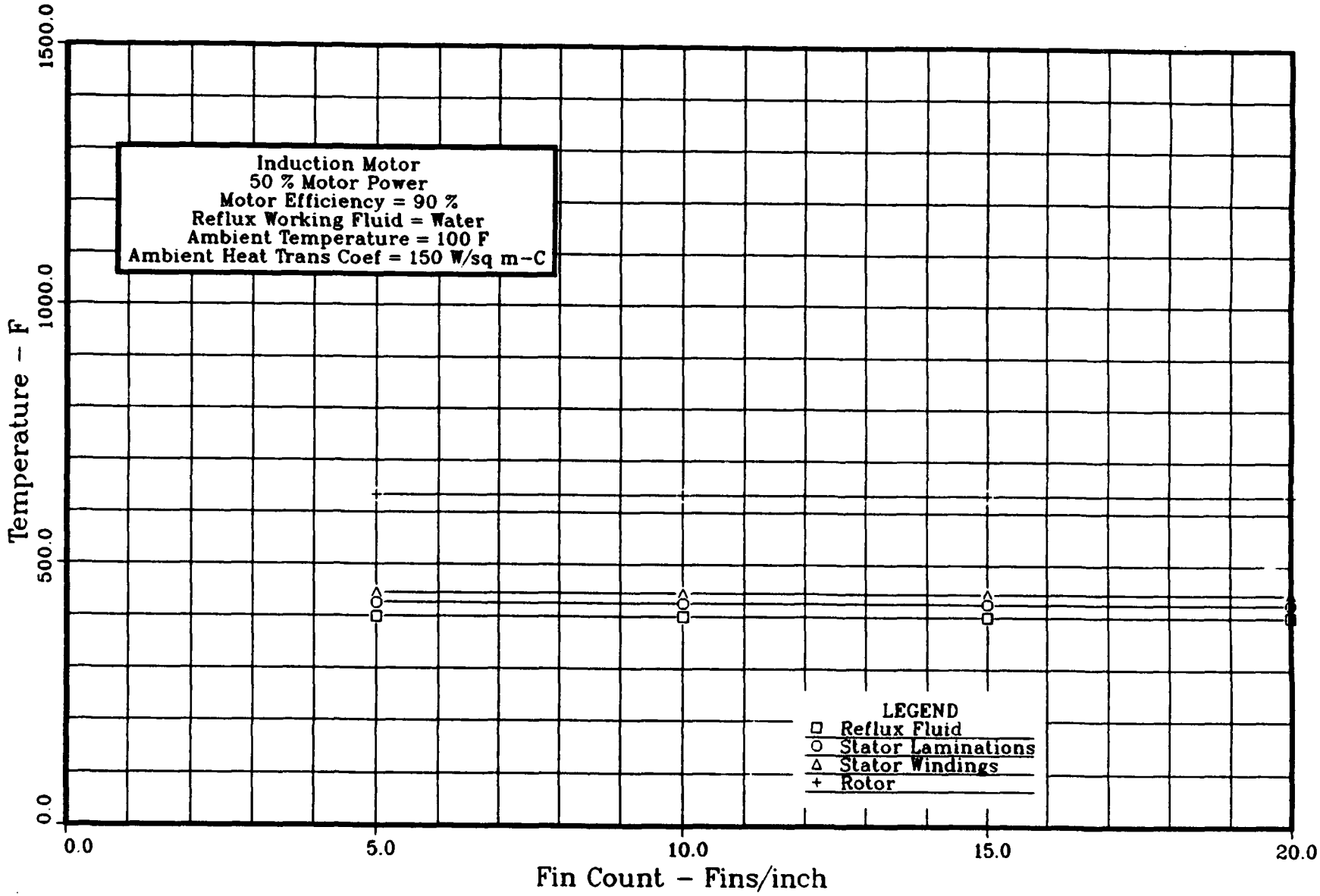

FIGURE A.7 ADVANCED ACTUATOR COOLING
Steady State Temperature vs Fin Count

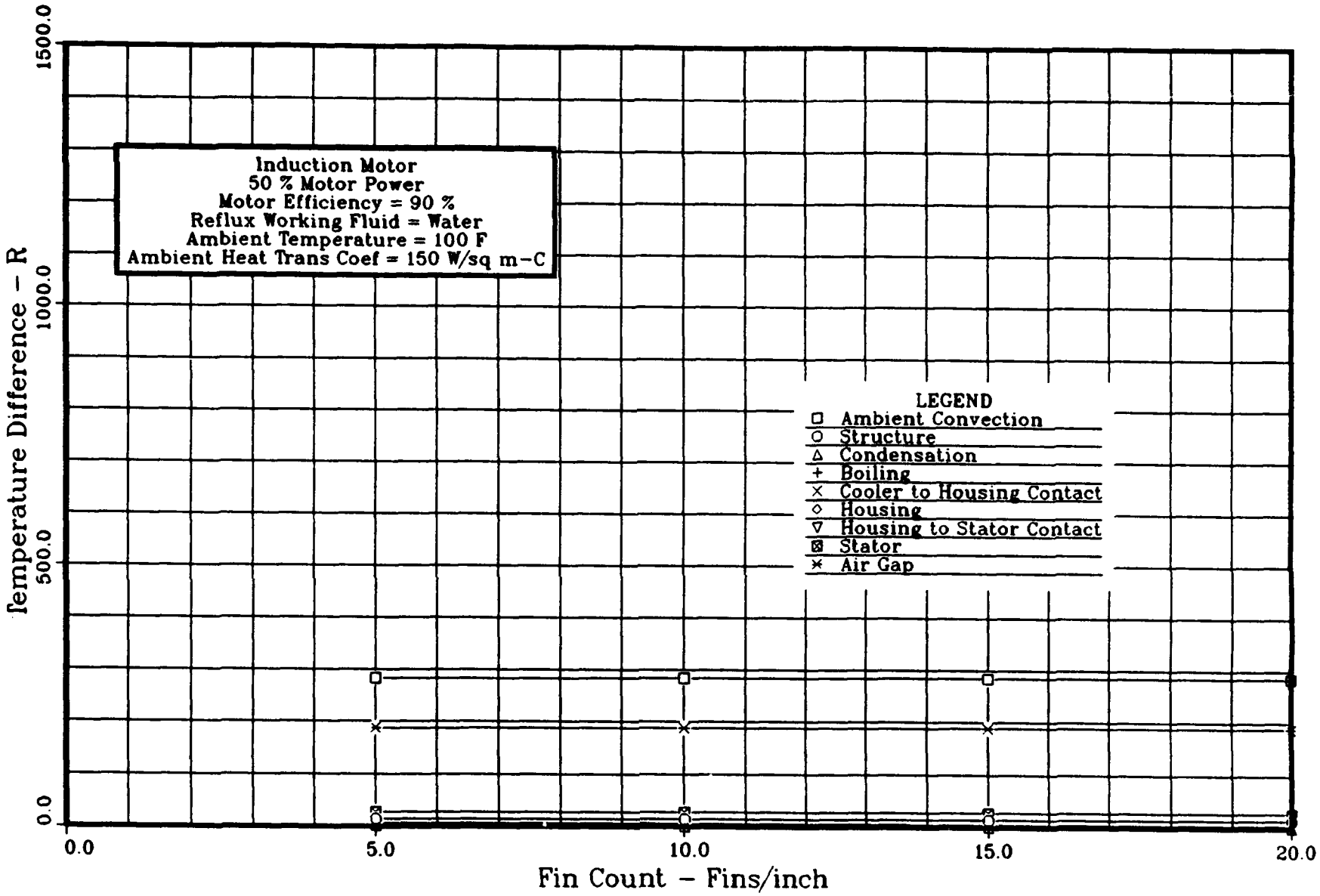

FIGURE A.8 ADVANCED ACTUATOR COOLING
Steady State Temp. Differences vs Fin Count

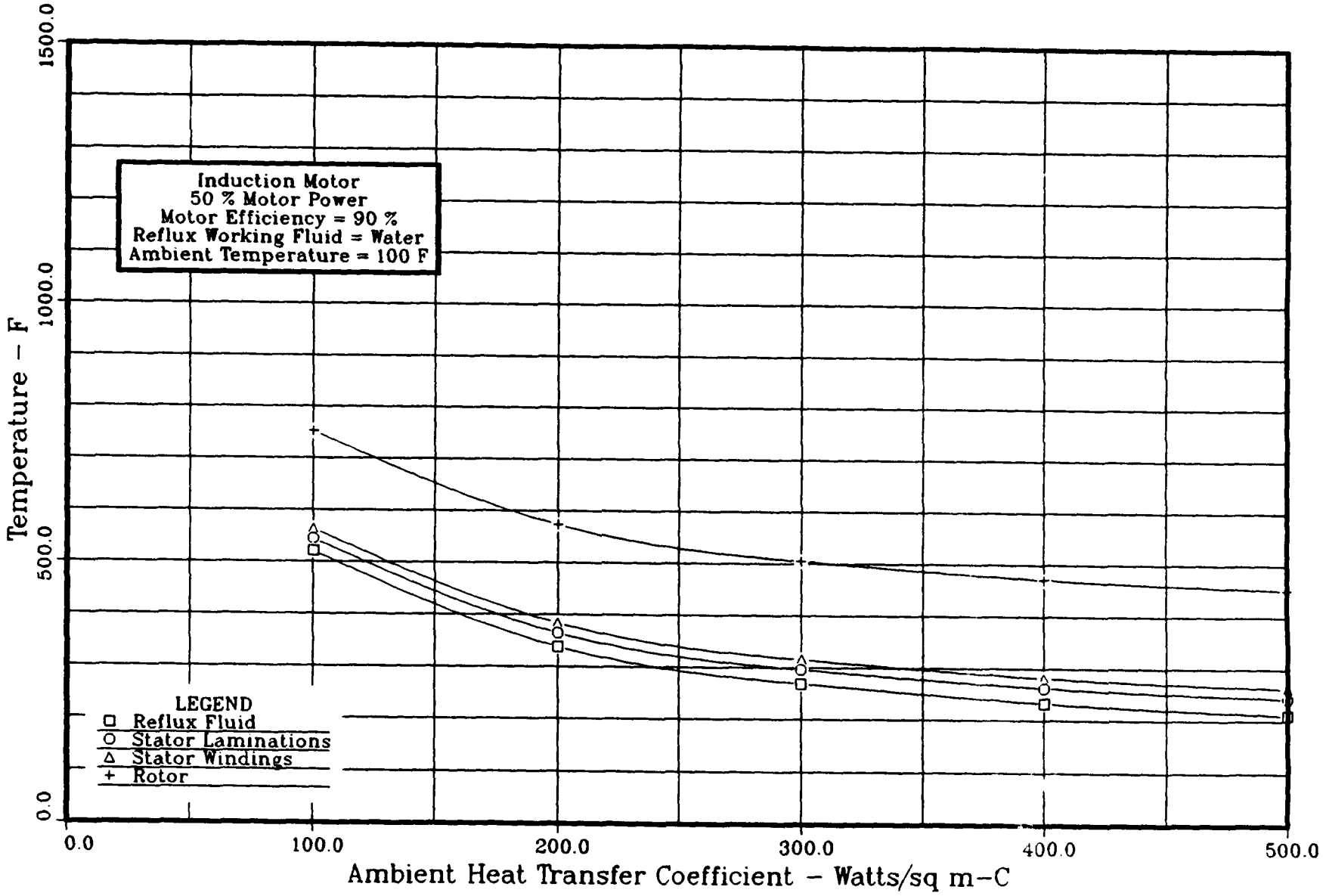

FIGURE A.9 ADVANCED ACTUATOR COOLING
Steady State Temp vs Ambient Heat Transfer Coefficient

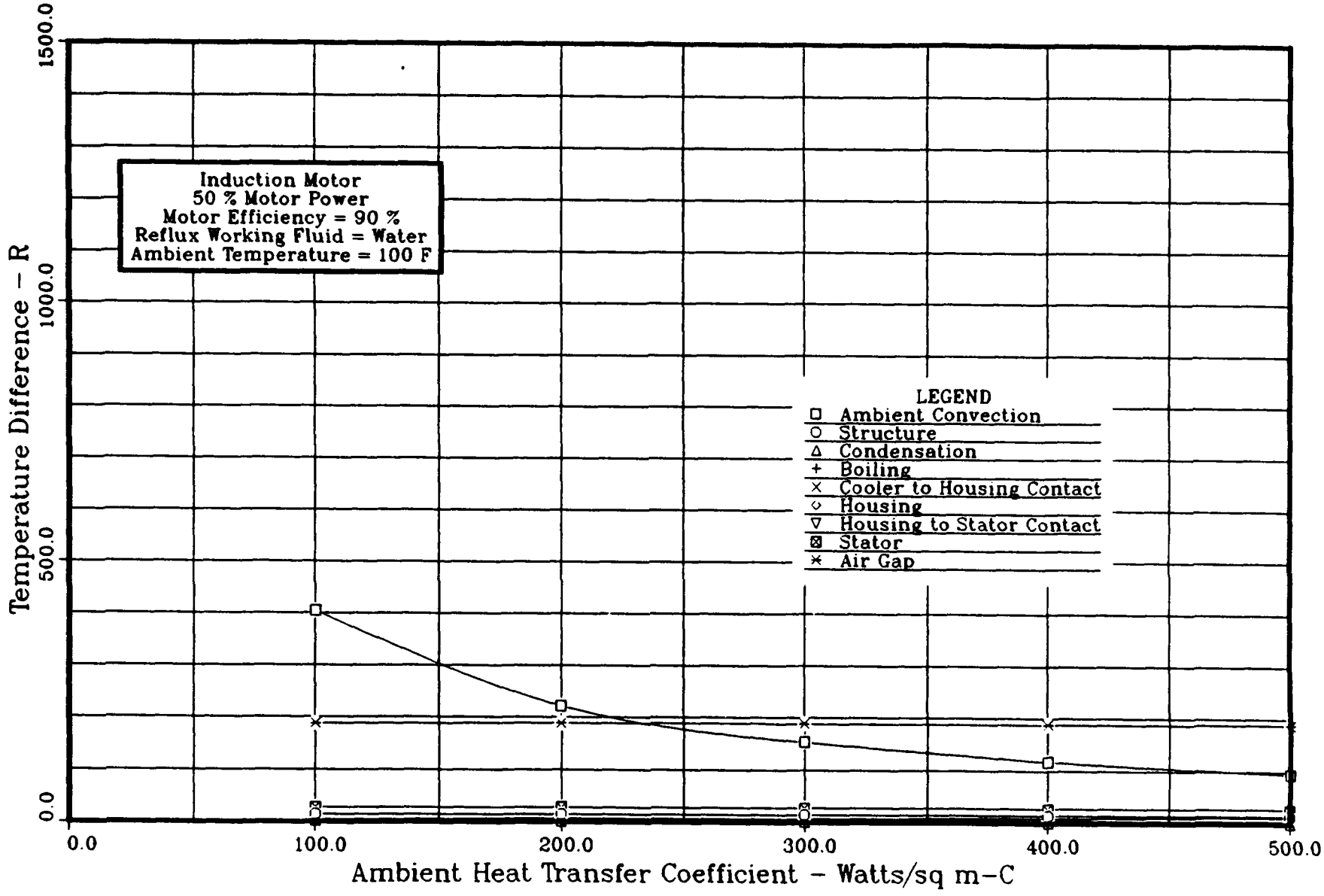

FIGURE A.10 ADVANCED ACTUATOR COOLING
Steady State Temp Diff vs Ambient Heat Trans Coef

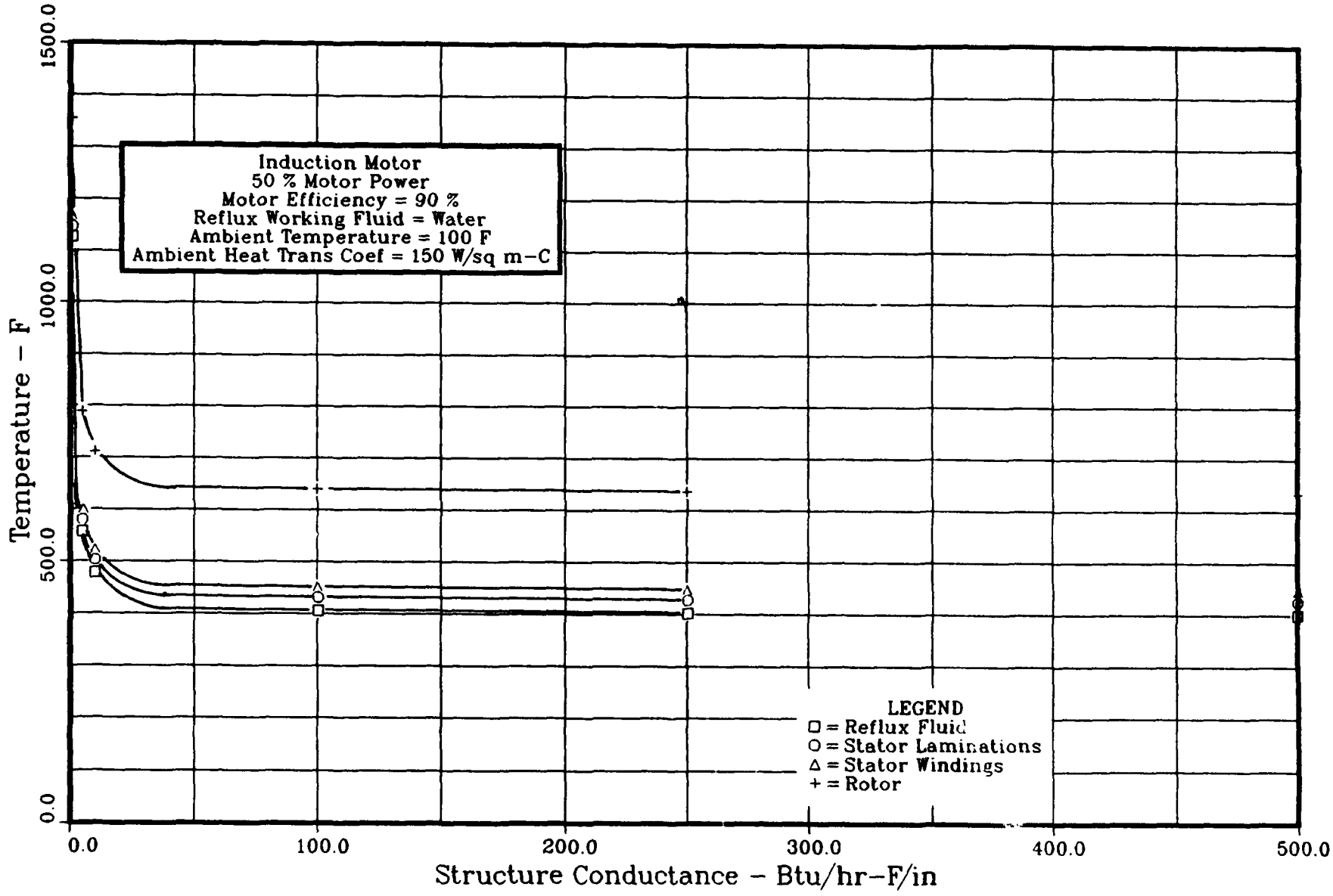

FIGURE A.11 ADVANCED ACTUATOR COOLING
Steady State Temperature vs Structure Conductance

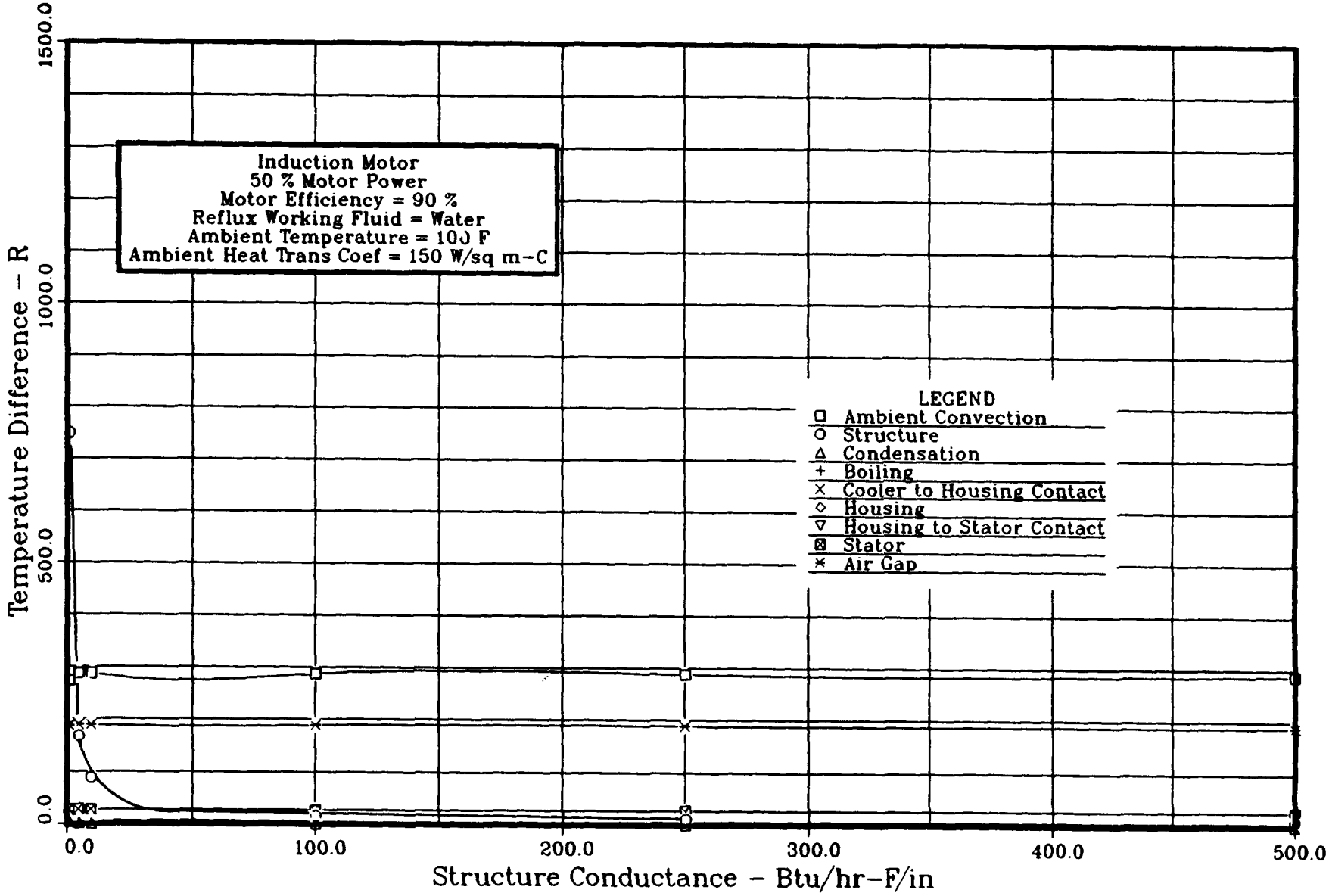

FIGURE A.12 ADVANCED ACTUATOR COOLING
Steady State Temp Differences vs Structure Conductance

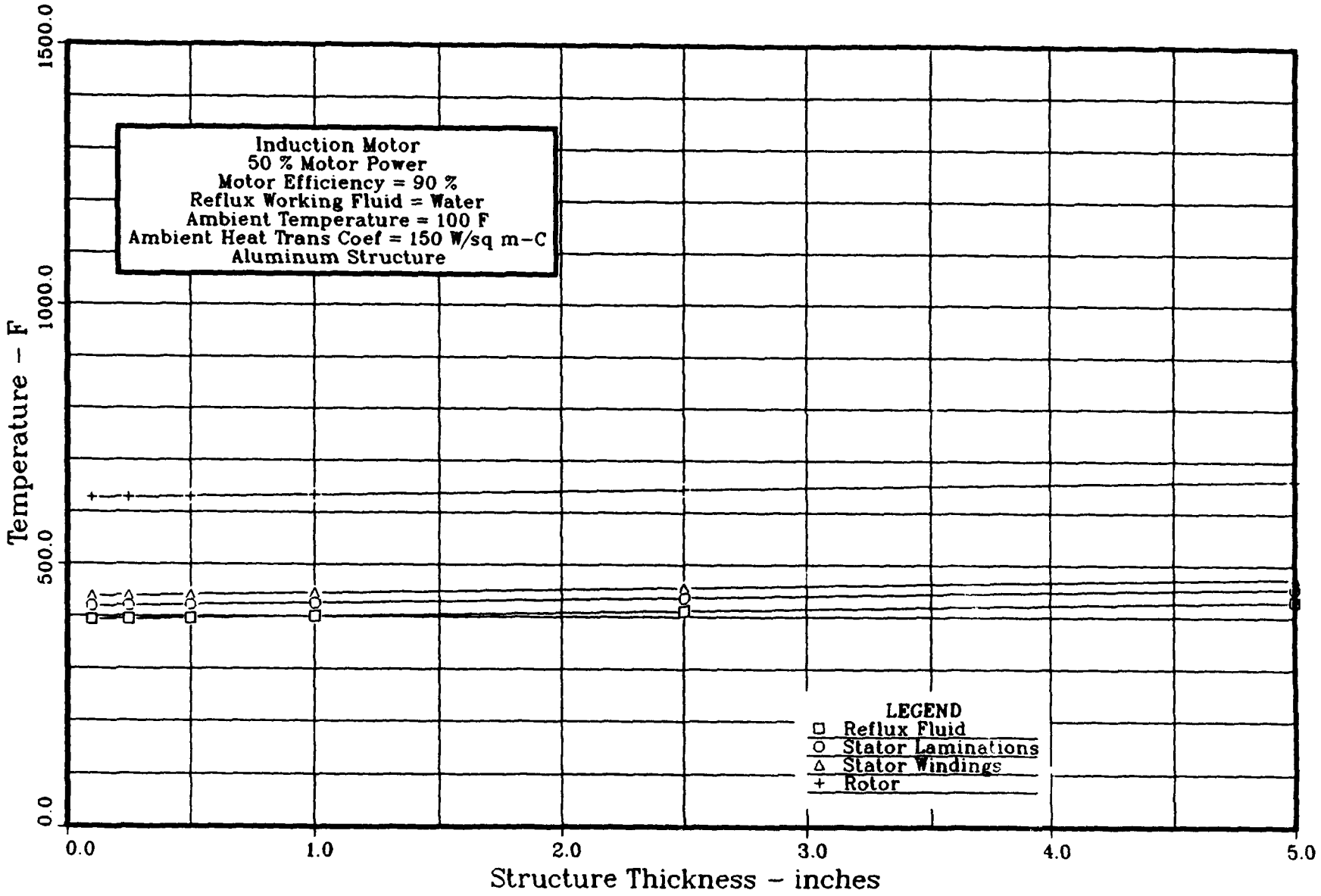

FIGURE A.13 ADVANCED ACTUATOR COOLING
Steady State Temperature vs Structure Plate Thickness

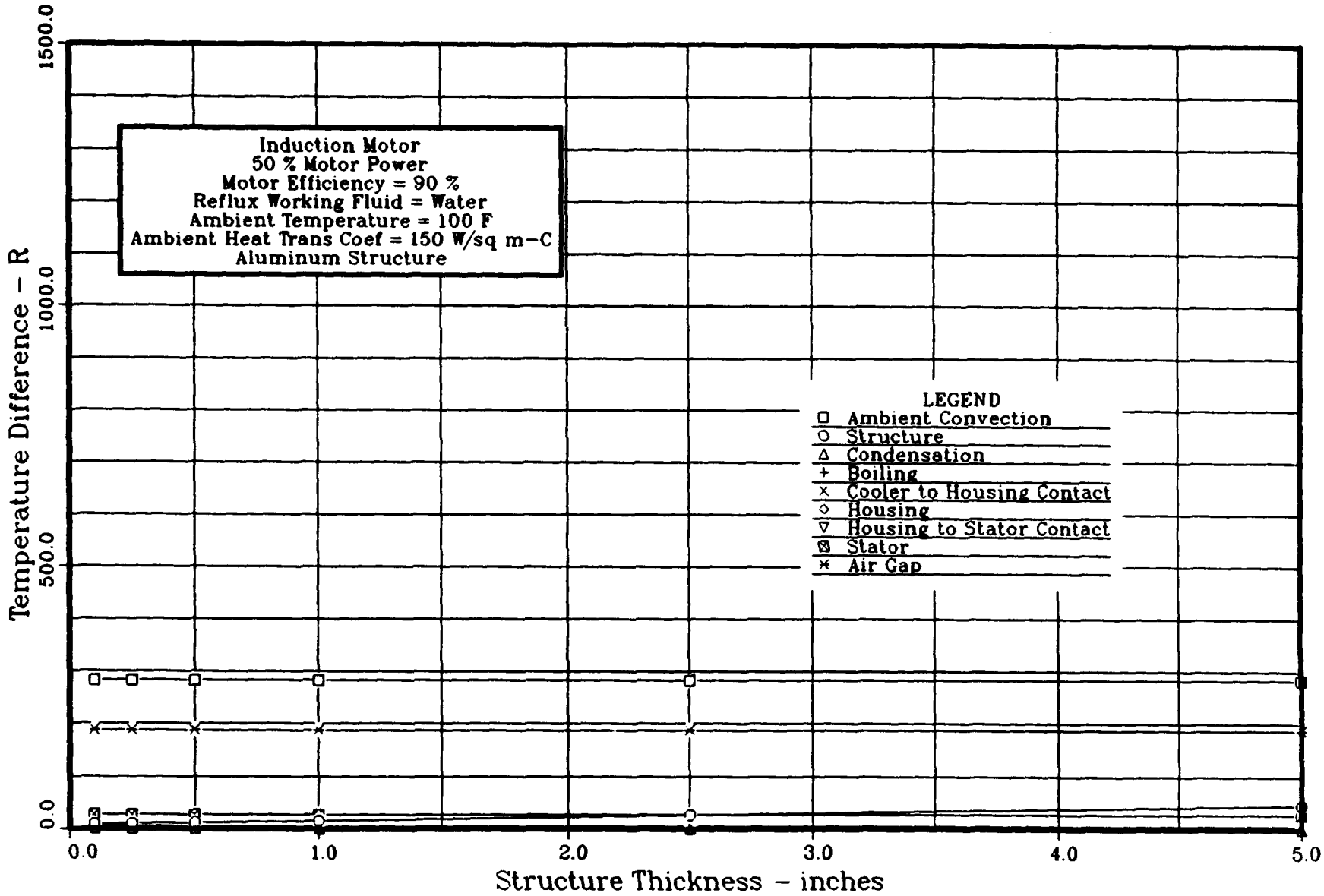

FIGURE A.14 ADVANCED ACTUATOR COOLING
Steady State Temp Differences vs Structure Plate Thickness

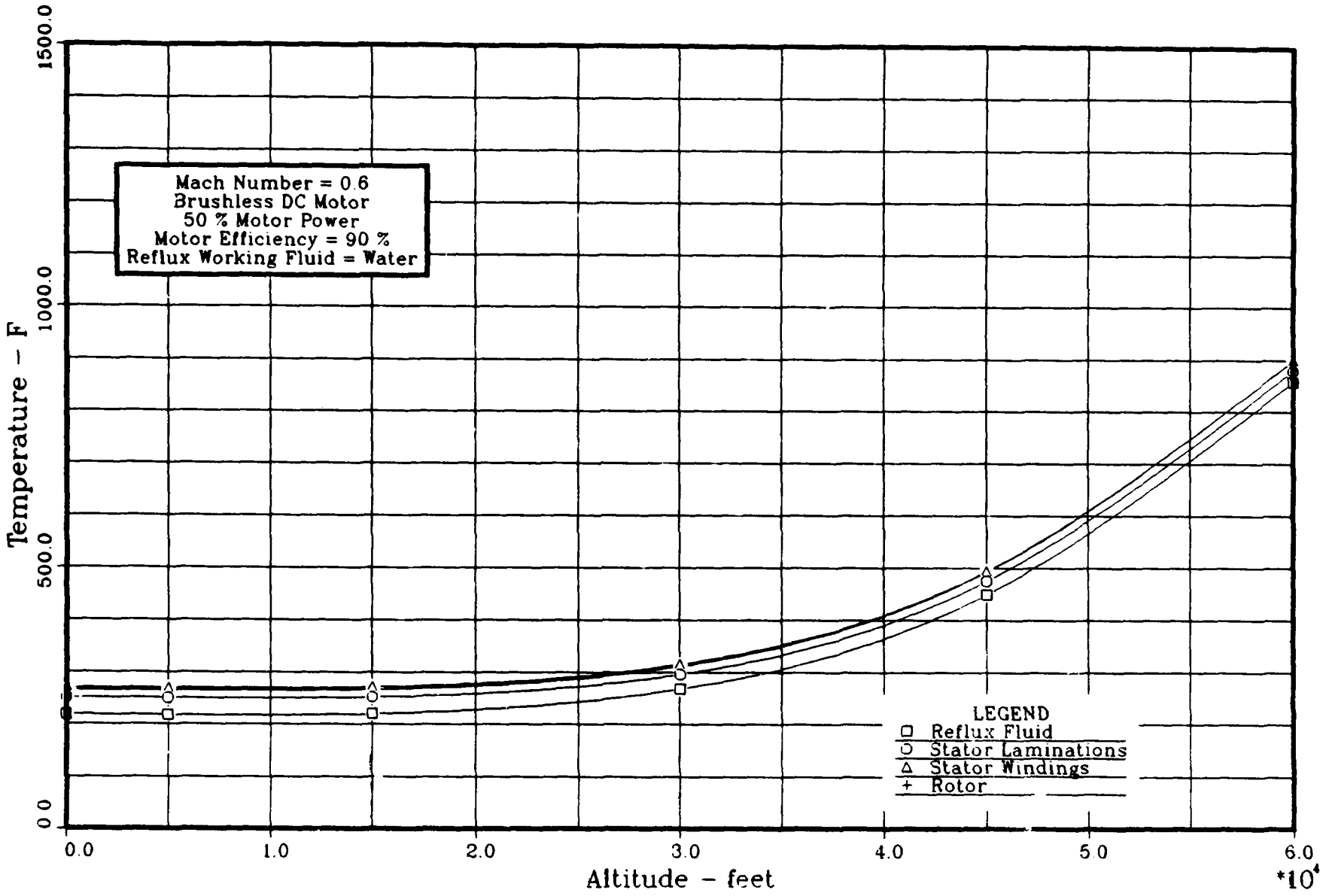

FIGURE A.15 ADVANCED ACTUATOR COOLING
Steady State Temperature vs Altitude

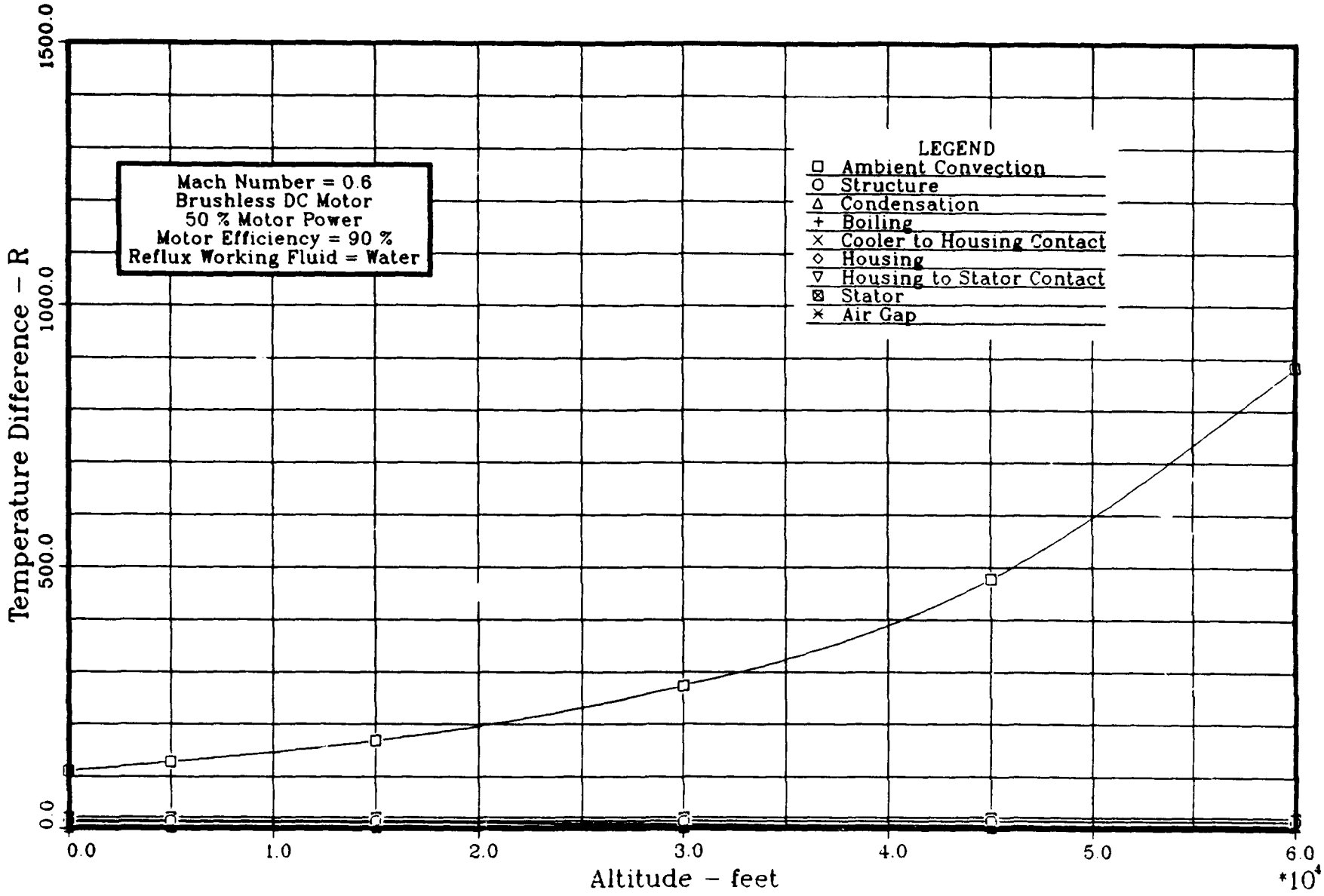

FIGURE A.16 ADVANCED ACTUATOR COOLING
Steady State Temp Differences vs Altitude

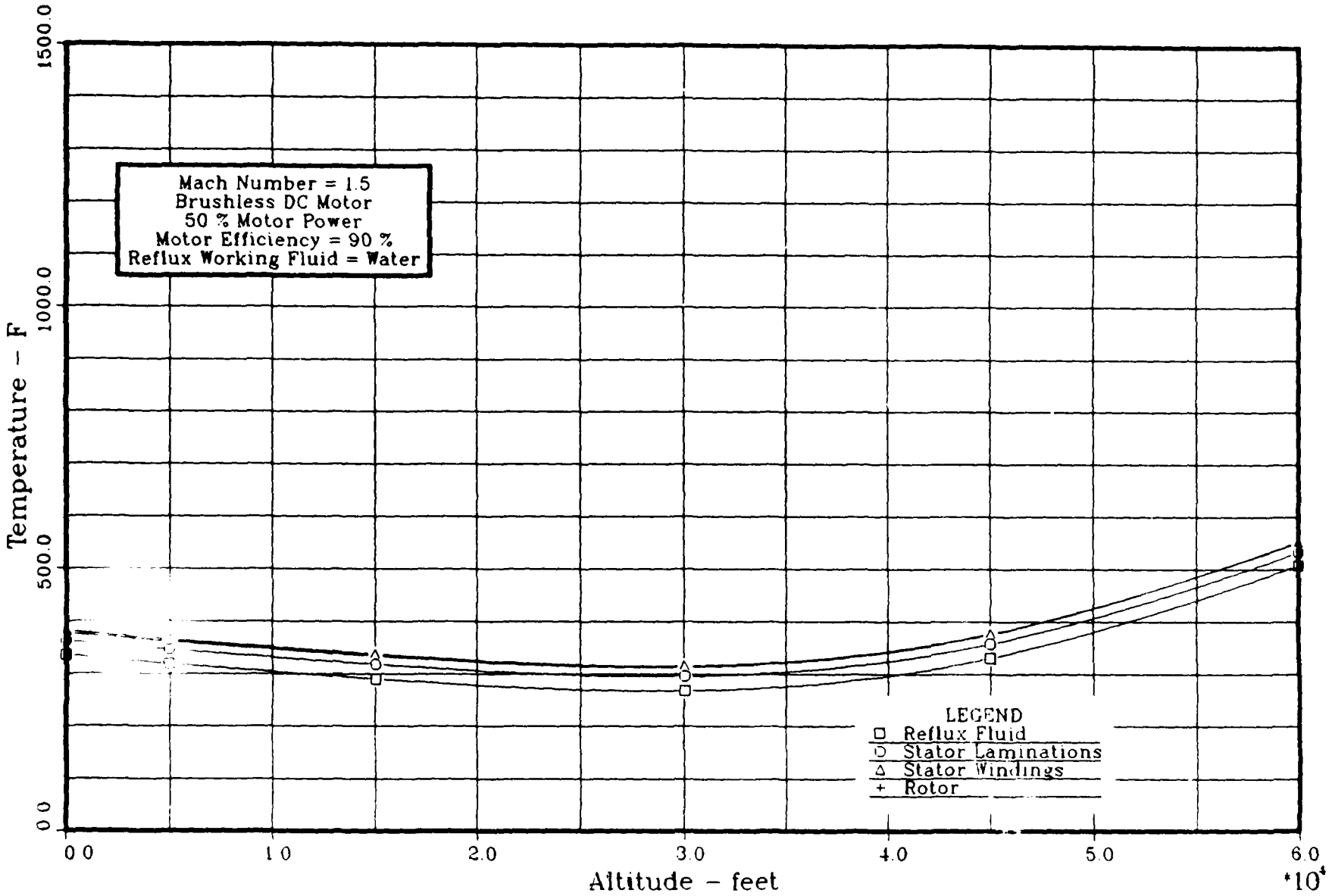

FIGURE A.17 ADVANCED ACTUATOR COOLING
Steady State Temperature vs Altitude

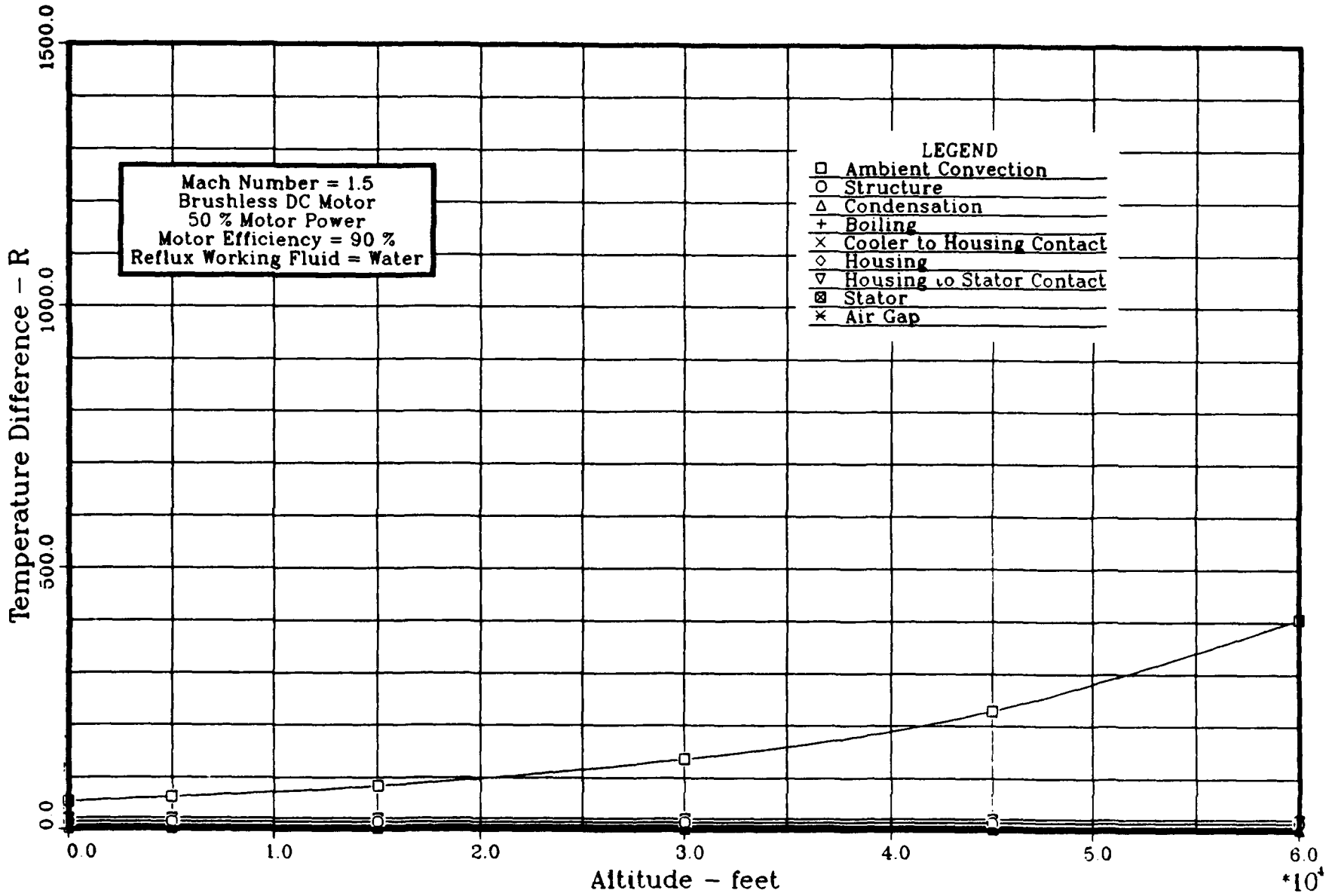

FIGURE A.18 ADVANCED ACTUATOR COOLING
Steady State Temp Differences vs Altitude

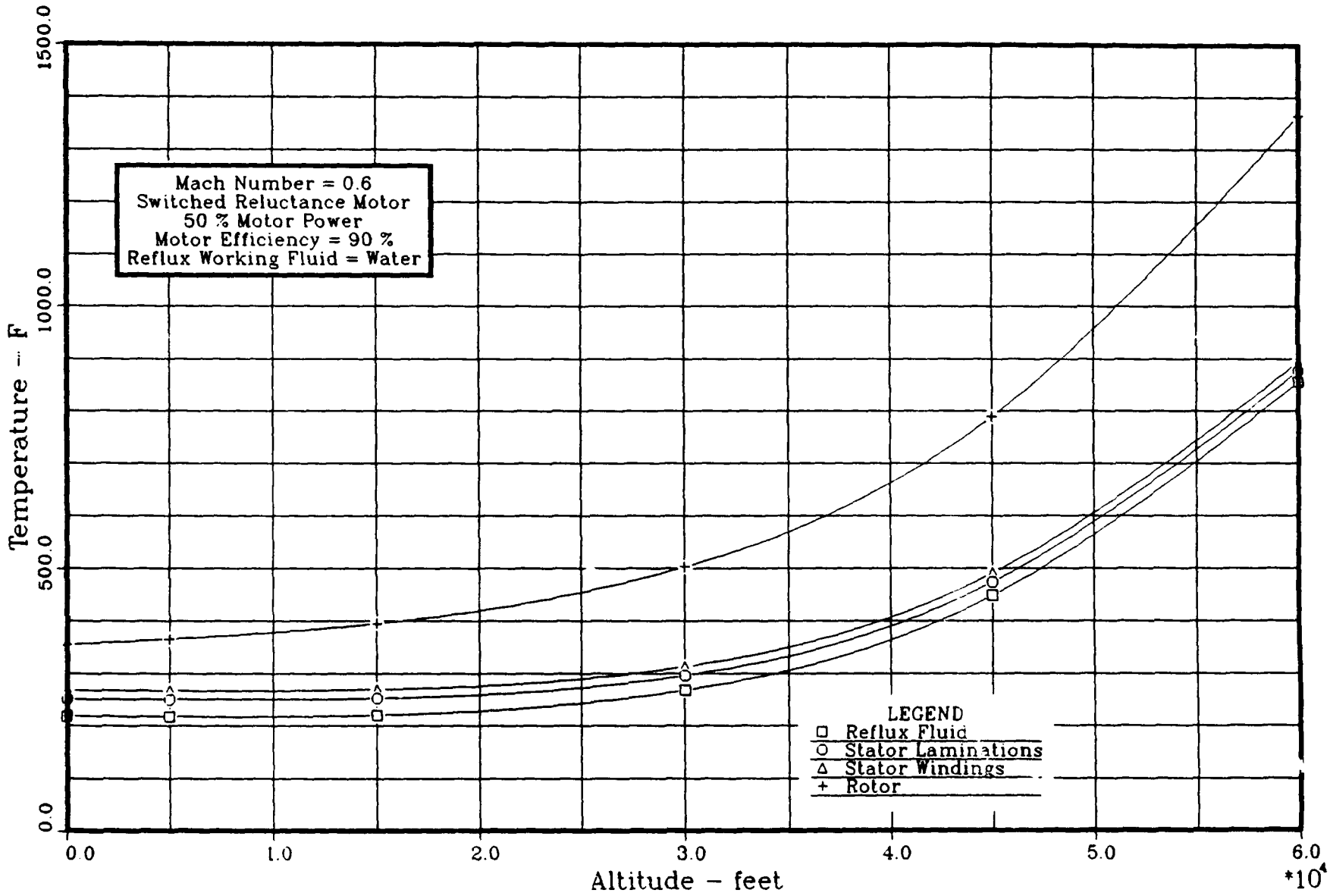

FIGURE A.19 ADVANCED ACTUATOR COOLING
Steady State Temperature vs Altitude

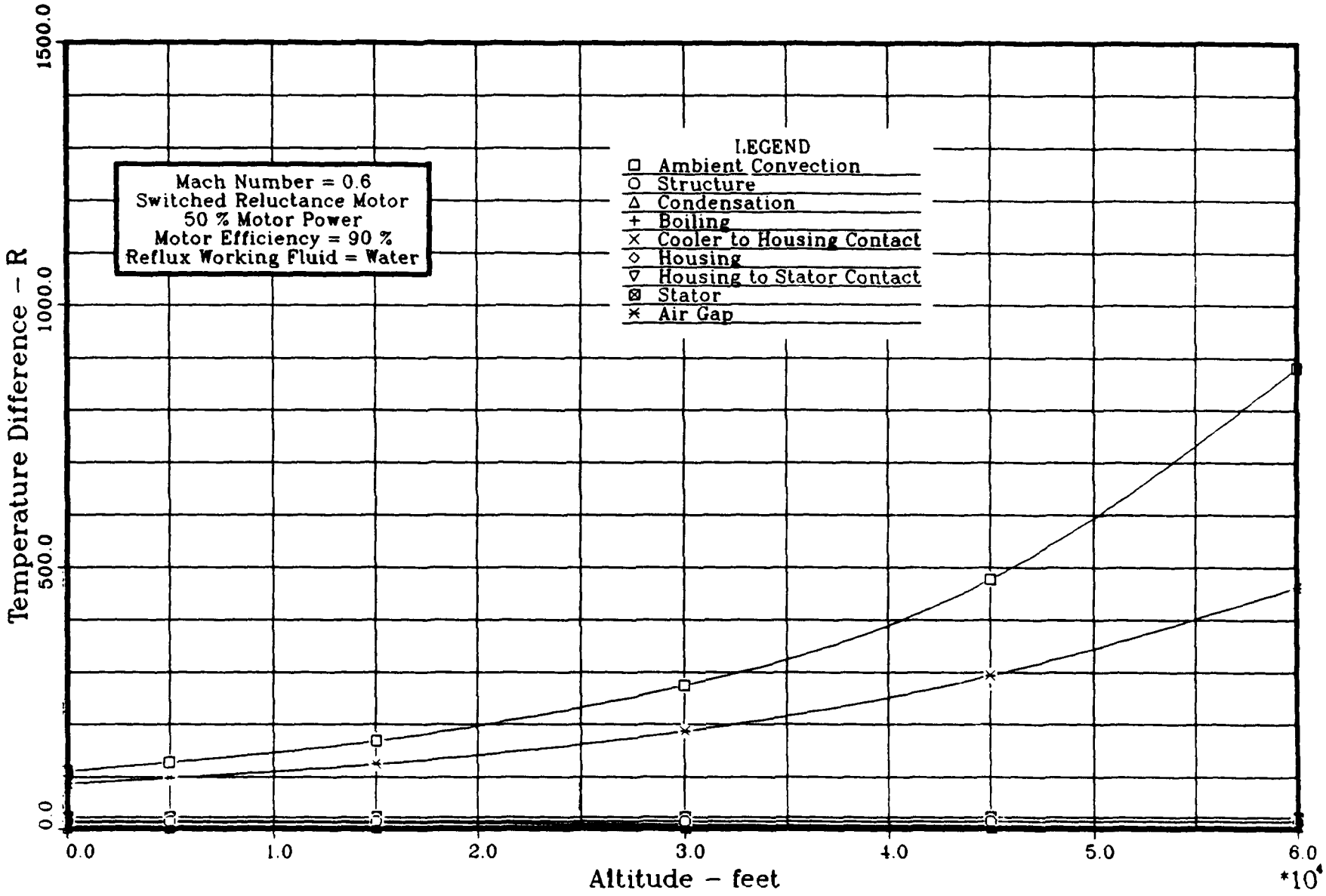

FIGURE A.20 ADVANCED ACTUATOR COOLING
Steady State Temp Differences vs Altitude

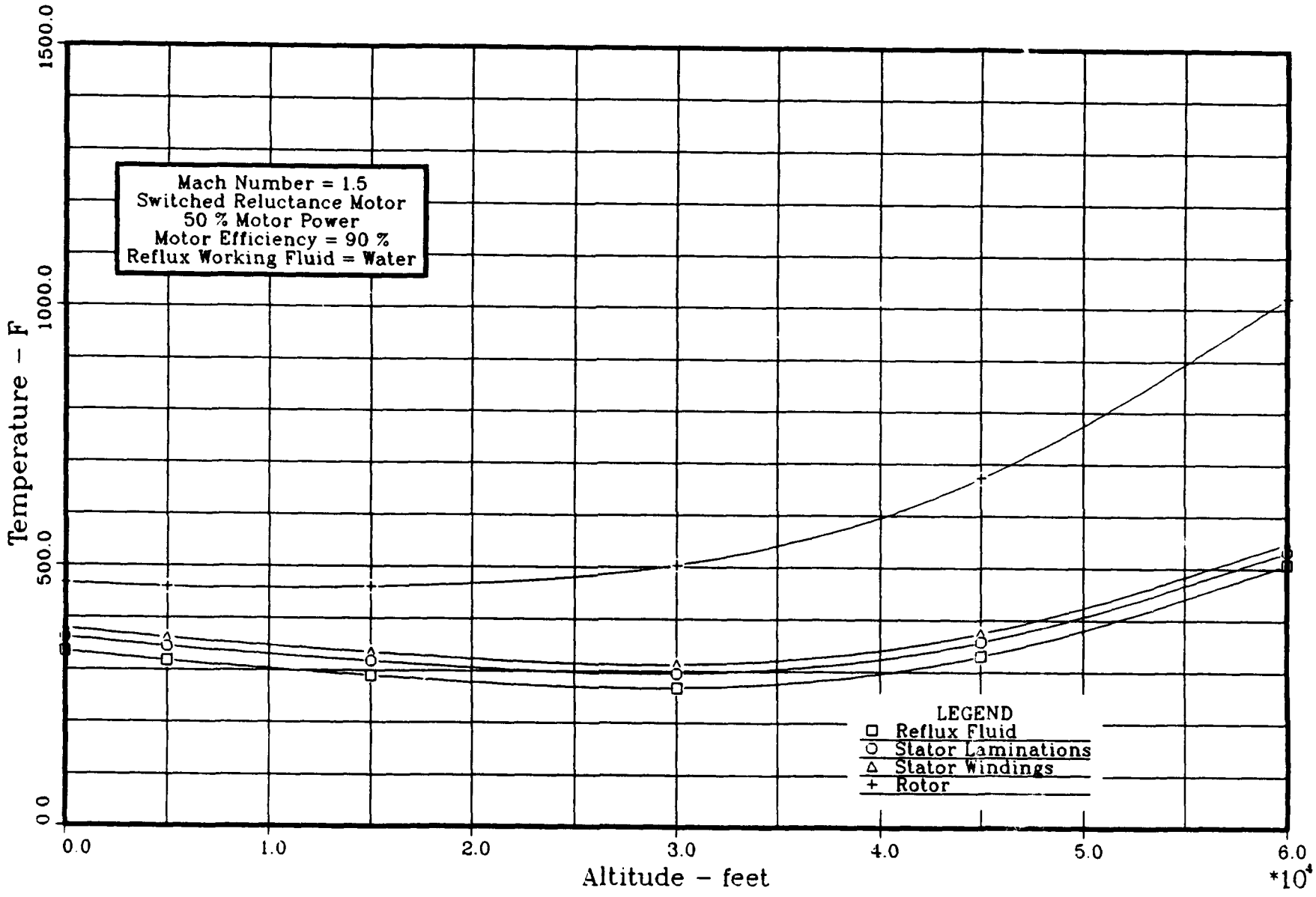

FIGURE A.21 ADVANCED ACTUATOR COOLING
Steady State Temperature vs Altitude

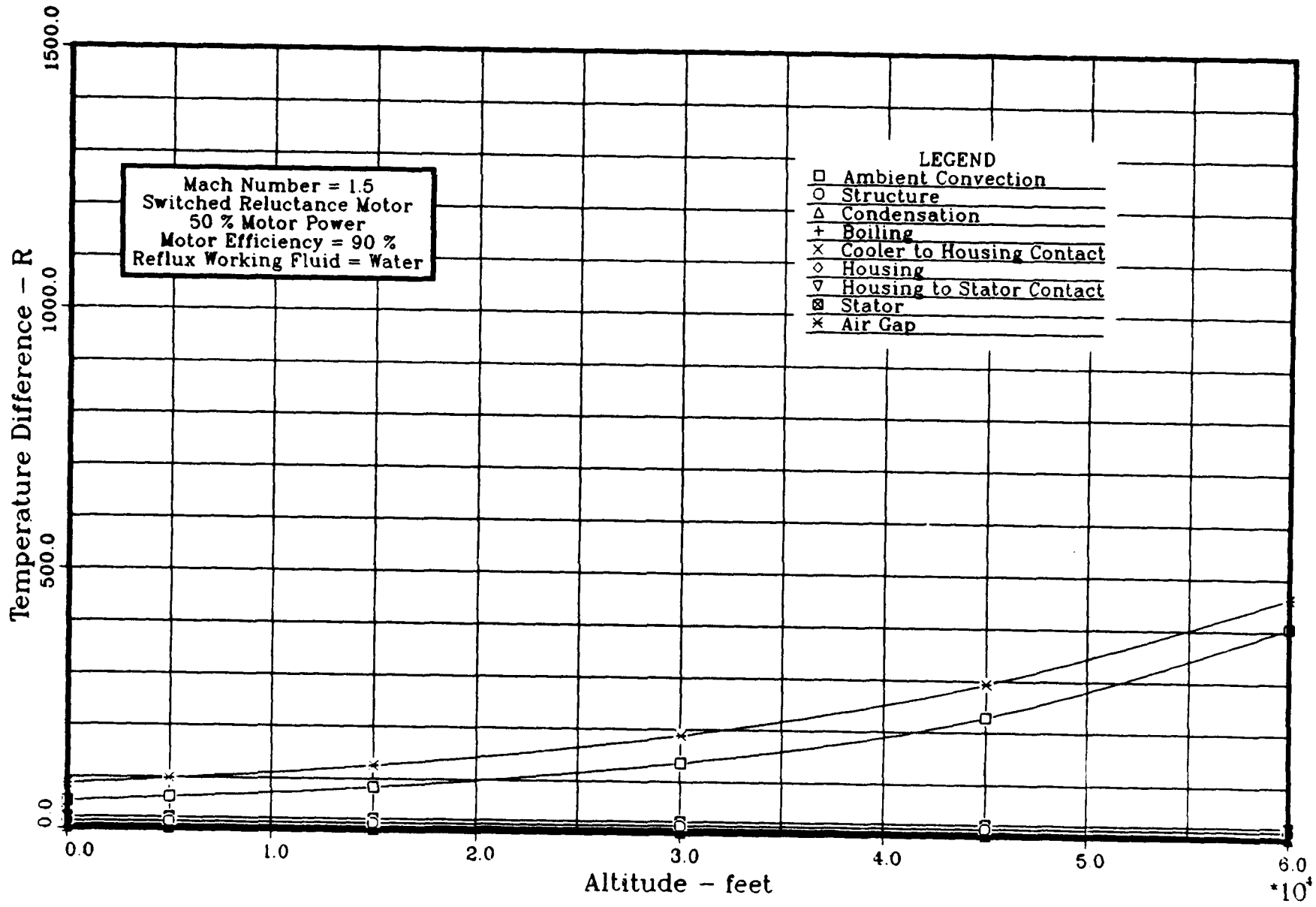

FIGURE A.22 ADVANCED ACTUATOR COOLING
Steady State Temp Differences vs Altitude

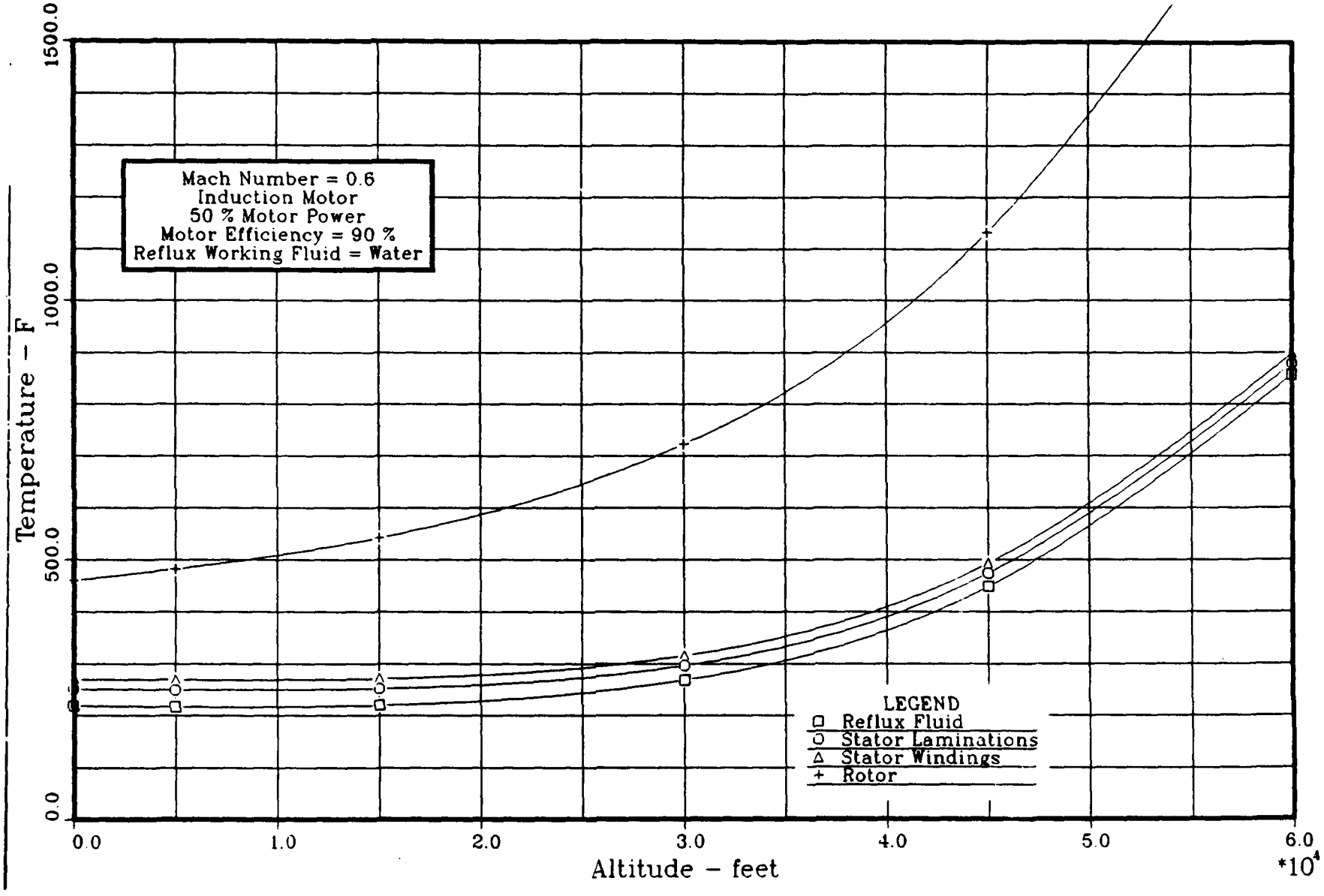

FIGURE A.23 ADVANCED ACTUATOR COOLING
Steady State Temperature vs Altitude

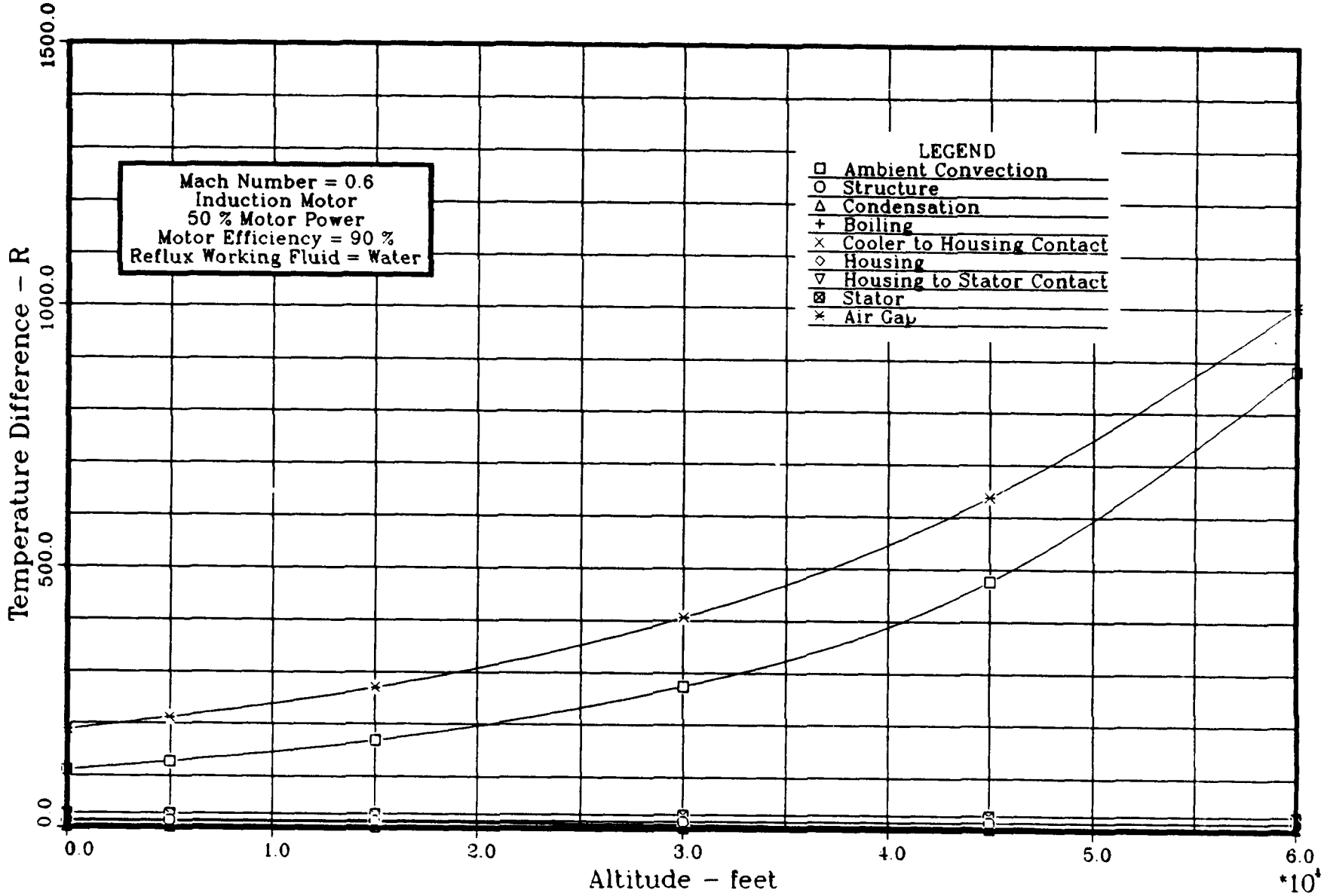

FIGURE A.24 ADVANCED ACTUATOR COOLING
Steady State Temp Differences vs Altitude

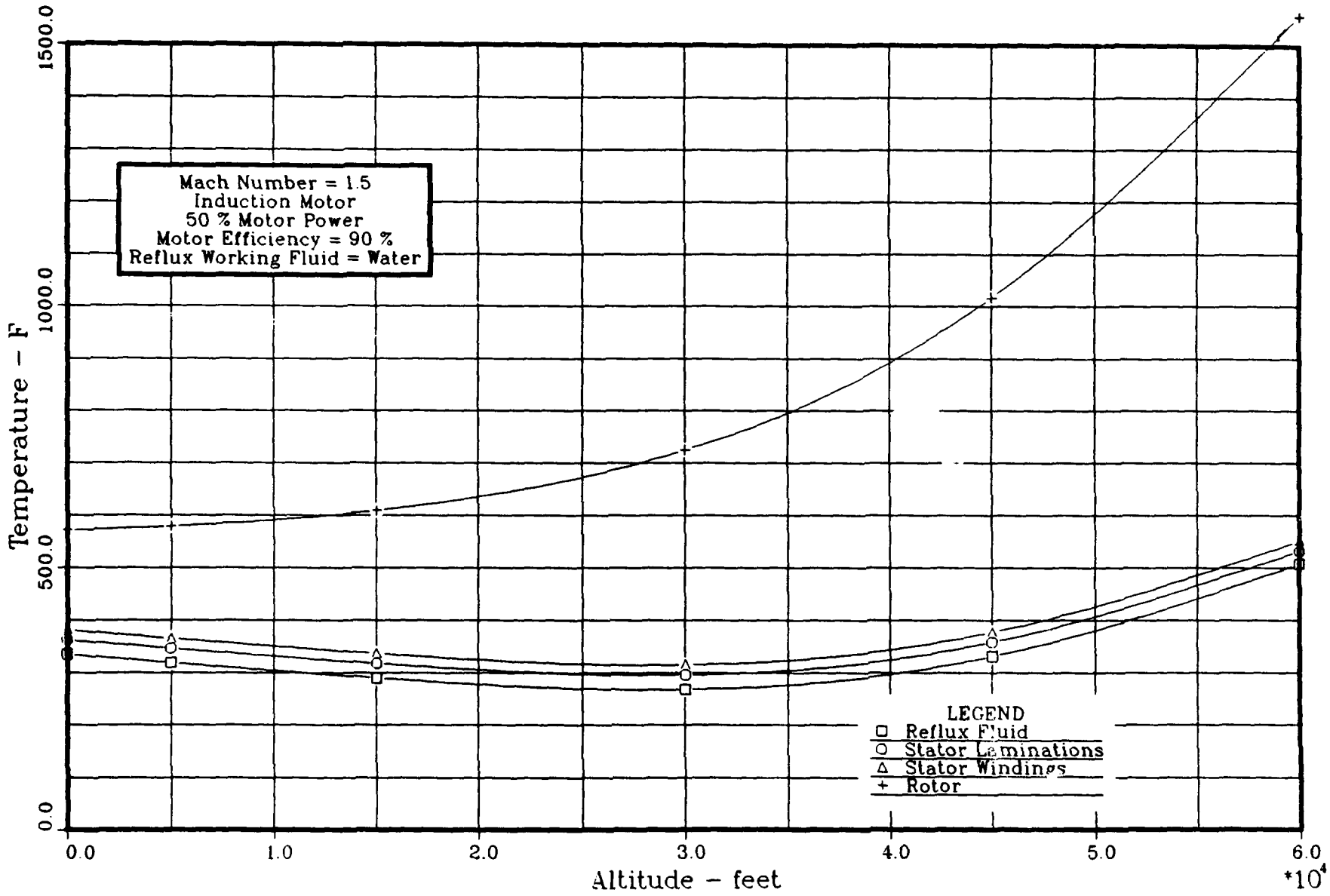

FIGURE A.25 ADVANCED ACTUATOR COOLING
Steady State Temperature vs Altitude

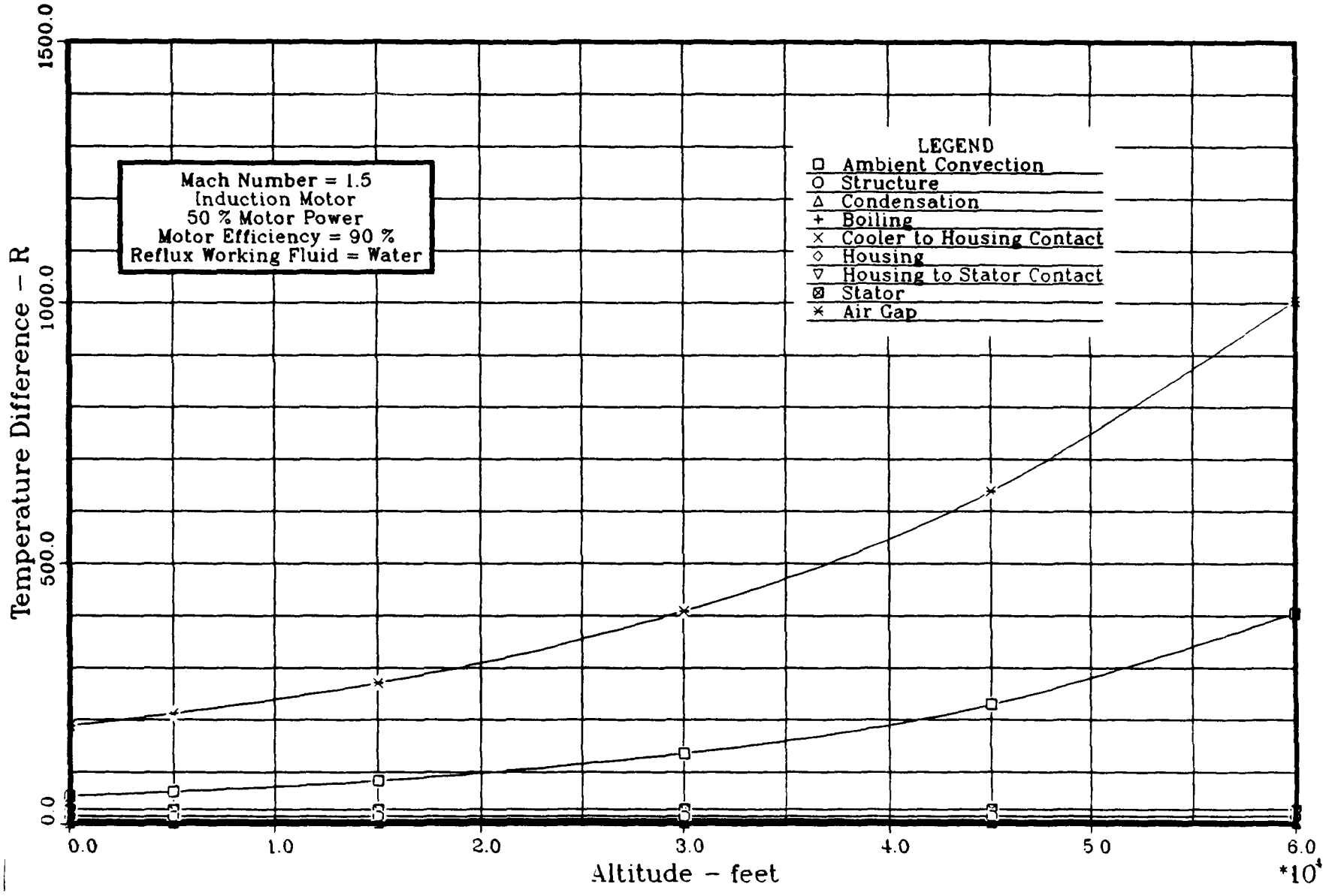

FIGURE A.26 ADVANCED ACTUATOR COOLING
Steady State Temp Differences vs Altitude

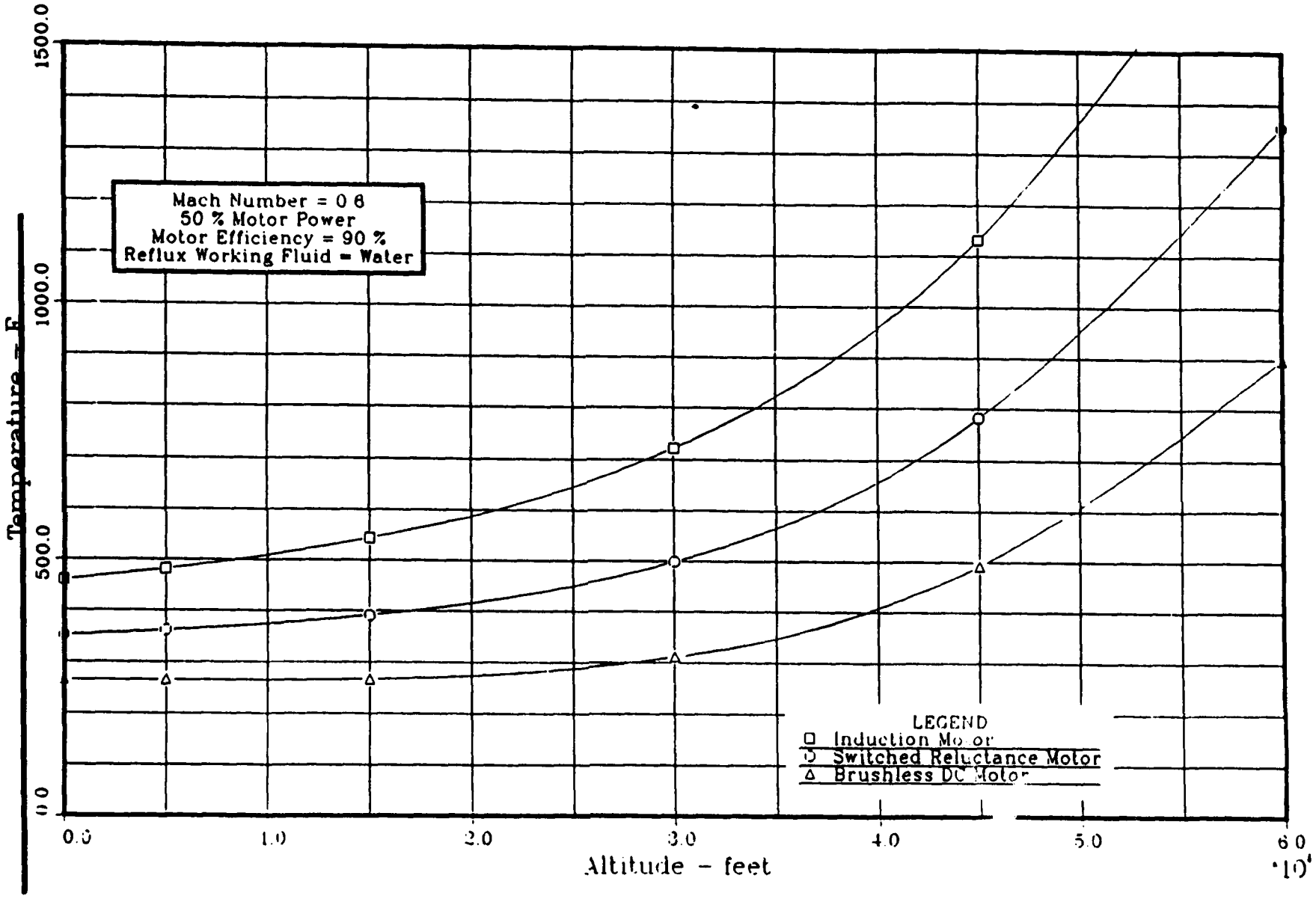

FIGURE A.27 ADVANCED ACTUATOR COOLING
Steady State Rotor Temperature vs Altitude

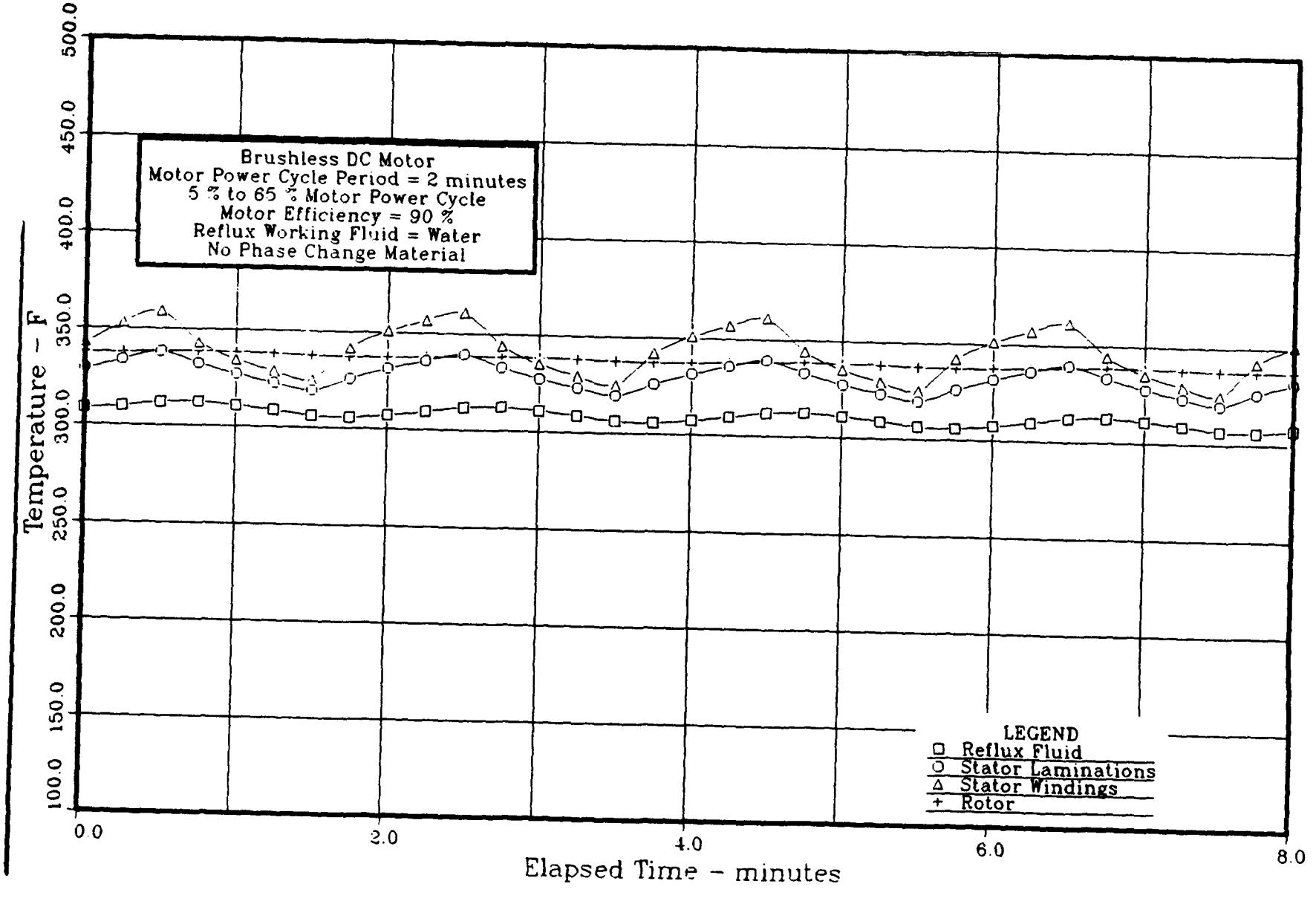

FIGURE A.28 ADVANCED ACTUATOR COOLING
Frequency Response - Temperature vs Time

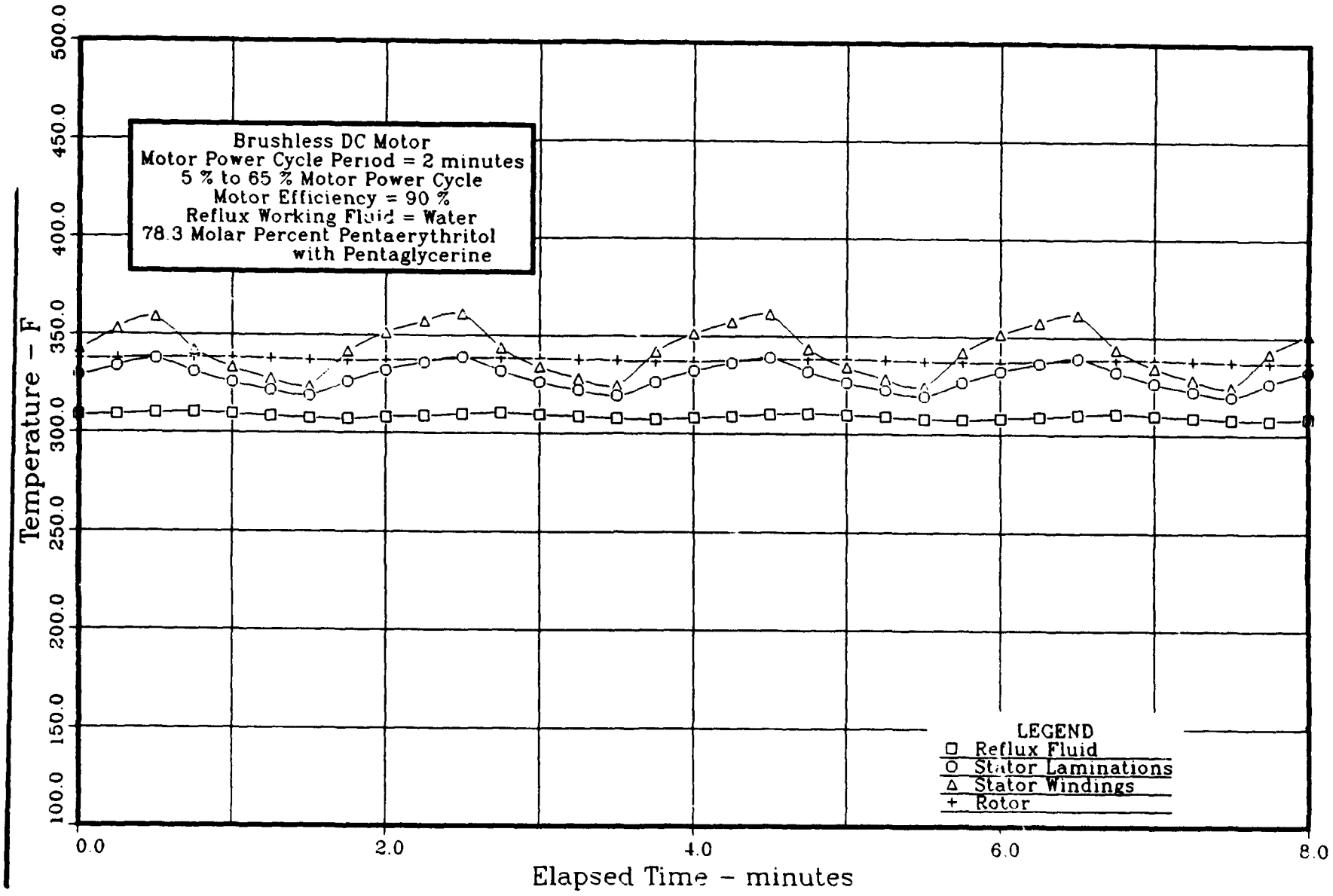

FIGURE A.29 ADVANCED ACTUATOR COOLING
Frequency Response - Temperature vs Time

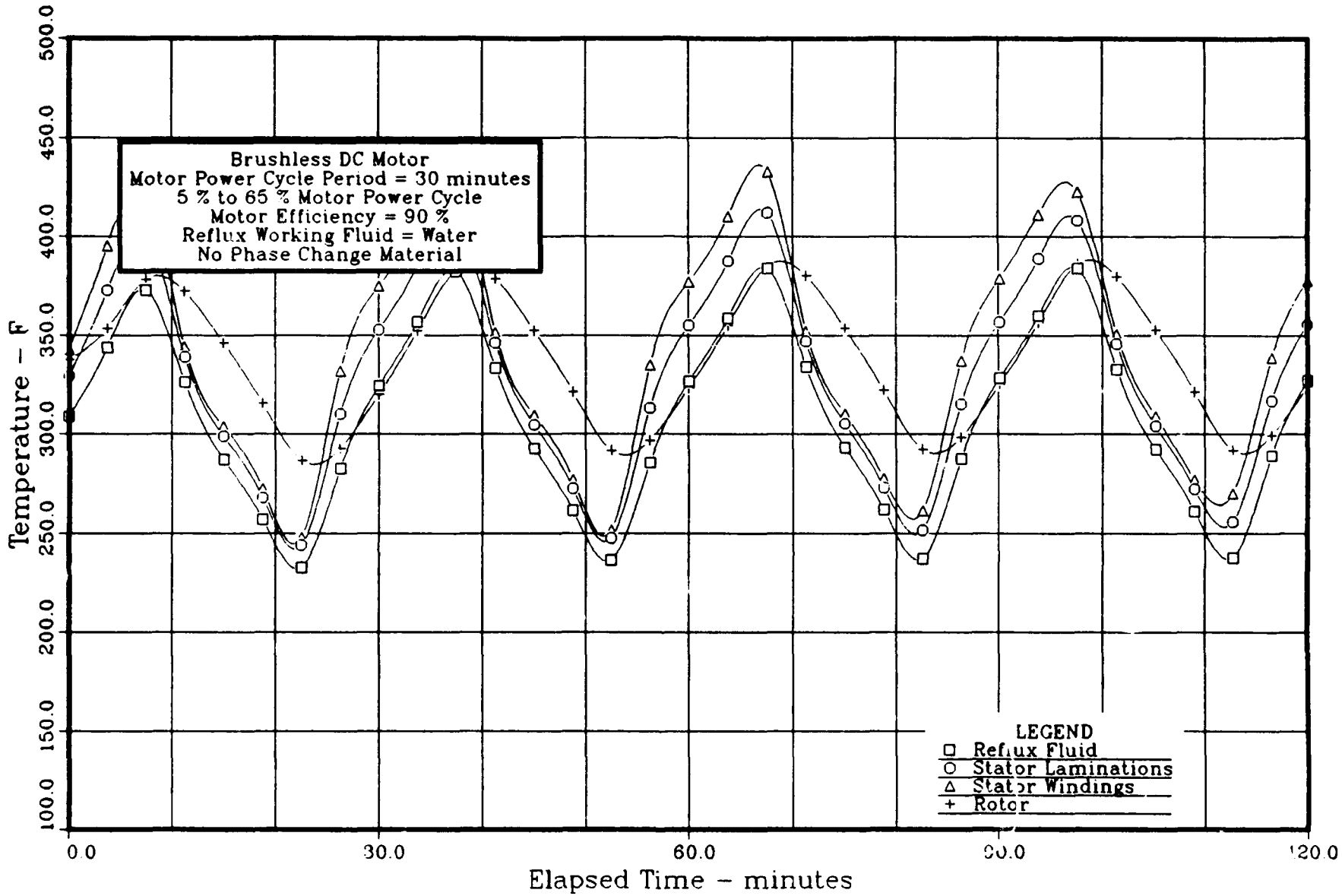

FIGURE A.30 ADVANCED ACTUATOR COOLING
Frequency Response - Temperature vs Time

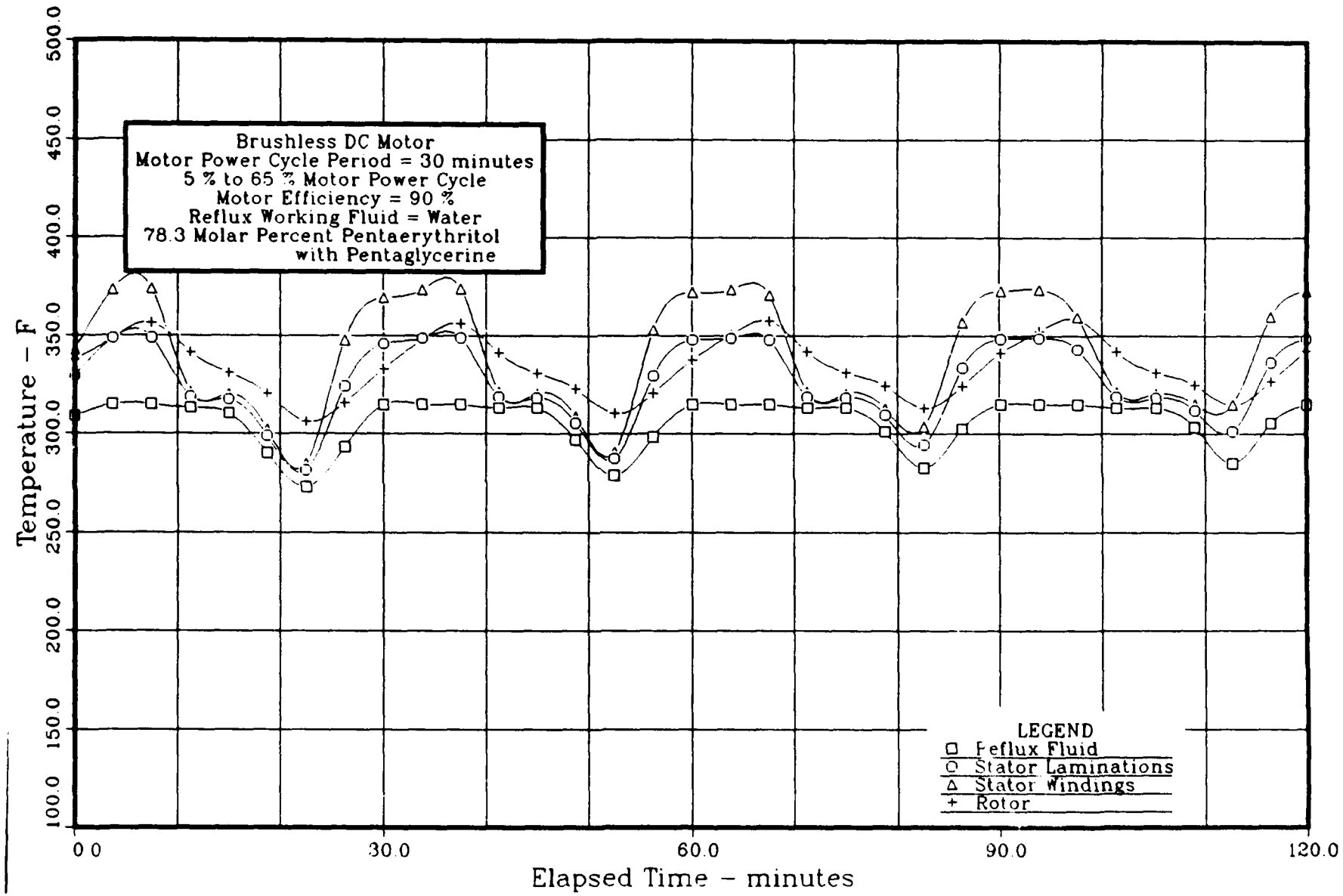

FIGURE A.31 ADVANCED ACTUATOR COOLING
Frequency Response - Temperature vs Time

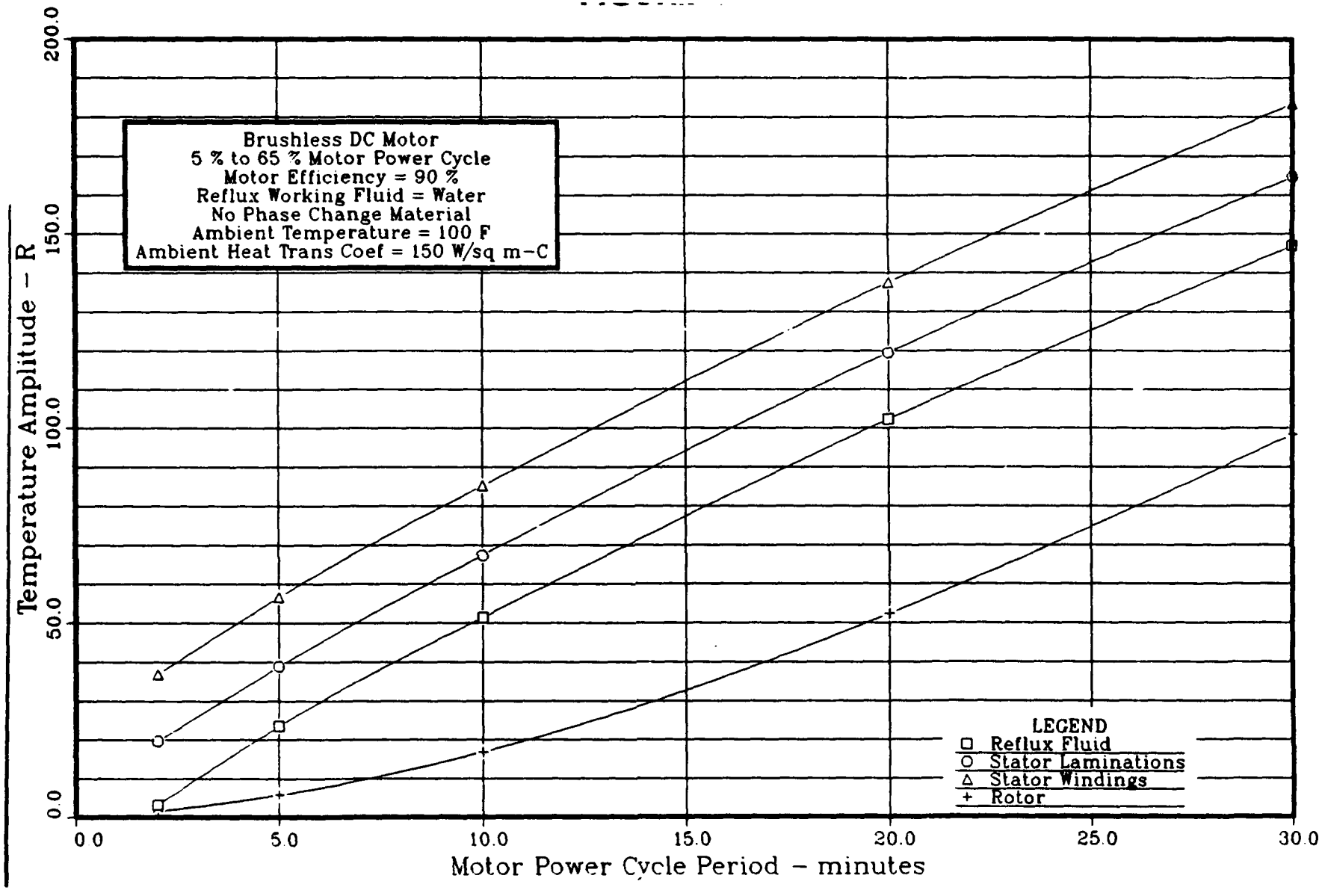

FIGURE A.32 ADVANCED ACTUATOR COOLING
Frequency Response

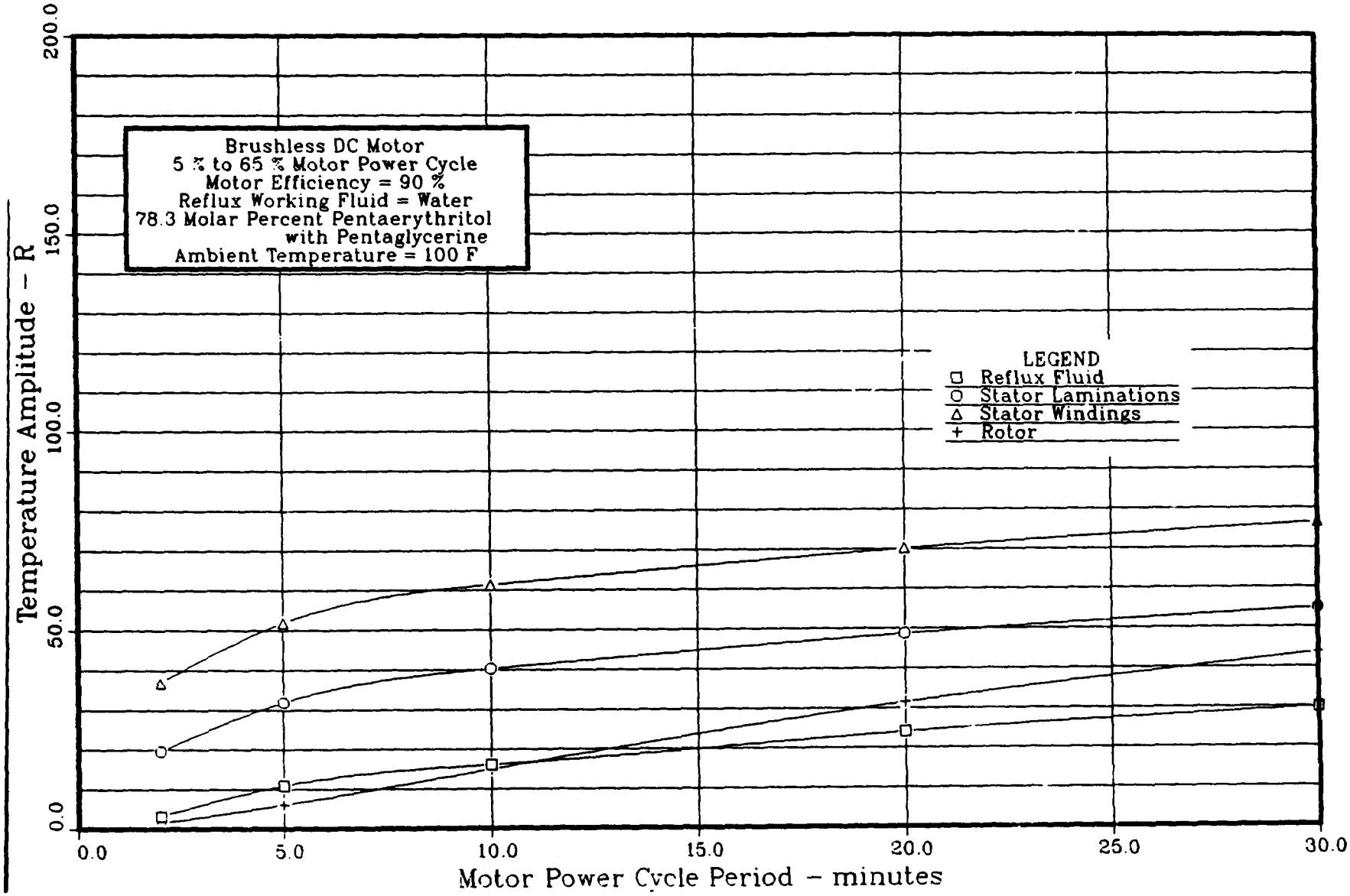

FIGURE A.33 ADVANCED ACTUATOR COOLING
Frequency Response

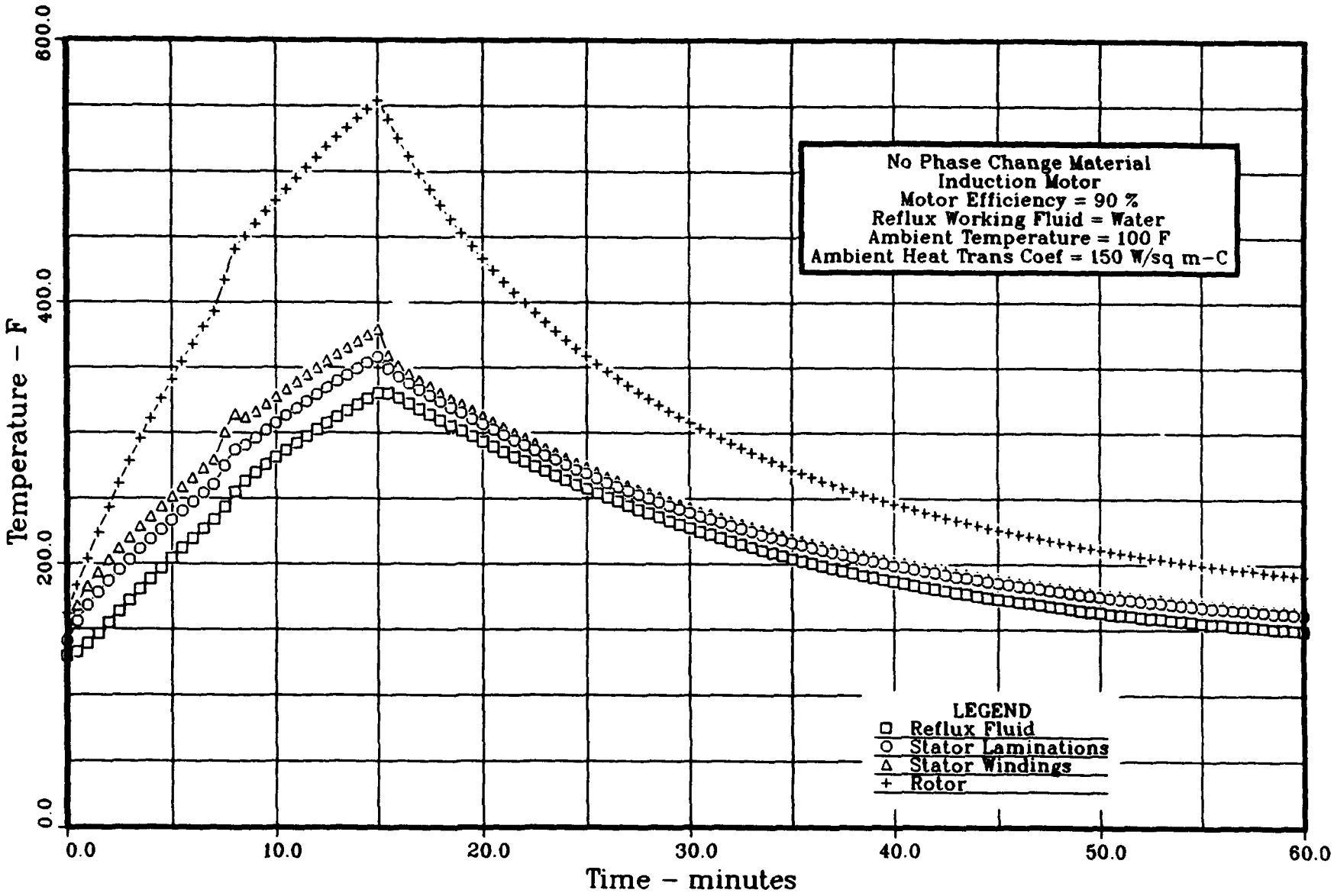

FIGURE A.34 ADVANCED ACTUATOR COOLING
Temperature vs Time

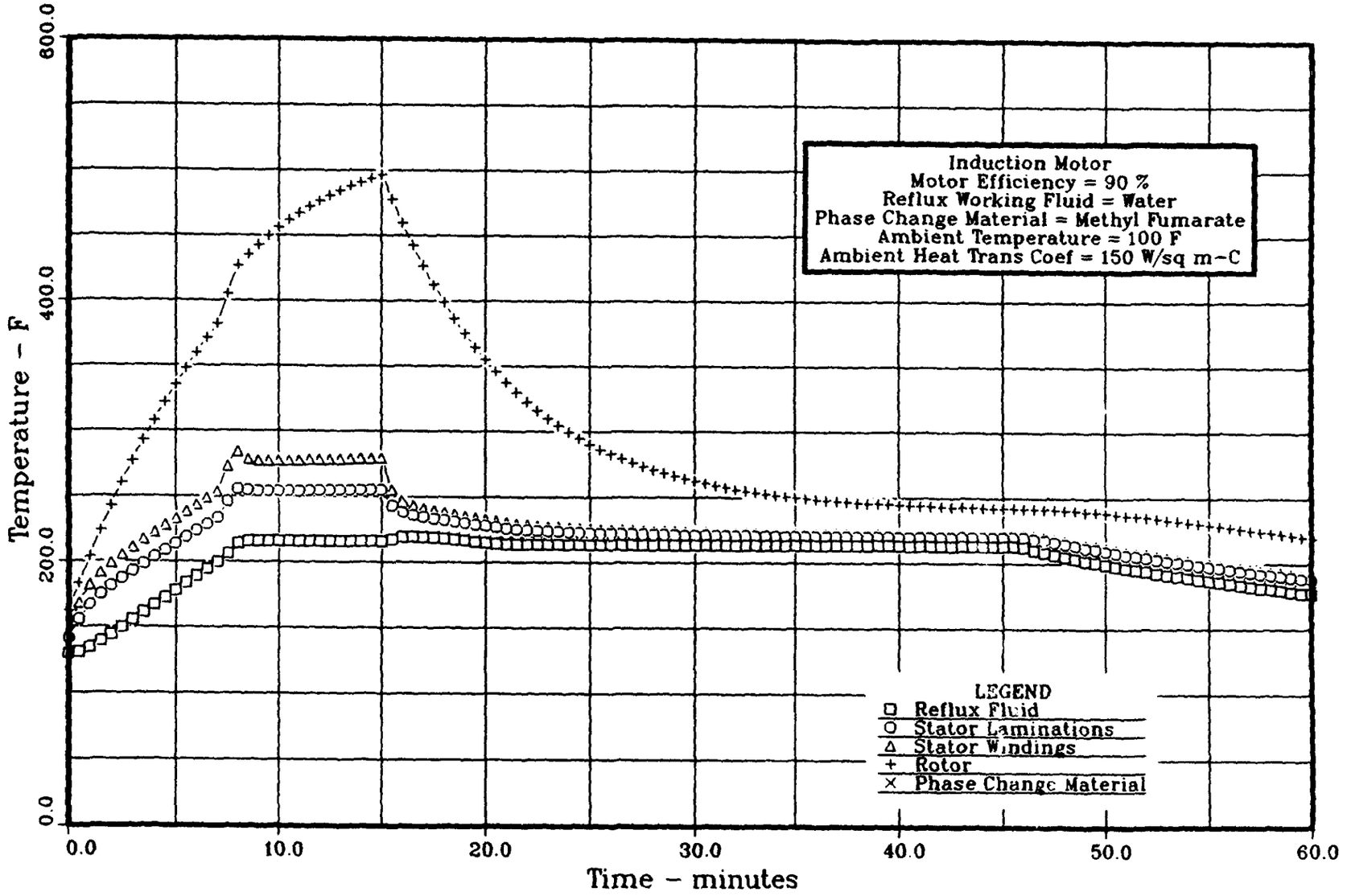

FIGURE A.35 ADVANCED ACTUATOR COOLING
Temperature vs Time

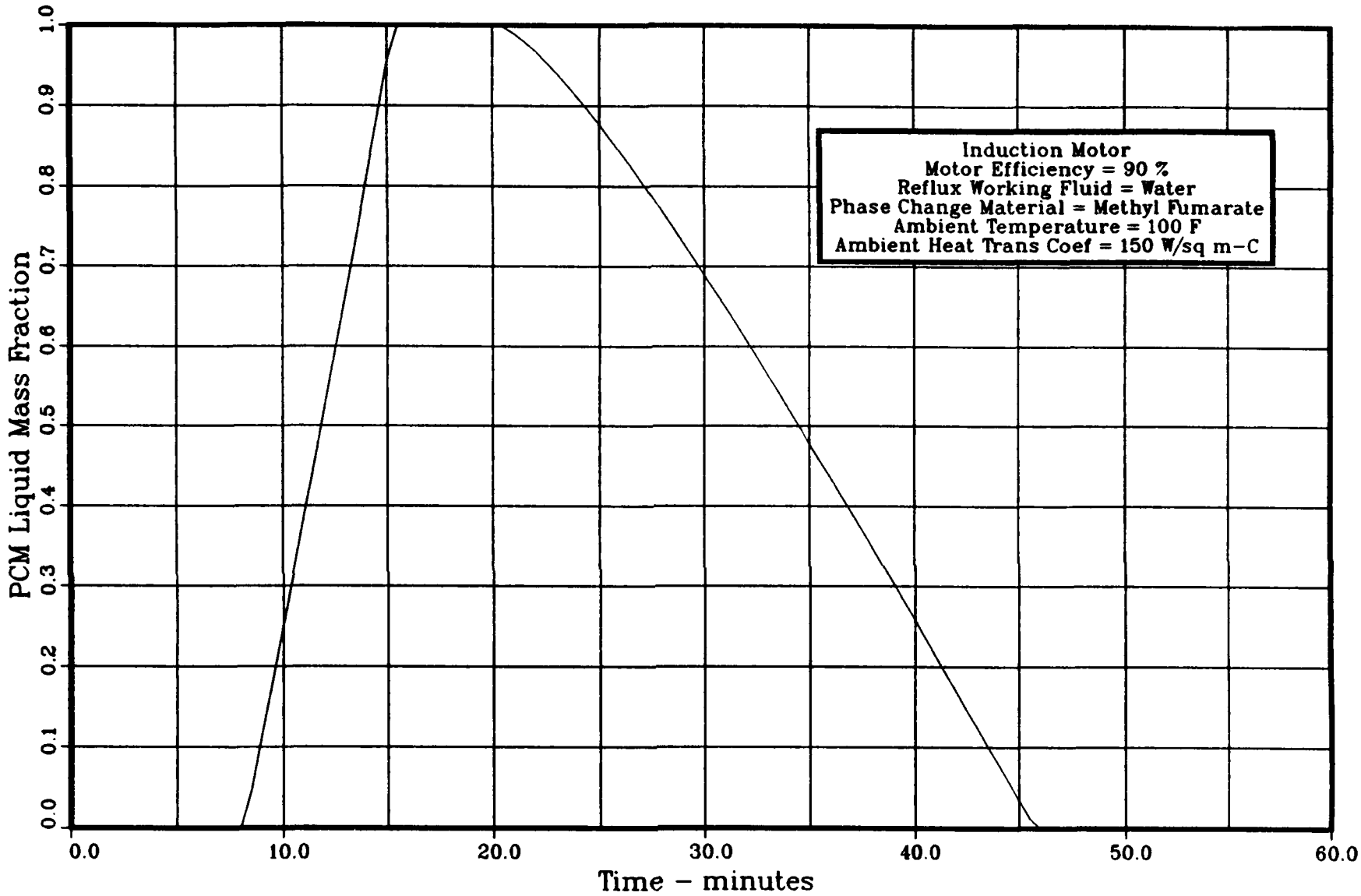

FIGURE A.36 ADVANCED ACTUATOR COOLING
PCM Liquid Mass Fraction vs Time

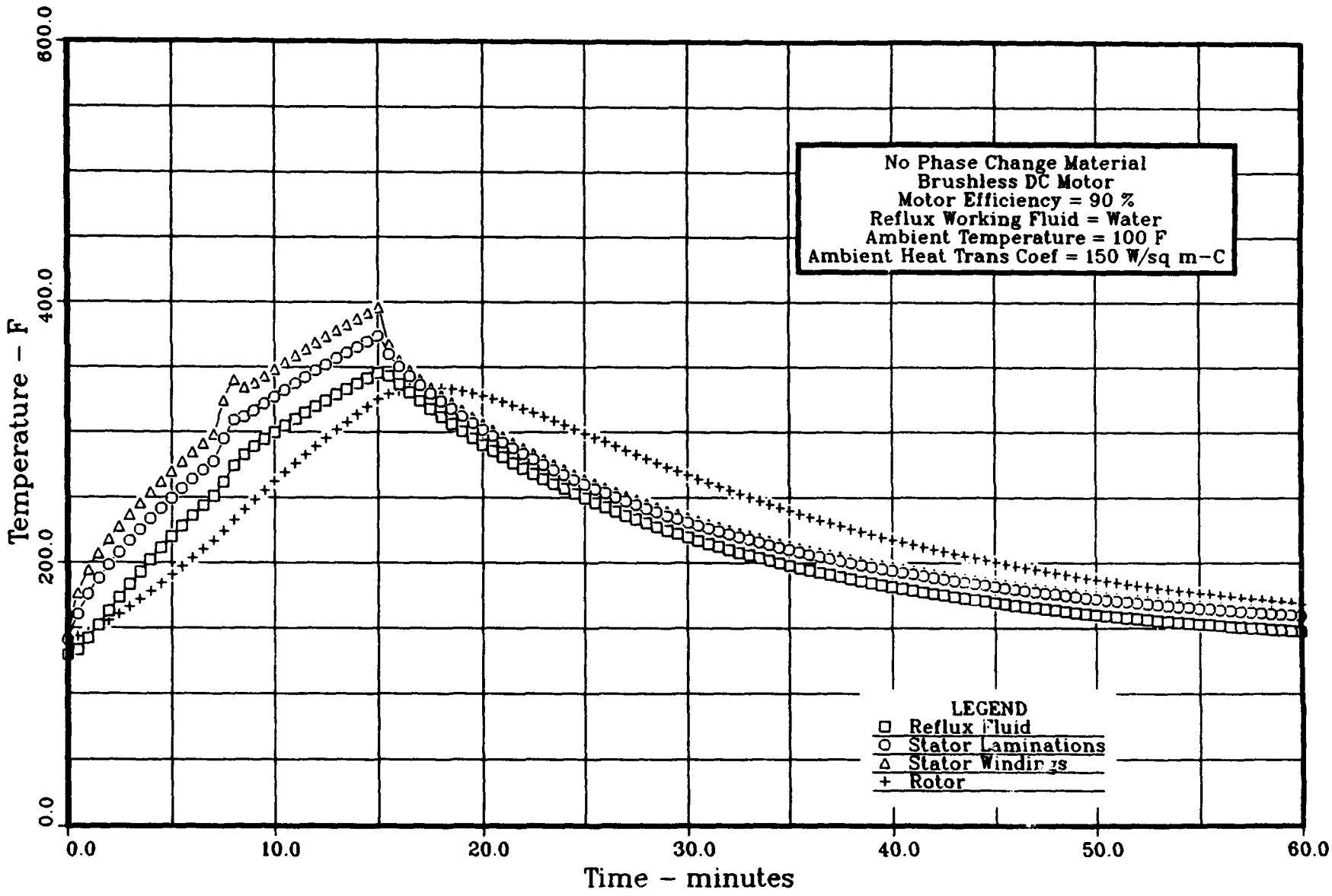

FIGURE A.37 ADVANCED ACTUATOR COOLING
Temperature vs Time

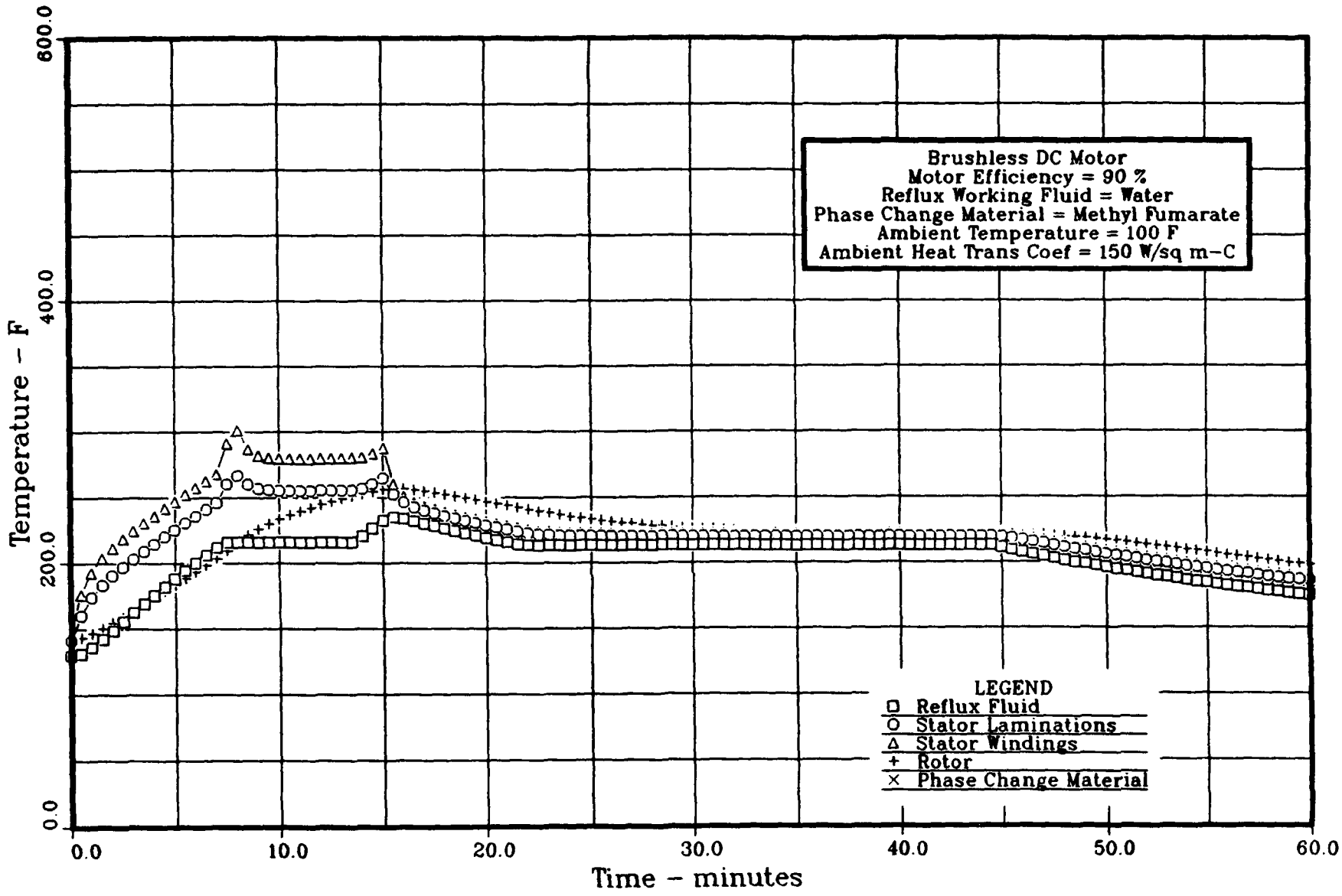

FIGURE A.38 ADVANCED ACTUATOR COOLING
Temperature vs Time

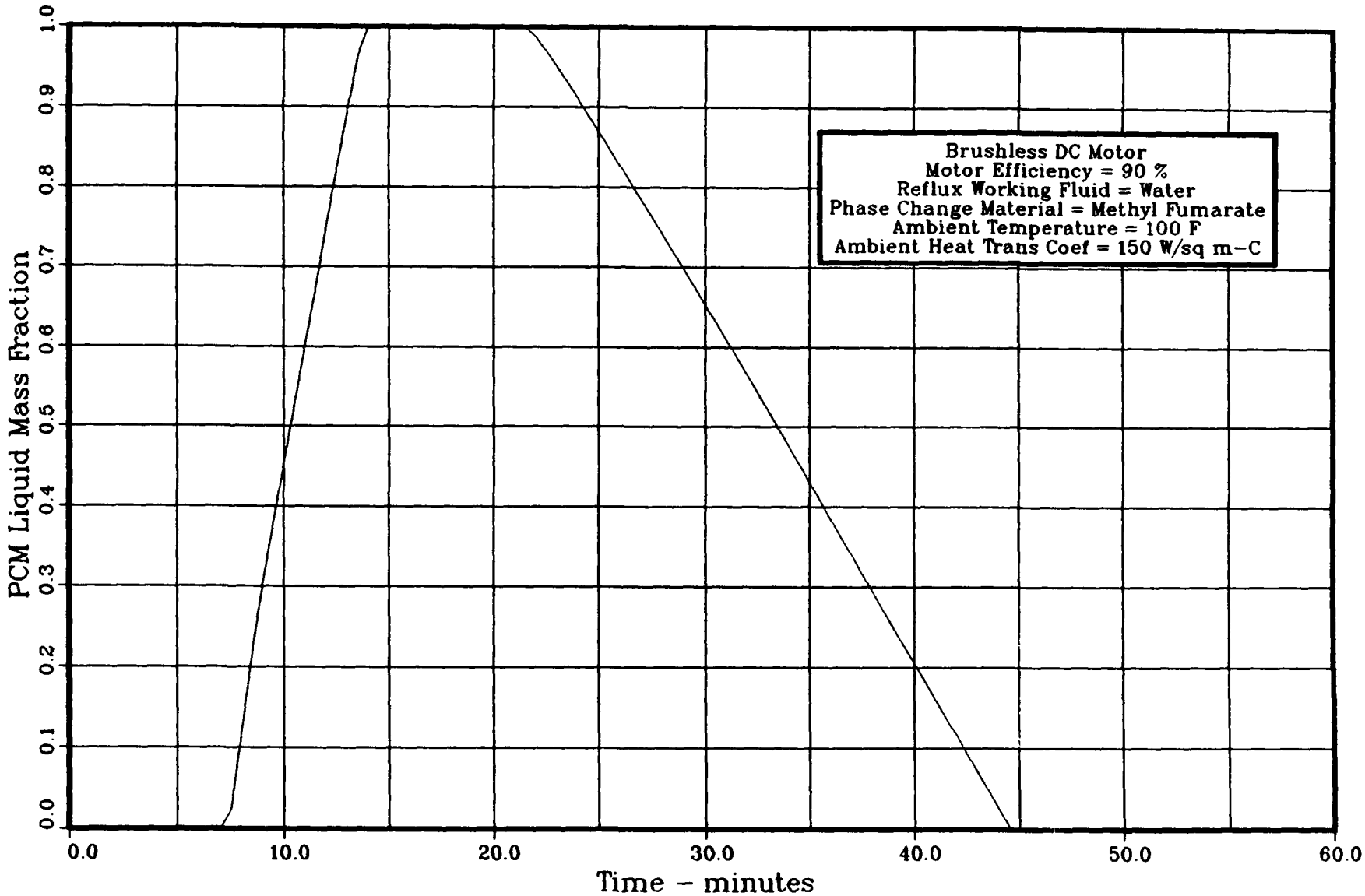

FIGURE A.39 ADVANCED ACTUATOR COOLING
PCM Liquid Mass Fraction vs Time

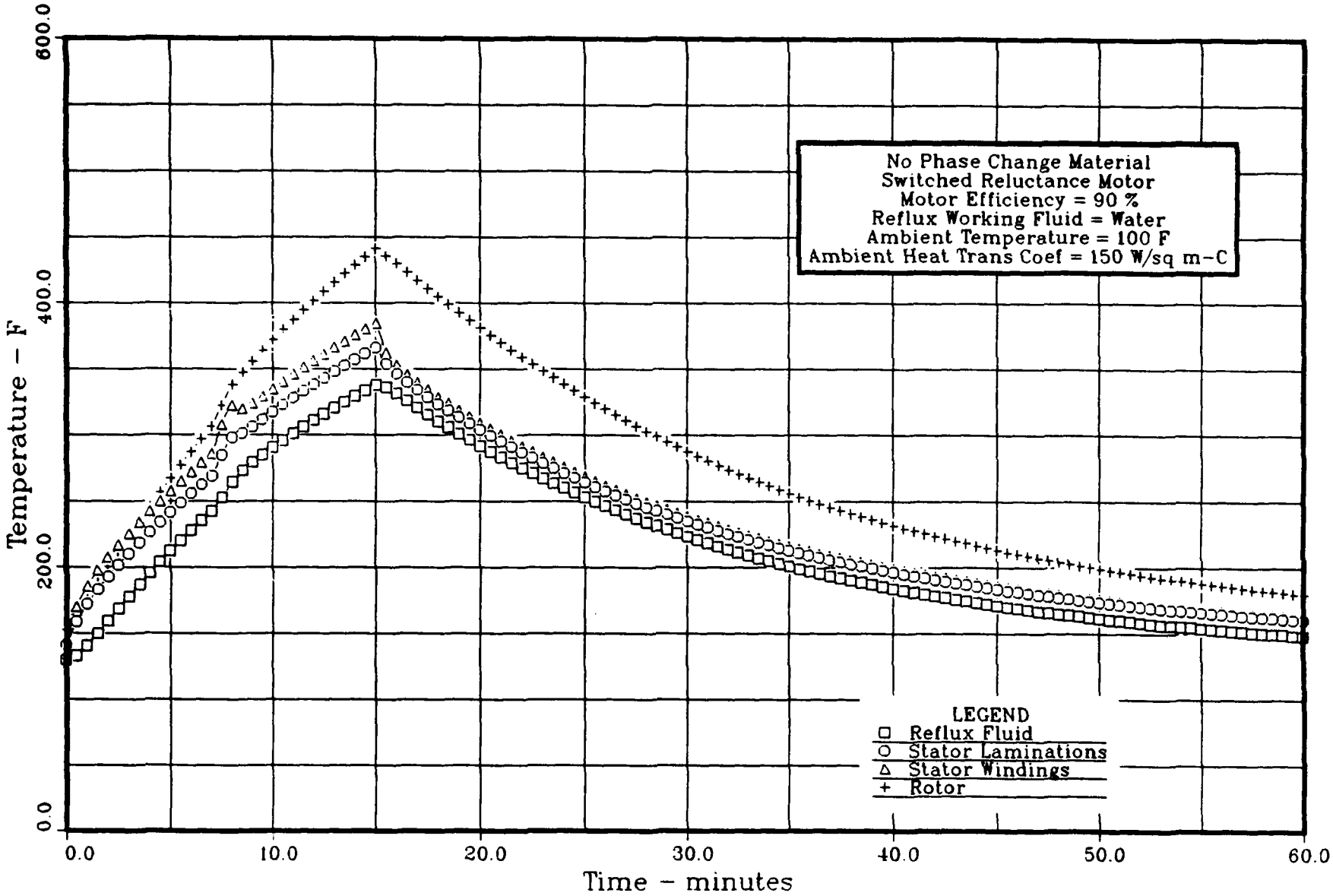

FIGURE A.40 ADVANCED ACTUATOR COOLING
Temperature vs Time

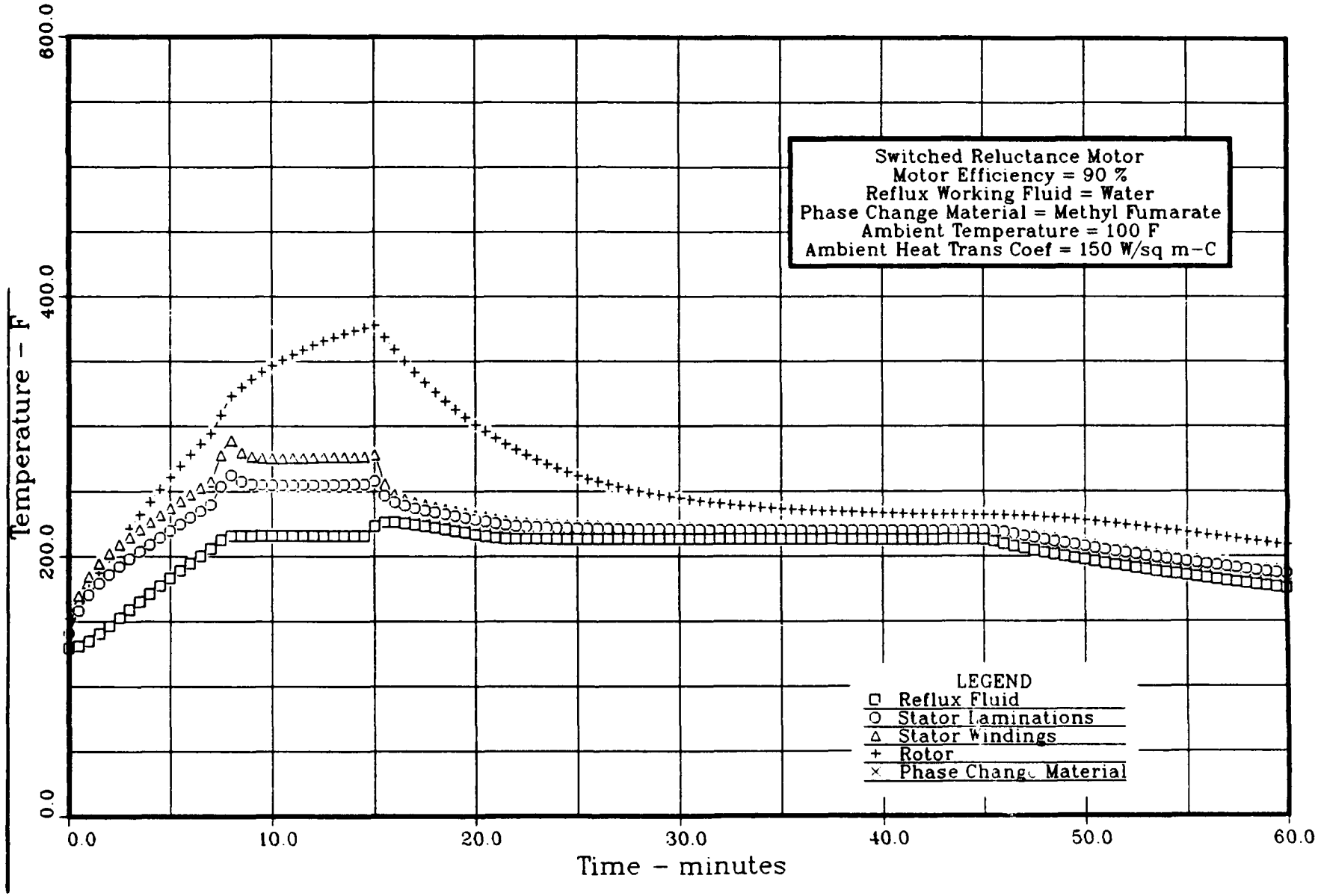

FIGURE A.41 ADVANCED ACTUATOR COOLING
Temperature vs Time

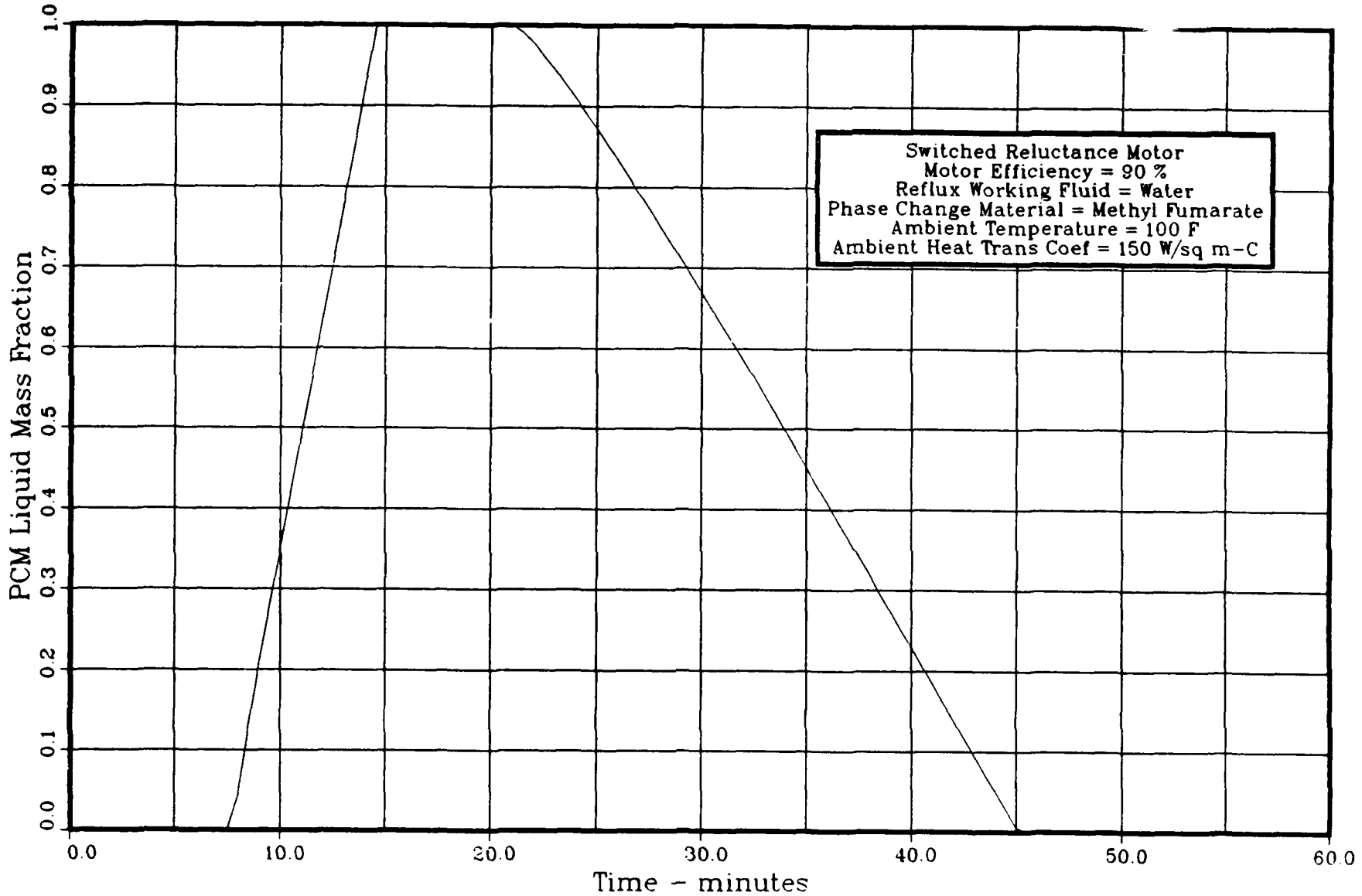

FIGURE A.42 ADVANCED ACTUATOR COOLING
PCM Liquid Mass Fraction vs Time

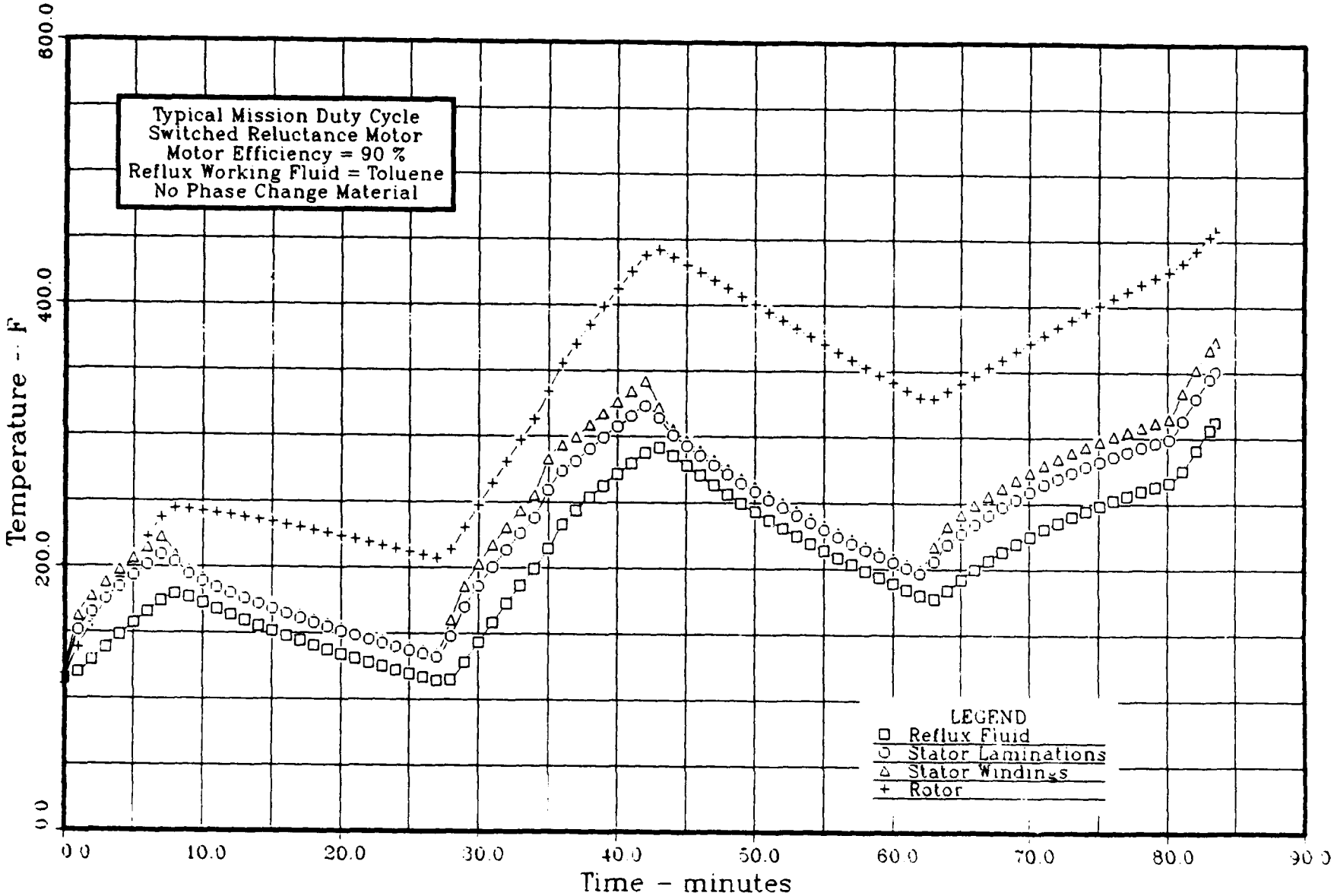

FIGURE A.43 ADVANCED ACTUATOR COOLING
Temperature vs Time

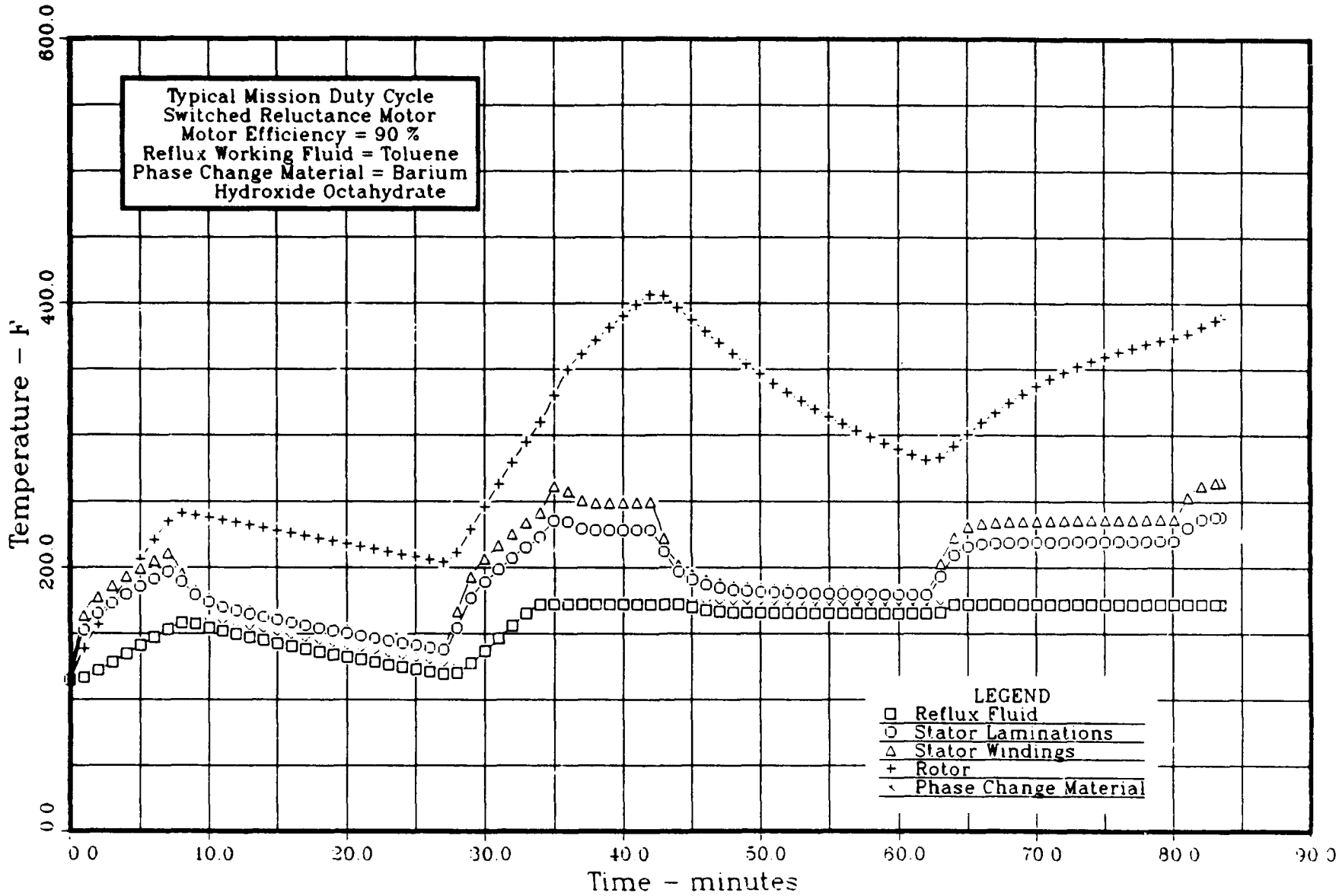

FIGURE A.44 ADVANCED ACTUATOR COOLING
Temperature vs Time

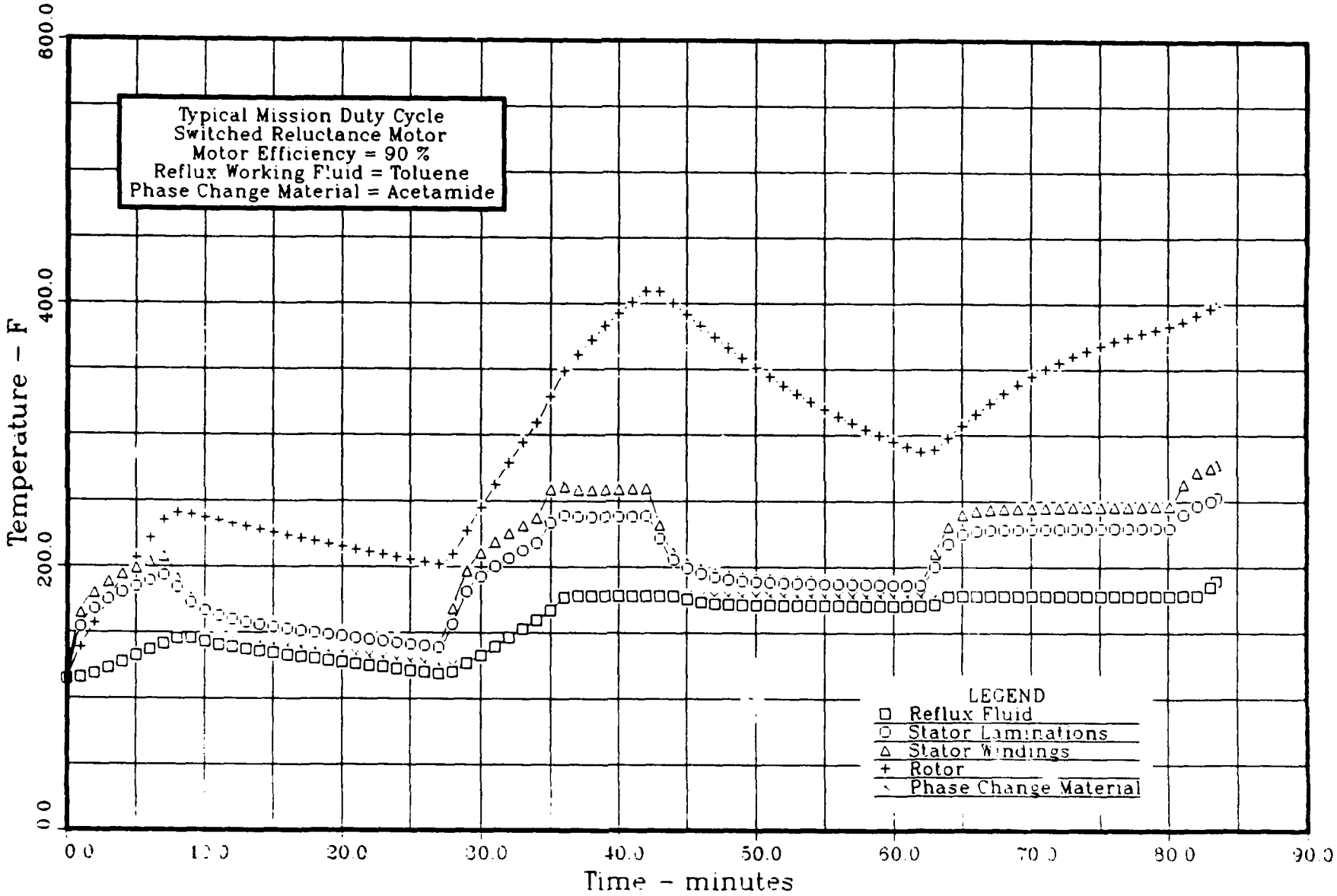

FIGURE A.45 ADVANCED ACTUATOR COOLING
Temperature vs Time

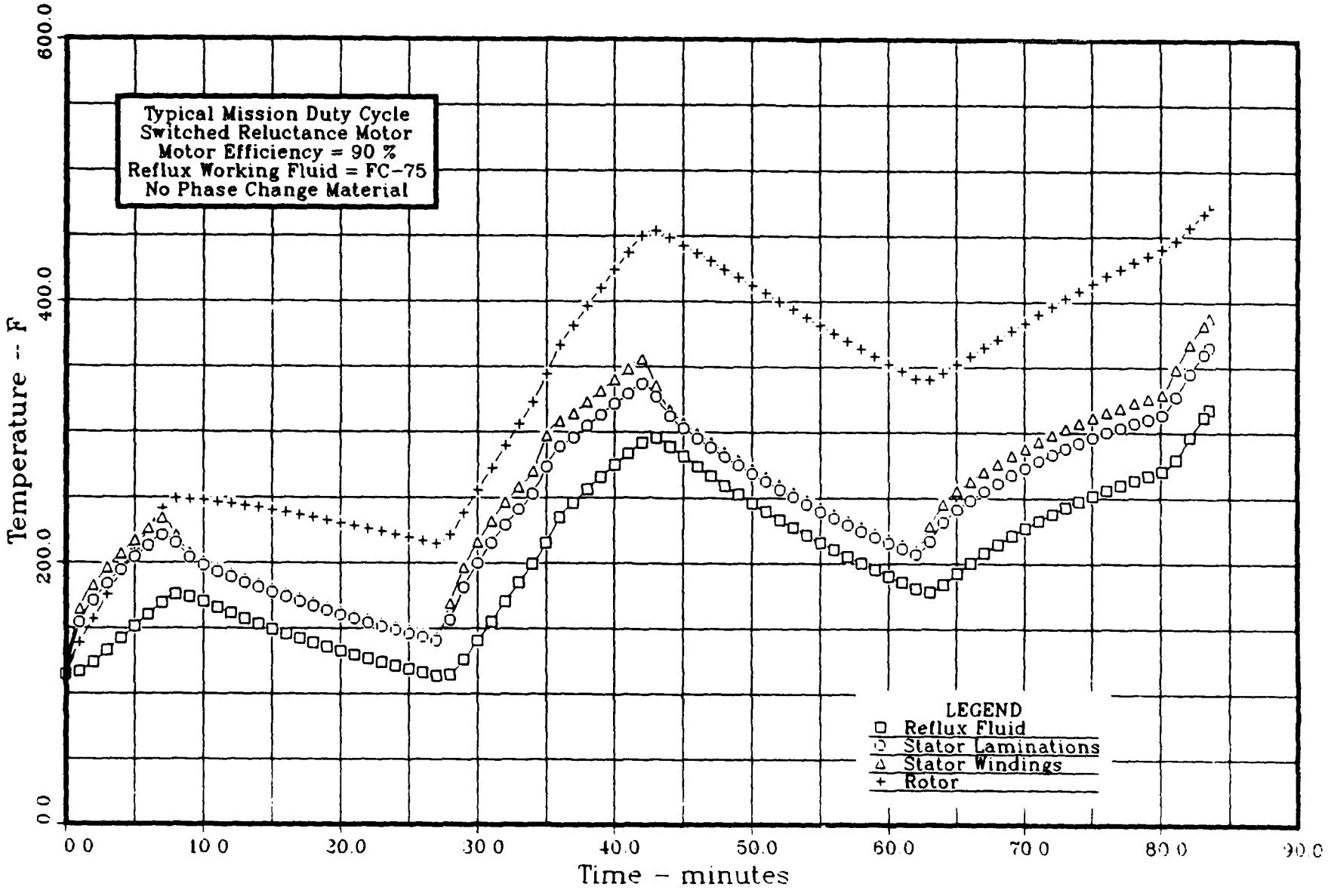

FIGURE A.46 ADVANCED ACTUATOR COOLING
Temperature vs Time

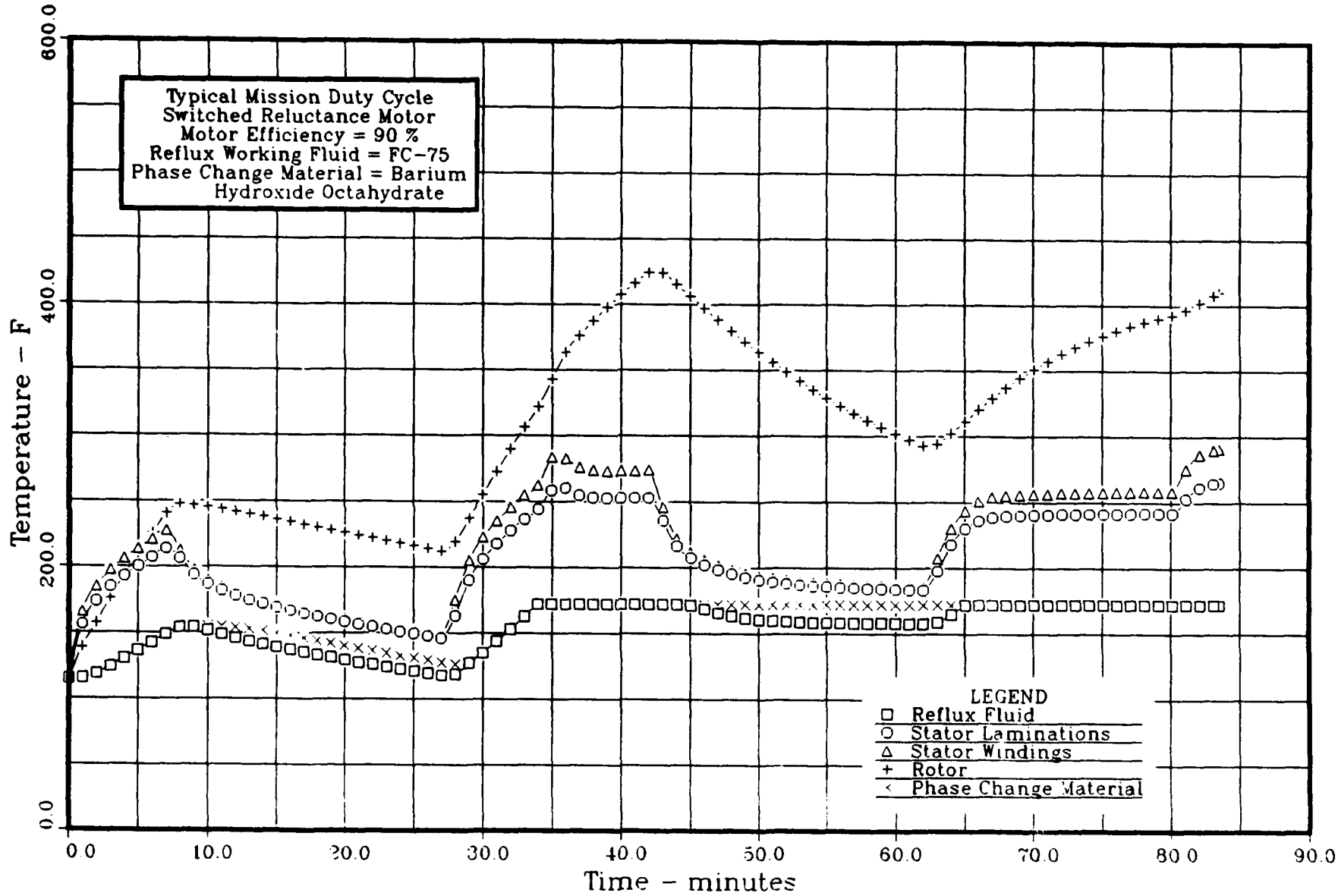

FIGURE A.47 ADVANCED ACTUATOR COOLING
Temperature vs Time

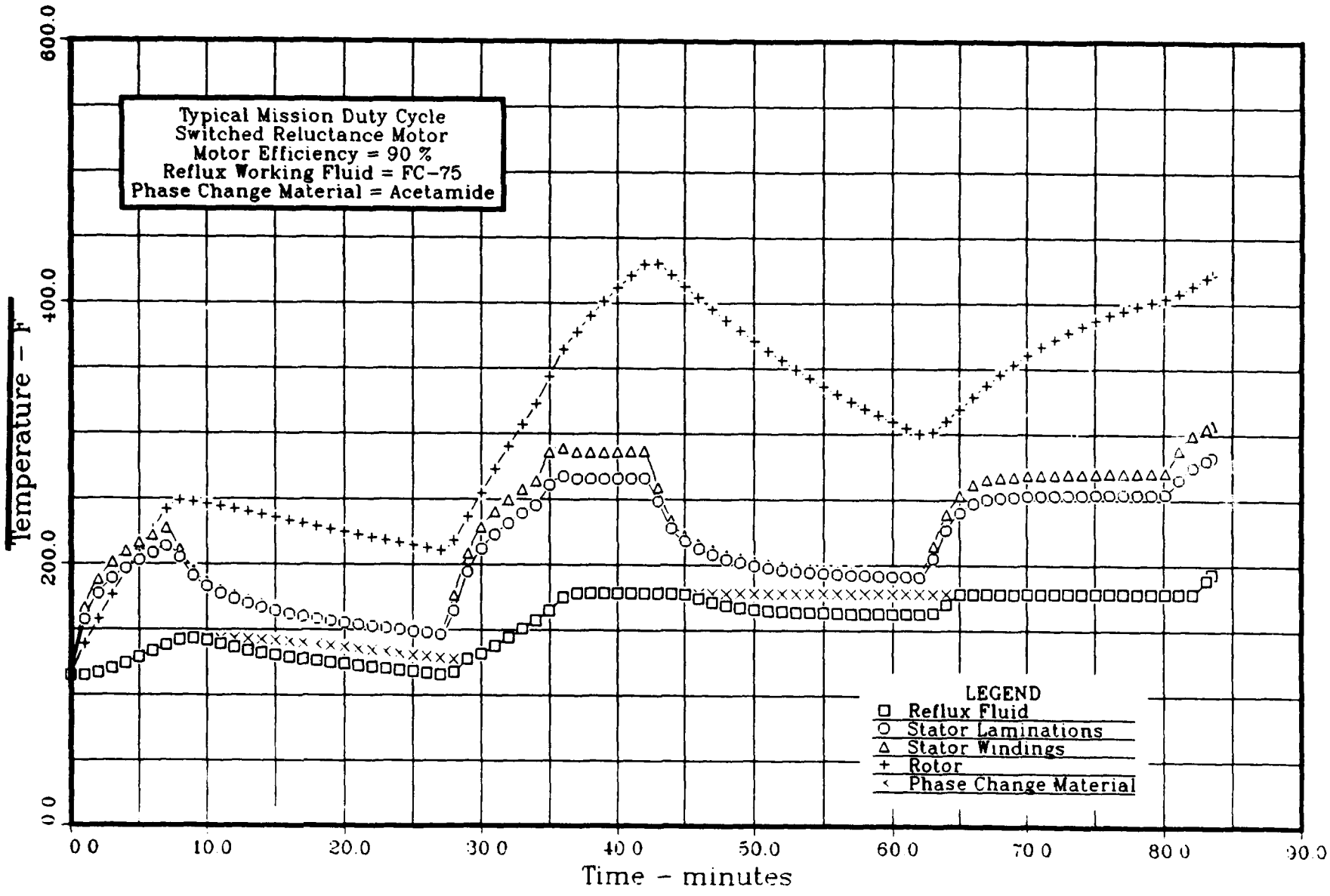

FIGURE A.48 ADVANCED ACTUATOR COOLING
Temperature vs Time

U.S. GOVERNMENT PRINTING OFFICE 750-113